Development of variational models and algorithmic strategies for coupled problems

Jorge de Anda Salazar

UNIVERSITE BRETAGNE SCIENCES LOIRE POUR L'INGENIEUR

CENTRALE NANTES

THESE DE DOCTORAT DE

L'ÉCOLE CENTRALE DE NANTES
COMUE UNIVERSITE BRETAGNE LOIRE

ECOLE DOCTORALE N° 602
Sciences pour l'Ingénieur
Spécialité : Mécanique des Solides, des Matériaux, des structures et des surfaces

Par
Jorge DE ANDA SALAZAR

Development of variational models & algorithmic strategies for coupled problems

Thèse présentée et soutenue à Centrale Nantes, le 11/12/2019
Unité de recherche : UMR6183, Institut de recherche en Génie Civil et Mécanique (GeM)

Rapporteurs avant soutenance :

J. Antonio GIL	Professeur des Universités, Swansea University
Marc-André KEIP	Professeur des Universités, Universität Stuttgart

Composition du Jury :

Président :	Yann MONERIE	Professeur des Universités, Université Montpellier
Examinateurs :	J. Antonio GIL	Professeur des Universités, Swansea University
	Marc-André KEIP	Professeur des Universités, Universität Stuttgart
	Kerstin WEINBERG	Professeur des Universités, Universität Siegen
	Wolfgang A. WALL	Professeur des Universités, Technische Universität München
Dir. de thèse :	Laurent STAINIER	Professeur des Universités, Centrale Nantes
Co-dir. de thèse :	Thomas HEUZÉ	Maître de Conférences, Centrale Nantes

Acknowledgments

This thesis has been possible thanks to the SEED program, which is one of the programs from Erasmus Mundus Joint Doctorate. I have been very lucky for having the opportunity to participate in such an interesting program. Despite being in its early stage, the program allowed me to benefit from a unique experience. I have been able to meet and collaborate in different research environments with two amazing workgroups in Nantes (GeM) and Munich (LNM).

First and foremost I wish to thank two people in particular. My advisor and co-advisor, Prof. Laurent Stainier and Dr. Thomas Heuzé. I have learned a lot from both of you and this work could not have been possible without the continuous support and interest you have provided me. Prof. Laurent, in particular, I am grateful to you for making me aware of some of my flaws but at the same time reminding me that those traits are also my strongest suit. Thanks for making me aware of it. This has been a lesson that has transcended by far my work during the Ph.D. and I will keep improving and benefiting from knowing it on the days to come. Dear Thomas, you have been for me a continuous source for advice, teachings, and patience. You have been able to understand my ideas when I was not able to state them clearly and helped me incredibly in this task. I appreciate deeply the talks we have had during this period and the honesty in your feedback every time. Thanks to both of you for all your support and concern, which you made me feel beyond the university and work. I deeply appreciate it.

In addition, I would like to acknowledge Prof. Wolfgang A. Wall, for his inspiration and being always welcoming to my ideas and always giving me the push of support I needed to hear. Thanks to all my colleges in both groups GeM and LNM. I feel humble from the opportunity to work with both amazing groups. It is said that one is the average of the people you one is surrounded by. I am delighted to have spent all those years of growth thanks to all of you and I am lucky if I can consider myself the average of all of you. In special thanks to Rui Fang with whom I worked during my time in LNM. Thanks for giving me your time and guidance in the last steps of my Ph.D. research, where you had no duty to do it, but you made it just for the sake of exploring ideas and enjoying research. Furthermore, I would like to thank my colleagues. I have been blessed by having the opportunity to meet you and consider many of you not only colleagues but friends.

Continuing on a personal level, I want to especially thank my parents who have been the best teachers I could have ever asked for such thing as life. You have formed me and have made a big part of who I am today. Both of you have taught me how to see the joy in life always, independently of any situation. Thanks for always encourage me to pursue my dreams, even if that goes against what you would like. I can only feel admiration, respect, and love for both of you. Thanks to my siblings, Moni because you opened me the eyes, and showed me that life was bigger than what I could just envision some years back with my narrow sight. Rodrigo, because you are one of the persons I aspire to be. You are my constant reminder of how to keep living my life to the fullest in all aspects. I know with both of you if I get lost I know I will always have you. In general, I want to thank all my family, and family in law for all your love and good energy you irradiate which makes me feel I am blissful and loved. You make my heart full

and clear my head to focus on the things I love and enjoy as it was this Ph.D. Thanks also to all the friends we have made along our way in Nantes in Munich, you have made us feel that we have been always surrounded by family. To our friends in Mexico, thanks for keeping our friendship always strong despite the distance.

Finally, the last person I am infinitely grateful for, is the most important person in my life. It is my best friend who also happens to be my wife. Shanti, thanks for all your support, laughs, friends and experiences that we shared together during this process. Thanks also for sticking along with me through all the difficulties we had to traverse in this period. Thanks for choosing the hard path for you, just because you knew it will lead me to follow my dreams. The fact of you just being there for me independently of everything has been my constant source of energy to keep pushing forward even when I felt I could not do it anymore. One of the things I treasure the most from this experience is the opportunity and luck I got to go along with you all the way in this journey.

Contents

List of Figures

List of Tables

List of Symbols

δ	Variation

Domains, boundaries and interfaces

Ω	Reference Domain
$\overline{\Omega}$	Closure = Reference Domain + boundary domains
$\partial\Omega_X$	Boundary domain for the field X
$\vec{n}$	Outward pointing unit normal vector

Finite Elements

$\cdot\langle a\rangle$	Node (a)
$S_X^{(a)}$	Shape function of field X at node (a)
$X\langle a\rangle$	Field X at node (a)

Number Sets

$\mathbb{C}$	Complex Numbers
$\mathbb{H}$	Quaternions
$\mathbb{R}$	Real Numbers

Other Symbols

ρ	Friction Index
V	Constant Volume

Physical Constants

c	Speed of light in a vacuum inertial system
g	Gravitational Constant
h	Plank Constant

Operators

$:=$	Definition *(from right to left)*

$=:$	Definition *(from left to right)*
$\approx$	Approximation
$\bigcup$	Union
$\equiv$	Equivalence through different notation / Imposed condition
$\hat{\Delta}$	Iteration operator
∇	Spatial gradient
$\otimes$	Dyadic (tensor) product

Part I

Basics

Chapter 1

Introduction

Sommaire

Ce premier chapitre présente la perspective et les motivations de ce travail, et aussi les concepts de base essentiels pour les chapitres suivants. Les applications touchent des sujets de recherche actuels impliquant des problèmes multiphysiques. Les concepts présentés sont structurés en deux catégories: l'une présente le jargon utilisé pour les problèmes couplés et l'autre les définitions précises à utiliser pour travailler avec les solutions numériques des problèmes.

> "The central task of theoretical physics in our time is no longer to write down the ultimate equations but rather to catalogue and understand emergent behavior in its many guises".
>
> R. B. Laughlin & David Pines
> *The Theory of Everything, 2000*

The area of *multiphysics* is a branch of Physics which deals with the coupling of two or more physical systems each one governed by its own principles. In this work, we explore some of the modeling and numerical implications *multiphysics* entails. The approach taken is based mainly from the standpoint of variational principles, focused on the development of mathematical models and its corresponding numerical solution strategies as a systematic process for multiphysic problems.

1.1 Perspective

Multiphysics tackles problems which have a direct impact on our everyday life. Due to the current advances in science and technology the urge to compute solutions of these problems and a deeper understanding of their features gains importance. Due to its complexity and emergent properties, these problems required an understanding beyond single branches of Physics such as *chemistry*, *electricity and magnetism*, *thermodynamics*, *mechanics*, among others, to give us an answer. It is here where multiphysics appears as a viable option. Moreover, such problems are often out of reach for the most fundamental current theories in Physics, namely *relativity* and *quantum mechanics*. For most of the phenomena we are interested, relativistic effects can be neglected and models based on quantum mechanics suffer from the so-called *curse of dimensionality* when the number of particles exceeds ten [Laughlin and Pines, 2000]. Multiphysics is able

to produce an answer through the use of concepts, which despite not being fundamental,[1] can provide us an accurate answer. *Variational principles* and the *continuum approach*, among others are examples of these ideas.

Furthermore, the need of more practical theories also questions the limits of the *reductionist approach* often used by science, where a system to be understood is decomposed into simpler components. Single branches of Physics are based on this approach. A drawback from the reductionist approach is the loss of information regarding the interaction among the simpler components themselves since as stated in Brown et al. [2008] "Reductionist approaches that seek to obtain understanding by breaking complex systems into simpler components may miss emergent, and often significant behavior that arises due to the interaction of these components in nonlinear ways". Therefore, one of the main topics in multiphysics is to answer how these components are coupled in the system, raising the concept of *coupled problems*.[2] We can identify two methodologies in coupled problems, namely, "*bottom-up*" and "*top-down*". A *bottom-up* methodology constructs the whole system from its individual parts, a *top-down* theorizes an hypothetical whole system and observes if its reduction leads to the individual components. Keyes et al. [2013], recently reviewed the state of the art in multiphysics, illustrating opportunities and identifying gaps in our understanding. As they also highlight, most of the used methodologies are *bottom-up* on that regard. They proposed the following motto

"Coupled until proven decoupled"

as a perspective worthy of 21st century simulation purposes and resources, favoring thus a *top-down approach*.

Two main difficulties in multiphysics are the construction of the mathematical model and its solution. The models are highly dependent on the nature of the problem and the type of couplings it involves. As it is for their solutions, the numerical implementations used are most of the time specifically-tailored for the problem and do not leverage algebraic insights from related problems [Keyes et al., 2013]. Therefore, generic techniques to model and solve multiphysic problems are a viable way to standardize and push forward our understanding of multiphysic problems.

The aim of this research is twofold since it concerns both, the modeling and the implementation of the numerical solution for multiphysic problems. The framework on which we base ourselves is that of variational principles. From the standpoint of the modeling, we propose a generic variational form (VF) technique for coupled problems having a *top-down* methodology. To this end, we explore the area of multifield chemical diffusion, for which mixed formulations can be derived and hence be treated as a multiphysic problem. We abstract ideas based on energies, balance and constitutive laws which are common in all of Physics and propose a generic VF scheme for multiphysic problems. The fact that the model can be constructed from a generic scheme allows us to propose a *top-down* methodology. On the other side, for the numerical solution of the VF model we propose to simplify the computation of the solution by deriving[3] from the VF itself three different families of solution strategies.

[1] By fundamental we mean a unified, coherent description of all of nature. Since here we consider multiphysics based on branches of Physics based on a continuum approach, these frameworks are not suitable to establish concepts subatomic particles, therefore, we do not consider them fundamental.

[2] The terms *multiphysics* and *coupled problems* are often interchangeable in the literature

[3] usually, numerical strategies are rather imposed than derived.

1.2 Applications

We present some applications below for multiphysic problems as illustrative examples, which can serve as motivation. The applications considered here focus on electrochemistry and chemomechanical problems in multiphysics. More examples can be found in Keyes et al. [2013]

1.2.1 Lithium-ion batteries

Lithium-ion batteries are common in consumer electronics. They are one of the most popular types of rechargeable batteries for portable electronics. Beyond consumer electronics, Lithium-ion batteries are also growing in popularity for military, battery electric vehicle and aerospace applications. What makes lithium-ion batteries preferable over alternative technologies is their long life, high specific energy, and high efficiency at moderate size and weight [Scrosati and Garche, 2010], [Fang et al., 2017]. A deeper insight into the behavior and understanding of these type of batteries is therefore a current interest for the industry. We explore this application in chapter §5.

A brief description into the functioning of Lithium-ion batteries is now presented. The three primary functional components of a Lithium-ion battery are the positive and negative electrodes and the electrolyte. Generally, the negative electrode of a conventional Lithium-ion cell is made of carbon. The positive electrode is a metal oxide, and the electrolyte is a Lithium salt in an organic solvent. The electrochemical roles of the electrodes reverse between anode and cathode, depending on the direction of the current flow through the cell. Both electrodes of a Lithium-ion battery are hosts of Lithium. During charge and discharge, Lithium diffuses out of one electrode, migrates across the electrolyte, and then diffuses into the other electrode, while the electrodes deform. A high-capacity silicon[4] electrode, can absorb a large amount of Lithium and is expected to swell more than three times its initial volume roughly. The deformation is inelastic: after a cycle of lithiation and delithiation, silicon atoms are rearranged. When a thin film of silicon on a substrate is lithiated and delithiated, the stress in the film may reach the yield stress. Atomistic simulation shows that Lithium assists the flow of silicon by participating in bond breaking and reforming. This flow changes the shape of the electrode, preserves its composition and volume, and is driven by the deviatoric stress. By contrast, reaction changes the composition and volume of the electrode, and is driven by a combination of the mean stress and the chemical potential of Lithium in the environment [Brassart and Suo, 2012] , [Brassart and Suo, 2013].

Hence, one can regard the diffusion of Lithium ions into the film of silicon affects its mechanic behavior elastically and inelastically. In Brassart and Suo [2012] and Brassart and Suo [2013] a theory of reactive flow in solids is formulated by regarding both flow and reaction as non-equilibrium processes.

1.2.2 Hydrogels

Hydrogels are a network of polymer chains that are hydrophilic, in essence, they readily absorb or dissolve in water. It possesses a degree of flexibility very similar to natural tissue, due to their significant water content. Therefore, a variety of medical applications can be related to hydrogels, as an example is the tissue reconstruction of the intervertebral disc (IVD).

[4] As mentioned by Kingshuk et al. [2019], silicon Li-ion electrodes can theoretical suffer 300% volume changes during lithiation/delithiation due to its absorption capacity.

In a word, IVD is the fibro-cartilage structure between two consecutive vertebrae, and it consists of three main components: *nucleus pulposus* damping in the center, the *annulus fibrosus* at its periphery, and the cartilaginous end plates, which surround the whole. Each of these structures are mainly composed of water, collagen and an extracellular matrix. The mechanical role of the IVD is both to ensure the mobility and flexibility of the spine while absorbing shocks. However, due to aging or a disease process, the IVD and particularly its *nucleus pulposus* undergoes gradual degradation phenomenon called "disc degeneration". It is characterized by severe changes in the macroscopic appearance and composition (major water loss, especially), causing a profound alteration of the mechanical functions of the IVD [Brulliard, 2014].

In the context of IVD tissue reconstruction, hydrogels can be used as a replacement material for degraded *nucleus pulposus*. Hydrogels are materials formed of two ingredients: a three-dimensional network of long polymer chains connected to each other at the points of cross linking and water (solvent). Nowadays, research attempts to associate hydrogels to stem cells to achieve mid-organic hybrid mid-synthetic grafts to replace the damaged tissue. The issue concerns both the development of injectable biomaterials so that the surgery is minimally invasive, but also the required properties of these materials for the mechanical function of the IVD to be preserved, at least for the cell proliferation phase. In the work of Brulliard [2014] a chemomechanical model coupling diffusion with large deformation is proposed in order to model this phenomenon.

1.2.3 Further Applications

Now just a brief mention to other potential options related to reactive flow in solids[5] which appear in the literature where chemomechanical phenomena can be applied. A reference to some of these works is presented next.

Chemical reactions in cement can cause inelastic deformations. This deformations can be triggered by thermal or chemical diffusion of different substance into the concrete [Ulm et al., 2000].

Oxide formation is another example. When a metal reacts with oxygen in the environment to form a layer of oxide, much of the new oxide forms at either the metal/oxide interface or the oxide/environment interface, depending on the relative rate of diffusion of metal and oxygen through the oxide; however, new oxide also forms inside the existing oxide, causing the oxide to flow inelastically [Tolpygo and Clarke, 2004], [Oh and Thompson, 2011]. As a closely related phenomenon, when an aluminum-containing alloy oxidizes, oxygen preferentially reacts with aluminum, driving aluminum atoms to diffuse out and changing the composition of the alloy, so that the alloy flows [Suo et al., 2003] [Kadiri et al., 2008].

The *Kirkendall effect* is a phenomenon where the coupling mechanics-diffusion also appears. When different species of atoms mix by diffusion, inert markers move in the direction of diffusion [Kirkendall et al., 1938], and dimensional changes normal to the direction of diffusion occur [Balluffi and Alexander, 1952].

Metal deposition is also subjected to the physics of mechanic-diffusion since it develops stress and flow [Chason et al., 2002] and electromigration [Pharr et al., 2011];

[5]Change of the internal structure of a solid material due to chemical reactions

Self-diffusion and *Self-reaction* are phenomena that may occur in solids when atoms interact with defects such as vacancies, dislocations, and grain boundaries [Balluffi and Seigle, 1955] [Suo, 2004] [Svoboda and Fischer, 2009].

The applications above have been some of the initial targets considered in the beginning of this research. As mentioned, we have chosen the Lithium-ion batteries (§5) as a benchmark example, the reason being the wide spectrum of aspects this problem entails as a coupled problem. Now, the rationale behind tacking variational principles as our standpoint is explained below.

1.3 Variational principles

Variational principles have been used for a long time to understand nature. These ideas can be traced back even to Greek philosophers as Aristotle and Archimides [Berdichevsky, 2009, dell'Isola and Placidi, 2011]. It is often believed that VF models derived from variational principles can not represent dissipative systems. We know by facts the latter is no longer true, as shown by several works in the literature. To mention a few diverse examples, Bourdin [2011] presents a VF to model fracture phenomena, Pandol et al. [2001] model frictional contact through a VF, in Yang et al. [2006] a VF model is derived which allows to represent boundary value problems of thermo-mechanical dissipative structures, and Miehe [2011] presents a VF for solids with dissipative micro-structures. In Miehe et al. [2014] a VF is derived for diffusion in solids and Gay-Balmaz [2019] derives a VF describing the dynamics of the moist atmosphere that includes the irreversible processes of viscosity, heat conduction, diffusion, phase transition, and rain. Furthermore, the latter examples show that VFs are suitable to be used for multiphysics problems.

There are several reasons why a VF can be preferred over balance principles. As it concerns the model, it allows the handling of boundary conditions by providing a natural framework to state them, whereas balance postulates do not [dell'Isola and Placidi, 2011]. For multifield models, as Berdichevsky [2009] states, "If the interactions between various fields are absent or simple enough then one does not need the variational approach to construct the governing equations. However, if the interactions in the system are not trivial the variational approach becomes the only method to obtain physically sensible governing equations". A VF also offers theoretical advantages as regards the selection of trajectories in cases of non-uniqueness [Pandol et al., 2001]. The perks of the VF reside in its corresponding numerical implementation too. For instance, a VF goes hand by hand with FEM since there is always a *Galerkin method* associated with it [Finlayson, 2013]. One can derive a fundamental approach to a monolithic finite element solution via a VF as suggested in Miehe et al. [2014] within the framework of multiphysics. Furthermore, a VF can highlight an inherent symmetry of the evolution problem [Miehe, 2011], which can be exploited also by numerical methods. In general, as stated in Pandol et al. [2001] a VF provides a basis for formulating numerical algorithms. Unfortunately, as it concerns the development of sound generic solution strategies based on the VF itself seems to be lacking.

In this work we follow the line of variational principles based on a thermodynamic approach to constitutive modeling, closely following the Generalized Standard Materials approach of Halphen and Son Nguyen [1975]. This approach is followed by Yang et al. [2006], Miehe [2011], Stainier and Ortiz [2010], Stainier [2011], and Miehe et al. [2014]. These works present a VF for multiphysic phenomena involving mechanics. A generalization of these VF approach is described in Miehe [2011]. In contrast, we present a generalized VF based on these ideas but keeping the formulation independent of any of the branches of physics. We achieve this by proposing a top-down[6] approach which differs from the bottom-up construct described in

[6]Here, by *top-down* we mean the initial model can be reduced to derive models containing less field variables. In contrast, a *bottom-up* approach starts with a model containing a few field variables, and can be transform into formulations with a

Miehe [2011]. The difference in perspective allows us to formulate multiphysics directly as optimization problems, where we optimize in time and space the cost function which is the addition of internal energy and dissipation potential of the system, constrained by the balance laws it must satisfy. In addition, a novel contribution of this work, is the derivation of different families of numerical solution strategies based on the VF itself. Furthermore, we show how these solution strategies can be linked to variants of the Newton method. But before moving forward, we need to introduce the required definitions we will use along this manuscript.

1.4 Definitions

Standard definitions for subjects involving multiphysics, coupled problems and numerical solution techniques is not the subject of consensus. Therefore, we present below the definitions considered in this work.

1.4.1 Multiphysics and coupled problems

The definitions in this subsection are mainly in line with the work of Keyes et al. [2013].

To start we consider as *multiphysics* phenomena in which more than one component is involved, each one following its own principles. Individual components can be different branches of Physics, different time or spatial scales, different discretizations or even different system of Partial Differential Equation (PDE)s. Therefore, individual branches of Physics, −which we refer as *uniphysics*− can compose a multiphysic problem. Moreover, there are two aspects of a multiphysic application, *algorithmic* and *architectural*. The *algorithmic* perspective accounts for the mathematical analysis and computational complexity, while the *architectural* is related to the software and hardware environments.

1.4.2 Coupling strength

Considering an *algorithmic perspective* as defined above, of a multiphysic application, the strength of the coupling may be different, from physical and algorithmic viewpoints. We emphasize that these two different types of strength coupling are independent of each other.

1.4.2.1 Physical coupling

To represent the idea of a physical coupling, we consider two stand-alone systems, $f_1(y_1) = 0$ and $f_2(y_2) = 0$. Each system represents a certain uniphysic application. However, in a more detailed analysis, we can infer both systems are influencing each other, in essence, they are coupled. But how exactly is that influence, is what leads us to define the different types of physical couplings.

Strong coupling:

A *strong coupling* is when both systems have a mutual influence which cannot be neglected through their respective variables. In essence,

$$\begin{bmatrix} f_1(y_1, y_2) \\ f_2(y_1, y_2) \end{bmatrix} = \begin{bmatrix} 0 \\ 0 \end{bmatrix} \tag{1.1}$$

higher number of them.

Weak coupling:

A *weak coupling* is when the influence between variables is not reciprocal, only one system influences significantly the other system. Thus, we have the following options

$$\begin{bmatrix} f_1(y_1) \\ f_2(y_1, y_2) \end{bmatrix} = \begin{bmatrix} 0 \\ 0 \end{bmatrix}; \qquad \begin{bmatrix} f_1(y_1, y_2) \\ f_2(y_1) \end{bmatrix} = \begin{bmatrix} 0 \\ 0 \end{bmatrix} \tag{1.2}$$

1.4.2.2 Algorithmic coupling

An *algorithmic coupling* is concerned with the solution procedure taken to solve the system of equations modeling the physical system. The solution is almost always obtained numerically through the use of computer programs. The selection of the system is a decision of the designer which despite of being guided by empirical knowledge is independent of the Physics. This is the reason behind the independence between *algorithmic* and *physical* couplings. Hence, an *algorithmic coupling* represents the relation between the unknowns used inside the algorithm in order to solve the system. We consider three different types of algorithmic coupling, *tight*, *moderate*, *loose*. For the moment we can consider the linear system of equations which the algorithm needs to solve.

$$\begin{bmatrix} \mathbb{F}_{11} & \mathbb{F}_{12} \\ \mathbb{F}_{21} & \mathbb{F}_{22} \end{bmatrix} \begin{bmatrix} \mathbb{Y}_1 \\ \mathbb{Y}_2 \end{bmatrix} = \begin{bmatrix} \mathbb{B}_1 \\ \mathbb{B}_2 \end{bmatrix} \tag{1.3}$$

where we are using the blackboard font to denote a system of equations represented by blocks.

Tight coupling:

A *tight coupling* stands for an algorithm which gives no special privilege to some unknowns over the others. It means that, if we look at all the unknowns of the problem at any step of the solution process, these are updated at the same time. In this case, the algorithm may solve the system of equations 1.3 or a similar system which gives an approximate solution. In essence, the algorithm solves a system which has the following form, where Y is the vector containing ALL the unknowns of the system.

$$\tilde{\mathbf{F}} Y = \tilde{\mathbf{B}} \tag{1.4}$$

moderate coupling:

A *moderate coupling* is an algorithm which partitions the system unknowns into different sets and solve them asynchronously under a feedback loop. The solution can lead to a similar solution as a tight coupling algorithm. This type of coupling requires a feedback or close loop between the different chosen partitions.

Loose coupling:

A *loose coupling* is also an algorithm which partitions the system unknowns into different sets and solve them asynchronously under an open loop.

In the paper of Keyes et al. [2013] only the *tight* and *loose* couplings are mentioned. However, in order to be more precise with the results of our work we have introduced the *moderate* coupling. We justify this by means of the dependency between variables as shown below.

Algorithmic dependencies Consider a system $\tilde{\mathbf{F}}(y_1, y_2)$ as shown in (1.3) as the best approximation of the system when solved iteratively. Independent of the specific form of $\tilde{\mathbf{F}}$, the algorithmic coupling of such system is **tight** and it can be observed through the implicit dependencies, in essence

$$\tilde{\mathbf{F}}\big(y_1, y_2\big) \equiv \tilde{\mathbf{F}}\big(y_1(y_2), y_2(y_1)\big) \qquad \textbf{Tight coupling} \tag{1.5}$$

both variables are considered equally important for the algorithm. However, we can benefit by turning the implicit dependencies into explicit ones. As an example, let only y_1 depend on y_2. Depending on the algorithmic, this imposes a change of dependencies which under a feedback loop may lead to the same result as those obtained by a tight algorithmic dependence (1.5). If this is the case the explicit dependence denotes a **moderate** coupling

$$\tilde{\mathbf{F}}\big(y_1, y_2\big) = \tilde{\mathbf{F}}\big(y_1(\tilde{y}_2), y_2\big) \qquad \textbf{moderate coupling} \tag{1.6}$$

However, if the system after a change of algorithmic dependencies is solved through an open loop it can lead to an approximation of the solution. In this case, the the coupling is **loose**

$$\tilde{\mathbf{F}}\big(y_1, y_2\big) \approx \tilde{\mathbf{F}}\big(y_1(\tilde{y}_2), y_2\big) \qquad \textbf{Loose coupling} \tag{1.7}$$

1.4.3 Domain Coupling

Domain coupling is another important classification for coupled problems. It concerns the spatial domain on which the coupling takes place. The domain coupling can be considered to be a *bulk coupling* or an *interface coupling*.

Bulk coupling :

Bulk coupling is when there exists two or more fields acting in the same domain arising from different types of Physics. As an example, the deformation of a structure when subjected to heat.

Interface coupling :

Interface coupling makes reference when there are two or more non-overlapping domains governed by different types of Physics. The different fields interact with each other at the interface of the contiguous domains. An example of interface coupling can be seen by the deformation of an object submerged in a liquid, which in turn modifies the behavior of the liquid surrounding it.

1.4.4 Numerical solutions

In the current literature, it appears there is not a unique consensus in the meaning of *preconditioner*, *solver* and *strategy*. We present below the adopted definition in this work.

1.4.4.1 Preconditioner

A *preconditioner*, as mentioned in Benzi [2002] refers to transforming a system like

$$\mathbf{T}\hat{\Delta}\mathbf{Y} = -\mathbf{R} \tag{1.8}$$

into another system with more favorable mathematical properties. We change the variables name to emphasize that the system we describe is discrete now, where $\mathbf{T}$ denotes the *tangent matrix* and $\mathbf{R}$

the *residual* of a system as described by the Newton method,[7]. This adjustment may allow solving (1.8) through a more stable process. Roughly speaking, the application of a preconditioner implies the following

$$\mathbf{T}\hat{\Delta}\mathbf{Y} = \mathbf{R} \qquad \underset{\text{preconditioner}}{\rightarrow} \qquad \tilde{\mathbf{T}}\hat{\Delta}\mathbf{Y} = \tilde{\mathbf{R}} \tag{1.9}$$

where the tilde ($\tilde{\cdot}$) indicates a change may have occurred in $\mathbf{T}$ and (not necessarily) the vector $\mathbf{R}$. There are cases when the preconditioner works on the system through blocks, −block preconditioner−. Some of these scenarios arise naturally when working with coupled problems, since such block preconditioners can help to partition the full-system into smaller problems, in the same way one thinks of multiphysics problems being decomposed into uniphysic problems. The fact that a preconditioner receives a system and outputs another system as shown in (1.9), highlights its "recursive" property, since we can connect as many preconditioners we want sequentially.

1.4.4.2 Solver

A *solver* is a numerical method whose task is to obtain the solution of a linear system like (1.8). In contrast with the preconditioner, after applying a solver we expect to get the unknown, in essence

$$\mathbf{T}\hat{\Delta}\mathbf{Y} = \mathbf{R} \qquad \underset{\text{solver}}{\rightarrow} \qquad \hat{\Delta}\mathbf{Y} \tag{1.10}$$

We will use the specific word "solver" instead of the more general "method" to do a concrete connection with the goal of the process, nevertheless, *method* might be used in order to not reiterate the word *solver* within a phrase. A characteristic of some solvers is that they may be embedded within a preconditioner implicitly.[8]. In such cases, the coupling between the embedded preconditioner and the solution process is so strong, that it's needed to think of them as a whole in order to define these solvers properly. That is why some types of solvers are often called *point preconditioners* [Sala and Heroux, 2005]. However, to be consistent with the definition above, we refer to this type of methods also as solvers.

1.4.4.3 Strategy

A *strategy* just like a solver, takes a linear system like (1.8) and obtains its solution. The difference with a *solver* is that a *strategy* is a composition of a preconditioner and a solver that are not mutually dependent. Basically, we can pick a preconditioner and select a solver as it suits us the best, or the other way around. In essence, one example might be

$$\mathbf{T}\hat{\Delta}\mathbf{Y} = \mathbf{R} \quad \overbrace{\underset{\text{preconditioner}}{\rightarrow} \qquad \tilde{\mathbf{T}}\hat{\Delta}\mathbf{Y} = \tilde{\mathbf{R}} \qquad \underset{\text{solver}}{\rightarrow}}^{\text{strategy}} \quad \hat{\Delta}\mathbf{Y} \tag{1.11}$$

It is precisely this composition which allows different authors to refer at a *strategy* like a synonym for preconditioner or solver. However, we emphasis on the distinction due to the following. A strategy, can take a preconditioner (or several preconditioners) and output the unknown through the use of different solvers if desired. Notice that defining a strategy as a composition, allows to define a *strategy* even through the composition of other strategies. This property of the strategies is explained through the "recursivity" of the preconditioners, creating thus a whole family of techniques to solve a linear system. A strategy gives in a sense more malleability to the solution process of a system, as shown in the works of Gee et al. [2010], Verdugo and Wall [2016]. Furthermore, in the case when we use a solver directly without preconditioning the system, a *strategy* and a *solver* are equivalent, we only have to think that *strategy* is using the identity

[7] as previously stated, this numerical method is a point of comparison along this work

[8] sometimes refer as *splitting*, e.g. [Strang, 2007, §7]

matrix as a preconditioner.

Before moving to the current preconditioners, solvers and strategies used in the literature, we summarize the above through the table (1.1). This table shows the main difference between numerical methods aiming to solve linear(ized) systems like that on (1.8). Figure 1.1 depicts graphically the relation

Method	Input	Output	Objective
Preconditioner	$\mathbf{T}\hat{\Delta}\mathbf{Y} = \mathbf{R}$	$\tilde{\mathbf{T}}\hat{\Delta}\mathbf{Y} = \tilde{\mathbf{R}}$	Reduces computational cost of the system to solve.
Solver	$\mathbf{T}\hat{\Delta}\mathbf{Y} = \mathbf{R}$	$\hat{\Delta}\mathbf{Y}$	Numerical method to solve a complete or partial system. Computational cost is fixed.
Strategy	$\mathbf{T}\hat{\Delta}\mathbf{Y} = \mathbf{R}$	$\hat{\Delta}\mathbf{Y}$	Defines an algorithm to solve the system by composition of solvers, preconditioners and even more strategies.

Table 1.1: Difference between numerical methods aiming to solve $Ax = b$

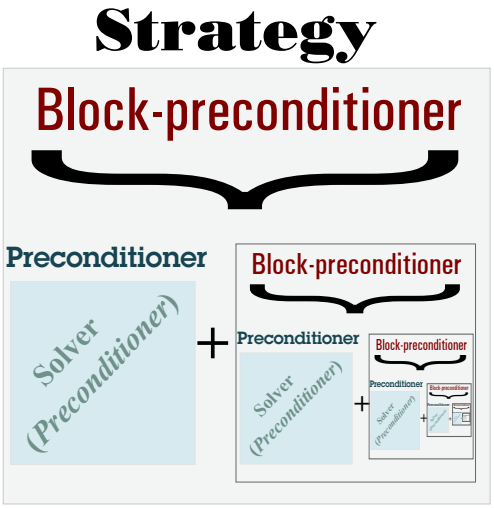

Figure 1.1: Relation between preconditioners, solvers, and strategy

1.5 What to expect from this research

1.5.1 Objectives

We conclude this chapter by taking up the goal of this work. We focus on multiphysic problems due to the current important applications[9] and the theoretical perspective in Physics this subject involves. We settle our work in the framework of variational form (VF) as a starting point for our models, fruitful among others for building new models and designing numerical strategies. The specifics of the multiphysic phenomena we are interested concerns the use of different fields of Physics which are coupled through the bulk and/or interface of the domain. We deal with the *algorithmic perspective* of the problem. The strength of the physical couplings we use is *strong* and *weak* and the algorithmic couplings explored are *tight*, *moderate* and *loose*. The aim is the development of a generic VF for multiphysic problems and the derivation of different solution strategies which can help to reduce the computational cost of the solution process and provide a further insight to the subject.

1.5.2 Structure of the document

In this introductory chapter we laid down the motivation and key ideas to be used in this research. The next chapter contains some of the generalities for the modeling and computation of multiphysic problems. We start in §2.1 by showing some notation and some basic results from Calculus of Variations (CoV) as a main mathematical tool for variational principles. Afterward, the notation which will be used for Finite Element Method (FEM) is laid down since it is the technique we use to transform the model from a continuum to a discrete setting in order to solve it numerically. We also introduce the Newton method as the initial technique to start the solution of our models and from which we will reduce its computational cost using the proposed solution strategies in this work. We conclude chapter §2 with a review of numerical strategies, where we also establish some of their properties. These initial chapters provide the general knowledge needed in order to follow up the ideas that are presented in the consequent chapters.

Chapters §3, §4 and §5 concern the mathematical modeling while chapter §6 is devoted to the solution strategies of the models proposed. Chapter §3 presents the multifield problem of chemical diffusion, for which mixed formulations can be derived and hence be treated as a multiphysic problem. In here we present some key concepts and procedures useful to abstract the problem and extrapolate it into a generic formulation. As a consequence, chapter §4 presents a generic VF for multiphysic problems. At the end of the chapter we apply the general formulation into the direction of electrochemistry. Chapter §5 makes use of that result to develop a concrete VF model for a lithium-ion battery cell from current theories in the literature. Finally, chapter §6 proposes a family of solution strategies derivable from the proposed VF. The proposed strategies are defined and analyzed in this chapter. We conclude in chapter §7 with a brief summary of the ideas presented, highlighting the contributions of this work and present a possible outlook of the work which can be followed based on this research.

[9] as lithium-ion batteries

Chapter 2

Generalities for the modeling and computation of multiphysic problems

Sommaire

Dans ce deuxième chapitre, nous présentons les notations à utiliser tout au long du document, nous fournissons le cadre sur lequel nous allons travailler et nous présentons une revue des stratégies numériques de pointe en la matière. Dans l'examen des stratégies numériques, compte tenu du fait qu'il n'existe pas de concepts globaux unanimes, nous fournissons des définitions qui nous aideront à mettre en évidence certains des résultats que nous présenterons dans les chapitres suivants.

In this chapter we present the basics of Calculus of Variations (CoV), Finite Element Method (FEM) and numerical solutions strategies since these are the main tools we us in this work. We start with CoV as it is the core instrument when dealing with variational principles which allow us to construct the mathematical models. Once we derived the models we solve them numerically, we have chosen a classical approach to FEM to move the problems from a continuous to a discrete setting and set the *Newton method* as the solution approach towards all the solution strategies we propose will direct at. We conclude the chapter with a review on numerical strategies, where we propose a set of attributes which will help us to categorize the strategies proposed and revised in this work.

2.1 Calculus of variations : Variational framework

Calculus of Variations (CoV) is the main mathematical tool used when we talk about variational principles. Since our framework is that of variational principles, we explore the notation to be used and the basics of CoV.

2.1.1 Notation

Functional and integrand Consider the fields c & μ. We denote the dependence on the fields (c, μ) of a *functional* Π with square brackets as $\Pi[c, \mu]$, where we refer to π as the *integrand* of the functional Π

.

$$\Pi[c,\mu] = \int_\Omega \pi(c,\mu) dV \tag{2.1}$$

Partial derivatives *Partial derivatives* of a function will be presented in the following form

$$\pi_\mu = \frac{\partial \pi}{\partial \mu} \qquad\qquad \pi_{\mu c} = \frac{\partial \pi}{\partial c \partial \mu}$$

Variations A *variation* is denoted with δ. We add a subindex indicating the field it applies the variation to when necessary. When applied to a functional, the variation can be written as

$$\delta_c \Pi \equiv \frac{\delta \Pi}{\delta c} \equiv \delta_c \Pi[c,\mu] = \delta_c \int_\Omega \pi(c,\mu) dV = \int_\Omega \delta_c \pi(c,\mu) dV \tag{2.2}$$

where we have use the commutative property of the variation with the integral [Lanczos, 1949, chap 2.9].

When a functional depends on a variable but it does not depends on its spatial derivatives we say the variable is a *local field*. Instead, when there exists a dependence of the functional in at least one of the spatial derivatives, the variable is considered to be a *global field*. On the one hand, if the variation of a *local field* is applied to a function we write it as

$$\delta_c \pi(c,\mu) \equiv \partial_c \pi(c,\mu) \delta c \equiv \frac{\partial}{\partial c} \pi(c,\mu) \delta c \tag{2.3}$$

On the other hand, when the variation of a *global field* is applied to a function we have the following expressions

$$\delta_\mu \Pi[c,\mu;\nabla\mu] \equiv \frac{\delta}{\delta \mu} \Pi[c,\mu;\nabla\mu] \qquad \text{variation Functional} \tag{2.4a}$$

$$\int_\Omega \delta_\mu \pi(c,\mu,\nabla\mu) d\Omega = \int_\Omega \frac{\delta \pi}{\delta \mu} dV \qquad \text{variation integrand} \tag{2.4b}$$

$$= \int_\Omega \left[\frac{\partial \pi}{\partial \mu} \delta\mu + \frac{\partial \pi}{\partial \nabla \mu} \cdot \delta \nabla \mu \right] dV \qquad \text{variation PD} \tag{2.4c}$$

$$\equiv \int_\Omega \left[\frac{\partial \pi}{\partial \mu} \delta\mu + \frac{\partial \pi}{\partial \mu_{,i}} \delta\mu_{,i} \right] d\Omega \qquad \text{index notation} \tag{2.4d}$$

Finally we refer to the *variational derivative* with the expression

$$\langle \delta_\mu \Pi \,|\, \delta\mu \rangle \equiv \int_\Omega \left[\frac{\partial \pi}{\partial \mu} + \nabla \cdot \frac{\partial \pi}{\partial \nabla \mu} \right] \delta\mu d\Omega - \int_{\partial\Omega} \left[\frac{\partial \pi}{\partial \nabla \mu} \cdot \vec{n} \right] \delta\mu dS$$

where $\vec{n}$ is the unit outer vector of the domain.

2.1.2 Basics of calculus of variations

As mentioned in [Courant and Hilbert, 1989, §4], the origin of calculus of variations and its "simplest problem" is to determine the minimum of an integral. This is at some level, the same problem we are going to tackle in this research. Indeed, a physical problem can be recasted into a mathematical statement, which in order to be solved requires to seek the minimal or/and maximal value of an integral. Thus, we need to know some of the basic tools from calculus of variations.

2.1.2.1 Variations

A variation is an infinitesimal change in a function output. Formally this concept can be described as follows. Consider a function $\mu(x) \in \mathbb{V}_\mu$ which satisfies the boundary conditions and the requirements of differentiability and continuity. A perturbation of this function $\mu_p(x)$, being defined as follows

$$\mu_p(x) := \mu(x) + \epsilon\eta(x)$$

where $\eta(x) \in \mathbb{V}_\eta$ is any function with compact support satisfying also differentiability and continuity requirements, and ϵ is any number such that $\epsilon > 0$. From the perturbation, we can say that if ϵ is an infinitesimal, then we can define $\mu(x)$ variation's $\delta\mu(x)$ as

$$\delta\mu(x) := \epsilon\eta(x) \qquad \rightarrow \qquad \delta\mu(x) = \mu_p(x) - \mu(x)$$

The expression above defines the idea of a *variation* in calculus of variations. As mentioned, it is an infinitesimal change in the output of $\mu(x)$ in this case, disconnected from any increment dx.

In the case where Dirichlet boundary conditions $\partial_D\Omega$ are imposed in a problem, the variation must vanish in that boundary, in essence, $\delta\mu = 0 \quad \forall \quad x \in \partial_D\Omega$. Some properties of the variation which follow from the definition and we are going to use are presented below.

Permutability with differentiation The *permutability with differentiation* of the variation, states the following.

$$\delta\left(\frac{d}{dx}\mu\right) = \frac{d}{dx}\Big(\delta\mu\Big) \tag{2.5}$$

This arises from the definition, as shown below

$$\delta\left(\frac{d}{dx}\mu\right) = \delta\mu'(x) = \mu'_p(x) - \mu'(x) = \epsilon\eta'(x) \qquad \& \qquad \frac{d}{dx}\Big(\delta\mu\Big) = \frac{d}{dx}\Big(\epsilon\eta(x)\Big) = \epsilon\eta'(x) \tag{2.6}$$

Permutability with integration Similarly, the *permutability with integration* of the variation, states the following.

$$\delta\int_\Omega \mu(x)d\Omega = \int_\Omega \delta\mu(x)d\Omega \tag{2.7}$$

because

$$\delta\int_\Omega \mu(x)d\Omega = \int_\Omega \mu_p(x)d\Omega - \int_\Omega \mu(x)d\Omega = \int_\Omega \mu_p(x) - \mu(x)d\Omega = \int_\Omega \delta\mu(x)d\Omega \tag{2.8}$$

The properties above rely on the fact that the domain Ω is fixed, in essence, independent of μ.

2.1.2.2 The Gâteaux variation

The idea of a variation has its impact when we are dealing with functions whose arguments are also functions. Take as an example a function $\pi(\mu)$, dependent of $\mu(x)$. Hence, we can think on how will π change if we allow $\mu(x)$ to change a little bit. In this case, the usual idea of the derivative will not hold, because $\mu(x)$ is also a function, but instead, we can benefit of the concept of a variation.

The *Gâteaux variation* [Simo and Hughes, 2000], whose definition is closely related to that of the directional derivative in the usual calculus, allows to address the question regarding the change of $\pi(\mu)$. The definition of the *Gâteaux variation* is the following

$$\delta\pi[\mu](\eta) := \lim_{\epsilon\to 0} \frac{\pi(\mu+\delta\mu)-\pi(\mu)}{\epsilon} = \frac{d}{d\epsilon}\pi(\mu+\delta\mu)\Big|_{\epsilon=0} \tag{2.9}$$

where as before η needs to belong to the same space $\mathbb{V}$ as μ, and ϵ is defined as a positive infinitesimal. Both representation of the Gâteaux variation are useful for us. With the first one, we can explain the necessary condition for the functional to have an stationary point (maximum,minimum), whilst with the second, we can reach more concrete computations of the variations in terms of partial derivatives. We start with a necessary condition for a functional to have an extremum.

Functional Optimization condition

As mentioned earlier, we are interested in the optimization of a functional. Thus, let $\Pi[\mu]$ be the integral with integrand π, thus depending on the function $\mu(x)$ over a domain $\Omega \subset \mathbb{R}^3$. If μ^* is the function which gives a minimum on $\Pi[\mu]$, hence we have the following conditions

$$\Pi[\mu^*+\epsilon\eta]-\Pi[\mu^*] \geq 0 \quad \forall\epsilon>0 \qquad \& \qquad \Pi[\mu^*+\epsilon\eta]-\Pi[\mu^*] \leq 0 \quad \forall\epsilon<0 \tag{2.10}$$

Thus, applying the *Gâteaux variation* to the functional $\Pi(\mu^*)$ defines a condition for the extremum

$$\lim_{\epsilon\to 0}\frac{\Pi[\mu^*+\epsilon\eta]-\Pi[\mu^*]}{\epsilon} = \delta\Pi[\mu^*](\eta) \equiv 0$$

The equation above states, that in order to find the extremum of the functional $\Pi[\mu]$, its *Gâteaux variation* $\delta\Pi[\mu](\eta)$ must be zero.

To make things more clear, we use a specific definition for Π which we will encounter commonly along this research. Consider the following definition for Π where it depends on μ and its gradient $\nabla\mu$

$$\Pi[\mu] = \int_\Omega \pi(\mu,\nabla\mu)dV \qquad \text{such that} \qquad \Pi[\mu+\delta\mu] = \int_\Omega \pi(\mu+\delta\mu,\nabla\mu+\delta\nabla\mu)dV$$

we would like to know the value of μ such that the optimal condition for Π is reached. Using what has been presented so far, we can arrive to the following expression

$$\begin{aligned}
\delta\Pi[\mu](\eta) &= \delta_\eta\left(\int_\Omega \pi(\mu,\nabla\mu)dV\right) \\
&= \int_\Omega \delta_\eta\pi(\mu,\nabla\mu)dV && \because \quad (2.7) \\
&= \int_\Omega \frac{d}{d\epsilon}\pi(\mu+\epsilon\eta,\nabla\mu+\epsilon\nabla\eta)\Big|_{\epsilon=0} dV && \because \quad (2.9.2) \\
&= \int_\Omega \left[\frac{\partial\pi}{\partial(\mu+\epsilon\eta)}\eta + \frac{\partial\pi}{\partial(\nabla\mu+\epsilon\nabla\eta)}\cdot\nabla\eta\right]\Big|_{\epsilon=0} dV && \because \quad \text{(chain rule)} \\
&= \int_\Omega \left[\frac{\partial\pi}{\partial\mu}\eta + \frac{\partial\pi}{\partial\nabla\mu}\cdot\nabla\eta\right] dV && \because \quad \epsilon=0 \qquad (2.11)
\end{aligned}$$

This expression, represents the Gâteaux variation in terms of partial derivatives of the integrand π from the functional Π and the corresponding derivatives of η

2.1.2.3 The functional first variation

Once we have a functional like $\Pi[\mu]$, the *functional first variation*[1], is an element of the dual space $\frac{\delta\pi}{\delta\mu} \in \mathbb{V}^*$ such that the following relation with the Gâteaux variation holds

$$\delta\Pi[\mu](\eta) := \int_\Omega \left[\frac{\partial\pi}{\partial\mu} - \nabla\cdot\left(\frac{\partial\pi}{\partial\nabla\mu}\right)\right]\eta d\Omega \tag{2.12}$$

as higlighted in Simo and Hughes [2000], the expression for the *functional first variation* can be obtained through the use of integration by parts into the Gâteaux variation as follows. Using integration by parts in the last term of (2.11), and in a second step the divergence theorem we arrive to

$$\int_\Omega \left[\frac{\partial\pi}{\partial\nabla\mu}\cdot\nabla\eta\right] dV = \int_\Omega \nabla\cdot\left[\frac{\partial\pi}{\partial\nabla\mu}\eta\right] dV - \int_\Omega \left[\nabla\cdot\left(\frac{\partial\pi}{\partial\nabla\mu}\right)\eta\right] dV \tag{2.13}$$

$$= -\int_\Omega \left[\nabla\cdot\left(\frac{\partial\pi}{\partial\nabla\mu}\right)\eta\right] dV + \int_{\partial\Omega}\left[\frac{\partial\pi}{\partial\nabla\mu}\cdot\vec{n}\right]\eta dS \tag{2.14}$$

where $\partial_D\Omega$ stands for the Dirichlet boundary of the domain Ω, and $\vec{n}$ is the unit normal vector pointing outwards of the boundary $\partial_D\Omega$. Substituting the latter into (2.11) leads to

$$\delta\Pi[\mu](\eta) = \int_\Omega \left[\frac{\partial\pi}{\partial\mu} - \nabla\cdot\left(\frac{\partial\pi}{\partial\nabla\mu}\right)\right]\eta d\Omega + \int_{\partial_D\Omega}\left[\frac{\partial\pi}{\partial\nabla\mu}\cdot\vec{n}\right]\eta dS \tag{2.15}$$

where the boundary term vanishes, because the variation at the Dirichlet boundary is zero. Therefore, we have

$$\delta\Pi[\mu](\eta) = \int_\Omega \left[\frac{\partial\pi}{\partial\mu} - \nabla\cdot\left(\frac{\partial\pi}{\partial\nabla\mu}\right)\right]\eta d\Omega \tag{2.16}$$

From above, we get the expression for functional derivative of $\Pi[\mu]$

$$\frac{\delta\Pi}{\delta\mu} := \int_\Omega \left[\frac{\partial\pi}{\partial\mu} - \nabla\cdot\left(\frac{\partial\pi}{\partial\nabla\mu}\right)\right] d\Omega \tag{2.17}$$

Notice that due to the *fundamental lemma of calculus of variations* Courant and Hilbert [1989] the functional Π reaches a stationary condition when its first variation is equal to zero. This special condition defines the so-called *Euler-Lagrange* equations [Courant and Hilbert, 1989, Simo and Hughes, 2000].

In the following chapters we will use the first variation to establish an equivalence between different formulations. In specific, we reach an equivalence with the strong form by means of the Fréchet derivative, and with the weak form via the Gâteaux variation. The case of the *Euler-Lagrange* equation (2.17), makes the equivalence with the *strong form* of the problem, whilst the equation (2.11) with the *weak form*. Furthermore, notice that in the special case were the functional Π does not depend on the derivatives of $\mu(\vec{x})$, hence, the first variation is equivalent to the integral over Ω of the partial derivative $\frac{\partial\pi}{\partial\mu}$.

2.1.2.4 The functional second variation

With the results of the *functional first variation* we obtain a stationary condition, a extremum. Nevertheless, we do not know if the extremum is a minimum, a maximum or a saddle point. In an analogy

[1] also known as the *functional derivative*, or Fréchet derivative, Demanet [2015]

with standard calculus, we can use the *functional second variation*[2] to get an answer. Once we have obtained the *functional first variation*, the *functional second variation* can be obtained under proper smooth conditions of the functional, as follows

$$\begin{aligned}\delta\Big(\delta\Pi[\mu](\eta_1)\Big)(\eta_2) &= \lim_{\epsilon\to 0}\frac{\delta}{\delta\mu}\left[\frac{\Pi[\mu+\epsilon\eta_1]-\Pi[\mu]}{\epsilon}\right](\eta_2)\\ &= \lim_{\epsilon\to 0}\frac{\delta}{\delta\mu}\left[\frac{\Pi[\mu+\epsilon(\eta_1+\eta_2)]-\Pi[\mu+\epsilon\eta_1]-\Pi[\mu+\epsilon\eta_2]+\Pi[\mu]}{\epsilon}\right]\\ &= \frac{\delta^2}{\delta\mu\delta\mu}\Pi[\mu] \end{aligned} \tag{2.18}$$

Before finishing this section, we present a notation which turns out to be fruitful while dealing with the solution of our problems.

2.1.2.5 Algebraic form of variations

We use the tools from calculus of variations to be able to represent and solve the multiphysic problem at hand. As it will be clarified below, after some discretization the problem can be turned into an algebraic system of equations by means of the Newton method (linearization). This algebraic system of equations can be better understood through the right notation. A depiction of the system of equations we are going to be dealing with will have the following block form considering m physical fields.

$$\begin{bmatrix}\mathbb{A}_{11} & \mathbb{A}_{12} & \dots & \mathbb{A}_{1m}\\ \mathbb{A}_{21} & \mathbb{A}_{22} & \dots & \mathbb{A}_{2m}\\ \vdots & \vdots & \ddots & \vdots\\ \mathbb{A}_{m1} & \mathbb{A}_{m2} & \dots & \mathbb{A}_{mm}\end{bmatrix}\begin{bmatrix}\hat{\Delta}\mathbb{X}_1\\ \hat{\Delta}\mathbb{X}_2\\ \vdots\\ \hat{\Delta}\mathbb{X}_m\end{bmatrix} = -\begin{bmatrix}\mathbb{B}_1\\ \mathbb{B}_2\\ \vdots\\ \mathbb{B}_m\end{bmatrix} \tag{2.19}$$

when applying the Newton method, we will see the blocks $\mathbb{B}$ correspond to the first variations of our functional and the blocks $\mathbb{A}$ to the second variations. Thus, instead of using a subindex to denote the position of the blocks, we use the variation of the field which has taken place. This change, besides helping locate the blocks, adds the functionality of giving a direct physical interpretation. For a functional Π dependent upon m fields x_i with $0 < i \leq m$, we use the following notation to relate the blocks to the corresponding variation

$$\Pi_{x_i} := \frac{\delta}{\delta x_i}\Pi[x_1, x_2, \dots, x_m] \qquad \to \qquad \text{first variation} \tag{2.20a}$$

$$\Pi_{x_j x_i} := \frac{\delta^2}{\delta x_j \delta x_i}\Pi[x_1, x_2, \dots, x_m] \qquad \to \qquad \text{second variation} \tag{2.20b}$$

As an example, consider the functional $\Pi[\mu, c]$, which we will encounter in §3. In this case, the matrix form obtained by the Newton method, will be given by

$$\begin{bmatrix}\Pi_{\mu\mu} & \Pi_{\mu c}\\ \Pi_{c\mu} & \Pi_{cc}\end{bmatrix}\begin{bmatrix}\hat{\Delta}\mu\\ \hat{\Delta}c\end{bmatrix} = -\begin{bmatrix}\Pi_{\mu}\\ \Pi_{c}\end{bmatrix} \tag{2.21}$$

To see that the block diagonal of the Matrix holds the uncoupled system and the off-diagonal section the coupling becomes evident with this notation. Moreover, since the integrand is continuos for c and μ the off-diagonal elements satisfy $\Pi_{\mu c} = \Pi_{c\mu}$. We now conclude the section on calculus of variations and the mathematical tools which are required to follow this text. For more information on the topic of calculus of variations, please confer to Lanczos [1949], Courant and Hilbert [1989], Simo and Hughes [2000].

[2] also known as the *Hessian* or the *Fréchet Hessian* ,Demanet [2015]

2.2 Finite Element discretization of the variational principle

Analytical solutions of mathematical models are often difficult and scarce, variational models are not the exception. Therefore, the models are solved through numerical methods. This often implies the change of the problem from a continuum setting to a discrete one. One of the most successful methods for this endeavor is the Finite Element Method. This is the technique we use in this work. Good references for this topic can be found in Strang and Fix [2008], Brenner and Scott [2013], Bergheau and Fortunier [2010] & Donea and Huerta [2003]. This section presents the notation we used for it in this work.

We can use the FEM to approximate a field μ as

$$\mu(\vec{x},t) \approx \bigcup_{\forall a} \mu^{(a)}(t) S_\mu^{(a)}(\vec{x}) \tag{2.22}$$

where the index (a) stands for a node in the discrete domain, and $S_\mu^{(a)}(\vec{x})$ refers to the shape function associated to μ defined at the node (a).

We denote the rate of change at a node (a) of the approximate field and also to its gradient as

$$\frac{\delta\mu}{\delta\mu^{(a)}} = S_\mu^{(a)}(\vec{x}); \qquad\qquad \frac{\delta\nabla\mu}{\delta\mu^{(a)}} = \nabla S_\mu^{(a)}(\vec{x}) \tag{2.23}$$

When we apply a variation to a field which is FEM discrete as in (2.22), we specify the variation at a node (a) as

$$\begin{aligned}\frac{\delta\Pi}{\delta\mu^{(a)}} &= \int_\Omega \left[\frac{\partial\pi}{\partial\mu}\frac{\delta\mu}{\delta\mu^{(a)}} + \frac{\partial\pi}{\partial\nabla\mu}\cdot\frac{\delta\nabla\mu}{\delta\mu^{(a)}}\right] d\Omega \\ &= \int_\Omega \left[\frac{\partial\pi}{\partial\mu}S_\mu^{(a)} + \frac{\partial\pi}{\partial\nabla\mu}\cdot\nabla S_\mu^{(a)}\right] d\Omega\end{aligned}$$

as an example, by applying a second variation we get the element matrices

$$\frac{\delta^2\Pi}{\delta c^{(b)}\delta\mu^{(a)}} = \int_\Omega \left[\left(\frac{\partial^2\pi}{\partial c\partial\mu}S_\mu^{(a)}S_c^{(a)}\right) + \left(\frac{\partial^2\pi}{\partial c\partial\nabla\mu}\cdot\nabla S_\mu^{(a)}S_c^{(a)}\right)\right] dV$$

In the context of FEM, we use the following shorthand. For vectors we have

$$\mathbb{S}_\mu^{(a)}\Big(\pi_\mu\Big) \equiv \int_\Omega \left[\frac{\partial\pi}{\partial\mu}\frac{\partial\mu}{\partial\mu^{(a)}}\right] d\Omega = \int_\Omega \left[\frac{\partial\pi}{\partial\mu}S_\mu^{(a)}\right] d\Omega \tag{2.24a}$$

$$\nabla\mathbb{S}_\mu^{(a)}\Big(\pi_{\nabla\mu}\Big) \equiv \int_\Omega \left[\frac{\partial\pi}{\partial\nabla\mu}\frac{\partial\mu}{\partial\mu^{(a)}}\right] d\Omega = \int_\Omega \left[\frac{\partial\pi}{\partial\mu}\nabla S_\mu^{(a)}\right] d\Omega \tag{2.24b}$$

where we use $\mathbb{S}_\mu$ to denote the shape function to be used in that integral. For matrices we have

$$\mathbb{M}_{c\mu}^{(a,b)}\Big(\pi(c,\mu)\Big) = \int_\Omega \left[\frac{\partial^2\pi}{\partial\mu\partial c}S_c^{(a)}S_\mu^{(b)}\right] dV \qquad \textbf{Mass Matrix} \tag{2.25a}$$

$$\mathbb{K}_{c\mu}^{(a,b)}\Big(\pi(c,\mu)\Big) = \int_\Omega \left[\frac{\partial^2\pi}{\partial\mu\partial c} : \nabla S_c^{(a)} \otimes \nabla S_\mu^{(b)}\right] dV \qquad \textbf{Stiffness Matrix} \tag{2.25b}$$

$$\mathbb{C}_{c\mu}^{(a,b)}\Big(\pi(c,\mu)\Big) = \int_\Omega \left[\frac{\partial^2\pi}{\partial\mu\partial c} \cdot \nabla S_c^{(a)}S_\mu^{(b)}\right] dV \qquad \textbf{Coupling Matrix} \tag{2.25c}$$

where as shown above, we choose the variable according with the name the matrix is popularly known in mechanics.

2.3 Numerical solution approach

As mentioned, the FEM takes the VF model from a continuum to a discrete setting. As with all variational problems, the solution of problem becomes an optimization problem. Thus, we need to solve numerically a problem having the following form

$$\nabla\boldsymbol{\pi} \equiv \frac{\partial\boldsymbol{\pi}}{\partial\mathbf{Y}} = \mathbf{0} \qquad \text{with} \qquad \nabla\boldsymbol{\pi} := \begin{bmatrix} \nabla\pi_1(\mathbf{y}_1, \mathbf{y}_2, \dots \mathbf{y}_N) \\ \nabla\pi_2(\mathbf{y}_1, \mathbf{y}_2, \dots \mathbf{y}_N) \\ \vdots \\ \nabla\pi_N(\mathbf{y}_1, \mathbf{y}_2, \dots \mathbf{y}_N) \end{bmatrix}; \quad \mathbf{Y} := \begin{bmatrix} \mathbf{y}_1 \\ \mathbf{y}_2 \\ \vdots \\ \mathbf{y}_N \end{bmatrix}; \tag{2.26}$$

where the elements of $\nabla\boldsymbol{\pi}$ correspond to the discrete system of equations modeling the problem, thus, $\nabla\boldsymbol{\pi}$ represents the optimal condition of the variational problem and the elements of $\mathbf{Y}$ are the unknown fields. Since we are allowing $\boldsymbol{\pi}$ to be nonlinear, we use the well known iterative Newton Method [3], [Strang, 2007, §2.6] to solve the discrete optimal problem.

2.3.1 Optimization problem : Newton method for variational problems

As it will be detailed in the next chapters, a classical discretization of a variational form, leads to a set of nonlinear algebraic equations to be solved at each time step. In resemblance to what it is shown in [Verdugo and Wall, 2016, §2] for problems under a strong form, we briefly detailed the Newton method applied to a variational formulation. In this context, the problem to solve becomes

$$\mathbf{Y}^{n+1} = \hat{\Delta}\mathbf{Y}^n + \mathbf{Y}^n \qquad \text{with} \qquad \hat{\Delta}\mathbf{Y}^n := \mathbf{Y}^{n+1} - \mathbf{Y}^n \tag{2.27}$$

where the symbol $\hat{\Delta}$ corresponds to the iteration operator. The unknown $\hat{\Delta}\mathbf{Y}$ is being evaluated at the iteration n through the matrix problem

$$\mathbf{T}^n\hat{\Delta}\mathbf{Y}^n = -\mathbf{R}^n \qquad \text{with} \qquad \mathbf{T} := \left[\frac{\partial^2\boldsymbol{\pi}}{\partial\mathbf{Y}^2}\right]; \quad \mathbf{R} := \left[\frac{\partial\boldsymbol{\pi}}{\partial\mathbf{Y}}\right] \tag{2.28}$$

the symbol $\mathbf{R}$ stands for the residual and $\mathbf{T}$ for the tangent. Under a variational framework those two terms can be interpreted correspondingly as the *optimal conditions* and the *Hessian* of the variational problem. In a closer look to (2.28) we need to solve at each iteration n the following system

$$\begin{bmatrix} \frac{\partial^2\pi_1}{\partial\mathbf{y}_1^2} & \frac{\partial^2\pi_1}{\partial\mathbf{y}_1\partial\mathbf{y}_2} & \cdots & \frac{\partial^2\pi_1}{\partial\mathbf{y}_1\partial\mathbf{y}_N} \\ \frac{\partial^2\pi_2}{\partial\mathbf{y}_1\partial\mathbf{y}_2} & \frac{\partial^2\pi_2}{\partial\mathbf{y}_2^2} & \cdots & \frac{\partial^2\pi_2}{\partial\mathbf{y}_2\partial\mathbf{y}_N} \\ \vdots & \vdots & \ddots & \vdots \\ \frac{\partial^2\pi_N}{\partial\mathbf{y}_N\partial\mathbf{y}_1} & \frac{\partial^2\pi_N}{\partial\mathbf{y}_N\partial\mathbf{y}_2} & \cdots & \frac{\partial^2\pi_N}{\partial\mathbf{y}_N^2} \end{bmatrix} \begin{bmatrix} \hat{\Delta}\mathbf{y}_1 \\ \hat{\Delta}\mathbf{y}_2 \\ \vdots \\ \hat{\Delta}\mathbf{y}_N \end{bmatrix} = - \begin{bmatrix} \frac{\partial\pi_1}{\partial\mathbf{y}_1} \\ \frac{\partial\pi_2}{\partial\mathbf{y}_2} \\ \vdots \\ \frac{\partial\pi_N}{\partial\mathbf{y}_N} \end{bmatrix} \tag{2.29}$$

The process above describes the classical process of the Newton method. Nevertheless there exist several variants which can be classified into different classes, mainly: the *damped-Newton methods*, the *modified Newton methods* and the *Newton-like methods*, each one having sub-classes on its own. We are specially interested on a couple of subclasses of the latter *Newton-like methods*: the *inexact Newton methods* [Dembo et al., 1982] and the *Quasi-Newton methods* [J. E. Dennis and Moré, 1977]. These two subclasses are important because the numerical strategies we propose in this work fall within these categories.

[3] see Deuflhard [2005] for a deep analysis of the methods in different family of problems

The Newton method turns the nonlinear optimization problem (2.26) into a linearised problem $\mathbf{T}\hat{\Delta}\mathbf{Y} = -\mathbf{R}$ (2.28). Nevertheless, the price paid is to solve a big system of equations per iteration, therefore, economic methods to solve (2.28) are required. It is at this point where we turn our attention towards preconditioners, solvers and strategies. We will explore this direction in §6. For a quick overview of the classes related to the Newton method mentioned above and some references, as well as a review of the convergence properties, error stimates, numerical stability and computational complexity of the Newton method in general settings, one can refeer to Galántai [2000]. A study of the affine invariance of the Newton method is shown in Deuflhard [2005], and finally an interesting geometrical approach for the complex Newton method, can be found Yau and Ben-Israel [1998].

2.3.2 Review on numerical strategies

In this work we also derive different solution strategies for the general VF we propose, all of them leading or be defined as variations of the Newton method. Therefore, this section presents a review on concepts related to numerical strategies from current literature. However, we do not aim to give a complete analysis of the state of the art. As mentioned, the definitions pertaining to numerical solutions introduced in this manuscript are not directly tied to a specific work but rather to several, due to the lack of standardized definitions. In addition, we go in depth into the concepts and mention some methods used to highlight some properties. Some new concepts are also proposed and defined when consider relevant for the sake of clarity within this work.

2.3.2.1 Preconditioners

As mentioned in [Allaire and Kaber, 2007, §5.3.5], the task to find good preconditioners is difficult and there is no universal solution for it. It is therefore hard to find a consensus on how the preconditioners must be classified. A comprehensive attempt is done at Chen [2005] but as highlighted in Wathen [2006] in the review of Chen's book, "A good preconditioning book not geared to a particular application area is therefore hard to write". Thus, below we focus on a few preconditioners which target coupled problems. Specially in the so-called *partitioned approaches*.

Roughly speaking, a *partitioned approach* is the block-preconditioning of a coupled system in order to decompose it into different smaller subproblems (usually fields corresponding to uniphysics). The partitioning may be physically or mathematically based. When the partitioning is physically based, the subproblems are usually related with a reductionist perspective of the coupled problem, in essence, with the single field-problems. This technique −may− allow the use of standard solvers available for the single field-problems [Keyes et al., 2013]. If the partitioning is mathematically based, as shown in the work of Verdugo and Wall [2016], generic preconditioners can be developed independently of the type of Physics we are dealing with. As mentioned "[the issue in] preconditioning essentially comes down to whether one is *given a problem* or *given a matrix*"[4]. Physically based preconditioners require an insight of the problem to solve, while mathematically based, an insight of the matrix. We explore a few of those approaches below.

Mathematically-based:

Algebraic preconditioners: *Algebraic preconditioners* are understood as matrices that help at system of equations like (2.28) to ease the solution's computation. This type of

[4] Quote credited to M. Neytcheva (1999), see Wathen [2015]

preconditioners are found mainly as the following cases

$$\mathbf{T}\hat{\Delta}\mathbf{Y} = -\mathbf{R} \quad \underset{\text{Preconditioned}}{\rightarrow} \begin{cases} \mathbf{P}\,\mathbf{T}\hat{\Delta}\mathbf{Y} = -\mathbf{P}\,\mathbf{R} & \text{(left)} \\ \mathbf{T}\,\mathbf{P}\,\mathbf{P}^{-1}\hat{\Delta}\mathbf{Y} = -\mathbf{R} & \text{(right)} \\ \mathbf{P}_L\,\mathbf{T}\hat{\Delta}\mathbf{P}_R\,\mathbf{P}_R^{-1}\mathbf{Y} = -\mathbf{P}_L\,\mathbf{R} & \text{(split)} \\ (\mathbf{P}+\mathbf{T})\hat{\Delta}\mathbf{Y} = \mathbf{P}\hat{\Delta}\mathbf{Y} - \mathbf{R} & \text{(additive)} \end{cases} \rightarrow \tilde{\mathbf{T}}\hat{\Delta}\mathbf{Y} = -\tilde{\mathbf{R}} \tag{2.30}$$

In essence, we used an identity element whether additive or multiplicative to modify the expression of the original equation (2.28), however, its solution has remained intact. The first three cases are examples of multiplicative preconditioners Saad [2003], Gutknecht [2007], some examples used in the literature of this type of preconditioners are the **Schur complement** [Badia et al., 2014], **Incomplete LU (ILU)(0)** [Mayr et al., 2015] and **split+GMRES** Saad [2003]. The last *(additive)* preconditioner, is mainly used to define some solvers, as is the case of the *Richardson's iterations* method. However, in §6 we will show an example of how an additive preconditioner can be used on its own, which to our/my best knowledge has not been done before.

block Gauss-Seidel (BGS): The *BGS* block preconditioner allows to uncouple the different physical fields derived from the different uniphysic problems (refer to Verdugo and Wall [2016] for details). The big disadvantage of this method is that it cannot deal with a system having a zero block on the main diagonal, as it might happen with saddle point problems. This preconditioner is presented in the works of Gee et al. [2010], Verdugo and Wall [2016].

SIMPLE: The *SIMPLE* block preconditioner is a generalization of the Semi-Implicit Method for Pressure-Linked Equations (SIMPLE) proposed in [Caretto L. S. and B., 1973], to solve the Navier-Stokes equations for steady, fully three-dimensional flows. In contrast with BGS, this preconditioner allows to work with systems having zero block elements on its diagonal. The price to pay, is the preconditioning is Schur complement based. Thus, a further selection of the right approximation of the Schur complement must be made. This preconditioner is presented in Verdugo and Wall [2016].

Uzawa block preconditioner: The *Uzawa method* used as a solver for concave problems Uzawa and Arrow [1958], has been proved useful to multiphysics problems as seen in Bouery [2012]. In some cases, the implicit preconditioner of the method which is based on the Schur complement, can be used for multiphysic problems as highlighted in Badia et al. [2014], where they also describe the process on how this preconditioner can be thought as a building block for more robust preconditioners as the **Cahouet–Chabard block preconditioner** and the **pressure convection–diffusion preconditioner**.

AMG-(Restriction & Projection): As it will be shown below, a famous strategy is the algebraic multigrid strategy (AMG). As mentioned above, a strategy is a composition of preconditioners, solvers and/or strategies. The preconditioners which define a AMG strategy are the *Restriction* $\mathbf{R}_{\text{AMG}}$ and *Projection* $\mathbf{P}_{\text{AMG}}$ matrix, these matrices are applied not to the system of equations, but to the domain. This change of perspective, allows to construct a procedure for the systematical implementation of the preconditioners and solvers. In essence, $\mathbf{R}_{\text{AMG}}$ is used to make the mesh coarser, and $\mathbf{P}_{\text{AMG}}$ when we refine again the mesh. A most detail description of the method and some sources of information will be given when we

describe it as a strategy.

As mentioned, when we focus on solving the physical problem instead of the matrix problem, it is possible to change the condition number of the system (in essence, preconditioning) before reaching its matrix form. This leads to the lack of an algebraic description of the preconditioner, nevertheless, we are still preconditioning the original problem. In some cases, an algebraic description is possible despite not preconditioning the matrix directly, hence, a categorization regarding if the preconditioner is physically or mathematically based can be difficult. For the classification we use the following thought, if the preconditioner has a strong physical intuition, then it is physically based. We show some examples below

Physically-based:

Iso-thermal split: This block-preconditioner is used for *thermo-mechanical* problems. It can be traced back to Simo and Miehe [1992]. This preconditioner decomposes the original system $\mathbf{T}$ into two blocks $\mathbf{T} \approx \mathbf{T}_{T0} + \mathbf{T}_T$. The block $\mathbf{T}_{T0}$ describes the mechanical phase at a fixed temperature −therefore its name−, while $\mathbf{T}_T$ represents the heat conduction phase. The downside of this approach, is that it leads at best to conditional stable schemes Armero and Simo [1992].

Adiabatic split: This preconditioner is also used for thermo-mecanical systems. It was developped to outcome the conditionally stability of the iso-thermal split by Armero and Simo [1992]. This preconditioner divides the problem into two subproblems, one containing the elasto-dynamic phase with local adiabatic conditions and other the remaining heat conduction phase. Since energy dissipation occurs only at the heat conduction phase, this split presents the contractivity property of the fully coupled problem, see Bouery [2012].

Artificial added mass effect split: When the coupling in multiphysics problems is at the interface, as it is in FSI, a block preconditioner can be used based on the *Schur complement*, as the *artificial added mass effect split*. This partition despite being physically based can also be represented algebraically. A study of the instabilties raised by this type of block preconditioning can be found in Förster et al. [2007].

This is just a brief overview of the different preconditioners used for coupled problems. For a broader perspective, the reader can refer to Keyes et al. [2013], Benzi [2002] and Wathen [2015] for example. In addition, the TRILINOS project, offers a set of packages useful to precondition a system. An example is the IFPACK package [Sala and Heroux, 2005] which offers block preconditioners like the BGS preconditioner.

Algebraic definitions Due to the importance of two specific type of algebraic preconditioners in this research, we define them below. As mentioned an *algebraic* preconditioner is defined by a matrix $\mathbf{P}$. We can apply the preconditioner $\mathbf{P}$ by two different algebraic operations, namely, addition and multiplication.

Additive preconditioner

An *additive preconditioner* $\mathbf{P}$ is introduced via an additive identity

$$\mathbf{P}x = (\mathbf{P} - \mathbf{A})x + b \qquad \textbf{: Additive Identity} \tag{2.31}$$

From the equation above it can be seen that we can pick a preconditioner $\mathbf{P}$ having different mathematical properties which will ease the computational cost of solving the system. This type of preconditioner is most commonly used under an iterative approach.

Multiplicative preconditioner

A *multiplicative preconditioner* $\mathbf{P}$, as the name suggests, is defined through similar steps as before, the only difference being the use instead of the multiplicative identity

$$\mathbf{PA}x = \mathbf{P}b \qquad \textbf{: Multiplicative Identity} \tag{2.32}$$

In here, the matrix properties we try to improve should now reside in the product $\mathbf{PA}$. Notice that the transformation of the *additive* or *multiplicative* preconditioner into the system leaves the solution invariant in any case.

2.3.2.2 Solvers

Once we have mentioned some preconditioners, is time to proceed to solvers which is the final tool to use. As we did with the preconditioners, we will focus our attention towards solvers which are used in the literature to tackle multyphisic problems. There is a fundamental difference when thinking about solvers and preconditioners. As mentioned above, in a preconditioner it is important to distinguish the approach we want to exploit, namely, if it is based on the physical or mathematical properties. In a solver, such distinction is meaningless thanks to the PDE's classification, where a close connection can be drawn of the type of Physics and its mathematical properties. However, for the choice of a solver within multiphysics we mainly focus on methods to solve a sparse matrix. This direction is considered since the sparsity of the matrix can arise from the discretization of PDE's by finite element, finite volume or finite difference methods, as mentioned in Wathen [2015]. Therefore the solution of this type of systems is an active area of research. In addition, there exist a consensus on the classification for the solvers. We benefit from it to mention some of the methods and point towards the corresponding references.

Direct methods:

A *direct method* is a method that allows to compute the solution of a system like in (2.28) within a finite number of operations in exact arithmetic, as described by Allaire and Kaber [2007]. The downside of the method is that computationally they are expensive. However, in a compromise between the cost and accuracy, they may be a good choice, specially if the original system has been partitioned already. Some of the solvers considered as *direct methods* are **Gaussian elimination**, **LU decomposition**, **Cholesky**, **QR factorization**, for detailed information you may refeer to Allaire and Kaber [2007], Davis et al. [2016].

Iterative solvers:

A *iterative solver* creates a sequence of approximate solutions which improve at each iteration. Therefore, in contrast with direct methods, they require an infinite number of operations to remove the round-off errors of the method. Nevertheless, these solvers may achieve a good approximation of the solution quite fast. Some of the most famous iterative solvers are the **Jacobi method**, the **Gauss-Seidel** method and **incomplete LU**, see for more details Strang [2007], Saad [2003], Axelsson [1994].

Krylov subspace methods:

This family of solvers was initially derived as a direct method, based on the idea of the *Krylov space* $\mathcal{K}$ van der Vorst [2003], Ipsen and Meyer [1998]. However, it was until they where used as iterative methods to approximate the solution, that they have acquired great importance among solvers for sparse matrices [Benzi, 2002]. A key aspect of this class of solvers, is that it can be used as direct or iterative solver, however, as an iterative solver it requires only a finite number of iterations. From this class, the most prominent solvers are:

• **Conjugate gradient** which is the solver of choice when the matrix to solve is symmetric and positive definite Hestenes and Stiefel [1952] [5].
• **Minimum Residual (MINRES)** if the matrix is symmetric but not positive definite Paige and Saunders [1975].
• **General Minimum Residual (GMRES)** in the most general case where the matrix is non symmetric Saad and Schultz [1986]. However, GMRES is not a direct choice when choosing a solver as pointed out in Wathen [2015].

For a general review on solvers, one can refer to the following bibliography Axelsson [1994], Saad [2003], Allaire and Kaber [2007]. As it is for the preconditioners, there is a set of packages for solvers in the TRILINOS project. AMESOS is the Direct Sparse Solver Package [Sala et al., 2006a,b]. For Iterative solvers, the package ILFPACK [Sala and Heroux, 2005] provides access to solvers known also as point preconditioners[6], whereas AZTEC00 is a package of Krylov solvers [M. A., 2004].

2.3.2.3 Strategies

As mentioned above, it is a common practice to apply a *preconditioner* to a matrix, after which we use a *solver* to obtain the unknown fields. We name this whole process of using a preconditioner followed by a solver, a *numerical strategy* or for short a *strategy*. Therefore, a *strategy* details an algorithmic procedure to solve a system of equations through the use of possibly many preconditioners and solvers, or even strategies themselves. A strategy is considered a numerical method, thus, sometimes strategies are also correctly called *solution methods* or *partitioned methods* (e.g. Felippa et al. [2001]). We will stick to the term *strategy* most of the time. Given the overview of the preconditioners and solvers shown above, we present some of the current strategies used for multiphysic problems.

Multigrid:

The *multigrid strategy (MG)* started with the paper of Brandt [1977], which has been widely explored and developed by many others. Roughly, this method consists of the system's iterative solution through different discrete representations of the domain (mesh) at hand. If these representations are considered explicitly we talk of a **geometric multigrid strategy (GMG)** as considered in Wesseling and Oosterlee [2001]. Instead, if computed algebraically we talk of a **algebraic multigrid strategy (AMG)** [Briggs et al., 2000].

What **AMG** does to obtain the different meshes algebraically, is to define the process of refinement and projection on the domain through the matrices $\mathbf{R}_{\text{AMG}}$ and $\mathbf{P}_{\text{AMG}}$ correspondingly. These matrices can be considered as the preconditioners of the AMG strategy as mentioned above. In the case of **GMG**, the preconditioning can not be represented algebraically since the different meshes are obtained as an external source.

Part of the success of this strategy is the liberty on choosing different solvers for the different discretizations. As pointed out by Fedorenko [1964], Bakhvalov [1966], economic solvers like Jacobi or Gauss-Seidel method can help to solve the expensive −finer− meshes. With these solvers we can remove high frequency errors[7]. This leaves a direct solver for the solution of the cheapest −coarsest− mesh, to remove low frequency errors. This attibute has proven

[5] Confeer to Shewchuk [1994] for simple introduction to the method
[6] Refer to the definition above of a solver, for a brief discussion on the name of the solvers as point preconditioners
[7] That is why the solvers applied in this partitions are called *smoothers*

useful specially in elliptic problems [Gee et al., 2010], where the work to compute the solution scales linearly with the dimension of the discretized problem as highlighted by Wathen [2015]. Further details in **AMG** can be found in Trottenberg et al. [2000].

As mentioned before, the definition through composition of a *strategy*, allows the possibility to define it through several preconditioners, solvers or strategies themselves. This idea can be seen in the following techniques.

BGS(AMG) : The *BGS(AMG)* strategy presented in Gee et al. [2010] and generalized by Verdugo and Wall [2016], starts with a partition of the full system using the block Gauss-Seidel preconditioner mentioned earlier. Afterwards it proceeds by applying at each partitioned block the AMG strategy.

SIMPLE(AMG) : The *SIMPLE(AMG)* strategy [Verdugo and Wall, 2016], works in a similar fashion as the BGS(AMG), the difference being that a SIMPLE block-preconditioner is applied instead of the block Gauss-Seidel. The practical difference between these methods, arises as one would expect from the block preconditioners. Nevertheless, in both cases when applied to coupled problems the coupling is altered by the first block partition without any compensation for the coupling error like it might be needed in some cases like FSI with the "artificial added mass effect".

Preconditioned Krylov: A *Preconditioned Krylov* strategy, in contrast with the later two methods, is mainly defined by its solver instead of the preconditioner. As pointed out in Gutknecht [2007], normally a *krylov solver* converges slowly for real world applications, therefore, nearly always the solver is used along with a preconditioner Saad [2003]. This approach gives raise to the *Preconditioned Krylov* strategy also found in the literature as Krylov subspace preconditioning (KSP) methods, or *preconditioned Krylov subspace* methods [8]. .

AMG(BGS) and/or AMG(SIMPLE) : The *AMG(BGS)* [Gee et al., 2010, Verdugo and Wall, 2016] and *AMG(SIMPLE)* [Verdugo and Wall, 2016], are two strategies which start by using the AMG strategy to solve the system. However, when it is time to solve each mesh, a further preconditioning is applied. In these cases, the second preconditioners is the block Gauss-Seidel for AMG(BGS) or the SIMPLE block preconditioner for AMG(SIMPLE). The change on the ordering solves the issue of uncoupling in all AMG levels[9], achieving a better performance of the strategy. Examples of this type of strategies applied to multiphysic problems can be found in Gee et al. [2010], Danowski et al. [2013]

There exists a classification for strategies which is sometimes taken into account, specially when physically based block-preconditioners are used. As with the solvers, we benefit from this classification to present more strategies currently used in the literature. However, a detail description of the classification is reserved for §6 where we are going to analyze more the strategies proposed in this work.

Monolithic :

[8] confer to Zhang [2000] as an example and for short overview on the subject

[9] however, not in the approximation of the solution

Monolithic strategies are characterized by the fact that the unknowns of the full system are solved synchronously, in essence, ALL the unknowns get their value (or update) at the same time. This is the standard approach, when solving a linear matrix system using a direct method. Nevertheless, as it will be shown in §6, it is possible to apply a partition on the system and still get back to a Monolithic strategy. For methods under this classification having a general setting we can find the **Newton-Krylov methods** Brown and Saad [1994], whilst in the context of multiphysics some examples can be found in the works of Blom [1998], Solin et al. [2010], Mayr et al. [2015], just to mention a couple of examples.

Staggered :

Staggered strategies, partition the system and proceed to solve each partition in a sequential manner. Some of the examples which can be found in the literature are the **iso-thermal & adiabatic strategies:** used in thermo-mechanical problems, using as its basis the *iso-thermal split* or *adiabatic split* as preconditioners. However, different choices of predictors[10] and solvers give raise to a variety of methods −strategies− to solve the thermomechanical problem. As examples please confeer to Miehe [1995], Martins et al. [2017], Vaz M. [2017] and the references within.

Nested :

Nested strategies also involve the partitioning of the system. The difference with the staggered strategy is that the partitions are not solved sequentially but rather in a nested loop fashion. Examples of these type of methods can be found in the works of Ortiz and Stainier [1999], Miehe et al. [2014], Simo and Hughes [2000], de Souza Neto et al. [2011].

To conclude we go into a final example which leaves clear how strategies can be composed within strategies themselves.

MG(Nested) : This strategy has the following compositions of strategies: MG ∘ Nested. Basically, it applies the multigrid preconditioners, whereas to solve each mesh it applies a nested method, and adds up the error corrections at each level as the usual in the MG strategy. A example in the literature of this technique can be found in [Alonso and Jameson, 1994].

Under the TRILINOS project, there are a couple of packages: PLAYA [Howle et al., 2012] and TEKO [Cyr et al., 2016] which allow the manipulation of block matrices and implementation of block preconditioners respectively. It is also possible to use the combination of the previously mentioned packages, ILFPACK and AZTEC00 to develop different strategies.

2.3.2.4 Properties

Now that we have finally seen the definitions of preconditioner, solver and strategy with current examples in the literature, it is time to highlight some of the distinguishable properties each of these methods has. These properties help to build up a justification for the definitions taken in §1.4.4. Most of the notions for the following properties comes as a collection of ideas from all the references cited in this research. Nevertheless, there are two main papers which must be mentioned, Keyes et al. [2013] and Felippa et al. [2001].

[10] A predictor is the technique used to choose the initial guess in iterative solvers

Preconditioners
Some important properties which define a preconditioner are its *basis*, *structure*, *characterization*, *fragmentation*. Below we present a definition for each one of those, along with some examples.

Basis: This property has already come out in the text. It refers to whether a preconditioner exploits the physical or mathematical properties of the system. Thus, a preconditioner might be *physically-based* or *mathematically-based*.

- Physically-based
  - Isothermal split
  - Adiabatic split
  - Artificial Added Mass Effect split
- Mathematically-based
  - AMG (R_{AMG}, T_{AMG})
  - BGS
  - Simple
  - Uzawa block
  - ILU (precondtioner)

Structure: When a preconditioner is formulated into blocks, then we can say it has a *block structure*. If it is not the case, we say it has a *point structure*.

- Point-structure
  - ILU (preconditioner)
  - QR factorization
  - LU
- Block-structure
  - AMG (R_{AMG}, T_{AMG})
  - BGS
  - Isothermal split
  - Adiabatic split

Characterization: When we can define a preconditioner through matrices, we say it has an *algebraic characterization*. In the case it is possible to define it without the need of a matrix, it has an *algorithmic characterization*. In contrast with the latter properties, these two possibilities are not exclusive.

- Algorithmic characterization
  - GMG (external meshes)
  - Isothermal split
  - Adiabatic split
- Algebraic characterization
  - AMG (R_{AMG}, T_{AMG})
  - BGS
  - Isothermal split

Fragmentation: If the preconditioner arises as a decomposition of the original operator it has a *natural fragmentation*, whereas the preconditioner arises as an artifact it has an *artificial fragmentation*

- Natural fragmentation
  - ILU (preconditioner)
  - Isothermal split
  - QR factorization
- Artificial fragmentation
  - AMG (R_{AMG}, T_{AMG})
  - BGS
  - Diagonal(Jacobi)

Target: The *target* let us know what the preconditioner is modifying. It may be targeting the *system of equations*, or the *domain*.

- System of equations
  - ILU (preconditioner)
  - Isothermal split
  - BGS
- Domain
  - AMG (R_{AMG}, T_{AMG})
  - GMG
  - Schwartz preconditioners

Solvers

For the solvers we can distinguish the main couple of properties: the *approach* and the *algorithmic dependence*.

Approach: This property is in line with the classification shown above. Thus, it has a *direct approach*, or an *iterative approach*. From an iterative approach we can do a further distinction between *finite* and *infinite* approaches.

- Direct Approach
  - Gaussian elimination
  - LU decomposition
- Iterative Approach
  - Finite Iterations
    - Krylov methods
  - Infinitely Iterations
    - Jacobi, Gauss-Seidel

Algorithmic dependence: A solver can assume the type of dependence between the variables, independently of the dependence they have in the original system. Therefore we can talk in this property about *implicit algorithmic dependence* and *explicit algorithmic dependence*.

- Implicit algorithmic dependence
  - Krylov methods
  - Gaussian elimination
- Explicit algorithmic dependence
  - Jacobi
  - Gauss-Seidel

Strategies

We conclude with the properties a strategy may have. In general those are: the *computational path*, *Target*, *power structure*, and *algorithmic coupling*. The first, is related with the solver-mode of the strategy, the second relates to its preconditioner-mode, while the last two can not be related to any of those two.

Computational path: The computational path, describes the way on which the unknowns are being solved. When the unknowns are being solved synchronously, we have a *monolithic computational path*, the opposite tells about a *partitioned computational path*. A further subdivision of the *partitioned computational path* will be explored within this research in §6

- Monolithic
  - Identity Preconditioner ∘ Direct solver
  - ILU(x) ∘ Krylov method
- Partitioned
  - Staggered
  - Nested
  - AMG(BGS)
  - SIMPLE ∘ Krylov methods

Target: The *target* let us know what is the strategy modifying in the solution process. As with the preconditioner its target may be the *system of equations*, the *domain*, or a mixture of both, in essence *system/domain*.

- System of equations
  - Staggered
  - Nested
- Domain
  - AMG
  - GMG
- System/Domain
  - AMG(BGS)
  - BGS(AMG)
  - AMG(Nested)

Power structure: Power structure establishes if there exist some hierarchical process defined by the strategy, specially into the different subproblems it might decompose the system. If such a hierarchical process exists, it has a *hierarchical structure*, otherwise it has an *egalitarian structure*

- Egalitarian structure
  - Identity Precond. ∘ Direct solver
  - ILU(x) ∘ Krylov methods
  - Monolithic
- Hierarchical structure
  - Staggered
  - Nested
  - MG

Algorithmic coupling: This property describes the feedback process of the unknowns. We can talk about a *thigh coupling*, when in the solution process the variables are considered implicitly related at all times[1], thus the notion of feedback does not exists. A *loose coupling*, assumes a explicit dependence[1], hence there is no feedback, in essence is an open loop system. A further possibility is that the systems assumes an explicit dependence[1], but there is a feedback between variables at some later time, in such case we say the strategy has a *moderate coupling*.

- Tight Coupling
  - Monolithic
  - MG
- moderate Coupling
  - Nested
  - AMG (BGS)
- Loose Coupling
  - Staggered
  - BGS(AMG)

All the properties just described are summarized in Figure (2.1).

[1] independent of the physical system

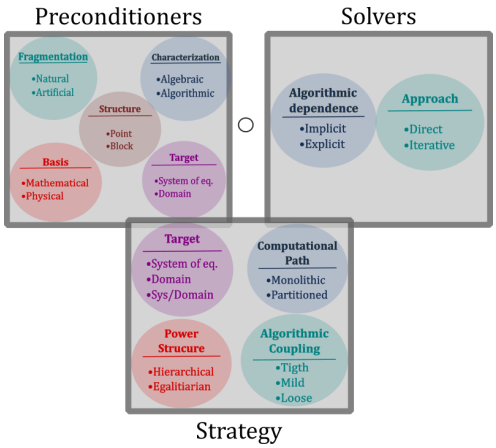

Figure 2.1: Properties: Preconditioner, solver, Strategy

Part II

Physical Models

Chapter 3

Chemical Diffusion

Sommaire

Ceci est le premier chapitre concernant la modélisation et la résolution numérique des problèmes tels qu'ils vont être traités dans la suite. En considerèrant le problème multiforme de la diffusion chimique au lieu d'un problème multiphysique, nous présentons, sous une forme simplifiée, la procédure que nous proposons pour développer les modèles variationnels. Les premiers modèles variationnels présentés ici sont validés en utilisant notre modèle simplifié et en montrant ainsi la congruence avec les résultats de la littérature. À la fin du chapitre, nous résolvons et analysons un problème 1D numériquement.

> "It was quite natural to suppose, that this law for the diffusion of a salt in its solvent must be identical with that, according to which the diffusion of heat in a conducting body takes place; upon this law Fourier founded his celebrated theory of heat, and it is the same which Ohm applied with such extraordinary success, to the diffusion of electricity in a conductor."
>
> Adolf Eugen Fick
> *On liquid diffusion, 1855*

The quote above, is considered historically the first mathematical idea to represent the process of diffusion, which on those days was considered an obscure process. Fick's vision to see the same patterns into different fields and apply it to areas not so highly developed is in line with what we expect to present in this work. This chapter, is not about any multiphysic problem, but rather a multifield mathematical formulation for the uniphysic area of chemical diffusion. Why is it important to dedicate a Chapter for a uniphysic problem in a multiphysics work?. The reason to dedicate a Chapter only on chemical diffusion, is that the understanding and ideas which arise from this simple problem using multiple fields can be extended into multiphysic in the same way, giving a smooth transition towards our understanding of coupled problems.

The goal for this chapter is two fold. In a global perspective, we present the intuition that deriving a multifield mathematical formulation for the process of chemical diffusion is analogous for multiphysic problems. In a local perspective, we present a variational form (VF) for chemical diffusion, similar to that presented in Miehe et al. [2014]. However, we arrive to his formulation after reducing a first instance of our model. In general, the ideas we will develop are the cornerstone for the models we will derive in the

following chapters §4 and §5 for multiphysic problems.

3.1 The different formulations

By diffusion, we express the net movement of certain property in a system which reallocates itself, towards an equilibrium state. Usually diffusion is related to movement from areas of high concentration to areas of low concentration, as it was firstly proposed by Fick [1855]. Nowadays it is understood that the driving force behind diffusion of chemical substances is the chemical potential inherent to each substance, as mentioned by Job and Herrmann [2006], [Job et al., 2015, p. 317], [Callen, 1985, p. 45-46], [Sears and Salinger, 1975, p. 120], [Clemens, 2005, § 4]. The relation between concentration and chemical potential is usually defined through some algebraic dependency based on empirical observations. One of the most popular relations is the *logarithmic mass action law* [Job et al., 2015, § 6]. The former three ideas: how the concentration evolves in time, what happens with the chemical potential and how it is correlated with the concentration can be presented through different but equivalent mathematical formulations. We can distinguish between three of them the *strong form* (SF), the *weak form* (WF) and the *variational form* (VF).

3.1.1 An overview of the Strong form

The *strong form (SF)*, describes the problems for every point in the physical space. As an example we have

Fick's laws

$$\vec{j} = -D\nabla c \qquad \text{Fick's First law} \tag{3.1a}$$

$$\frac{\partial c}{\partial t} = -\nabla \cdot \vec{j} + f_c \qquad \text{Fick's Second law} \tag{3.1b}$$

Mass Action law

$$\mu = \mu_0 + RT \ln\left(\frac{c}{c_0}\right) \qquad \text{Logarithmic law (secondary reference state)} \tag{3.2}$$

initial conditions (IC)

$$c(0,\vec{x}) = \overline{c}_0(\vec{x}) \qquad \forall \vec{x} \in \partial_c\Omega \tag{3.3a}$$

$$\vec{j}(0,\vec{x}) = \overline{j}_0(\vec{x}) \qquad \forall \vec{x} \in \partial_{\vec{j}}\Omega \tag{3.3b}$$

boundary conditions (BC)

$$c(t,\vec{x}) = \overline{c}(t,\vec{x}) \qquad \forall t \in [t_0,t_f] \quad \& \quad \vec{x} \in \partial_c\Omega \tag{3.4a}$$

$$\vec{j}(t,\vec{x}) = \overline{j}(t,\vec{x}) \qquad \forall t \in [t_0,t_f] \quad \& \quad \vec{x} \in \partial_{\vec{j}}\Omega \tag{3.4b}$$

The first two equations are the Fick's laws. The *first law* (3.1a) is a constitutive law which defines the *massic flux* $\vec{j}$ depending on the *diffusion coefficient* D and the *gradient of the concentration* ∇c, the minus sign indicates that the flux opposes the direction of the gradient −which always points in the direction of greatest increase−, in this case the direction of greatest concentration. *Fick's second law* (3.1b), describes the evolution of the *concentration* c through time t. The concentration will change accordingly if we add

or subtract substance from *external sources* f_c, and will increase if the divergence of the flux is positive, in essence, $\nabla \cdot \vec{j} > 0$ or decrease when it is negative.

The *logarithmic mass action law* (5.18), is a mathematical approximation to describe the empirical relationship between the *chemical potential* μ and the concentration c, where μ_0 and c_0 can be seen as reference values for the chemical potential and concentration respectively, R is the universal gas constant and T represents the temperature at which the process is taking place. As mentioned in Newman and Thomas-Alyea [2004] the use of μ_0 is needed because according to thermodynamics there is no absolute value of chemical potential, that is why μ_0 can be refereed as *reference state*. The second term is the *secondary reference state* to describe an ideal dependence between μ and c. However, empiric results show the relation holds only for small values of c,[1] thus in a most general way we must add to (5.18) the term $RT \ln a$ where a is called the absolute activity coefficient and is dependent on different thermodynamic quantities than the concentration.

Finally, the set of equations in (3.4) and (3.3) impose the boundary conditions (BC) and initial conditions (IC) of the problem, where we have defined the boundary of the domain Ω as $\partial\Omega \equiv \partial_c\Omega \cup \partial_{\vec{j}}\Omega$, such that the two subdomains are non overlapping, in essence, $\partial_c\Omega \cap \partial_{\vec{j}}\Omega \equiv \emptyset$. The mass action law complements the BC and IC for the chemical potential $\mu \in \partial_\mu\Omega$. Hence, the domain $\partial_\mu\Omega$ is defined where $\partial_c\Omega$ is prescribed.

Equations (3.1a) and (5.18) can be seen as *constitutive laws*, selected according with the specific substance we are using or the scale we are working. In contrast, (3.1b) is an *evolution law* or *balance law* since it describes the dynamics of the system independently of material.

The process which is normally used to solve the set of equations, is to solve Fick's laws first to get the concentration. Once the concentration is obtained we plug it into (5.18) to compute the chemical potential. This post-process relation usually chosen to get the chemical potential, is equivalent to solve the system under a staggered scheme as it will be shown in §6. The implications of the algorithmic uncoupling of the system may hide information of the actual system we are solving.

3.1.2 An overview of the Weak form

The *weak form (WF)* in contrast with the strong form presents the problem globally. For chemical diffusion the WF formulation associated to the SF shown in (3.1) is the following

[1] for neutral substances it should satisfy $c < 100$ mol m^{-3} and for ions $c < 1$ mol m^{-3} [Job et al., 2015, §. 6.2]

Fick's laws

$$\int_\Omega \left(\frac{\partial c}{\partial t}\delta c + D\nabla c \cdot \nabla \delta c - f_c \delta c \right) dV = -\int_{\partial_j \Omega} \left(\vec{j} \cdot \vec{n} \right) \delta c \, dS \qquad \forall\, c \in \mathcal{V}_c,\ \delta c \in \mathcal{V}_{\delta c} \tag{3.5}$$

Mass Action law

$$\mu = \mu_0 + RT \ln\left(\frac{c}{c_0}\right) \qquad \text{Logarithmic law} \tag{3.6}$$

initial conditions (IC)

$$c(0, \vec{x}) = \overline{c}_0(\vec{x}) \qquad \forall \vec{x} \in \partial_c \Omega \tag{3.7a}$$

$$\vec{j}(0, \vec{x}) = \overline{j}_0(\vec{x}) \qquad \forall \vec{x} \in \partial_{\overline{j}} \Omega \tag{3.7b}$$

Solution space

$$\mathcal{V}_c := \left\{ c \in H^1 \;\middle|\; c = \overline{c}(t, \vec{x}) \quad \forall \vec{x} \in \partial_c \Omega \right\} \qquad \text{Admissible solution space } (c) \tag{3.8a}$$

$$\mathcal{V}_{\delta c} := \left\{ \delta c \in H^1 \;\middle|\; \delta c = 0 \quad \forall \vec{x} \in \partial_c \Omega \right\} \qquad \text{Test function space } (\delta c) \tag{3.8b}$$

where δc is the *test function*. This formulation is equivalent to the strong form showed above. Notice that the BC (3.4b) has been integrated into the right hand side (RHS) of the equation (3.5). As it is for the BC (3.4a) we impose the concept of an *admissible space* on the solution for the concentration field c (3.8). Equation (3.6) must hold for the IC and the BC the chemical potential c. The constraint in the WF solution is weaker since it requires a lower degree of differentiability (H^1) in comparison with the SF(H^2). To solve the system we solve the WF of Fick's laws in (3.5) obtaining the value for c. Since the chemical potential depends explicitly on the concentration, i.e. $\mu(c)$, we insert the obtained value of c into (3.6). We call this to be a *post-process* relation for μ.

3.1.3 The Variational form

A *variational form (VF)* is equivalent to a WF or a SF. However, the paradigm is different. Instead of solving a system of PDE's we optimize a functional. Thus, to find the functional to optimize is the principal task when modeling through a VF. Nevertheless, sometimes this turns out to be a difficult endeavour. Take as example the SF in (3.1) or the equivalent WF in (3.5), there is no direct VF equivalence in the continuum. At most we can declare a version which holds but in a time discrete setting, which we show below.

A discrete variational form

Optimization problem :

$$\{c\} = \arg\inf_{c} I[c] \tag{3.9}$$

$$I[c] := \int_{\Omega} \left[\frac{1}{2} (c - c_n)^2 + \Delta t \frac{D}{2} \nabla c \cdot \nabla c \right] dV - \int_{\partial_j \Omega} \Delta t \bar{j} c dS \tag{3.10}$$

Mass Action law

$$\mu = \mu_0 + RT \ln \left(\frac{c}{c_0} \right) \qquad \text{Logarithmic law}$$

initial conditions (IC)

$$\mu(0, \vec{x}) = \overline{\mu}_0(\vec{x}) \qquad \forall \vec{x} \in \partial_\mu \Omega \tag{3.11a}$$

$$\vec{j}(0, \vec{x}) = \bar{j}_0(\vec{x}) \qquad \forall \vec{x} \in \partial_{\vec{j}} \Omega \tag{3.11b}$$

Solution space

$$\mathcal{V}_\mu := \left\{ \mu \in H^1 \;\middle|\; \mu = \overline{\mu}(t, \vec{x}) \quad \forall \vec{x} \in \partial_\mu \Omega \right\} \qquad \text{Admissible space} \tag{3.12a}$$

Recalling two key ideas: the domain $\partial_\mu \Omega$ is defined where $\partial_c \Omega$ is prescribed and the mass action law draws the relation between their values. We choose for this formulation to state BC and IC in terms of the chemical potential instead of the concentration, since the chemical potential is the driving force for the chemical diffusion process.

The importance of dependencies: The formulations so far show the chemical potential depending explicitly on the concentration. However, there is no physical reason behind why we compute first the concentration and afterwards the chemical potential. This innocent procedure is a mere consequence of the equations we are using. Nevertheless, it obscures the physics we are aiming to describe. Some signals of this obscurity is that we only need Fick's laws to describe/solve the system. We do not need to consider the chemical potential, despite the chemical potential is the driving force for the process of chemical diffusion. Moreover, the equations tells us that there is an implicit dependency between c and $\vec{j}$, and an explicit dependency $\mu(c)$. The safest bet we can make is to assume that the dependency between the three of them is implicit. In fact, the importance about why and when we consider the dependencies is one of the core ideas we want to emphasize in this work. As we will show, awareness on this matter is useful to comprehend the type of couplings in models and numerical strategies we would like to use. All this should bring back to our heads the quote from Keyes et al. [2013].

"Coupled until proven decoupled"

where they propose the quote "as a perspective worthy of 21st century simulation purposes and resources."

A strongly coupled variational form

In contrast with the previous formulations we have shown so far. We present a VF which considers an implicit dependency between the three fields c, $\vec{j}$ and μ. This VF is one of the models we are going to derive in this chapter. In order to provide some context we present the formulation in a descriptive fashion. To start, the meaning we give to the functional is that of energy, or more properly said, an

energy-like functional. The distinction is just to clarify that the functional takes into account the energy of the system plus its power over a lapse of time, with this the coupled VF looks like

Optimization problem

$$\{\dot{c}, \mu\} = \arg\inf_{\dot{c}} \sup_{\mu} \Pi_2[\dot{c}, \mu] \tag{3.13}$$

$$\Pi_2[\dot{c}, \mu] = \int_\tau \left[\int_\Omega \left(\dot{U}(c) - \mu\dot{c} - \chi(\vec{g}, c) + \mu f_c \right) dV - \int_{\partial_j \Omega} \mu \bar{j} dS \right] dt \tag{3.14}$$

Now the optimal problem to solve involves the chemical potential and the concentration as seen in (3.13), while the functional to optimize is Π_2 and is detailed in (3.14). The term $\vec{g}$ defines the chemical field, this means $\vec{g} := -\nabla\mu$. The new parameters $U(c)$ and $\chi(\vec{g}, c)$, are functions which represent the Internal energy of the system and the dissipation potential respectively.

Before going into details of the equivalence with the previous models, let's review a brief description of the terms in the functional (3.14). The term $\dot{U}(c)$ describes the process which represents the internal energy rate of the system and its evolution through time, since this is embedded within a time integral it denotes it is conservative, in essence, the value of the time integral of this term is path independent, since only the initial and final values of the internal energy are needed to solve the system for a given lapse of time τ. Moreover, the internal energy acts as the link between μ and c for the system to be empirically consistent. This function must contain the logarithmic mass action law, or whatever constitutive law we are using.

The function $\chi(\vec{g}, c)$ represents an emergent property of the system, the energy which is lost or dissipated by the system for the process of chemical diffusion to take place. This function needs to be convex for the system to be consistent with the laws of thermodynamics. We will detail this idea further in §3.2.2. In addition, when $\chi(\vec{g}, c)$ equals zero it represents the system being in thermodynamic equilibrium. This can be understood by noting that this part of the integrand is a *Dirichlet principle* which solves the Laplacian $\Delta c = 0$ [Evans, 1998, §2.2.5, §8.1.2][2]. Another property, is that in contrast with $U(c)$ the function $\chi(\vec{g}, c)$ is not a state function.

The term $\mu\dot{c}$ considers the energy used −due to the minus sign− by the system to change the amount of concentration in a point during a lapse of time τ. The coupled μf_c takes into account the energy which is added to the system by external sources of concentration. And finally the boundary term $\mu\bar{j}$ represents the energy needed by the system to satisfy a flux constraint or a Neumann condition.

3.2 Deriving the coupled variational form

There are three main ingredients in the construction of a mathematical model: state variables, constitutive laws and balance laws. To construct the VF we propose to relate correspondingly to these ingredients the ideas of *conjugate variables*, *existence of energy-like potentials* and *system's constraints*.

Conjugate Variables : To describe the system we need some state variables. For the coupled chemical diffusion problem we use the concentration and chemical potential. A distinction in our model is that we

[2]The later is explained through our approach if we derived the steady problem, see 2.1.1

define state variables to act as conjugate variables. Hence, instead of coupling the fields through a weak coupling as a post-process relation does, now they become strongly coupled.

Energy-like potentials : We postulate the existence of energy-like potentials, namely, the *Internal energy* $U(c)$ and the *Dissipation potential* $\chi(\vec{j})$. Both functions represent *constitutive relations*, for the concentration c and the massic flux $\vec{j}$ respectively. These potentials will help us to relate the variables via the Legendre-Fenchel's transform.

Balance laws : The possible states the system can undergo should satisfy a set of general principles, in essence, the *balance laws*. Therefore, we impose balance laws as a constraint in our variational problem by means of the Lagrange multiplier method.

We make use of the Legendre-Fenchel's transform and the Lagrange multiplier method. The generality of these tools is what allow us to define a generic VF model for multiphysics from a uniphysic problem.

3.2.1 Description of the system's dynamics

To construct the functional we start by using Onsager's energy rate [Onsager, 1945]

$$\Pi_0[\dot{c},\vec{j}] := \int_\tau \left[\int_\Omega \Big(\dot{U}(c) + \chi^*(\vec{j},c) \Big)\, dV + \int_{\partial_\mu \Omega} \overline{\mu}(\vec{j}\cdot\vec{n}) dS \right] dt \tag{3.15}$$

with U and χ^* as the internal energy and the dual dissipation potential, $\vec{j}$ the massic flux, $\vec{n}$ the outward normal and $\overline{\mu}$ a known value for the chemical potential defined at the Dirichlet boundary $\partial_\mu\Omega$. This energy-like representation of the system has also been used for many others [e.g. Ziegler, 1963, Needleman and Rice, 1980, Svoboda and Turek, 1991, Parhami et al., 1999, Hackl and Fischer, 2008]. We impose on it a flux condition and the mass conservation law as constraints.[3] This raises the following primal problem which we aim to solve

$$\{\dot{c},\vec{j}\} = \arg\inf_{\dot{c},\vec{j}} \Pi_0 \qquad \textit{subject to} \qquad \begin{cases} \dot{c} + \nabla\cdot\vec{j} - f_c = 0 & \forall\, \vec{x}\in\Omega \\ \overline{j} - \vec{j}\cdot\vec{n} = 0 & \forall\, \vec{x}\in\partial_j\Omega \end{cases}$$

where $\overline{j}$ is a predefined flux at the boundary $\partial_j\Omega$, f_c is an external source and c the concentration. By means of the Lagrange multiplier method we can define the following functional

$$\begin{aligned} \Pi_\lambda[\dot{c},\lambda_1,\lambda_2,\vec{j}] := \int_\tau \Bigg[& \int_\Omega \Big(\dot{U} + \chi^* + \lambda_1(\dot{c} + \nabla\cdot\vec{j} - f_c) \Big)\, dV \\ & + \int_{\partial_\mu\Omega} \overline{\mu}(\vec{j}\cdot\vec{n}) dS + \int_{\partial_j\Omega} \Big(\lambda_2(\overline{j} - \vec{j}\cdot\vec{n}) \Big) dS \Bigg] dt \end{aligned} \tag{3.16}$$

where λ_1 and λ_2 are the Lagrange multipliers.

First Variations : The first variations of the functional should vanish since we look for a stationary point of the functional.

[3] A stationary law could also be imposed.

Variation of $\vec{j}$: The variations with respect to $\vec{j}$ leads to

$$< D_{\vec{j}}\Pi_\lambda, \delta\vec{j} >\equiv \vec{0} \qquad \Rightarrow \qquad \begin{cases} \lambda_1 = -\overline{\mu} & \forall \vec{x} \in \partial_\mu \Omega \\ \lambda_1 = \lambda_2 & \forall \vec{x} \in \partial_j \Omega \\ \nabla\lambda_1 = \dfrac{\partial \chi}{\partial \vec{j}} & \forall \vec{x} \in \Omega \end{cases} \tag{3.17}$$

From here several interesting facts can be observed. To start, (3.17).a indicates that the Lagrange multiplier λ_1 is equal to the negative chemical potential at the Dirichlet boundary shedding some light about true identity of this Lagrange multiplier. While (3.17).b declares that both Lagrange multipliers are actually the same variable confirming thus, that the Lagrange multipliers are nothing more than the negative chemical potential. With this in mind, (3.17).c states that the negative gradient of the chemical potential, in essence, the chemical field $-\nabla\mu := \vec{g}$ is the dual variable of the massic flux through the dissipation function.

Variation of $\dot{c}$: A look to the first variations of $\dot{c}$ leads to

$$< D_{\dot{c}}\Pi_\lambda, \delta\dot{c} >\equiv 0 \qquad \Rightarrow \qquad \begin{cases} -\lambda_1 = \dfrac{dU}{dc} & \forall \vec{x} \in \Omega \end{cases} \tag{3.18}$$

this outcome of (3.18) gives us the dual relationship between chemical potential and concentration which we were aiming for. Now we can see that c and μ are conjugated through the internal energy.

Variation of μ : To conclude, we apply the variations of the Lagrange multiplier, which now we know is the chemical potential

$$< D_\mu\Pi_\lambda, \delta\mu >\equiv 0 \qquad \Rightarrow \qquad \begin{cases} \dot{c} = -\nabla \cdot \vec{j} + f_c & \forall \vec{x} \in \Omega \\ \overline{j} = \vec{j} \cdot \vec{n} & \forall \vec{x} \in \partial_j \Omega \end{cases} \tag{3.19}$$

this result was to be expected from the use of the lagrange multipliers. Nevertheless, the characterization of lagrange multiplers as the chemical potential gives to this outcome a way to measure the sensibility to the balance laws in the model. The use of chemical potential as a Lagrange multiplier dates back to at least as far as Larché and Cahn [1973].

Second variations : The second variations on the functional Π_λ help us characterize the optimal conditions as a minimum or maximum for the different fields and to see the implications of that.

Variation of μ : The second variation with respect to μ is not computed, instead we make use of a result from convex optimization. Due to *strong duality* properties (cf. [Boyd and Vandenberghe, 2004, § 5.2.3]) the chemical potential −which we know is the Lagrange multiplier−, must have the opposite characterization than the concentration.

Variation of $\dot{c}$: For this we need to apply a further variation to (3.18) results in

$$< D^2_{\dot{c}}\Pi_\lambda, \delta\dot{c}^2 > = \int_\tau \left[\int_\Omega \frac{d^2U}{dc^2} dV \right] \delta\dot{c}^2 dt \qquad \Rightarrow \qquad \frac{d^2U}{dc^2} \begin{cases} > 0 & c \text{ is minimum} \\ < 0 & c \text{ is maximum} \\ = 0 & c \text{ is saddle} \end{cases}$$

As shown above the optimal condition for $\dot{c}$ depends on the second derivative of the internal energy. Hence, what can the internal energy tell us about the diffusing species?. To understand this, we need to do a small example. Consider a constitutive law for the massic flux as

$$\vec{j} = -M\nabla\mu$$

where M is a positive quantity called the *mobility* of the species. Recalling condition (3.18) we can get

$$\vec{j} = -M\nabla\mu \quad \text{with} \quad \mu := \frac{dU}{dc} \qquad \rightarrow \qquad \vec{j} = -M\frac{d^2U}{dc^2}\nabla c$$

Since M is positive, thus $\vec{j}$ points in the direction of greatest decrease of concentration if $\dfrac{d^2U}{dc^2} > 0$ which is the case of standard diffusion. In general, under this specific $\vec{j}$ it can be said that

$$\frac{d^2U}{dc^2}\begin{cases} > 0 & c \text{ is minimum} \quad \textit{(standard diffusion)} \\ < 0 & c \text{ is maximum} \quad \textit{(spinoidal decomposition)} \\ = 0 & c \text{ is saddle} \quad \textit{(equilibrium)} \end{cases} \tag{3.20}$$

where we recall according to A. D. [1997], the process of *spinoidal decomposition* to be "a clustering reaction in a homogeneous, supersaturated solution (solid or liquid) which is unstable against infinitesimal fluctuations in density or composition. The solution therefore separates spontaneously into two phases, starting with small fluctuations and proceeding with a decrease in the Gibbs energy without a nucleation barrier".

Variation of $\vec{j}$: Finally the second variation of $\vec{j}$, shows a similar dependence as the second variation of $\dot{c}$, but now, the dependence is with the dissipation potential

$$< D^2_{\vec{j}}\Pi_\lambda, \delta\vec{j}^2 >= \int_\tau \left[\int_\Omega \frac{d^2\chi}{d\vec{j}^2} dV\right] \delta\vec{j}^2 dt$$

However, thermodynamic consistency imposes a convex shape of χ^* as it will be shown in §3.2.2. Therefore, the second derivative of χ^* is positive, this gives a minimum condition on $\vec{j}$. This optimal condition on $\vec{j}$ is a way to ensure the entropy-like restriction is satisfied.

3.2.1.1 The different field variational formulations

As pointed out Felippa et al. [2001], coupled systems can be characterized by the number of different fields that appear in the first-level decomposition. Moreover, the functional in (3.16) satisfies our requirements to model a chemical diffusion problem equivalent to the SF in (3.1) or the equivalent WF in (3.5). Nevertheless, this is not the unique VF we can formulate to model the same system. We can easily reduce the number of fields on which the functional (3.16) depends upon. The field reductions are important since it makes the computations to solve the system easier. We must recall the SF and WF counterparts only solve for the concentration c as the unknown field.

3-Field variational form : We can rewrite the functional Π_λ in (3.16) by using the chemical potential instead of the lagrange multipliers and applying the divergence and Gauss theorem to the term containing $\nabla\vec{j}$. As a result, we get the *3-Field VF* shown below.

3-Field variational form

$$\{\vec{j}, \dot{c}, \mu\} = \arg \inf_{\vec{j},\dot{c}} \sup_{\mu} \Pi_3[\vec{j}, \dot{c}, \mu] \tag{3.21a}$$

$$\Pi_3[\dot{c}, \vec{j}, \mu] = \int_\tau \left[\int_\Omega \left(\dot{U} - \mu\dot{c} + \chi^*(c, \vec{j}) - \vec{g} \cdot \vec{j} + \mu f_c \right) dV - \int_{\partial_j \Omega} \mu \bar{j} dS \right] dt \tag{3.21b}$$

The physical insights gained by the derivation of the *3-field formulation* above which are missed in the SF and/or WF are the following.

1. The *massic flux* $\vec{j}$ and the *chemical field* $-\nabla\mu$ are conjugate variables. As conjugate variables they define a dissipation potential which must be convex in order to make the model thermodynamical consistent.
2. The *chemical potential* acts as a Lagrange multiplier. As a Lagrange multiplier, the chemical potential constraints the mass balance law to satisfy the mass action (constitutive) law.
3. The system can be easily interpreted in energy terms by the definition of the functional.

Notice that the physical insights, specially the first and second pose the physical problem in a mathematical framework. These are the keys to extrapolate the ideas from this uniphysic multifield problem to a general multiphysic coupled setting. However, this system contains two extra unknown fields to be solved, namely, μ and $\vec{j}$. Plus, $\vec{j}$ is not a scalar field bur rather a vector field. Therefore, to make the system more efficient to be solved we apply a field reduction to it. This reduction is given through the elimination of the massic flux $\vec{j}$.

2-Field variational form : The *2-Field variational form* is obtained by vanishing the massic flux as a needed field for the functional (3.21b). To do this job, we apply the Legendre-Fenchel transform as follows

$$\chi(\vec{g}, c) = \chi^*(c, \vec{j}) - \vec{g} \cdot \vec{j}$$

This equation exploits the fact that the chemical field is conjugate to the massic flux and the convexity of both χ and χ^*. Now the dissipation potential, depends only on the concentration and the chemical field, which is the negative gradient of the chemical potential. Using the substitution leads to the functional mentioned in (3.14)

2-Field variational form :

$$\{\dot{c}, \mu\} = \arg \inf_{\dot{c}} \sup_{\mu} \Pi_2[\dot{c}, \mu] \tag{3.22a}$$

$$\Pi_2[\dot{c}, \mu] = \int_\tau \left[\int_\Omega \left(\dot{U}(c) - \mu\dot{c} - \chi(\vec{g}, c) + \mu f_c \right) dV - \int_{\partial_j \Omega} \mu \bar{j} dS \right] dt \tag{3.22b}$$

The system above (3.22a) & (3.22b) has been presented earlier in the literature by Miehe et al. [2014]. Despite being the same model, they obtain the VF in a different manner. In general, they start from an analysis of forces taking into consideration the boundary conditions. The forces are used to postulate the existence of the potentials and by means of the Gauss law and divergence theorem they reconstruct the VF as shown in (3.22a) & (3.22b). In contrast, we have posed a constrained variational problem we

need to reduce to arrive to the same model. Computing the variations of (3.22b) we can observe that this reduction has the following implications.

1. We have lost the direct connection between $\vec{j}$ and $-\nabla\mu$. By taking the variations of the functional this insight can be inferred. However, we can not tell why does this relation arises.[4]
2. We lose the notion of the chemical potential as a Lagrange multiplier.
3. The system can be easily interpreted in energy terms by the definition of the functional.
4. The system becomes simpler to solve since we removed the massic flux $\vec{j}$ as an unknown. We are left with two scalar fields as unknowns.

Therefore, despite loosing some physical insights, there are no inconsistencies in what the model represents. This is a good compromise, since an easier to solve model becomes more useful. Hence, we will use this two field formulation as a starting point for the models we will develop in further chapters, but we will take as given principles the insights lost in the reduction.

1-Field variational form : A further field reduction can be made where only the chemical potential is the needed field to optimize. This leads to the *1-Field variational form* . Again, we use the Legendre-Fenchel transform but now on the rate of change of the internal energy as

$$\dot{U}^*(\mu) - \dot{\mu}c = \mu\dot{c} - \dot{U}(c)$$

and we substitute the concentration which appears after by the first derivative of the dual internal energy.

1-Field variational form

$$\{\mu\} = \arg\sup_{\mu} \Pi_1[\mu] \tag{3.23a}$$

$$\Pi_1[\mu] = \int_\tau \left[\int_\Omega \left(\dot{U}^*(\mu) - \dot{\mu}\frac{dU^*}{d\mu} - \chi(\vec{g}, \frac{dU^*}{d\mu}) + \mu f_c \right) dV - \int_{\partial_j\Omega} \mu\bar{j} dS \right] dt \tag{3.23b}$$

If we analyze the variations after this last field reductions, the problem can not be directly related any more to the SF in (3.1) nor the WF in (3.5).

3.2.2 Specification of the material

As mentioned through the definition of the potential functions U and χ we describe the specifics of our problem. To define the function of the internal energy $U(c)$, we use a constitutive law for the chemical potential μ in terms of the concentration c. For the dissipation potential $\chi(\vec{g})$, we use a constitutive law for the massic flux $\vec{j}$ in terms of the chemical field $\vec{g}$.

Two different materials are shown here, we refer to them as models. Each models, encloses a specific definition for the internal energy and dissipation potential. From those two models, one is the linear version of the other. We start by defining the linear model.

[4] ... unless we do the process of field reduction backwards, which makes non senses except that you already know what are you looking for

3.2.2.1 The Linear model

Internal energy : The mass action law derives from the internal energy potential since it describes a reversible process. The linear version of the logarithmic mass action law presented is

$$\mu = \mu_0 + \frac{RT}{c_0}(c - c_0) \tag{3.24}$$

As shown in (3.18), we know that μ is energetically-conjugated to c through the internal energy $U(c)$, in essence we have the relation $\mu \equiv \frac{dU}{dc}$. Thus, the integral of (3.24) with respect to c defines $U(c)$.

$$U(c) = \mu_0 c + \frac{1}{2}\frac{RT}{c_0}(c - c_0)^2\,; \qquad \frac{dU}{dc} = \mu_0 + \frac{RT}{c_0}(c - c_0)\,; \qquad \frac{d^2U}{dc^2} = \frac{RT}{c_0} \tag{3.25}$$

In the box above are displayed the internal energy obtained and its corresponding first two derivatives (recall the first derivative is the constitutive law).

Dissipation potential: To define the dissipation potential we need to make an incursion into thermodynamics as devised in the end of the last section.

Thermodynamic analysis To do the thermodynamic analysis, we start by analyzing the balance of mass equation.

$$\dot{c} + \nabla \cdot \vec{j} - f_c = 0 \tag{3.26}$$

by multiplying the above equation by the chemical potential and applying the divergence and Gauss' law we can get the following energy rate

$$\underbrace{\int_\Omega \mu \dot{c} dV}_{\dot{W}_{int}} - \left(\underbrace{\int_\Omega \mu f_c dV - \int_{\partial\Omega} \mu \vec{j} \cdot \vec{n} dS}_{\dot{W}_{ext}} \right) = - \underbrace{\int_\Omega -\nabla\mu \cdot \vec{j} dV}_{\mathcal{D}} \tag{3.27}$$

where the boundary term and the term on the right hand side have been obtained by using the divergence and Gauss theorems. The braces indicate whether the terms belong to the *internal energy rate* $\dot{W}_{int}$, the *external energy rate* $\dot{W}_{ext}$ or the *dissipation* $\mathcal{D}$.[5]. We can rewrite the equation above as

$$\dot{W}_{ext} - \dot{W}_{int} = \mathcal{D} \geq 0$$

To understand the last inequality we need to recall the following. Since we consider the chemical potential as the driving force for diffusion, when its gradient is zero it means that the system is in equilibrium. Now if the gradient is different from zero the system is out of equilibrium. In addition, we know from thermodynamics the difference between the external and internal energy rates of the system must be positive. This last statement imposes a condition on the dissipation $\mathcal{D}$. Recalling the chemical field is the negative gradient of the chemical potential $\vec{g} := -\nabla\mu$, plus the fact that the chemical field and the massic flux $\vec{j}$

[5]The existence of the *dissipation* $\mathcal{D}$ can be regard as an emergent properties of the system, do to its global nature in variables like $-\nabla\mu$ and $\vec{j}$

are energetically-conjugated. The next equation for the dissipation $\mathcal{D}$ follows from these statements

$$\mathcal{D} = \vec{j} \cdot \vec{g} = \frac{\partial \chi}{\partial \vec{g}} \cdot \vec{g} \geq 0 \tag{3.28}$$

Equation (3.28) imposes a condition on χ which can be satisfied by χ being convex. The same thought can also be used to construct the dual function χ^* which is mathematically consistent since the dual function of a convex function is itself convex.

As a remark, the inequality in (3.28) can be regarded as an entropy-like condition. This condition ensures the solution we obtain from the equations is physically meaningful. This thermodynamic analysis is independent of the model we aim to describe. Now, the simplest constitutive law satisfying (3.28) is a linear relation between massic flux and chemical field

$$\vec{j} = D_\mu \vec{g} \tag{3.29}$$

restricting $D_\mu > 0$. Since $\vec{g}$ and $\vec{j}$ are energetically conjugated through the dissipation potential, in essence $\vec{j} \equiv \frac{d\chi}{d\vec{g}}$. Integrating with respect to $\vec{g}$ we can construct χ which is shown below along with its two partial derivatives.

$$\chi(\vec{g}, c) = \frac{D_\mu}{2} \vec{g} \cdot \vec{g}; \qquad \frac{\partial \chi}{\partial \vec{g}} = D_\mu \vec{g}; \qquad \frac{\partial^2 \chi}{\partial \vec{g}^2} = D_\mu \tag{3.30}$$

A further property of the dissipation potential is that it can be seen as the function which leads the system to its steady state. This result arises from constraining the initial functional (4.4) to a steady conservation law. Both constitutive relations (3.25) and (3.29) are linear functions. The corresponding set of the two functions derived from them (3.25) and (3.30) form what we call the *linear model* of chemical diffusion.

3.2.2.2 The Fickean model

The next model is the non linear version of the linear model above. The main difference is the selection of the mass action law as detailed next.

Internal energy : In contrast with the linear model, to define the internal energy we use the logarithmic mass action law (5.18) displayed again below

$$\mu = \mu_0 + RT \ln\left(\frac{c}{c_0}\right) \qquad \text{Logarithmic mass action law}$$

Again, since we know μ and c are energetically-conjugated which is a material independent property, integrating with respect to c the equation (5.18) defines the corresponding internal energy.

$$U(c) = \mu_0 c + RT\left[c \ln\left(\frac{c}{c_0}\right) - c + c_0\right]; \qquad \frac{dU}{dc} = \mu_0 + RT \ln\left(\frac{c}{c_0}\right); \qquad \frac{d^2U}{dc^2} = \frac{RT}{c} \tag{3.31}$$

The box above describes the corresponding internal energy along with its two first derivatives.

The dissipation potential Now that we know that χ must be convex with respect to $\vec{g}$ −as constrained in (3.28)−, the only thing left to characterize the dissipation potential is to find a constitutive law which is in agreement with the condition (3.28). Another option for the constitutive law is to use the following relation from [Feynman et al., 1963]

$$\vec{j} = -cM\nabla\mu = cM\vec{g} \equiv \frac{\partial\chi}{\partial\vec{g}} \tag{3.32}$$

where c is the concentration and M is the mobility, both parameters are non-negative, thus this constitutive law is in agreement with (3.28). Using this relation the dissipation potential which can be derived is

$$\chi(\vec{g}, c) = \frac{cM}{2}\vec{g}\cdot\vec{g}; \qquad \frac{\partial\chi}{\partial\vec{g}} = cM\vec{g}; \qquad \frac{\partial^2\chi}{\partial\vec{g}^2} = cM \tag{3.33}$$

where as in the linear model, we have exploited the fact that $\vec{g}$ and $\vec{j}$ are energetically-conjugated.

The functions defined in (3.31) and (3.33) defined what we call the *Fickean model*. The choice for this name resides in the relation the constitutive laws (3.32) and (5.18), hold with Fick's first law (3.1a), in specific with its diffusion parameter D.

3.2.2.3 Relation between models and the diffusion parameter D

Fickean model : The diffusion parameter D appearing in Fick's first law (3.1a) encloses information from the constitutive laws for the chemical potential μ and the massic flux $\vec{j}$. Focusing on the *Fickean model*, starting from (3.32) we get

$$\begin{aligned}
\vec{j} &= cM\vec{g} && \because && (\vec{g} := -\nabla\mu)\\
&= -cM\nabla\mu && \because && \text{(taking the gradient from (3.31).b and substituting)}\\
&= -cM\frac{RT}{c}\nabla c && \therefore \iff && (D \equiv MRT)\\
&= D\nabla c
\end{aligned}$$

the process above shows the equivalence between the diffusion parameter D and the terms MRT, where the mobility M comes from the constitutive law for $\vec{j}$ in (3.32) and the parameters R and T − gas constant and temperature correspondingly− come from the constitutive law for μ (3.31).b . Since R is an universal parameter −independent of the substance being described− and we are considering T as constant, thus the information of the material is enclosed in D as in M through the equivalence $D \equiv MRT$. The fact that the parameter D encompass the information from the parameters in the constitutive laws (3.32) and (3.31).b gives the *Fickean model* its name.

Linear model: The relation of D is not exclusive of the Fickean model, it can also be related to the linear model starting from (3.29) as follows.

$$\begin{aligned}
\vec{j} &= D_\mu\vec{g} && \because && (\vec{g} := -\nabla\mu)\\
&= -D_\mu\nabla\mu && \because && \text{(taking the gradient from (3.25).b and substituting)}\\
&= -D_\mu\frac{RT}{c_0}\nabla c && \therefore \iff && (D \equiv D_\mu\frac{RT}{c_0})\\
&= D\nabla c
\end{aligned}$$

In this model D again contains information from the parameters in the constitutive laws (3.25) and (3.29). However, it also contains an extra dependency with the initial values of the concentration c_0, whereas on the Fickean model, it is completely independent of any field.

3.2.2.4 Dual Functions

Now with the internal energy and the dissipation potential defined. We can derive their corresponding dual functions. The benefit of knowing the dual functions is to explore the different field formulations of the VF as derived in §3.2.1.1. To get the internal energy dual functions, we use the Legendre-Fenchel transform.

$$U^*(\mu) = \sup_c \{\mu c - U(c)\}$$

The corresponding functions and its two first derivatives are shown below for each model.

Dual Internal Energy → Linear model

$$\begin{aligned} &U^*(\mu) = (\mu - \mu_0)c_0 + \frac{1}{2}\frac{c_0}{RT}(\mu - \mu_0)^2; \\ &\frac{dU^*}{d\mu} = c_0 + \frac{c_0}{RT}(\mu - \mu_0); \qquad \frac{d^2U^*}{d\mu^2} = \frac{c_0}{RT} \end{aligned} \tag{3.34}$$

Dual Internal Energy → Fickean model

$$\begin{aligned} &U^*(\mu) = RTc_0\left[\exp\left(\frac{\mu - \mu_0}{RT}\right) - 1\right]; \\ &\frac{dU^*}{d\mu} = c_0 \exp\left(\frac{\mu - \mu_0}{RT}\right); \qquad \frac{d^2U^*}{d\mu^2} = \frac{c_0}{RT}\exp\left(\frac{\mu - \mu_0}{RT}\right) \end{aligned} \tag{3.35}$$

As it is for the dual dissipation potential, we use the following Legendre-Fenchel transform.

$$\chi^*(\vec{j}) = \sup_{\vec{g}} \{\vec{j} \cdot \vec{g} - \chi(\vec{g}, c)\}$$

where for each model we have

Dual Dissipation potential → Linear model

$$\chi^*(\vec{j}, c) = \frac{1}{2D_\mu}\vec{j} \cdot \vec{j}; \qquad \frac{\partial \chi^*}{\partial \vec{j}} = \frac{1}{D_\mu}\vec{g}; \qquad \frac{\partial^2 \chi^*}{\partial \vec{j}^2} = \frac{1}{D_\mu} \tag{3.36}$$

Dual Dissipation potential → Fickean model

$$\chi^*(\vec{j},c)=\frac{1}{2cM}\vec{j}\cdot\vec{j};\qquad \frac{\partial\chi^*}{\partial\vec{j}}=\frac{1}{cM}\vec{j};\qquad \frac{\partial^2\chi^*}{\partial\vec{j}^2}=\frac{1}{cM} \tag{3.37}$$

3.2.2.5 Material Models

As a summary, we have set up two different models. A non-linear model constituted by the logarithmic mass action law for the internal energy and Fick's first law for the dissipation. We refer to this model as the *Fickean model*.

Fickean Model

Internal energy

$$U(c)=\mu_0 c+RT\left[c\ln\left(\frac{c}{c_0}\right)-c+c_0\right]$$
$$\frac{dU}{dc}=\mu_0+RT\ln\left(\frac{c}{c_0}\right)$$
$$\frac{d^2U}{dc^2}=\frac{RT}{c}$$

Dissipation Potential

$$\chi(\vec{g},c)=\frac{1}{2}\frac{D}{RT}c\vec{g}\cdot\vec{g}$$
$$\frac{\partial\chi}{\partial\vec{g}}=\frac{D}{RT}c\vec{g}$$
$$\frac{\partial^2\chi}{\partial\vec{g}^2}=\frac{D}{RT}c$$

The second model is the linear counterpart of the Fickean model, and we refer to it as the *linear model*.

Linear Model

Internal energy

$$U(c)=\mu_0 c+\frac{1}{2}\frac{RT}{c_0}(c-c_0)^2$$
$$\frac{dU}{dc}=\mu_0+\frac{RT}{c_0}(c-c_0)$$
$$\frac{d^2U}{dc^2}=\frac{RT}{c_0}$$

Dissipation Potential

$$\chi(\vec{g},c)=\frac{1}{2}\frac{D}{RT}c_0\vec{g}\cdot\vec{g}$$
$$\frac{\partial\chi}{\partial\vec{g}}=\frac{D}{RT}c_0\vec{g}$$
$$\frac{\partial^2\chi}{\partial\vec{g}^2}=\frac{D}{RT}c_0$$

The choice between primal and dual functions can be selected in accordance to the field formulation chosen (see §3.2.1.1). We choose to present this selection as it is the one corresponding to the 2-Field VF shown in(3.22). We recall the justification to retain the 2-Field formulation is presented in §3.2.1.1.

Finally, we should highlight that both models, still solve Fick's first law (3.1a). This can be verified by defining $\vec{g}\equiv-\nabla\mu$ in each model and substituting it into $\vec{j}\equiv\frac{\partial\chi}{\partial\vec{g}}$. Thus in both models, the dynamics of c is the same independent of the model selected. This assertion can be corroborated through numerical simulation, for this, we need to make the VF discrete.

3.3 The discrete variational form

So far we have derived a complete VF for the problem of chemical diffusion. This formulation is taken in the continuum setting for time and space. Unfortunately, the analytical solution is often hard to find or non-existent. In order to make the formulation useful, we need to move them from a continuum to a discrete setting were computers can be used to obtain a solution. In general, these problems need to be dealt in time and space we need to make both domains discrete. This section presents the process chosen to make time and space discrete, followed up by a summary on the consistency between the continuum and discrete formulations.

As justified in §3.2.1.1 the 2-Field formulation is going to be the one we are using for the rest of the chapter, however, the developments we show are applicable also for the for the 3-Field or 1-Field VF.

3.3.1 Time discretization

To make time discrete, we approximate the integrand and time integral in (3.22b) through n time steps, using implicit finite difference approximations. Thus, we obtain the following *implicit time discretization*

$$\begin{aligned}\Pi_2[c_{n+1},\mu_{n+1}] =& \sum_{i=1}^{n}\Bigg[\int_\Omega\left(\frac{\Delta U}{\Delta t}-\mu_{n+1}\frac{\Delta c}{\Delta t}-\chi(\vec{g}_{n+1},c_{n+1})+\mu_{n+1}f_c(t_{n+1})\right)dV-\\ &\int_{\partial_j\Omega}\mu_{n+1}\bar{j}_{n+1}dS\Bigg]\Delta t\\ =&\sum_{i=1}^{n}\Pi_2^n[\mu_{n+1},c_{n+1}]\end{aligned}\tag{3.42}$$

where the Δ operator, is the *time difference operator*, in essence, $\Delta U := U(c_{n+1}) - U(c_n)$, or, $\Delta t := t_{n+1} - t_n$. As it can be seen, this changes the problem into n different problems, each one corresponding with one of the n partitions of time. The functional *incremental functional*[6] Π_2^n which we refer as the *incremental variational formulation* is defined as

$$\begin{aligned}\Pi_2^n[\mu_{n+1},c_{n+1}] :=& \int_\Omega\left(\Delta U-\mu_{n+1}\Delta c-\Delta t\chi(\vec{g}_{n+1},c_{n+1})+\Delta t\mu_{n+1}f_c(t_{n+1})\right)dV\\ &-\int_{\partial_j\Omega}\Delta t\mu_{n+1}\bar{j}_{n+1}dS\end{aligned}\tag{3.43}$$

This choice is not the only way to make time discrete in a variational approach, but due to its simplicity we are going to use it for the numerical implementation.

3.3.2 Space discretization

To make fully discrete the incremental VF (6.13c), we need to make space discrete too. For this end, we use a classical finite element approach due to its flexibility for numerical implementation. Therefore, in accordance to the solution space we have defined the fields, we select its spatial discrete form. One

[6] Yang et al. [2006]

plausible option by looking the spatial dependencies in(3.22b) is

$$c \in L_2 \qquad \rightarrow \qquad c(\vec{x},t) \approx \sum_{\forall q} S_q(\vec{x}) c_h^{\{q\}} \tag{3.44a}$$

$$\mu \in \mathcal{V}_\mu := \{\mu \in H^1 \,|\, \mu = \overline{\mu} \quad \forall \vec{x} \in \partial_\mu \Omega\}$$
$$\rightarrow \qquad \mu(\vec{x},t) \approx \sum_{\forall a} S_a(\vec{x}) \mu_h^{\{a\}} \tag{3.44b}$$

where $S_a(\vec{x})$ is any shape function. The index $^{\{a\}}$ and $^{\{q\}}$ denotes a spatial node on the mesh.

Different discrete version can be defined, as an example, we can also take

$$c \in \mathcal{V}_c := \{c \in H^1 | c = \overline{c} \forall \vec{x} \in \partial_\mu \Omega\} \qquad \rightarrow \qquad c(\vec{x},t) \approx \sum_{\forall a} S_a(\vec{x}) c_h^{\{a\}} \tag{3.45a}$$

$$\mu \in \mathcal{V}_\mu := \{\mu \in H^1 \,|\, \mu = \frac{dU}{dc}\Big|_{\overline{c}}; \quad \forall \vec{x} \in \partial_\mu \Omega\} \qquad \rightarrow \qquad \mu(\vec{x},t) \approx \sum_{\forall a} S_a(\vec{x}) \mu_h^{\{a\}} \tag{3.45b}$$

Notice that this formulation also allows different solution spaces −and hence discrete forms− for the two variables.

3.3.3 Consistency with the continuum formulation

Now that we have moved the VF from the continuum to the discrete setting we must check if this transition has raised artifacts on our model. To check this, we apply and analyze the first variations now to the discrete version of the model. To avoid an overload notation, from this point forward all variables are consider to be discrete in space and time, hence, we remove correspondingly the sub-index $_h$ and $_{n+1}$ denoting the mentioned discretization. Only the sub-index $_n$ will be kept to differentiate between different time steps. When the notation is hold is to make an emphasis on the discrete form.

First Variations : As in the continuum case, we set the first variations of the functional to zero since we want to optimize the functional.

Variation of μ_h : The variations of the discrete chemical potential lead to

$$< D_\mu \Pi_2^n, \delta\mu > \equiv 0 \qquad \Rightarrow \qquad \begin{cases} c_{n+1} = -\nabla \cdot \frac{\partial \chi}{\partial \vec{g}} + f_c(t) & \forall \vec{x} \in \Omega_h \\ \overline{\vec{j}} = \frac{\partial \chi}{\partial \vec{g}}\Big|_{\vec{g},c} \cdot \vec{n} & \forall \vec{x} \in \partial_j \Omega_h \end{cases}$$

This variation, recalling the equivalence $\vec{j} \equiv \frac{\partial \chi}{\partial \vec{g}}$, is nothing more than the discrete conservation law and flux condition. Hence, as for μ_h concerns, there exists a consistency with its continuum counterpart.

Variation of c_h : The variations with respect to c_h leads to

$$< D_{\dot{c}} \Pi_2^n, \delta\dot{c} > \equiv 0 \qquad \Rightarrow \qquad \left\{\mu = \frac{dG}{dc}\Big|_c - \Delta t \frac{\partial \chi}{\partial c}\Big|_{\vec{g},c} \quad \forall \vec{x} \in \Omega_h \right. \tag{3.46}$$

this outcome in comparison with its continuum counterpart (3.18) suffers a modification with the addition of the second term. The expression is consistent as $\Delta t \to 0$. One way to remove this extra term, is to evaluate the concentration in the dissipation potential at times t_n for the concentration.

2-Field discrete variational form (Semi-Implicit scheme):

$$\{c,\mu\} = \arg\inf_{c}\sup_{\mu}\Pi_2^{SI}[c,\mu] \tag{3.47a}$$

$$\Pi_2^{SI}[c,\mu] = \int_{\Omega_h}\Big(\Delta U - \mu\Delta c - \Delta t\chi(\vec{g},c_n) + \ldots \\ \ldots + \Delta t\mu f_c(t)\Big)dV - \int_{\partial_j\Omega_h}\Delta t\mu\bar{j}dS \tag{3.47b}$$

By doing so, the system we are solving is not a fully implicit scheme any more, it becomes *semi-implicit*. However, we can still define the parameter c at c_{n+1} within the diffusion potential χ. Thus, we define a fully implicit scheme as

2-Field discrete variational form (Fully-Implicit scheme):

$$\{c,\mu\} = \arg\inf_{c}\sup_{\mu}\Pi_2^{FI}[c,\mu] \tag{3.48a}$$

$$\Pi_2^{FI}[c,\mu] = \int_{\Omega_h}\Big(\Delta U - \mu\Delta c - \Delta t\chi(\vec{g},c) + \ldots \\ \ldots + \Delta t\mu f_c(t)\Big)dV - \int_{\partial_j\Omega_h}\Delta t\mu\bar{j}dS \tag{3.48b}$$

where we have change the color on the dependence on c of χ, to recall that this term makes reference to the concentration, while the rest c terms come up from the finite difference approximation of the rate of concentration.

3.3.4 Setting for the numerical non-linear solver

In the more general case we are dealing with a non-linear problem. We need to set-up a non-linear solver to it. For this end, one of the most direct algorithms we can use is the *Newton Method*.

Newton Method The Newton Method algorithm help us transform the discrete nonlinear optimization problem we have set in (3.47) or in (3.48), −the semi-implicit and fully-implicit schemes respectively− into a sequence of linear algebra problems, suitable to solve for a computer. Using as an example the *fully implicit two-Field VF* (3.48), the needed *residual vector* $\mathbf{R}$ and the *tangent matrix* $\mathbf{T}$ are constructed through the following block-matrix form

$$\underbrace{\begin{bmatrix}\mathbb{T}_{\mu\mu} & \mathbb{T}_{\mu c}\\ \mathbb{T}_{c\mu} & \mathbb{T}_{cc}\end{bmatrix}}_{=:\mathbf{T}}\begin{bmatrix}\hat{\Delta}\mu\\ \hat{\Delta}c\end{bmatrix} = -\underbrace{\begin{bmatrix}\mathbb{R}_{\mu}\\ \mathbb{R}_{c}\end{bmatrix}}_{=:\mathbf{R}} \tag{3.49}$$

where the corrections in each field are denoted by the operator $\hat{\Delta}$. Each block subindex denotes the field which we need to variate to define the block. In addition, due to the continuity in Π_2^{FI} the above matrix

[**T**] is symmetric (cf. Schwarz's theorem [Stewart, 2015]). We use the variations to obtain **R** and **T**. Thus, the specific form of each block is detailed below

$$\mathbb{R}_{\mu}^{(a)} := \frac{\partial \Pi_2^{FI}}{\partial \mu^{(a)}} = \int_{\Omega_h} \Big[-\Delta c \quad S^{(a)} \Big] \, dV + \int_{\Omega_h} \left[\Delta t \frac{\partial \chi}{\partial \vec{g}} \cdot \nabla S^{(a)} \right] dV \tag{3.50a}$$

$$\mathbb{R}_{c}^{(a)} := \frac{\partial \Pi_2^{FI}}{\partial c^{(a)}} = \int_{\Omega_h} \left[- \left(\frac{dU}{dc} - \mu \right) \, S^{(a)} \right] dV \tag{3.50b}$$

$$\mathbb{T}_{\mu\mu}^{(a,b)} := \frac{\partial \mathbb{R}_{\mu}^{(a)}}{\partial \mu^{(b)}} = \int_{\Omega_h} \left[- \left(\Delta t \frac{\partial^2 \chi}{\partial \vec{g}^2} \right) \, : \, \nabla S^{(a)} \otimes \nabla S^{(b)} \right] dV \tag{3.50c}$$

$$\mathbb{T}_{cc}^{(a,b)} := \frac{\partial \mathbb{R}_{c}^{(a)}}{\partial c^{(b)}} = \int_{\Omega_h} \left[- \left(\frac{\partial^2 U}{\partial c^2} \right) \, S^{(a)} S^{(b)} \right] dV \tag{3.50d}$$

$$\mathbb{T}_{\mu c}^{(a,b)} := \frac{\partial \mathbb{R}_{\mu}^{(a)}}{\partial c^{(b)}} = \int_{\Omega_h} \Big[-S^{(a)} S^{(b)} \Big] \, dV \tag{3.50e}$$

$$\mathbb{T}_{c\mu}^{(a,b)} := \frac{\partial \mathbb{R}_{c}^{(a)}}{\partial \mu^{(b)}} = \int_{\Omega_h} \Big[-S^{(a)} S^{(b)} \Big] \, dV \tag{3.50f}$$

The former can also be written in a more compact fashion using the notation introduced in (2.24) and (2.25) as

$$\mathbf{R} = \begin{bmatrix} \mathbb{S}_{\mu}^{(a)} \Big(-\Delta c + f_c \Big) + \nabla \mathbb{S}_{\mu}^{(a)} \Big(\Delta t \frac{\partial \chi}{\partial \vec{g}} \Big) \\ \mathbb{S}_{c}^{(a)} \Big(\frac{\partial U}{\partial c} - \mu \Big) \end{bmatrix} \tag{3.51a}$$

$$\mathbf{T} = \begin{bmatrix} -\mathbb{K}_{\mu\mu}^{(a,b)} \Big(\Delta t \frac{\partial^2 \chi}{\partial \vec{g}^2} \Big) & \mathbb{M}_{\mu c}^{(a,p)} \Big(-1 \Big) \\ \mathbb{M}_{c\mu}^{(p,a)} \Big(-1 \Big) & \mathbb{M}_{cc}^{(a,b)} \Big(\frac{\partial^2 U}{\partial c^2} \Big) \end{bmatrix} \tag{3.51b}$$

where the Neumann boundary conditions have their contributions in

$$\mathbf{R} = \begin{bmatrix} \Big[\mathbb{S}_{\mu}^{(a)} \Big(-\Delta t + \bar{j} \Big) \Big] \\ [\mathbb{O}] \end{bmatrix} \tag{3.52}$$

Implementation remarks . There are some implementation remarks which should be considered while implementing the algorithm. These remarks are listed below.

- **Errors in numerical integration :** Despite the solution being an approximation, theoretically numerical errors arising from the numerical integration can be vanished. From the tangent matrices in (3.50c) - (3.50f) it can be seen that the higher order polynomial to solve resides in the mass-matrix $\mathbb{T}_{cc}$ in (3.50d). Since the order of the quadrature is given by $p = 2q - 1$, being p the order of the polynomial and q the number of integration points. The order of the polynomial on $\mathbb{T}_{cc}$ is $p = N_p^2$, where N_p is the order of the element. Thus, to avoid some of the errors from the numerical integration we need to select the number of quadrature points given by

$$q = \left\lceil \frac{N_p^2 + 1}{2} \right\rceil$$

- **Negative concentration at integration points:** Concentration differences can be positive or negative, however, concentrations must be always positive. This point is specially important for the

non-linear Fickean model, where the concentration works as argument of a logarithm, see (3.31). However, negative concentration can arise as an artifact of interpolation, despite having positive concentration at the nodes. Quadratic elements in 1D, or quads in 2D can lead to this issue. To solve it, we can try two things: to evaluate the internal energy (3.31) at the nodes and interpolate it afterwards to avoid the negative arguments of the logarithm. Or, to use hierarchical shape functions, were locally negativity can be eliminated. In this work, we have obtained good results with the first option.

- **Negative concentration at nodes:** Negative concentration can also arise at the nodes while solving at the same time −monolithically− for the chemical potential and the concentration. This may happen due to the unfulfilled of the maximum and/or minimal principles. These principles, which naturally arise in the continuum setting from the nature of the PDE, are imposed as a condition in its discrete counterpart. When this condition is not satisfied, spurious oscillations may appear.

3.4 Numerical example: Initial-Dirichlet discontinuity

Due to the simplicity of the physics in this chapter, we conclude with a numerical example of *initial-Dirichlet discontinuity* which proves challenging to solve numerically due to the appearance of spurious oscillations even for implicit schemes. By doing this, we show how the proposed VF performs when compared with different formulations. The toy problems of *initial-Dirichlet discontinuity* have the property that the initial condition which we define to be constant along the entire domain Ω, is different that the values imposed at the Dirichlet boundaries $\partial_\mu\Omega$.

One of the chapter's goals is to present the basis for the numerical implementation using a VF. The data used to work the examples shown are the following

Parameter	**Value**	**Units**
$\overline{\mu}$	$-175.0 \cdot 10^{-3}$	$J\,mol^{-1}$ (Gibbs *"G"*)
μ_0	$-190.0 \cdot 10^{-3}$	$J\,mol^{-1}$ (Gibbs *"G"*)
c_0	Eq (3.25) or Eq (3.31)	mol m^{-3}
R	8.3144598	kg m^2 sec^{-2} K^{-1} mol^{-1}
T	298.0	K
D	$0.84 \cdot 10^{-9}$	m^2 sec^{-1}
L	$1.0 \cdot 10^{-3}$	m
t_f	1190.47619048	sec

Table 3.1: Table of parameters

*The values for c_0 are made through the models from the given equations.

3.4.1 1D Problem

We start by posing the problem in the SF. We will describe it and analyze some of the properties which are useful to evaluate the results. Afterwards, we will do the same for the WF and the proposed VF. Finally, we will present a comparison of the results obtained and discuss the results.

3.4.1.1 Strong Form

The strong form (SF) of the *initial-Dirichlet discontinuity* 1D problem to solve is defined as

Strong Form

Equations

$$\vec{j} = -D\nabla c \qquad \forall x \in \Omega \qquad (3.53a)$$

$$\dot{c} + \nabla \cdot \vec{j} = 0 \qquad \forall x \in \Omega \qquad (3.53b)$$

Conditions

$$\vec{j}(0,t) \cdot \vec{n} = 0 \qquad (3.54a)$$

$$c(L,t) = c_{ext} \qquad (3.54b)$$

$$c(x,0) = c_0 \quad \text{with} \quad c_0 \neq c_{ext} \qquad (3.54c)$$

with the spatial domain defined as $\Omega := [0, L]$ and temporal domain $\tau := [0, t_f]$, with $t_f := L^2/D$.

The definition for t_f is justified at the end of this section. The equations in (3.53a) to solve are Fick's laws which were already presented in (3.1). The boundary condition (3.54a) at the left of Ω imposes a zero flux condition. The condition (3.54b) sets a Dirichlet value for the concentration at the right. Finally (3.54c) the initial condition is defined as constant and stipulates a discontinuity between the Dirichlet and initial values.

The analytical solution for this problem can be found in Crank [1979]. Two results are presented: A trigonometrical-type solution which converges rapidly for large values of time t. See [Crank, 1979, p. 24]. [7]

$$\frac{c(x,t) - c_0}{c_{ext} - c_0} = \left(1 - \frac{4}{\pi} \sum_{m=0}^{\infty} \frac{(-1)^m}{2m+1} \exp\left(-D\left[\frac{(2m+1)\pi}{2L}\right]^2 t\right) \cos\frac{(2m+1)\pi x}{2L}\right) \qquad (3.55)$$

And another solution as series of error functions, which converges rapidly for all except large values of time t is [Crank, 1979, p. 22]

$$\frac{c(x,t) - c_0}{c_{ext} - c_0} = \sum_{m=0}^{\infty} (-1)^m \left(\operatorname{erfc}\frac{(2m+1)L - x}{2\sqrt{D\,t}} + \operatorname{erfc}\frac{(2m+1)L + x}{2\sqrt{D\,t}}\right) \qquad (3.56)$$

Figures 3.1 depict the analytical solution, using the values displayed in the table 3.1. The vertical axis is the concentration, while the orthogonal plane to it represents the temporal and spatial domain of the problem. A plane cutting each domain at half is presented for each figure for ease of visualization. Thus, the intersection between the solution and the plane in 3.1a describes the concentration's evolution at all times for $x = L/2$, while the intersection in 3.1b can be seen as a snapshot of the domain at time $t = t_f/2$;

Some useful notions and remarks from the analytic form are detailed in the list below.

- **PDE's class:** The class of PDE described by Fick's laws can be two: *elliptic* or *parabolic*. When the concentration is time independent, in essence, $\dot{c} \equiv 0$, the system is elliptic, while on the contrary the system is parabolic. Hence, *steady state* and *transient state* are a solution of the corresponding parabolic and elliptic PDEs.

[7] The *cosine* in the original formula is presented here instead with a *sine*, since the boundary conditions are interchanged in contrast with the books statement of the problem. Plus, the term on the left-hand side of the equation adjust the value for the desire range of concentrations.

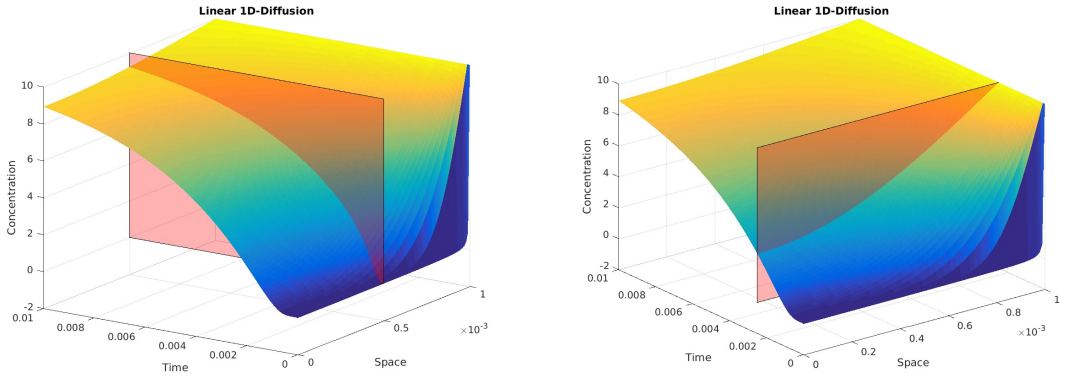

(a) Plane $x = L/2$ (b) Plane $t = t_f/2$

Figure 3.1: Analytical Solution for concentration.

- **Maximum principle :** The *maximum principle* is a solution property for elliptic and parabolic PDEs. Roughly it states that the maximum values of the system must be found in the boundary of the domain when sink, sources and initial conditions are homogeneous in the problem.
- **Time needed for the system to be steady :** From (3.55) by letting $t \equiv L^2/D$ the solution reaches approximately 89.2% of the steady solution (see [Crank, 1979, p. 24]). This fact is useful to define a meaningful temporal domain $0 \leq t < t_f := L^2/D$ with $t \in \tau$ for the transient behavior of the system.
- **Distance of penetration :** The *distance of penetration* x_l is the average length the substance has diffuse in a certain amount of time. This can be represented through the proportionality relation $x_l \propto 2\sqrt{Dt}$ as mentioned in [Crank, 1979, p. 38].

To conclude, we recall that to get the chemical potential μ with the SF, we do a post-process computation, in essence, solve for the concentration c and apply equations (5.18) or (3.24) afterwards.

3.4.1.2 Weak Form

For the WF we have used for time discretization the *generalized trapezoidal rule* and for spatial discretization classical FEM is used. For reference into this process see [Bergheau and Fortunier, 2010, Chapter 2,3,4], the similarity between heat conduction and diffusion makes some of the results obtained in the book applicable in our case. The matrix and residual vector are defined as

Weak Form

$$\mathbb{A}^{\{a,b\}} := \int_{\Omega_h} S^{\{a\}} S^{\{b\}} dx + \int_{\Omega_h} \Delta t \nu \nabla S^{\{a\}} \nabla S^{\{b\}} dx$$

$$\mathbb{R}^{\{a\}} := c_n \left(\int_{\Omega_h} \nabla S^{\{a\}} S^{\{b\}} dx - \int_{\Omega_h} \Delta t (1-\nu) \nabla S^{\{a\}} \nabla S^{\{b\}} dx \right)$$

where $\nu \in [0, 1]$ is the algorithm parameter. Letting $\nu \equiv 0$ gives an explicit scheme, while $\nu \equiv 1$ turns the system of equations into an implicit scheme.

Spurious oscillations may arise in the numerical solution of the problem. There are two type of spurious oscillations we can identify in this case. Each type imposes a lower or upper bound in the time step.

Time step - upper bound constraint: A stability analysis of the system rises the following condition (see [Bergheau and Fortunier, 2010, p. 122])

$$\Delta t \leq \Delta t_{max} \qquad \text{where} \qquad \Delta t_{max} := \frac{1}{(1-\nu)\alpha_{max}} \tag{3.57}$$

with α_{max} being the maximum eigenvalue of the system. It can be seen from (3.57) that for implicit schemes $\nu \equiv 1$, this oscillation has no impact on the solution. In contrast, for different values of ν this type of spurious oscillation have the effects as shown in the figure 3.2. Here we have implemented the Crank-Nicolson scheme, in essence $\nu \equiv 0.5$. It can be seen from the image 3.2 how this spurious oscillations mainly propagates through time, close to the Dirichlet boundary.

Time step - lower bound constraint: A second type of spurious oscillations may appear even in implicit schemes, imposing a lower bound constraint on the time step Δt. This type of spurious oscillations rises as a constraint needed in order to satisfy the discrete *maximum principle* of the PDEs. To derive the condition we check the relations needed to keep a monotonic solution. For a reference on the derivation see [Bergheau and Fortunier, 2010, p. 124]. Thus, the critical time step is given by

$$\Delta t > \Delta t_{min} \qquad \text{where} \qquad \Delta t_{min} := \frac{h_{min}^2}{6D\nu} \tag{3.58}$$

where h_{min} is the size of the smallest element. Figure 3.3 depicts how this oscillation appears as we cross the minimal time step Δt_{min} for an implicit scheme $\nu \equiv 1$. This type of spurious oscillations has a higher impact on the first time steps taken by the numerical solution. Figure 3.3 shows how the oscillation may appear in the first time step depending on the value selected for the time step dt.

3.4.1.3 Variational Form & comparison of results

Finally we solve the system using the proposed VF. The results obtained come from the fully-implicit scheme described in (3.48). In general we present two approaches to check the results, the behavior of the spurious oscillations and a couple of test to do a convergence analysis on the system.

Spurious oscillations :

The behavior of spurious oscillations is interesting because the field variables c and μ are conjugate variables in the VF, whereas in the weak form is a post-process relation. We explore whether conjugacy affects the behavior of spurious oscillations. Furthermore, we also explore the behavior of spurious oscillations for the two different VF models we have derived, namely, semi-implicit and fully implicit.

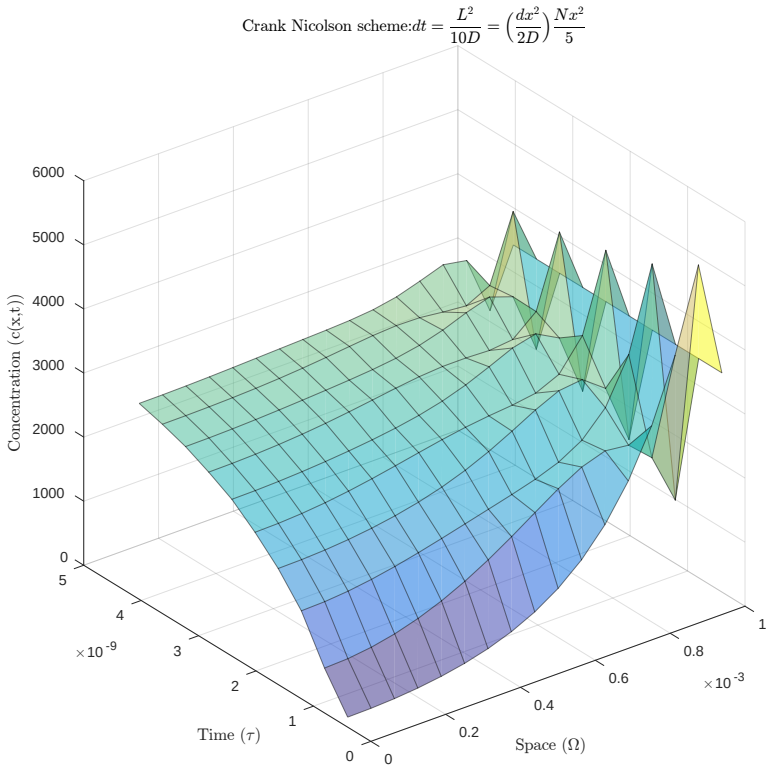

Figure 3.2: Crank-Nicolson scheme - Spurious oscillation (Δt_{max})

To perform the analysis, we consider the parameters in table 3.1 considering having $N_x = 50$ spatial elements. From here we define a threshold in the number of time steps N_t as a Deborah number [Reiner, 1964]. We consider a number N_t of equally spaced time steps. The duration is given by the constant time step Δt. These allows us to write the following relations

$$t_f = \Delta t\, N_t \qquad \Rightarrow \qquad N_t = \frac{t_f}{\Delta t} \tag{3.59}$$

where t_f is the final time prescribed for the simulation. The term on the right of (3.59) resembles the definition of the Deborah number under the right assumptions, meaning, t_f should represent a relaxation time whilst Δt the time taken for the observation. If we define t_f as $t_f := L^2/D$ [8] we can consider t_f as some relaxation time for the diffusion process, while Δt per se is the observation time.

Lower boundary spurious oscillation For the lower boundary of spurious oscillation, we have a minimum condition on Δt from (3.57). By allowing the equivalence $\Delta t \equiv t_{min}$ into (3.59) we get a threshold in the number of time steps to get spurious oscillations

$$Nt_{osc} := \frac{t_f}{t_{min}} = \frac{L^2/D}{(L/N_x)^2/(6D)} = 6N_x^2 \tag{3.60}$$

[8] as suggested when revising the strong form

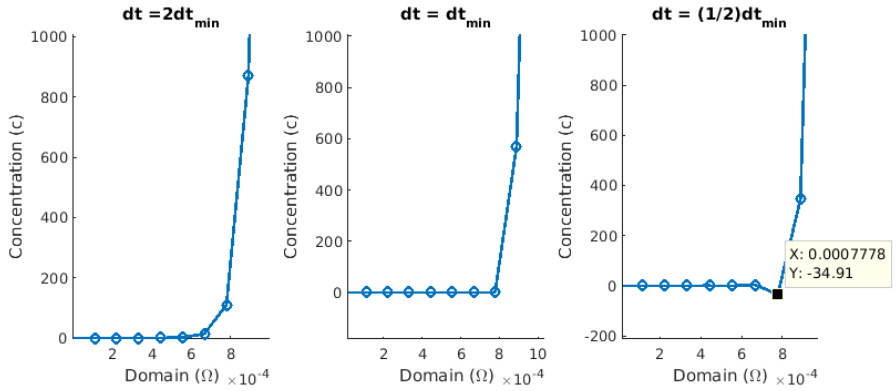

Figure 3.3: Implicit scheme - Spurious oscillation (Δt_{min})

when $N_t > 6N_x^2$ we can be sure that spurious oscillations will appear for the WF using linear elements.

Convergence analysis (description):

For the convergence analysis we need to measure the error of the numerical solution. Hence, we start by recalling the L_p and ℓ_p norms as:

$$L_p \text{ norm refers to} \qquad ||f(x)||_{L_p} := \left(\int_{\mathcal{V}} |f(x)|^p d\mathcal{V} \right)^{\frac{1}{p}} \tag{3.61a}$$

$$\ell_p \text{ norm refers to} \qquad ||f||_{\ell_p} := \left[\sum_{i=1}^{\infty} |f_i|^p \right]^{\frac{1}{p}} \tag{3.61b}$$

These norms will help us to measure the difference between numerical and analytical solutions. In addition, we need to compare the results coming from several runs or simulations. Since we are interested in the effects of the discrete model upon the solution, we will analyze runs for different number of time steps N_t and spatial elements N_x. Therefore, we define a couple of test for this task: Ω *fix* test and a *fix ratio* test. The Ω *fix* test, as the name suggests, keeps a fix number of elements N_x in the mesh while solving the system for a set of different time steps $N_t \in Nt_{list}$. The *fix ratio* test satisfies the relation $N_x = ratio\ N_t$, where *ratio* is a constant integer. This last test, changes the number of elements N_x, given a $N_t \in Nt_{list}$ keeping thus, the ratio N_x/N_t fix for all runs. The results obtained are summarized in the form of three different errors. The three errors we present for the Ω *fix* and *ratio fix* tests are: a L_2 relative error in the time step t_n, a L_1 relative error in time and finally a mean ℓ_1 relative error per time step.

L_2 relative error in the time step t_n : The L_2 relative error gives us the first result to compare the VF performance. This error is computed as

$$E_{\%y}(t_n) := \frac{||y_h - y||_{L_2}}{||y||_{L_2}} \tag{3.62}$$

where the sub-index $_y$ represents the field we are measuring the error from; being y_h the numerical solution and y the analytical solution. As it can be seen this error is time dependent. We compute the integral by Gaussian quadrature over the domain Ω, where the number of quadrature points are selected in accordance to the type of element used. By doing this we avoid further integration errors.

L_1 relative error in time : The results above show some of the convergence results expected from the discrete problem. Nevertheless, a lot of information is missing by only looking at the error in a given time step. In a attempt to take into account the errors in all the temporal domain τ, we define the L_1 relative error in time as

$$\hat{E}_{\%y} := ||E_{\%y}(t_n)||_{L_1} \tag{3.63}$$

where we are integrating over the temporal domain τ. To compute the integral the trapezoidal rule is used.

To see how meaningful this error is, imagine two different simulations giving the same result but having different time steps which are proportional. From this we would expect to have the same error outcome. One simulation has as time step $dt_1 = dt$ and the other one $dt_2 = 2dt$. At the nodal points they have in common in time we see the same error, however, if we integrate in time the error, the simulation having finer time step $-dt_1-$ will only have the same value as the other one, if the sample in between is the average of the nodes after and before it.

Mean ℓ_1 relative error per time step : To avoid the problems of the previous norm, we use the mean ℓ_1 norm, this means, we divide the ℓ_1 error by the number of time steps N_t taken by each simulation. We define it as

$$\tilde{E}_{\%y} := \frac{||E_{\%y}||_{\ell_1}}{N_t} \tag{3.64}$$

This approach gives impartial errors using the same thought experiment as before.

Convergence analysis (results):

The parameters used for the simulations are displayed in the table 3.1. The collection of time steps Nt_{list} we use to define the tests is $Nt_{list} := \{2^3, 2^4, \ldots, 2^{13}\}$. The results are present through a set of different plots, which will have the following format

Plot description

Subplots
The format of the following figures is as follows. The figure is divided into 1x2 subplots corresponding to the concentration (left) and chemical potential (right) errors.

Axis
The *horizontal axis* shows the time step, thus its units are seconds (s), while the *vertical axis* displays the corresponding error norm.

Annotations
The numbers between each segment of the curves, represent the slope at that segment.

Legends

Type of Strategy + Strategy's Name + Scheme + Model

where for now these are defined as follows

$$\begin{aligned} \text{Type of Strategy} &:= \{\text{Monolithic(Mono)}\} \\ \text{Strategy's Name} &:= \{\text{Newton Method(NM)}\} \\ \text{Scheme} &:= \{\text{Fully Implicit (FI), Semi-Implicit (SI)}\} \\ \text{Model} &:= \{\text{Linear(Lin), Fickean(Fick)}\} \end{aligned}$$

L_2 relative error in the time step t_n: The first plots presented in figures 3.4 & 3.5 display the convergence for the Linear and Fickean model correspondingly, using the L_2 relative error in the time step $t_n \equiv t_f$. The plots in the upper part of the page 3.4a & 3.5a show the results for the simulations under the *Omega fix* text (with $N_x = 512$) whilst the lower plots 3.4b & 3.5b are for the *Ratio fix test* (with $ratio = 1$).

From figure 3.4, we can see that for the linear model we have the expected convergence rate of one, since we made the functional discrete in time using an implicit scheme. In either the semi-implicit (3.47) and fully-implicit (3.48) schemes, the error is the same. The same can be said for the type elements − linear or quadratic −. The only remark to be done here where a difference can be perceived is in the size of the error between concentration and chemical potential. In this case, we observe the error of the chemical potential is one order less than that of the concentration, fact which can not be achieved using a post-process relation. As it is for the Fickean model in figure 3.5, we also have a convergence rate of one, however, a distinction between *semi-implicit* and *fully-implicit* is observed in the Fickean model. The samples taken for the fully-implicit scheme have a lower y-intercept on the error and reach the convergence of one faster. The semi-implicit scheme seems to have a slight concavity by looking at its slopes under the both tests. Still, the main difference resides on the scheme used, the type of element seems not to play a major role. A difference on the order of the error between chemical potential and concentration can also be observed, but now, the difference is that of two order of magnitude. A final comparison between errors in the linear and Fickean model, shows that the error for the chemical potential is the same despite the problem being linear or non-linear, in contrast with the concentration where the order of magnitude increases by an order of one for the non-linear (Fickean) model.

L_1 relative error in time: The next results in figures 3.6 & 3.7 display the convergence for the Linear and Fickean model correspondingly, using the L_1 relative error in time. Again, the plots in the upper part of the page 3.6a & 3.7a show the results for the simulations under the *Omega fix* text (with $N_x = 512$) whilst the lower plots 3.6b & 3.7b are for the *Ratio fix test* (with $ratio = 1$).

For the linear model there is not much to be said if we compare the type of scheme −fully-implicit or semi-implicit−, or the type of element −linear or quadratic−, or magnitude of the errors. The analysis of the Fickean model give us more things to say under this new error measure. The difference between schemes, and type of elements still hold in comparison with the previous error. But, the magnitude of the errors has changed, now the concentration and chemical potential only differs by one order of magnitude. Another fact worth noticing is the decrease of the slope in the convergence plot, however, this is explained by the initial discontinuity of the problem.

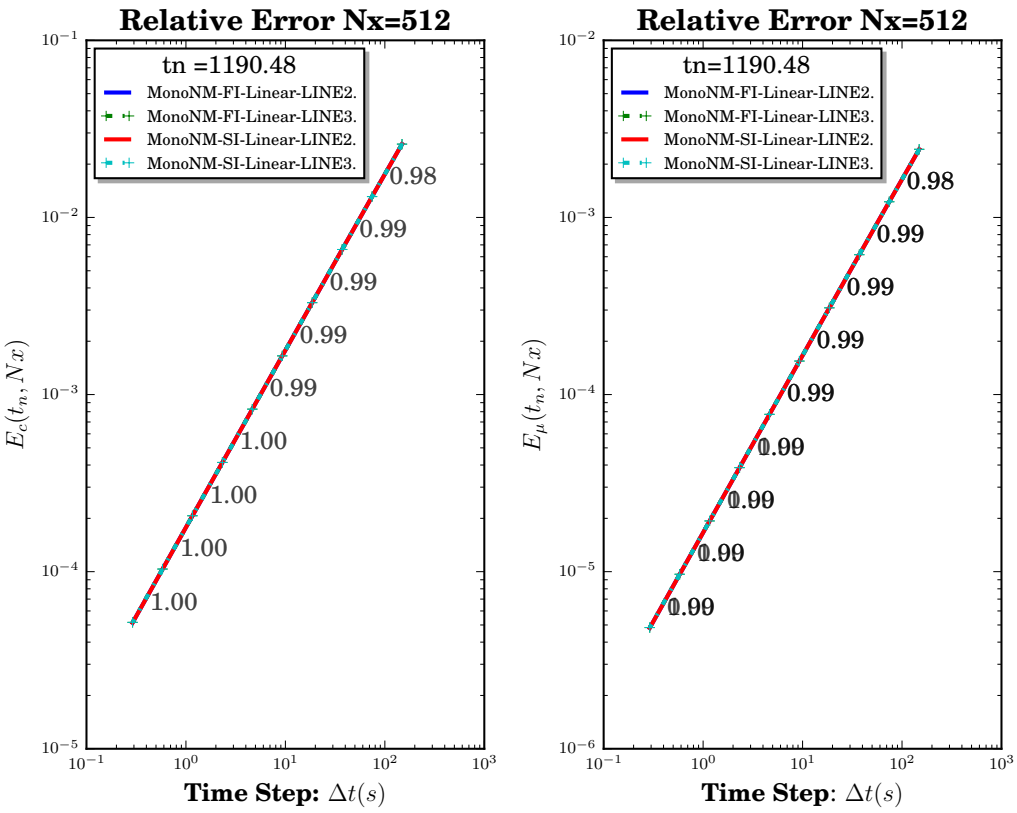

(a) Omega fix test: $N_x = 512$

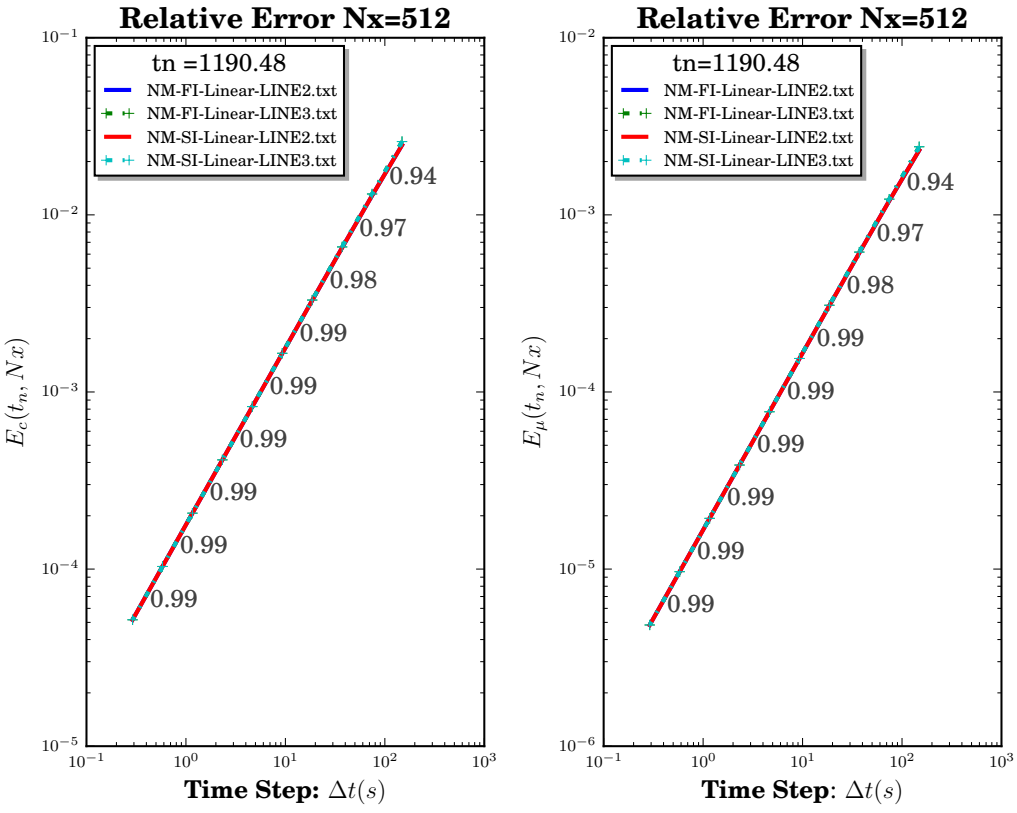

(b) Fix ratio test : $ratio = 1$

Figure 3.4: Tests for the Linear model
with $Nt_{list} = \{2^3, 2^4, \ldots, 2^13\}$

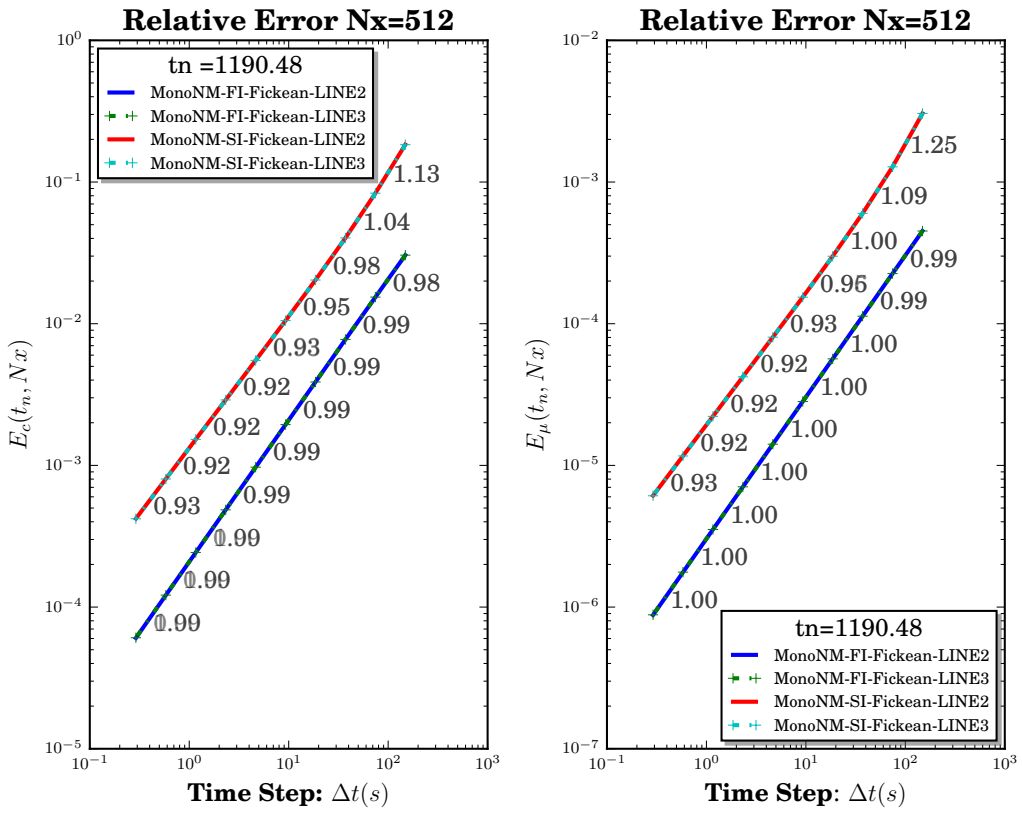

(a) Omega Fix Test: $N_x = 512$

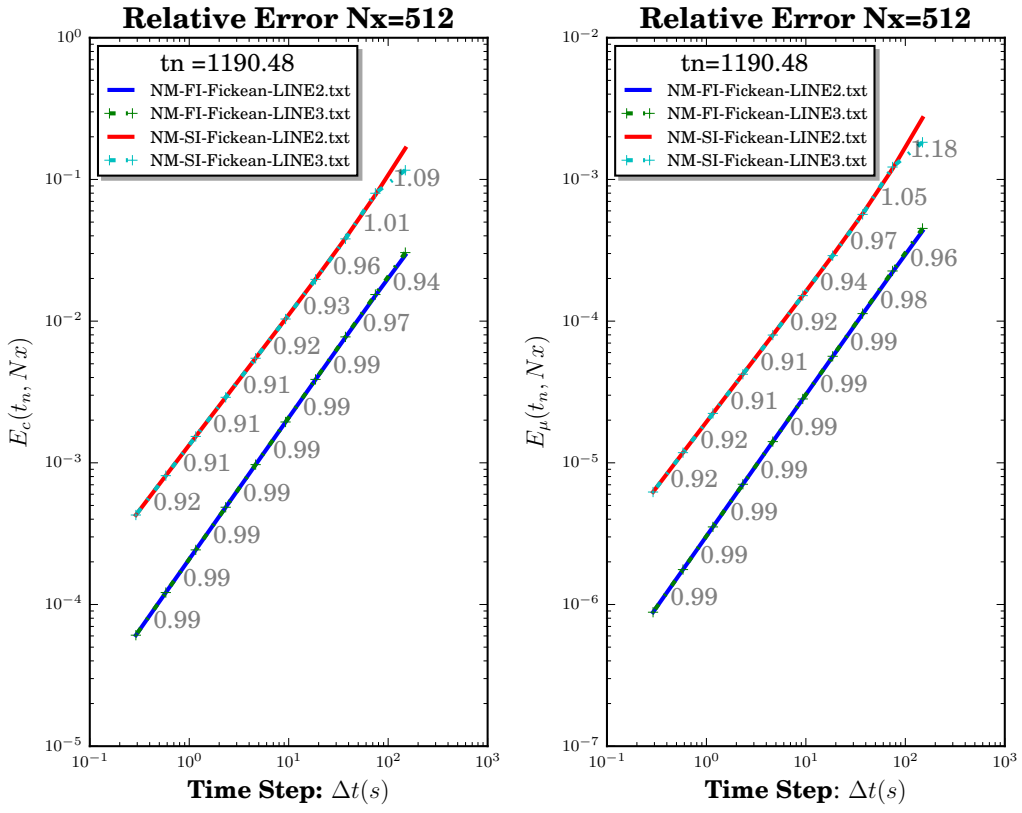

(b) Ratio Fix test: $ratio = 1$

Figure 3.5: Tests for the Fickean model
with $Nt_{list} = \{2^3, 2^4, \ldots, 2^13\}$

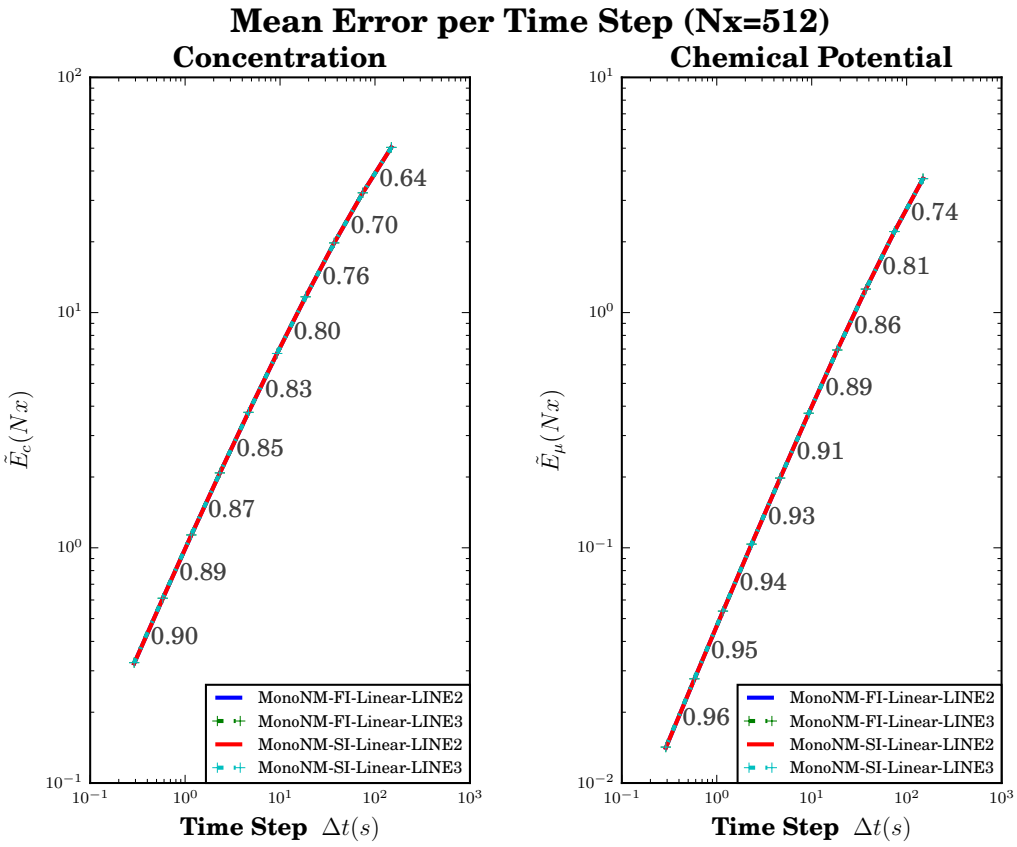

(a) Omega fix test: $N_x = 512$

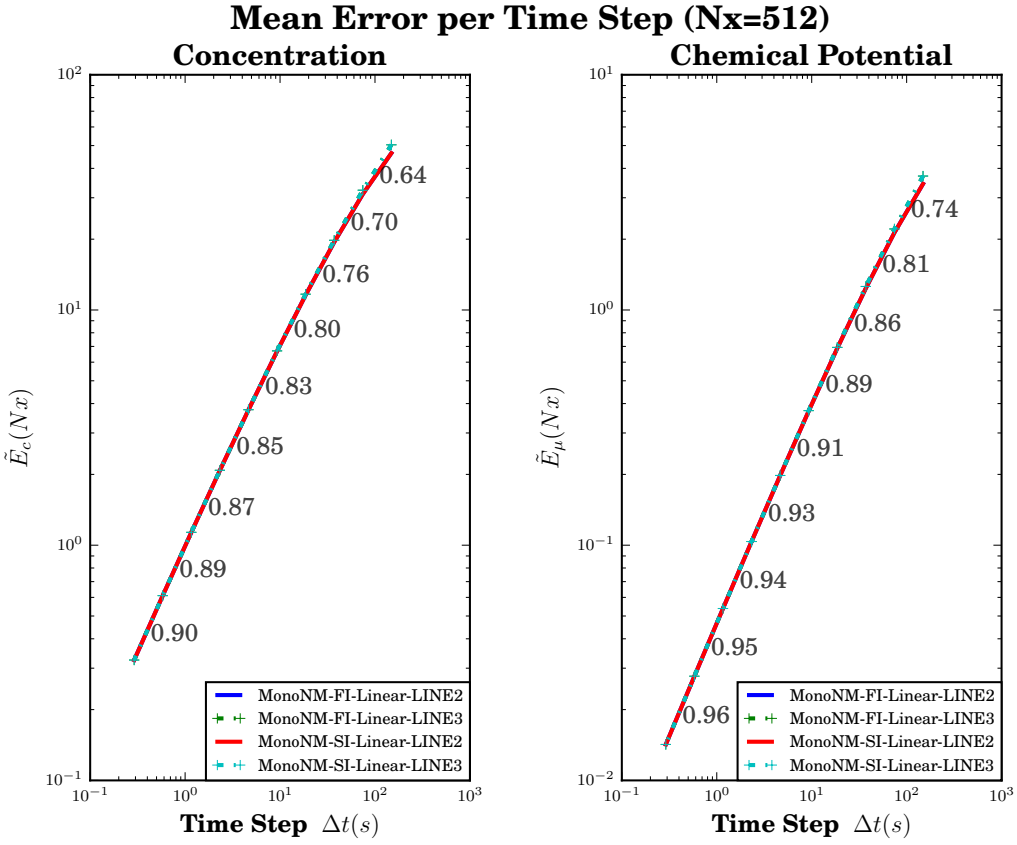

(b) Fix ratio test : $ratio = 2$

Figure 3.6: Linear model : L_1 relative error in time with $Nt_{list} = \{2^3, 2^4, \ldots, 2^1 3\}$

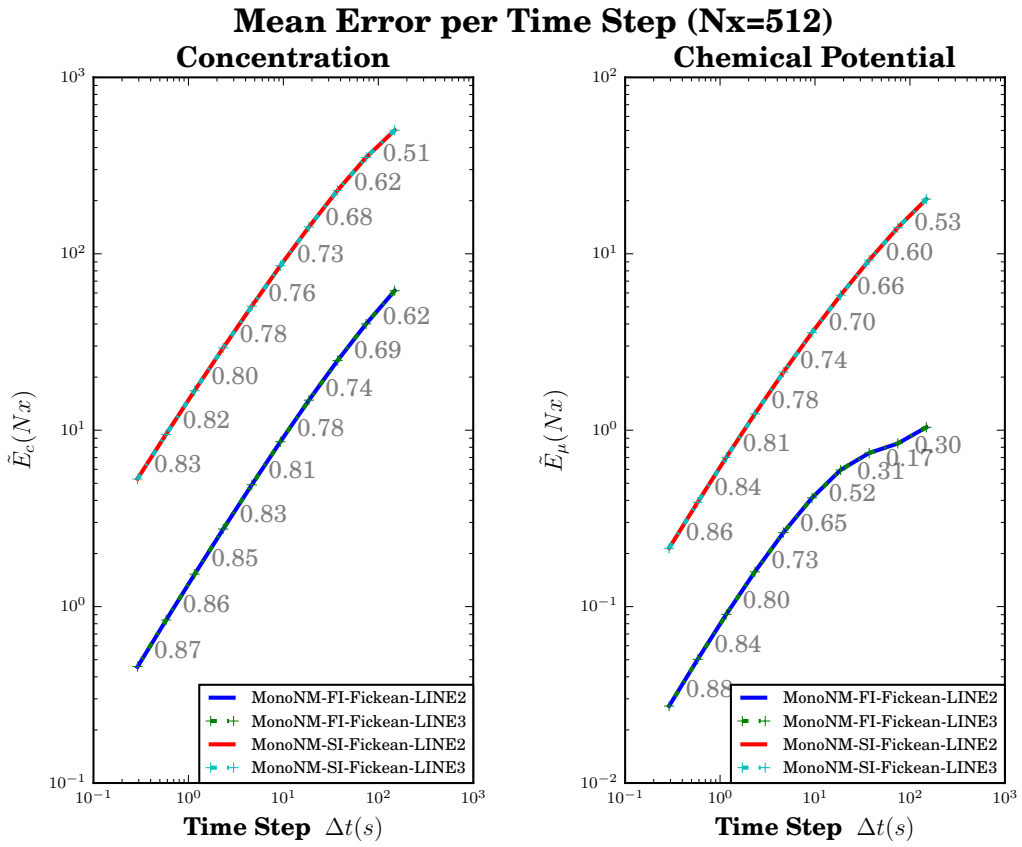

(a) Omega Fix Test: $N_x = 512$

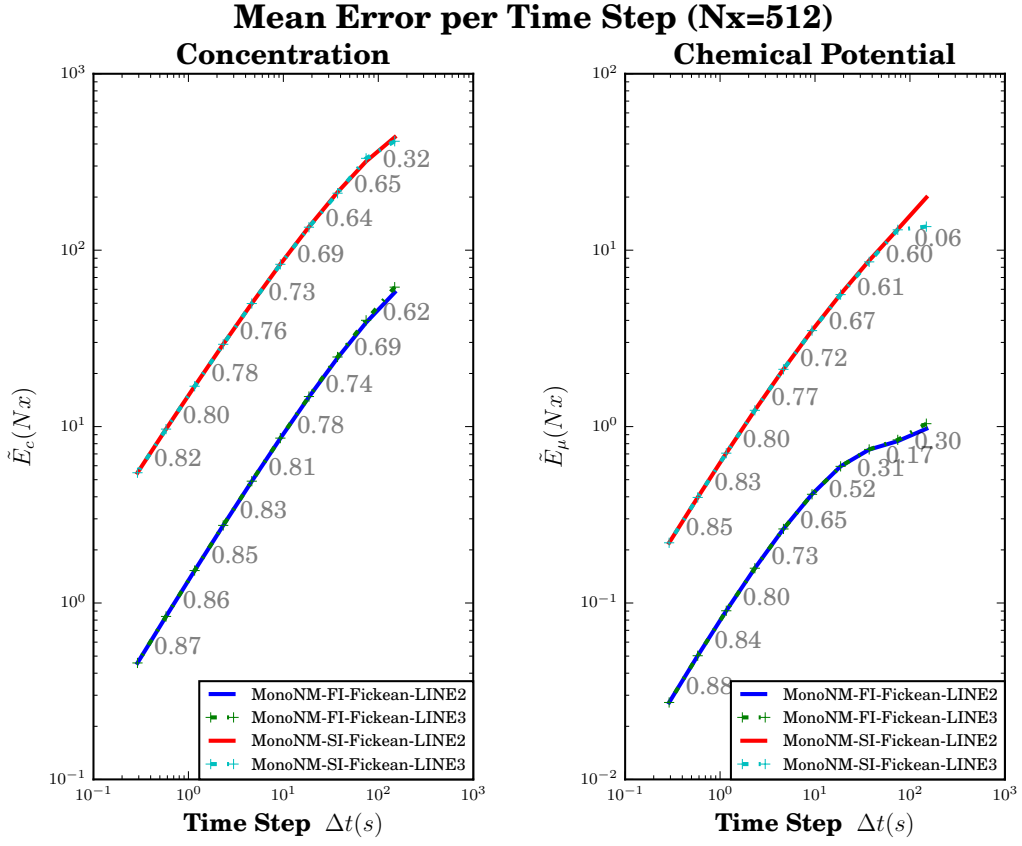

(b) Ratio Fix test: $ratio = 1$

Figure 3.7: Fickean model: L_1 relative error in time
with $Nt_{list} = \{2^3, 2^4, \ldots, 2^13\}$

Mean ℓ_1 relative error per time step: The next results in figures 3.8 & 3.9 display the convergence for the Linear and Fickean model correspondingly, using the mean ℓ_1 relative error per time step. The plots in the upper part of the page 3.8a & 3.9a show the results for the simulations under the *Omega fix* text (with $N_x = 512$) whilst the lower plots 3.8b & 3.9b are for the *Ratio fix test* (with $ratio = 1$).

In general this error, despite having a more meaningful interpretation of the results, gives us the same information as the L_1 relative error in time. What seems to be the most important results which can be drawn form these tests in 1D is that we might consider the interpretation of the fully implicit scheme valid. Still, the curvature displayed for the chemical potential must be understood, to know if its an artifact of the fully-implicit scheme, or maybe some extra information about the system which we can retrieve by considering a full feedback of the system, as done under this scheme.

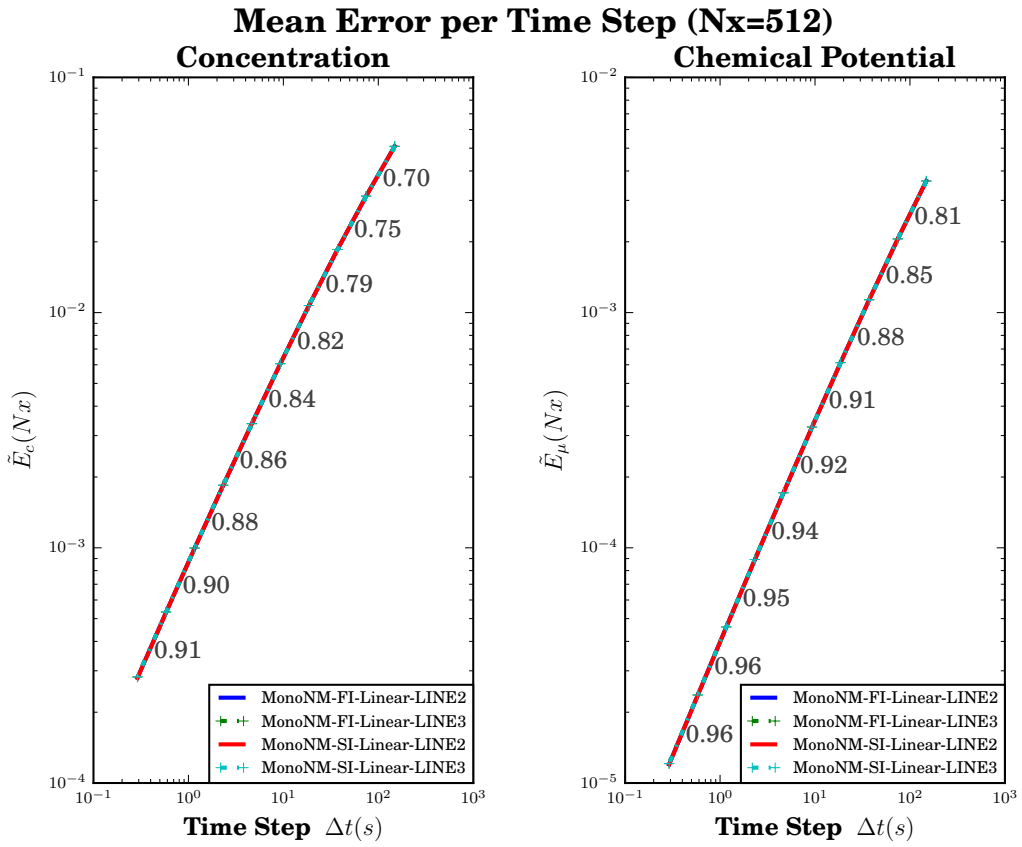

(a) Omega fix test: $N_x = 512$

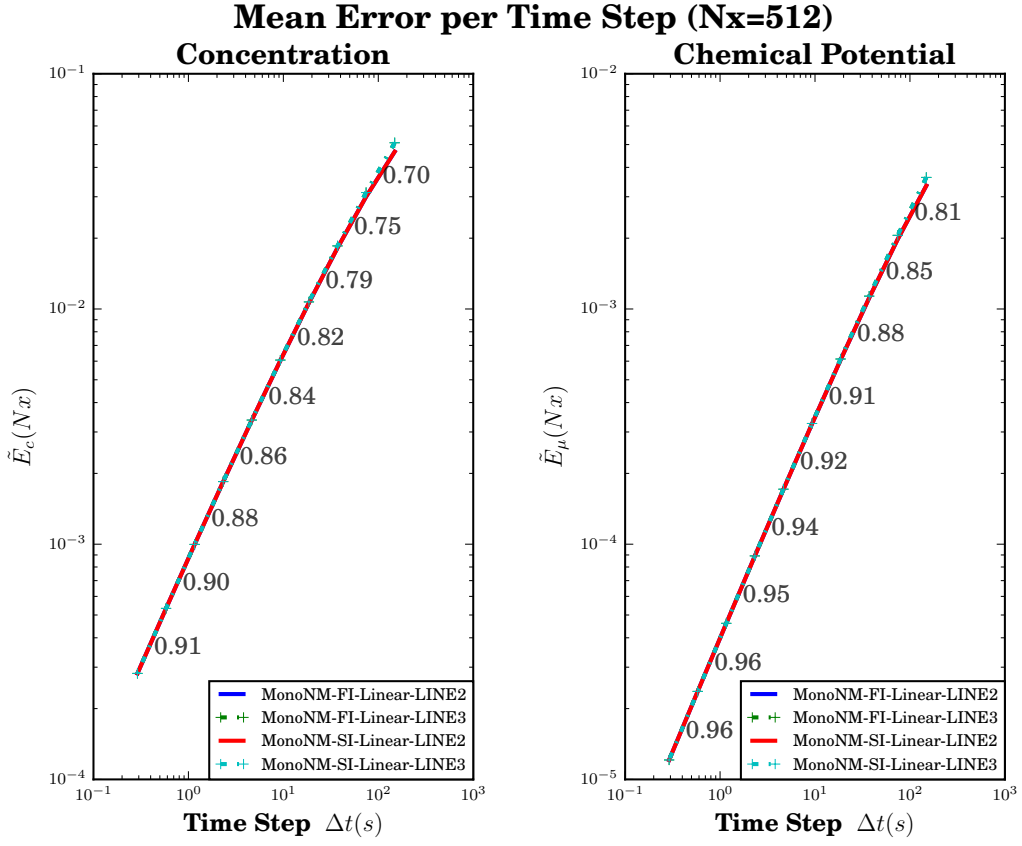

(b) Fix ratio test : $ratio = 1$

Figure 3.8: Linear model : mean ℓ_1 relative error per time step with $Nt_{list} = \{2^3, 2^4, \ldots, 2^13\}$

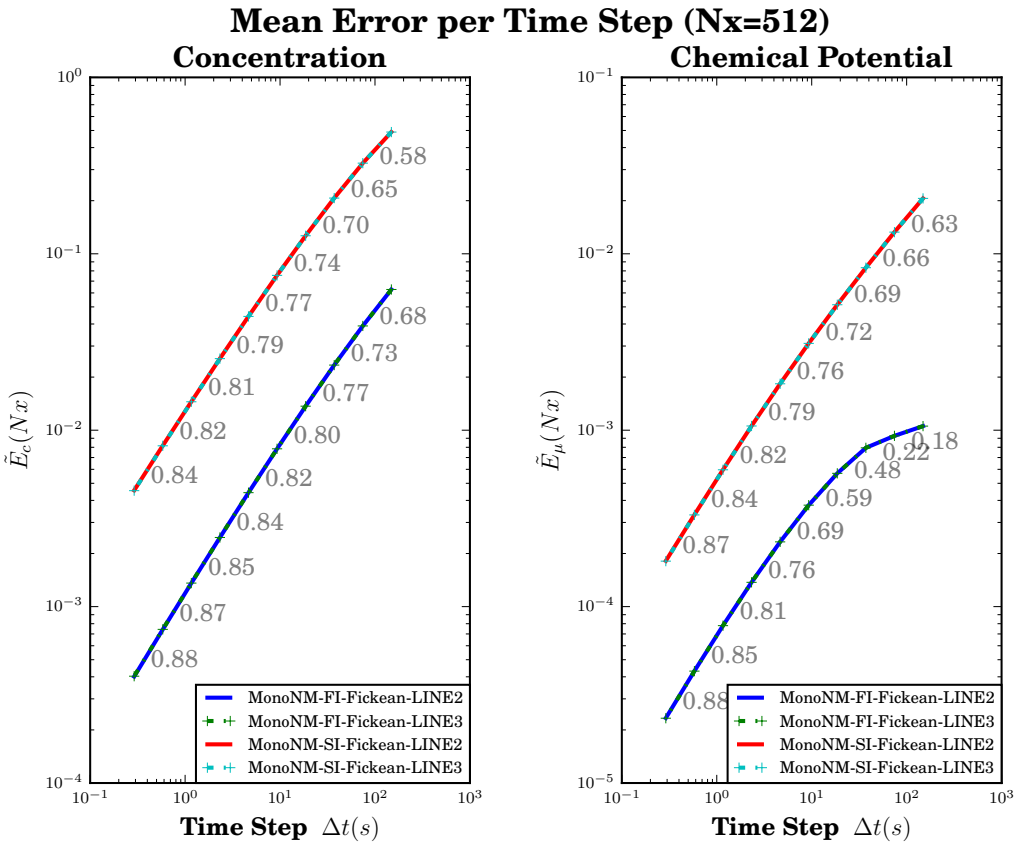

(a) Omega Fix Test: $N_x = 512$

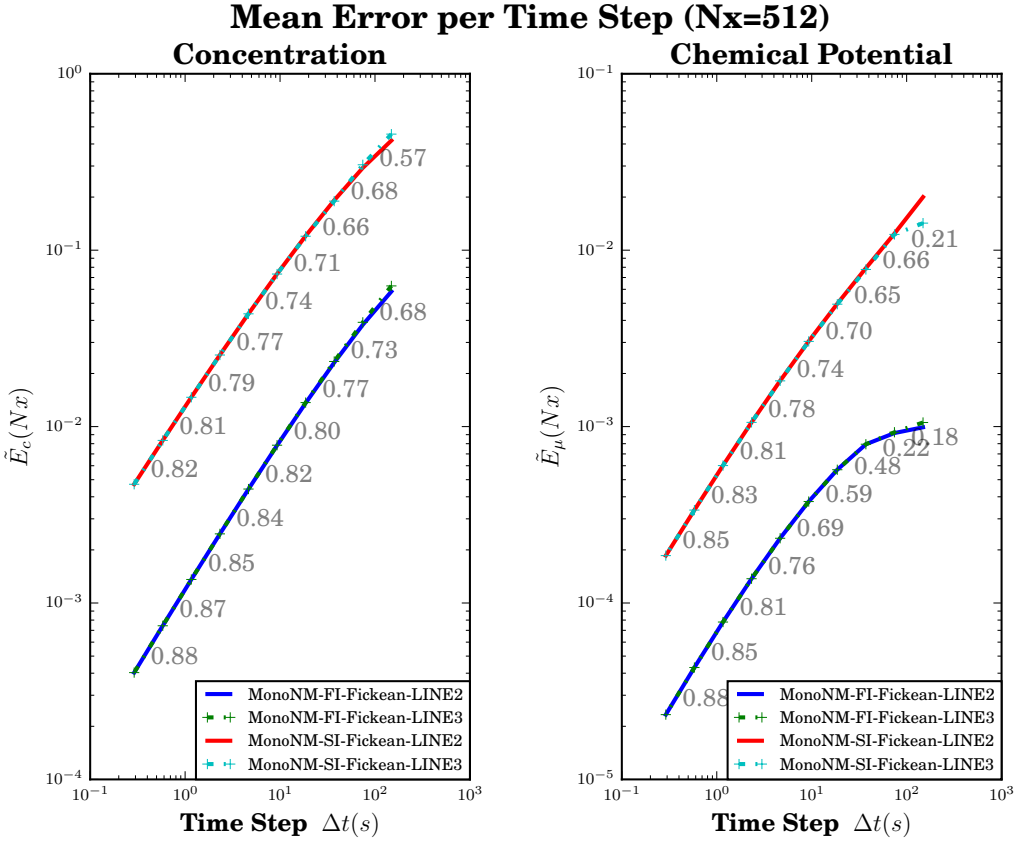

(b) Ratio Fix test: $ratio = 1$

Figure 3.9: Fickean model : mean ℓ_1 relative error per time step with $Nt_{list} = \{2^3, 2^4, \ldots, 2^13\}$

3.5 Summary

In this chapter we have explored the multifield problem of chemical diffusion. We proposed a process to derive a VF, presented three different field VF and solve one of them for a 1D problem. Our interest on this topic resides on the fact that mixed formulations can be treated as a multiphysic problem. On the following chapters, we take the ideas developed here to formulate generic VF models for multiphysic problems. These ideas are the following. The use of conjugate properties through the Legendre-Fenchel's transform allowed us to hide the specifics of the problem into abstract statements of energy rate potentials and helped to model a strong coupling between conjugate fields. The dissipation potential not only brought thermodynamic consistency to the model in the language of convex optimization, it also allowed to couple variables in terms of driving forces. The use of the Lagrange multiplier method set the basis to understand the use of the mass balance law as constraints in our VF. Moreover, we can observe the dynamics of the system are solely described by the functional, while the specifics of the problem, like material variables and constitutive laws, are defined through the potentials.

Chapter 4

General VF framework for multiphysic applications

Sommaire

Ce chapitre résume les idées utilisées pour développer le modèle variationnel du chapitre précédent et les explore dans un contexte général. Nous proposons une approche systématique pour créer des formulations variationnelles pour des problèmes couplés, indépendamment des types de physique utilisés. À la fin du chapitre, nous générons une instance du modèle général appliqué au problème couplé de l'électrochimie.

In chapter §3, we explored the problem of chemical diffusion from a multifield perspective deriving a corresponding variational form (VF). Now, we propose a systematic way or a generic model to construct the VF in the general scenario where different fields describing the problem arise from different areas of Physics, in essence, multiphysic problems. The notation will hence remain generic. These general results will be settled in more specific grounds at the end of the chapter, where a general VF for electrochemistry is proposed. Later on a concrete example with different specific models will be derived, to model the behavior of a lithium-ion battery.

In order to construct the systematic approach we propose to develop VFs for multiphysic applications, we need three key ingredients, namely, balance laws, energy and energy-like potentials and conjugate variables. Once those requirements are identified in the coupled problem, a systematic procedure to develop VF's is proposed. We construct this methodical approach by means of the generalized Onsager's energy rate [Onsager, 1945], from which we derive a constrained problem enhanced with tools from convex optimization. The obtained VF can be shown to be equivalent to the SF and WF of the problem. The following two sections concern the detailed description and justification of all the points mentioned above. As we describe each one, we will be constructing the general VF framework.

4.1 Modeling

4.1.1 Balance Laws

In general, we describe mathematically a balance law locally as

$$\dot{a}_i + \nabla \cdot A_i = b_i \qquad \textbf{Differential balance Law} \tag{4.1}$$

supplemented with appropriate boundary and initial conditions, where a_i is the *balanced quantity* volumic density, A_i the *associated flux-type* quantity and b_i an *external source*. The subindex i is introduced as an index for equations, since we will be working with several equations similar to (4.1). When the external source b_i is zero, the balance law is called a *conservation law* [Evans, 1998]. From (4.1) it is important to highlight that a_i and A_i are tensors, for which we do not need to specify for now the degree. However, consistency of the equation allows us to induce that A_i is a tensor with one order more than a due to the divergence operator. The physical meaning of (4.1) is to describe the evolution of the property a_i locally in time, in essence, variation in time of the balanced quantity should equal the sum of its surface and internal supplies. This evolution is taken considering changes due to an associated "flux-type" A_i, and external forces b_i.

A balance law can be written globally in a differential or integral form. The equation (4.1) shows the differential form. Its integral counterpart is given by

$$\int_\Omega (\dot{a}_i + \nabla \cdot A_i - b_i)\, dV = 0 \tag{4.2a}$$

$$\int_\Omega (\dot{a}_i - b_i)\, dV = -\int_{\partial\Omega} A_i \cdot \vec{n} dS \qquad \textbf{Integral balance Law} \tag{4.2b}$$

both equations in (4.2) describe the integral form of the balance law. To go from (4.1) to (4.2a) we restrict the equation to be satisfied only under the domain Ω, while to compute (4.2b) we have made use of the divergence theorem, where $\vec{n}$ is the unit outward orthogonal vector of the surface $\partial\Omega$. Notice that the zero at the RHS of the equation is a tensor of the same degree as a_i. The benefit of expressing the balance law as in (4.2b) is that it relates the evolution of a_i inside of the domain Ω with its corresponding boundary flux $A_i \cdot \vec{n}$ at $\partial\Omega$.

Balance laws have proven useful for the development of mathematical models in different areas of physics, providing a solid mathematical framework and sound understanding of the concerned problem. In coupled problems, we usually have a system of balance laws from the corresponding areas of Physics. Nevertheless, when developing coupled models the benefit in the similarity of the balance law's structure is rarely exploited. We will be pursuing this path.

4.1.2 Energy and energy-like potentials

Once we have identified the key variables in the system through the balance laws, we postulate the existence of potentials which we assume to be convex for thermodynamic consistency. In specific, we consider the energy and energy-like potential respectively $U(a_i)$ and $\chi(A_i, a_i)$. The potentials allow to describe reversible (U) and possible irreversible (χ) processes of the system. Furthermore, the fact that we define a potential for each type of variable allow to define constitutive laws in terms of the energy rates of the system rather than between the variables a_i and A_i.

4.1.3 Conjugate variables

Conjugate variables is what allows to encapsulate possible constitutive laws in the VF in a generalized fashion. We define as conjugate variables two variables which are related via the Legendre-Fenchel trans-

form. In specific we define the following Legendre-Fenchel transformations of the differentiable potentials (equations at the left)

$$U^*(a_i^*) = \sup_{a_i}\{a_i \cdot a_i^* - U(a_i)\} \qquad \rightarrow \qquad a_i^* = \frac{\partial U}{\partial a_i}(a_i) \tag{4.3a}$$

$$\chi^*(A_i^*, a_i) = \sup_{A_i}\{A_i \cdot A_i^* - \chi(A_i, a_i)\} \qquad \rightarrow \qquad A_i^* = \frac{\partial \chi}{\partial A_i}(A_i, a_i) \tag{4.3b}$$

where the upper index * is used to denote the corresponding duality, this means, the pairs $\{U(a_i), U^*(a_i^*)\}$ and $\{\chi(A_i), \chi^*(A_i^*, a_i)\}$ are convex dual functions, this defines the pairs of variables $\{a_i^*, a_i\}$ and $\{A_i^*, A_i\}$ as conjugate variables. This is shown by the equations at the right of (4.3). In (4.3b) we do not define a conjugacy with a_i since it has a lower tensor degree.[1]

Usually, constitutive relations are given between the variables[2] a_i and A_i. The constitutive relations in (4.3) defines the pairs of variables $\{a_i, a_i^*\}$ and $\{A_i, A_i^*\}$ as conjugate. The benefit of the later, is that it imposes an intrinsic dependence on the variables which contrasts with the artificial dependence imposed by algebraic constitutive relations[3]. The intrinsic dependence can be regard as a mutual-implicit relation between the variables, raised by the duality of the Legendre-Fenchel transform. We can think of this type of relation as the intrinsic dependence between a variable and its derivative.

4.2 Systematic approach

Now that the required ingredients have been detailed, it is time to describe the method used to develop a systematic VF for coupled problems. As mentioned, we will make use of a generalized version of the Onsager's energy rate, the Lagrange multiplier method and convex optimization tools. In the following we explain in detail how we can derive a general VF framework for coupled problems in a systematic fashion.

4.2.1 Onsager's Energy Rate

Energy is the language all fields of physics have in common. Hence, if we must add equations from n different fields of Physics into a single functional as expected from a VF, it is natural to think in terms of energy. An important step in this direction was taken by Onsager [1945] with the energy rate, which we express in a general form as

$$\begin{aligned}\Pi_0[\dot{\mathbf{a}}, \mathbf{A}] := \int_\tau \Bigg[\int_\Omega \Big(\dot{U}(\mathbf{a}) + \chi^*(\mathbf{A}, \mathbf{a}) \Big)\, dV \\ + \sum_{i=1}^{n} \int_{\partial_{D_i}\Omega} \overline{a_i^*}(A_i \cdot \vec{n}) dS \Bigg]\, dt; \qquad \forall \quad 1 \leq i \leq n\end{aligned} \tag{4.4}$$

where Π_0 is the *Onsager's energy rate functional* and $\overline{a^*}$ is a *known* value for the dual conjugate a^* defined over the domain $\partial_{D_i}\Omega$ as a Dirichlet condition. In addition, to reduce the expression we have used bold letters to denote the arrays as follows,

$$\Pi_0[\dot{\mathbf{a}}, \mathbf{A}] \equiv \Pi_0[\underbrace{\dot{a_1}, \dot{a_2}, \ldots, \dot{a_n}}_{=:\dot{\mathbf{a}}}, \underbrace{A_1, A_2, \ldots, A_n}_{=:\mathbf{A}},] \tag{4.5}$$

[1] We recall that the Legendre-Fenchel transform is also a functional, i.e. a mapping from a space $\mathcal{X}$ into the real numbers $\mathbb{R}$. A product like $a_i A_i$ cannot map to $\mathbb{R}$.

[2] e.g., Fick's first law

[3] To satisfy algebraic relations, we assign a dependent and an independent variable. This selection is guided by the numerical strategy we used to solve the system, rather than the actual physics.

Thus, with this notation the bold letters refer to the whole set of variables, and the non bold versions stand for an individual parameter, i.e., $i \in [1, 2, \ldots, n]$, where n is the number of balance laws from possibly different fields of Physics we would like to couple.

4.2.2 Constrained problem

The generalized Onsager's energy rate can be seen as a canvas where we can start sketching our model. It accounts for a system in energy-like terms, defined by the variables used to describe the balanced laws from the coupled problem. Moreover, it also takes into account the spatial domain on which we are working. What is missing on it, is the restriction that it should also satisfy the balance laws we observe or expect the coupled problem should have. Therefore, we define the *constrained problem* or *primal problem* by including the balance laws and the Neumann boundary conditions as constraints in the problem

$$\{\dot{\mathbf{a}}, \mathbf{A}\} = \underset{\dot{\mathbf{a}}, \mathbf{A}}{\operatorname{argstat}} \Pi_0 \qquad \textit{subject to} \qquad \begin{cases} \dot{a_i} + \nabla \cdot A_i - b_i = 0 & \forall\, \vec{x} \in \Omega \\ \overline{A_i} - A_i \cdot \vec{n} = 0 & \forall\, \vec{x} \in \partial_{A_i}\Omega\,; \quad 1 \leq i \leq n \end{cases} \tag{4.6}$$

The optimality with respect to the input arguments a_i and A_i, states that their value should render Π_0 stationary for all admissible variations. The former can be regarded as a kind of least action principle. Using the Lagrange multiplier method, this can be rephrased as

$$\{\dot{\mathbf{a}}, \mathbf{A}, \boldsymbol{\lambda_1}, \boldsymbol{\lambda_2}\} = \arg \underset{\dot{\mathbf{a}}, \mathbf{A}, \boldsymbol{\lambda_1}, \boldsymbol{\lambda_2}}{\operatorname{stat}} \Pi_\lambda \tag{4.7a}$$

$$\begin{aligned} \Pi_\lambda[\dot{\mathbf{a}}, \boldsymbol{\lambda_1}, \boldsymbol{\lambda_2}, \mathbf{A}] := \int_\tau \Bigg[\int_\Omega \left(\dot{U}(\mathbf{a}) + \chi(\mathbf{A}, \mathbf{a}) + \sum_{i=1}^{n} \lambda_{i1}(\dot{a_i} + \nabla \cdot A_i - b_i) \right) dV \\ + \sum_{i=1}^{n} \int_{\partial_{D_i}\Omega} \overline{a_i^*}(A_i \cdot \vec{n}) dS + \sum_{i=1}^{n} \int_{\partial_{A_i}\Omega} \Big(\lambda_{i2}(\overline{A_i} - A_i \cdot \vec{n})\Big) dS \Bigg] dt \end{aligned} \tag{4.7b}$$

$$\begin{aligned} \Pi_\lambda[\dot{\mathbf{a}}, \boldsymbol{\lambda_1}, \boldsymbol{\lambda_2}, \mathbf{A}] := \int_\tau \Bigg[\int_\Omega \left[\dot{U}(\mathbf{a}) + \chi(\mathbf{A}, \mathbf{a}) + \sum_{i=1}^{n} \Big(\lambda_{i1}\dot{a_i} - \lambda_{i1} b_i - (\nabla \lambda_{i1}) A_i \Big) \right] dV \\ + \sum_{i=1}^{n} \int_{\partial_{D_i}\Omega} \Big[(\lambda_{i1} + \overline{a_i^*}) A_i \cdot \vec{n} \Big] dS \\ + \sum_{i=1}^{n} \int_{\partial_{A_i}\Omega} \Big[\lambda_{i2}\overline{A_i} + (\lambda_{i1} - \lambda_{i2}) A_i \cdot \vec{n} \Big] dS \Bigg] dt \end{aligned} \tag{4.7c}$$

where λ_{i1} and λ_{i2} are the corresponding Lagrange multipliers for the ith-field a_i. As shown, equations (4.7b) and (4.7c) are equivalent, they differ in the substitution of the term $\lambda_{i1} \nabla \cdot A_i$ in (4.7b), which has been substituted into (4.7c) using integration by parts and the divergence theorem. We will be using down the road both forms depending on which will ease the computations to perform. We can also refer to the functional Π_λ also as

$$\begin{aligned} \Pi_\lambda[\dot{\mathbf{a}}, \boldsymbol{\lambda_1}, \boldsymbol{\lambda_2}, \mathbf{A}] := \int_\tau \Bigg[\int_\Omega \pi(\dot{\mathbf{a}}, \lambda_{I1}, \lambda_{I2}, \mathbf{A}) dV \\ + \sum_{i=1}^{n} \int_{\partial_{D_i}\Omega} \pi_{D_i}(A_i) dS + \sum_{i=1}^{n} \int_{\partial_{A_i}\Omega} \pi_{A_i}(A_i, \lambda_{i2}) dS \Bigg] dt \end{aligned} \tag{4.8}$$

where the integrand is substituted by a function denoted with π and a corresponding subindex, namely

$$\pi(\dot{\mathbf{a}}, \boldsymbol{\lambda_1}, \boldsymbol{\lambda_2}, \mathbf{A}) := \dot{U}(\mathbf{a}) + \chi(\mathbf{A}, \mathbf{a}) + \sum_{i=1}^{n} \lambda_{i1}(\dot{a_i} + \nabla \cdot A_i - b_i) \tag{4.9a}$$

$$\pi_{D_i}(A_i) := \overline{a_i^*}(A_i \cdot \vec{n}) \tag{4.9b}$$

$$\pi_{A_i}(A_i, \lambda_{i2}) := \lambda_{i2}(\overline{A_i} - A_i \cdot \vec{n}) \tag{4.9c}$$

We have now represented the coupled model as a constrained problem by means of (4.7), we must analyze now what the stationarity of Π_λ yields.

4.2.2.1 Implications of the stationary condition

We recall that for a functional to be stationary, their corresponding first order variations should equate to zero. The first order variations on a functional like Π_λ are obtained when we apply the Fréchet derivative to it with respect to variable under variation (2.16).

1st order variation : $\dot{a_i}$

The first order variation we examine is the one corresponding to the variable $\dot{a_i}$ which denotes the rate of change of the balanced property a_i. Using equations (4.8) and (4.7b) we obtain

$$\begin{aligned}\left\langle \frac{\delta \Pi_\lambda}{\delta \dot{a_i}} \,\middle|\, \delta\eta_{\dot{a_i}} \right\rangle &= \int_\tau \left[\int_\Omega \frac{\delta \pi}{\delta \dot{a_i}}(\dot{\mathbf{a}}, \boldsymbol{\lambda_1}, \boldsymbol{\lambda_2}, \mathbf{A}) \delta\eta_{\dot{a_i}} \, dV \right] dt \\ &= \int_\tau \left[\int_\Omega \Big(\frac{\partial U}{\partial a_i} + \lambda_{i1} \Big) \delta\eta_{\dot{a_i}} \, dV \right] dt \equiv 0 \quad \rightarrow \quad \frac{\partial U}{\partial a_i} = -\lambda_{i1} \quad \forall \vec{x} \in \Omega \end{aligned} \tag{4.10}$$

As shown above, the variations of $\dot{a_i}$ characterize the Lagrange multiplier λ_{i1} as the negative conjugate variable of a_i inside Ω. In essence, from this variations we can conclude

$$a_i^* = -\lambda_{i1} \qquad \forall \vec{x} \in \Omega \tag{4.11}$$

this means, the Lagrange multipliers λ_{i1} are the opposite of the corresponding conjugate variables of a_i within Ω.

1st order variation : A_i

The next variation to examine, is the one corresponding to the variable A_i which denotes the flux-type of the corresponding balanced property. For this case, is more convenient the use of equations (4.8) and (4.7c) so that we obtain

$$\begin{aligned}\left\langle \frac{\delta \Pi_\lambda}{\delta A_i} \,\middle|\, \delta\eta_{A_i} \right\rangle &= \int_\tau \left[\int_\Omega \frac{\delta \pi}{\delta A_i}(\dot{\mathbf{a}}, \boldsymbol{\lambda_1}, \boldsymbol{\lambda_2}, \mathbf{A}) \delta\eta_{A_i} \, dV \right. \\ &\quad \left. + \int_{\partial_{D_i}\Omega} \frac{\delta \pi_{D_i}}{\delta A_i}(A_i) \delta\eta_{A_i} \, dS + \int_{\partial_{D_i}\Omega} \frac{\delta \pi_{A_i}}{\delta A_i}(\boldsymbol{\lambda_2}, \mathbf{A}) \delta\eta_{A_i} \, dS \right] dt \\ &= \int_\tau \left[\int_\Omega \Big(\frac{\partial \chi}{\partial A_i} - \nabla\lambda_{i1} \Big) \delta\eta_{A_i} \, dV \right. \\ &\quad \left. + \int_{\partial_{D_i}\Omega} \Big(\lambda_{i1} + \overline{a_i^*} \Big) \delta\eta_{A_i} \cdot \vec{n} \, dS + \int_{\partial_{A_i}\Omega} \Big(\lambda_{i1} - \lambda_{i2} \Big) \delta\eta_{A_i} \cdot \vec{n} \, dS \right] dt \equiv 0 \end{aligned} \tag{4.12}$$

The implications of the results above in each domain are

$$\frac{\partial \chi}{\partial A_i} = \nabla \lambda_{i1} \quad \rightarrow \quad \frac{\partial \chi}{\partial A_i} = A_i^* = -\nabla a_i^* \quad \forall \vec{x} \in \Omega \tag{4.13a}$$

$$\lambda_{i1} = -\overline{a_i^*} \quad \rightarrow \quad a_i^* = \overline{a_i^*} \quad \forall \vec{x} \in \partial_{D_i}\Omega \tag{4.13b}$$

$$\lambda_{i1} = \lambda_{i2} \quad \rightarrow \quad a_i^* = -\lambda_{i2} \quad \forall \vec{x} \in \partial_{A_i}\Omega \tag{4.13c}$$

From (4.11) and (4.13a) it can be seen that the conjugate flux-type variable A_i^* is the negative gradient of a_i^*. Therefore, it is defined as a *conservative field*. Alternately we can also state that a_i^* is potential for A_i^*. Furthermore, (4.13c) establishes that both Lagrange multipliers λ_{i1} and λ_{i2} are equal on $\partial_{A_i}\Omega$. Finally, (4.13b) determines both Lagrange multipliers as the conjugate variables a_i^* for all the spatial domain defined by the functional Π_λ.

To synthesize the former results we rewrite (4.7) as follows

$$\{\dot{\mathbf{a}}, \mathbf{A}, \mathbf{a}^*\} = \arg \underset{\dot{\mathbf{a}}, \mathbf{A}, \mathbf{a}^*}{\operatorname{stat}} \Pi \tag{4.14a}$$

$$\begin{aligned}\Pi[\dot{\mathbf{a}}, \mathbf{a}^* \mathbf{A}] := \int_\tau \Bigg[\int_\Omega \Bigg(\dot{U}(\mathbf{a}) + \chi(\mathbf{A}, \mathbf{a}) - \sum_{i=1}^{n} a_i^* (\dot{a}_i + \nabla \cdot A_i - b_i) \Bigg) dV \\ + \sum_{i=1}^{n} \int_{\partial_{D_i}\Omega} \overline{a_i^*} (A_i \cdot \vec{n}) dS - \sum_{i=1}^{n} \int_{\partial_{A_i}\Omega} \Big[a_i^* (\overline{A_i} - A_i \cdot \vec{n}) \Big] dS \Bigg] dt\end{aligned} \tag{4.14b}$$

$$\begin{aligned}\Pi[\dot{\mathbf{a}}, \mathbf{a}^*, \mathbf{A}] := \int_\tau \Bigg[\int_\Omega \Bigg(\dot{U}(\mathbf{a}) + \chi(\mathbf{A}, \mathbf{a}) + \sum_{i=1}^{n} \Bigg(-a_i^* \dot{a}_i + a_i^* b_i - \underbrace{(-\nabla a_i^*)}_{A_i^*} A_i \Bigg) \Bigg) dV \\ - \sum_{i=1}^{n} \int_{\partial_{D_i}\Omega} \Big[\underbrace{(a_i^* - \overline{a_i^*})}_{=0} A_i \cdot \vec{n} \Big] dS - \sum_{i=1}^{n} \int_{\partial_{A_i}\Omega} \Big[a_i^* \overline{A_i} \Big] dS \Bigg] dt\end{aligned} \tag{4.14c}$$

For completeness we have also shown the Dirichlet boundary condition in (4.14c). However, that contribution must vanish as indicated by the braces when we consider a_i^* to be an admissible homogeneous field.

4.2.2.2 Equivalence with other formulations

Above we have seen how the variations of the functional Π_λ with respect to the variables a_i and A_i appearing in the balance laws have helped us to compact the functional Π_λ into Π by reducing the Lagrange multipliers by the conjugate variables a_i^* and A_i^*. Now, we will validate the VF we have developed in (4.14). Hence, we seek its equivalence with other formulations, namely, with a SF and/or WF of the same problem. To achieve this, we appeal to the variations from the dual variables a_i^*.

1st order variation : a_i^*

We expect the first variation with respect to a_i^* to output that balance laws and flux boundary conditions, since it is the opposite of Lagrange multiplier of the constrained problem. We

use (4.14b) to perform the variations as follows

$$\begin{aligned}\left\langle \frac{\delta \Pi_N}{\delta a_i^*} \,\middle|\, \delta a_i^* \right\rangle &= \int_\tau \left[\int_\Omega \frac{\delta \pi}{\delta a_i^*}(\dot{\mathbf{a}}, \mathbf{a}^*, \mathbf{A}) \delta a_i^* \; dV + \sum_{i=1}^{n} \int_{\partial_{A_i}\Omega} \frac{\delta \pi_{A_i}}{\delta a_i^*}(\mathbf{A}, \mathbf{a}^*) dS \right] dt \\ &= \int_\tau \left[\int_\Omega \Big(\dot{a_i} + \nabla \cdot A_i - b_i \Big) \delta a_i^* \right. \\ &\left. + \int_{\partial_{A_i}\Omega} \Big(\overline{A_i} - A_i \cdot \vec{n} \Big) \delta a_i^* \; dV \right] dt \equiv 0 \end{aligned} \tag{4.15}$$

As shown above, the variations of a_i^* establish that the conservation law and the flux-type boundary condition are satisfied, since we obtain the following conditions through the variation

$$\dot{a_i} + \nabla \cdot A_i = b_i \qquad \forall \vec{x} \in \Omega \tag{4.16a}$$

$$\overline{A_i} = A_i \cdot \vec{n} \qquad \forall \vec{x} \in \partial_{A_i}\Omega \tag{4.16b}$$

Hence, through the Fréchet derivative of Π with respect to the conjugate variables a_i^* we have shown that the VF implies the SF of the problem. However, we must recall that constitutive laws focus in specific aspects of the model, which for the VF are encapsulated within the potentials $U(\mathbf{a})$ and $\chi(\mathbf{A}, \mathbf{a})$. Therefore, once we have specifically characterized $U(\mathbf{a})$ and $\chi(\mathbf{A}, \mathbf{a})$ we have a full equivalence with a specific SF for a given problem. The converse can also be shown, thus establishing the equivalence. The connection with the WF can be drawn by means of a process similar to that shown in 2.11.

4.2.2.3 Types of extrema provided by stationary conditions

In (4.14a) we have not specified the stationary condition the variable imposes on the functional, whether it minimizes it or maximizes it. This task, requires a knowledge of the specifics of the problem, i.e., the constitutive laws. However, we can draw a general type of extrema of the stationary conditions by knowing the properties of the functions $U(\mathbf{a})$ and $\chi(\mathbf{A}, \mathbf{a})$. To do this, we must compute the second variation of the functional.

Type of extrema: $\dot{a_i}$

We compute the second variation from the variables $\dot{a_i}$ from the first variation (4.10).

$$\begin{aligned}\left\langle \frac{\delta^2 \Pi_\lambda}{\delta \dot{a_i}^2} \,\middle|\, \delta \eta_{\dot{a_i}} \delta \xi_{\dot{a_i}} \right\rangle &= \int_\tau \left[\int_\Omega \frac{\delta^2 \pi}{\delta \dot{a_i}^2}(\dot{\mathbf{a}}, \mathbf{a}^*, \mathbf{A}) \delta \eta_{\dot{a_i}} \delta \xi_{\dot{a_i}} \; dV \right] dt \\ &= \int_\tau \left[\int_\Omega \Big(\frac{\partial^2 U}{\partial a_i^2} \Big) \delta \eta_{\dot{a_i}} \delta \xi_{\dot{a_i}} \, dV \right] dt \end{aligned} \tag{4.17}$$

The second variation above, only depends on the second derivative of $U(a_i)$ with respect of each a_i. Hence, we can conclude the type of extrema for the stationary condition of a_i depends upon the second derivative of $U(a_i)$ which we have restricted to be convex or concave. Thus, this type of extrema depends on the model and does not change during computation.

Type of extrema: a_i^*

To define the optimality with respect to a_i^* we make use of a well known result from convex optimization. Since we know a_i^* is the opposite of the Lagrange multiplier, due to *strong duality* properties of the problem [Boyd and Vandenberghe, 2004, § 5.2.3], a_i^* must have opposite type of extrema than its conjugate counterpart a_i.

Type of extrema: A_i^*

Finally, we need to compute the second variation from the variables A_i. Therefore, we take back the computations of the first variation from (4.12).

$$\begin{aligned}\left\langle \frac{\delta^2 \Pi_\lambda}{\delta A_i^2} \,\middle|\, \delta\eta_{A_i}\delta\xi_{A_i} \right\rangle &= \int_\tau \left[\int_\Omega \frac{\delta^2 \pi}{\delta A_i^2}(\dot{\mathbf{a}}, \mathbf{a}^*, \mathbf{A}) \delta\eta_{A_i}\delta\xi_{A_i} \, dV \right] dt \\ &= \int_\tau \left[\int_\Omega \Big(\frac{\partial^2 \chi}{\partial A_i^2} \Big) \delta\eta_{A_i}\delta\xi_{A_i} \, dV \right] dt \end{aligned} \tag{4.18}$$

As it was for a_i, now the second variation depends on the second derivative of $\chi(A_i)$ with respect to each A_i. Hence, we can conclude the type of extrema for the stationary condition of A_i depends upon the second derivative of $\chi(A_i)$. Nevertheless, in this case we have to restrict $\chi(A_i)$ to be convex or concave for thermodynamic consistency, as it is shown next.

4.2.3 Thermodynamic consistency

An advantage of the VF is that it can be defined to be thermodynamically consistent, i.e., the model is able to satisfy the laws of thermodynamics. To perform this, we have to go back to the basics. We analyze the balance laws and Neumann boundary conditions of the system under the domain of interest. If we apply the principle of virtual power to them, which is achieved through multiplication with the corresponding conjugate variable a_i^* we get

$$\int_\Omega \sum_i \Big(\dot{a_i} + \nabla \cdot A_i - b_i \Big) a_i^* \, dV + \int_{\partial_{A_i}\Omega} \sum_i \Big(\overline{A_i} - A_i \cdot \vec{n} \Big) a_i^* dS = 0 \tag{4.19a}$$

$$\int_\Omega \sum_i \Big(\dot{a_i} a_i^* + \underbrace{(-\nabla a_i^*)}_{A_i^*} A_i - b_i a_i^* \Big) \, dV + \int_{\partial_{A_i}\Omega} \sum_i \Big(a_i^* \overline{A_i} \Big) dS = 0 \tag{4.19b}$$

The last equation (4.19b) is achieved by means of integration by parts and the divergence theorem. The expression in (4.19b) can be expressed in terms of the thermodynamics laws as follows

$$\underbrace{\int_\Omega \sum_i a_i^* \dot{a_i} \, dV}_{=:\dot{W}_{int}} - \underbrace{\left(\int_\Omega \sum_i a_i^* b_i dV - \int_{\partial_{A_i}\Omega} \sum_i a_i^* \overline{A_i} dS \right)}_{=:\dot{W}_{ext}} = - \underbrace{\int_\Omega \sum_i A_i^* A_i \, dV}_{=:\mathcal{D}} \leq 0 \tag{4.20}$$

where we have defined the expressions $\dot{W}_{int}$ as the *internal power*, $\dot{W}_{ext}$ the *external power* and $\mathcal{D}$ the *Dissipation*. The second law of thermodynamics imposes a restriction on the Dissipation $\mathcal{D}$, which can be regarded as an entropy-like condition (4.21). Recalling that A_i^* and A_i are conjugate variables through $\chi(A_i)$ (4.3b), the entropy-like condition is expressed as

$$\int_\Omega \sum_i A_i^* A_i \, dV = \int_\Omega \sum_i \left(\frac{\partial \chi}{\partial A_i} A_i \right) dV \geq 0 \qquad \textbf{entropy-like condition} \tag{4.21}$$

This condition (4.21), can be satisfied by setting $\chi(A_i, a_i)$ convex of its arguments. This condition of convexity on $\chi(A_i, a_i)$ is what ensures the VF is thermodynamic consistent. It can be introduced into the model by defining on (4.14a) the optimality condition of A_i as a minimum condition.

4.2.4 Field reduction in the VF

So far we have described a systematic VF framework to deal with coupled problems through the equations (4.14) which we rewrite below

$$\{\dot{\mathbf{a}}, \mathbf{A}, \mathbf{a}^*\} = \arg \underset{\dot{\mathbf{a}},\mathbf{A},\mathbf{a}^*}{\text{stat}}\, \Pi \tag{4.22a}$$

$$\Pi[\dot{\mathbf{a}}, \mathbf{A}, \mathbf{a}^*] := \int_\tau \left[\int_\Omega \left(\dot{U}(\mathbf{a}) + \sum_{\forall i} \big(- a_i^* \dot{a}_i + a_i^* b_i \big) + \chi(\mathbf{A}, \mathbf{a}) - \sum_{\forall i} A_i^* \cdot A_i \right) dV - \sum_{\forall i} \int_{\partial_{A_i}\Omega} \left[a_i^* \overline{A_i} \right] dS \right] dt \tag{4.22b}$$

Specially, we have seen that our model is equivalent with the SF and WF, plus, it can be defined to be thermodynamic consistent thanks to the condition (4.21). A further word on it concerns how this model can be reduced. Roughly speaking per each balance law we add to the model[4], it is likely we can reduce it by one or two variables. These reductions are possible due to the interplay of dualities within the model. We explore these options and their implications now.

4.2.4.1 First reduction type

The first reduction type considers the elimination of a flux-type field A_i. The key point arises from combining (4.3b) and (4.14c), i.e., we eliminate the dependence on A_i by means of the dual function $\chi(A_i^*, a_i)$

$$\{\dot{\mathbf{a}}, \mathbf{a}^*\} = \underset{\dot{\mathbf{a}},\mathbf{a}^*}{\text{argstat}} \Pi \tag{4.23a}$$

$$\Pi[\dot{\mathbf{a}}, \mathbf{a}^*] := \int_\tau \left[\int_\Omega \left(\dot{U}(\mathbf{a}) + \sum_{\forall i} \big(- a_i^* \dot{a}_i + a_i^* b_i \big) + \underbrace{\chi(\mathbf{A}, \mathbf{a}) + \sum_{\forall i} \nabla a_i^* \cdot A_i}_{\chi^*(\mathbf{A}^*, \mathbf{a})} \right) dV - \sum_{\forall i} \int_{\partial_{A_i}\Omega} \left[a_i^* \overline{A_i} \right] dS \right] dt \tag{4.23b}$$

To make things clearer, we perform the reduction for all our flux-type variables A_i, the modified functional $\Pi[\dot{a}_i, a_i^*]$ will depend only on the variables $\dot{a}_i$ and a_i^*, the local pair of the conjugated variables. We go from a system of maximum $4n$ unknown fields, to a system only of $3n$ unknown fields. The functional after applying the first reduction becomes

$$\Pi[\dot{a}_i, a_i^*] := \int_\tau \left[\int_\Omega \Big(\dot{U}(\mathbf{a}) - \mathbf{a}^* \cdot \dot{\mathbf{a}} + \mathbf{a}^* \cdot \mathbf{b_i} + \chi^*(\mathbf{A}^*, \mathbf{a}) \Big) dV - \sum_{\forall i} \int_{\partial_{A_i}\Omega} \left[a_i^* \overline{A_i} \right] dS \right] dt \tag{4.24}$$

The implications of the reduction are observed when we apply the variations to the functional above (4.24). We have detailed this process for the specific case of Chemical diffusion in §3.2.1, the same idea holds for the general case. In essence, from the variations of Π with respect to A_i we analyzed in §4.2.2.1, we saw that these variables allowed us to define the Lagrange multipliers as opposite to a_i^* and established the conjugate variable condition between A_i and A_i^*. Therefore, the information is only hidden[5] by reducing these variables since we can take as given the functional $\Pi[\dot{a}_i, a_i^*]$ without thinking of it as a constrained problem. Furthermore, our initial postulates already establish the conjugate relation between A_i and A_i^*. In addition, this reduction removes the variable which has one degree more (tensor) in comparison with a_i

[4] Recall that each balance law adds three variables to the VF framework, namely, a_i, A_i, a_i^*.

[5] we say hidden, because we could always go back to (6.49b) from (4.24) to find out $-a_i^*$ works as a Lagrange multiplier and A_i and A_i^* are conjugate variables. However, those insights will kept pertaining to the $3n$ formulation (6.49b).

and a_i^*. Thus, this type of reduction is encouraged, since it is more convenient for numerical computational purposes and no side-effects are observed by performing it neither. In fact, we will stick to the use of this reduction in general when developing a VF.

4.2.4.2 Second reduction type

The second reduction type considers the elimination of the balance variable a_i. If we take the time derivative of (4.3a) we arrive to the following expression

$$\dot{U}^*(\mathbf{a}^*) - \sum_{\forall i} a_i \dot{a}_i^* = \sum_{\forall i} \dot{a}_i a_i^* - \dot{U}(\mathbf{a}) \tag{4.25}$$

by substituting the former below and use again (4.3a) for a further substitution on the term a_i we arrive to on (4.14c) as follows

$$\Pi[a_i^*, A_i] := \int_\tau \left[\int_\Omega \left(\cancelto{0}{\sum_{\forall i} \frac{\partial U^*}{\partial a_i^*} \dot{a}_i^* - \dot{U}^*(\mathbf{a}^*)} + \sum_{\forall i} a_i^* b_i + \chi(\mathbf{A}, \frac{\partial U^*}{\partial \mathbf{a}^*}) - \sum_{\forall i} A_i^* \cdot A_i \right) dV - \sum_{\forall i} \int_{\partial_{A_i}\Omega} \left[a_i^* \overline{A_i} \right] dS \right] dt \tag{4.26}$$

In this case again, if we were to apply this reduction to all a_i terms, the functional $\Pi[a_i^*, A_i]$ will depend only on the variables $\dot{a}_i^*$ and A_i, this means. If we were to apply the variations with respect to a_i^* to this reduced functional, we would see that the variations are no longer equivalent relation with neither the SF nor WF. Nevertheless, a numerical implementation of this model, can output the right results, being the price to pay the stability of the model, which shows to be less stable than other reductions. A possible cause for the lose of stability is thought to be when substituting (4.25), since theoretically we would need to have already optimal values before performing the time derivative.

A further word between the *first* and *second reduction types* is that those reductions can be combined in order to construct a VF depending only on the dual variable, this means, we would arrive to a functional $\Pi[a_i^*]$. However, despite of being able to reduce to a third the amount of unknowns, this combination of reduction is not recommend by the same constraints which were described for the second type of reduction.

4.2.4.3 Third reduction type

The third reduction type considers the elimination of the conjugate balance variable a_i^*. The simplest case is the elimination of a_i^* by means of (4.3a) and (4.3b) on (4.14c) as follows

$$\Pi[a_i, A_i] := \int_\tau \left[\int_\Omega \left(\dot{U}(a_i) - \sum_{\forall i} \dot{a_i} \frac{\partial U}{\partial a_i} + \sum_{\forall i} b_i \frac{\partial U}{\partial a_i} + \chi(A_i, a_i) - \sum_{\forall i} \frac{\partial \chi}{\partial A_i} \cdot A_i \right) dV - \sum_{\forall i} \int_{\partial_{A_i}\Omega} \left[\frac{\partial U}{\partial a_i} \overline{A_i} \right] dS \right] dt \tag{4.27}$$

With similar arguments as the other reductions, we can reduce all a_i^* variables. This reduction entails, as in the Second reduction type, a lack of direct correspondence with either the SF or WF if any. Unfortunately, this reduction has not been implemented to take into account the numerical performance.

To conclude this part, we emphasize that the *First reduction type* should be performed. In fact, during the work of this research this has been the standard. Moreover, The *first* and *second order type* reduction can be performed along side, which highly contrast with the *third type reduction* which excludes combinations with the other two type of reductions for the same index i. Moreover, if the second or third type of reductions is used, a further degree of differentiability is required on the internal energy.

4.2.5 Constitutive laws, special boundary conditions and coupling

Despite we are not dealing in depth in this section with constitutive laws or special type boundary conditions (since those concern a less general framework), we should say some words regarding its treatment and implications within the proposed VF framework. As mentioned before, a_i and A_i each one have their corresponding conjugate variables. We avoid in our framework to establish a constitutive law between such variables. However, both are related through its dual variable a_i^* and A_i^* correspondingly. Since our framework imposes $A_i^* = -\nabla a_i^*$. Therefore, we seek for a constitutive relation between a_i and its conjugate a_i^* [6]. Once this unique constitutive relation is defined we can define the internal energy $U(\mathbf{a})$ and the dissipation potential $\chi(\mathbf{A}, \mathbf{a})$. In the same way, if we have defined the internal energy $U(\mathbf{a})$ and/or the dissipation potential $\chi(\mathbf{A}, \mathbf{a})$, we can obtain a constitutive relation between the corresponding variables.

4.2.5.1 General properties of the internal energy and dissipation potential

The specifics of each problem characterize the functions $U(\mathbf{a})$ and $\chi(A_I, \mathbf{a})$. Nevertheless, the link between a_i and A_i given by (4.13a) through the conjugate variable a_i^* imposes that to define these functions we only need one constitutive law for a given pair $\{a_i, A_i\}$. This is expressed better through the equalities coming from (4.13a) and (4.3a)

$$\frac{\partial \chi}{\partial A_i} = A_i^* = -\nabla a_i^* = -\nabla \frac{\partial U}{\partial a_i} \tag{4.28}$$

However, to develop such relation we can make use of constitutive relations used already in the literature, despite the dependencies are not between the variables and their corresponding conjugates. We present below, possible ways to use constitutive laws with different dependencies into the VF. In addition, the specifics of how these functions are characterized is strongly influenced by the type of physical coupling, whether weak, or strong. Assuming strong coupling, we explore some plausible cases here.

Strong coupling

Constitutive law of the form $a_i = h(a_i^*)$ or $A_i = H(A_i^*)$

This case is the most simple since the dependencies are given through conjugate variables which fits the requirements of our VF framework. Assume we are given any of the following constitutive laws

$$a_i = \frac{\partial U^*}{\partial a_i^*} = h(a_i^*) \qquad \text{or} \qquad A_i = \frac{\partial \chi^*}{\partial A_i^*} = H(A_i^*) \tag{4.29}$$

where we have recalled the relationship of the variables with its conjugates by means of the Legendre-Fenchel transform (4.3a). If $h(a_i^*)$ or $H(A_i^*)$ are part of an exact differential, we are able to construct the corresponding functions by completing the differential. The fact that the constitutive law should be part of an exact differential, is not a theoretical requirement as far as we can tell. Nevertheless, as it will be shown in the next chapter for the specific case of the lithium-ion battery we will model, the exact differential requirement goes hand by hand with a physical principle known as the *Onsager's relations*.

If both constitutive relations are given, we must ensure they satisfy (4.28). When this happens, we can obtain relation between different parameters. In case of being given only one of the constitutive relations, then (4.28) can be used as the link to derive the missing function.

[6] or equivalently A_i and A_i^*

Constitutive law of the form $A_i(\nabla a_i)$

As mentioned, it is common practice to define constitutive equations between balance a_i and flux-type variables A_i from a balance equation as in (4.1). This type of constitutive equations can also be used but we must change the dependencies in accordance to our formulation. Luckily, there is a straight-forward procedure due to the conjugate relations between variables. Consider the constitutive law given by

$$A_i = H_i(\nabla a_i) \tag{4.30}$$

where H_i describes the constitutive relation at hand. In addition, from the conjugate relation (4.3a) between a_i and a_i^* we can compute the gradient of a_i as follows

$$\begin{aligned} a_i^* = \frac{\partial U}{\partial a_i}\Big(\mathbf{a}\Big) \qquad &\rightarrow \qquad \nabla a_i^* = \frac{\partial^2 U}{\partial a_i^2}\Big(\mathbf{a}\Big)\nabla a_i \\ &\rightarrow \qquad \nabla a_i = \left[\frac{\partial^2 U}{\partial a_i^2}\Big(\mathbf{a}\Big)\right]^{-1}\nabla a_i^* \end{aligned} \tag{4.31}$$

the former allows us to substitute (4.31) into (4.30) as follows

$$\begin{aligned} A_i &= H\left(\left[\frac{\partial^2 U}{\partial a_i^2}\Big(\mathbf{a}\Big)\right]^{-1}\nabla a_i^*\right) \qquad \because \qquad A_i^* = -\nabla a_i^* \qquad \text{from (4.13a)} \\ &= H\left(-\left[\frac{\partial^2 U}{\partial a_i^2}\Big(\mathbf{a}\Big)\right]^{-1} A_i^*\right) \end{aligned} \tag{4.32}$$

Hence, the change of variables given by (4.31) allows to change the dependency of the constitutive relation to its corresponding conjugate variable. Once this is done, we can apply the first procedure we described previously.

Weak coupling

In a coupled problem, in the case of weak coupling between Physics the VF can not be used in a straight forward fashion. This is because second order variations of the functional are no longer commutative. Nevertheless, a way around this problem is to develop several functionals of the form (4.14). Such functionals must be listed in a hierarchical structure, where the first functional is described only by pure independent variables, i.e., variables which have no explicit dependency against any other variable. The second functional in the hierarchy is described by variables which only have an explicit dependency against the variables in the first functional. The hierarchy must continue to decrease in the same manner, until the last functional in the hierarchy contains only variables having an explicit or no dependence with the rest.

According to the construction above, we need to define the same number of internal functions and dissipation potentials as the number of hierarchies describing the problem. Once the hierarchies are identified, we use in each hierarchy the methods described above for a strong coupling to obtain the internal energy and the dissipation potential. An example of weak coupling will be provided in §5 when we model the electrodes of a lithium-ion battery, where we consider the chemistry inside the to influence its electric behavior, whereas the opposite is not true.

Special boundary functions :

Special type of boundary functions can be defined by decomposing the Neumann boundary condition into non overlapping sets. These sets must correspond with the desired location where the special boundary condition resides. Once the domain has been decomposed we can allow $\overline{A_i}$ to be a function dependent on the conjugate variables a_i^*. i.e., $\overline{A_i}(a_i^*)$ which allows the equivalence between the VF and the SF and WF to hold. An example of special boundary functions is performed in §5 when we introduced the Butler-Volmer equation as a boundary condition into the model.

We conclude this part by highlighting a property of the VF framework we are proposing. Notice that theoretic knowledge help us create the functional whilst empiric knowledge defines the functions on it.

4.3 Applications

We settle the theory so far in the chapter through an example. We will derive a general VF framework for electrochemistry. This framework, will allow us to implement the required functional of the VF. We focus in a specific coupled problem, electrochemistry. In the next chapter §5 we will use the functional to go into the specifics of a concrete model, e.g. lithium-ion batteries.

4.3.1 Electrochemistry

As the name suggests, electrochemistry consists of the union of Electricity and Chemistry. Each of these fields can be related with specific balance laws, namely, conservation of electric charge and mass balance. Therefore, we have the following balance equations from each field

$$\dot{\rho} + \nabla \cdot \vec{i} = b_\rho \qquad \textit{(electric charge balance)} \tag{4.33a}$$

$$\dot{c}_k + \nabla \cdot \vec{j}_k = b_c \qquad \textit{(mass balance)} \tag{4.33b}$$

where ρ is the electric charge density, $\vec{i}$ the electric current density, b_ρ a external source of electric charge density[7], c_k the concentration of a species k, $\vec{j}_k$ the flux associated to the substance c_k and b_c an external source of concentration for the species k. Electromagnetic phenomena are most commonly modeled through Maxwell's equations. The conservation of electric charge is derived from Maxwell's equations by applying the divergence to Ampere's law and substituting Gauss law into it. Now that we have defined the balance equations in our coupled problem we seek for the energetically conjugate variables related to them. First we recall that ρ and $\vec{i}$ as it is also for c and $\vec{j}$ are related through its correspondent Lagrange multiplier, as suggested by the results obtained in (4.10) and (4.13) and the corresponding units, the conjugate pairs become

$$\{\rho, \phi\}, \qquad \{\vec{i}, \underbrace{-\nabla\phi}_{=:\vec{E}}\} \qquad \textit{Electricity} \tag{4.34a}$$

$$\{c_k, \mu_k\}, \qquad \{\vec{j}_k, \underbrace{-\nabla\mu_k}_{=:\vec{g}_k}\} \qquad \textit{Chemistry} \tag{4.34b}$$

where ϕ is the electric potential and μ_k the chemical potential of the species k. Notice that the conjugate of $\vec{i}$ is the electric field $\vec{E}$ and for $\vec{j}_k$ the conjugate variable is the chemical field $\vec{g}_k$. The equations defining

[7] Despite the fact that under the ElectroNeutrality condition (ENC) b_ρ is usually zero, we keep it to maintain the model general. We discuss the ENC in §5.2.1.2

the former are obtained in accordance to (4.3), which turns as

$$U^*(\phi,\mu_k) = \sup_{\rho}\{\rho\cdot\phi - U(\rho,c_k)\} \quad \rightarrow \quad \phi = \frac{\partial U}{\partial \rho} \tag{4.35a}$$

$$U^*(\phi,\mu_k) = \sup_{c_k}\{c_k\cdot\mu_k - U(\rho,c_k)\} \quad \rightarrow \quad \mu_k = \frac{\partial U}{\partial c_k} \tag{4.35b}$$

$$\chi^*(\vec{E},\vec{g}_k) = \sup_{\vec{i}}\{\vec{i}\cdot\vec{E} - \chi(\vec{i},\vec{j}_k)\} \quad \rightarrow \quad \vec{E} = \frac{\partial \chi}{\partial \vec{i}} \tag{4.35c}$$

$$\chi^*(\vec{E},\vec{g}_k) = \sup_{\vec{j}_k}\{\vec{j}_k\cdot\vec{g}_k - \chi(\vec{i},\vec{j}_k)\} \quad \rightarrow \quad \vec{g}_k = \frac{\partial \chi}{\partial \vec{j}_k} \tag{4.35d}$$

The final step in the development of the generic VF is the explicit definition of the functional.

$$\begin{aligned}\Pi[\dot{\rho},\dot{c}_k,\mu_k,\phi,\vec{j}_k,\vec{i}] = \int_\tau \Bigg[\int_{\Omega_{el}} \left(\dot{U}(\rho,c_k) - \dot{\rho}\dot{\phi} - \sum_k \mu_k\dot{c}_k - \sum_k \vec{j}_k\cdot\vec{g}_k - \vec{i}\cdot\vec{E} + \chi(\vec{j}_k,\vec{i})\right) dV \\ - \int_{\partial_{j_k}\Omega_{el}} \overline{j_k}(\mu_k)dS - \int_{\partial_i\Omega_{el}} \overline{i}(\phi)dS - \int_{\partial_Q\Omega_{el}} Q(\mu_k,\phi)dS\Bigg]\, dt\end{aligned} \tag{4.36a}$$

where the functions $\dot{U}(\rho,c_k)$ & $\chi(\vec{j}_k,\vec{i})$ show the possible bulk coupling. Furthermore, we have defined a special boundary condition on the domain $\partial_Q\Omega_{el}$ which allows for the interface coupling of electrical and chemical fields in that boundary. Moreover, we can apply to the functional above a first reduction type as described in §4.2.4.1 for both physics, this allows for a reduction of the system as shown below. The addition of the constraints and the final expression of the functional to describe the general VF is

$$\{\dot{\rho},\dot{c}_k,\mu_k,\phi\} = \arg\inf_{\mu_k,\phi}\sup_{\dot{\rho},\dot{c}_k}\Pi[\dot{\rho},\dot{c},\mu,\phi] \tag{4.37a}$$

$$\begin{aligned}\Pi[\dot{\rho},\dot{c}_k,\mu_k,\phi] = \int_\tau \Bigg[\int_{\Omega_{el}} \left(\dot{U}(\rho,c_k) - \dot{\rho}\dot{\phi} - \sum_k \mu_k\dot{c}_k + \chi^*(\vec{g}_k,\vec{E})\right) dV \\ - \int_{\partial_{j_k}\Omega_{el}} \overline{j_k}(\mu_k)dS - \int_{\partial_i\Omega_{el}} \overline{i}(\phi)dS - \int_{\partial_Q\Omega_{el}} Q(\mu_k,\phi)dS\Bigg]\, dt\end{aligned} \tag{4.37b}$$

The functional above should satisfy any general electrochemical problem, independently of the type of coupling.

Therefore, the abstract VF model based on balance laws, the definition of internal energy and dissipation potential to encapsulate constitutive laws and conjugate variables to represent the fields, has led to the definition of a more specific VF for electrochemistry. In addition, the generalization makes possible to describe the different physical couplings, whether it is by its type, in essence, strong/weak or by its region of coupling, bulk/interface coupling. The general framework allows to verify the thermodynamic consistency of different models by means of the entropy-like condition. In the following chapter, we explore through the VF for electrochemistry derived above, the model for a lithium-ion battery in order to explore all the options just mentioned.

Chapter 5

Application: Lithium-ion battery

Sommaire

Nous commençons ce chapitre en utilisant le modèle électrochimique généré dans le chapitre précédent. Nous l'appliquons aux théories actuelles des formes fortes pour modéliser des batteries lithium-ion. Nous explorons chaque théorie et déterminons sa faisabilité pour l'intégrer dans notre cadre variationnel. Les spécificités de cet exemple permettent d'identifier différentes propriétés pouvant être extraites de notre modèle, telles qu'une autre façon de comprendre les relations de Onsager et la capacité à évaluer la cohérence thermodynamique d'un modèle. À la fin du chapitre, nous présentons les résultats numériques d'un modèle 1D de l'électrolyte de batterie au lithium-ion utilisant les relations de Butler-Volmer comme conditions aux limites.

In this chapter we develop a VF for a benchmark problem, the model of a lithium-ion battery cell. The importance of this application beyond the increase in commercial demand for electromobility, is that it is a great example of a coupled system. A battery cell involves all the types of physical coupling defined in §1, namely, bulk and interface coupling. The physical fields the model can encompass goes from chemistry, electricity & magnetism, mechanics, heat conduction and fluid dynamics. However, we will mainly focus with the area covered by electricity and chemistry, in essence, electrochemistry. The electrochemistry model of the battery, will allow us to use the generic VF model we developed in §4. The main goal of this chapter is to introduce by means of an example the specifics needed to construct a concrete VF. We start in §5.1 introducing main concepts in the electrochemistry of a lithium-ion battery, where we decompose a lithium-ion battery cell in three main components, namely, the electrolyte, the interface and the electrodes. Afterwards we present and derive the VF for each component of the battery cell.

5.1 Introduction

In electrochemistry, a *battery* is a system which main function is to convert chemical energy into electric energy. It is composed of one or more electrochemical cells, which are the minimal units responsible to transform the energy. We refer to one cell as a *battery cell*. Inside a battery cell, the interaction between electrical and chemical forces is described through *RedOx* reactions, roughly speaking, a chemical process where electrons are exchanged. Hence, electrons can be lost or gained. These two reactions happen in different spatial domains within the battery cell. The most simple spatial description of a battery cell

consists of three contiguous but non-overlapping regions, namely, a positive electrode (*cathode*), the electrolyte and a negative electrode (*anode*), see figure 5.1. Under discharge of the battery, electric current is generated when atoms inside the anode loose an electron, transforming them into cations. On the one hand, electrons traverse an external metal conductor until they reach the cathode. On the other hand, cations are ejected from the anode, where they traverse the electrolyte and reach the cathode in order to be absorbed and reassembled on it. A similar process may occur in the cathode, where anions can be generated and expelled so they can also be absorbed by the anode. This process is similar for different types of batteries. Nevertheless, for lithium-ion batteries only lithium cations are exchanged between anode and cathode. We model the problem by focusing on the different spatial zones and their corresponding couplings in the battery cell. Therefore, we start by mentioning the specific reactions of a lithium-ion battery followed by a description of the electrodes and the electrolyte. For a more in depth description one can refer to Newman and Thomas-Alyea [2004], Xu [2004], Ehrl [2017], A. Lundgren et al. [2017] from where the information presented is based.

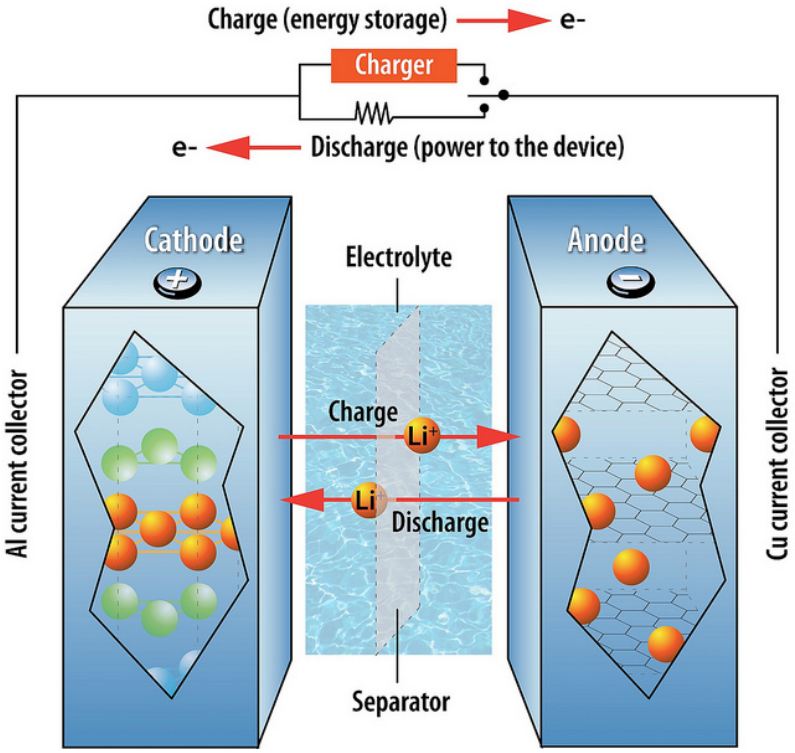

Figure 5.1: How a lithium-ion battery works
Source: Argonne National Laboratory. 27 Sep 2010. Online image. Flickr. 08 May 2017. <https://www.flickr.com/photos/argonne/5029455937>. Original image. (CC BY-NC-SA 2.0)

5.1.1 RedOx reaction

For a lithium-ion battery the whole process of RedOx reactions is the following.

$$x\mathrm{LiC_6} + \mathrm{Li_{(1-x)}CoO_2} \leftrightarrows x\mathrm{C_6} + \mathrm{LiCoO_2} \tag{5.1}$$

An amount of x molecules of LiC_6 react with $Li_{(1-x)}CoO_2$. The x missing atoms of Li in the $Li_{(1-x)}CoO_2$ are added by the decomposition of LiC_6 molecules. As a result we obtain x particles of C_6 and the expected $LiCoO_2$. As mentioned in the introduction, this is a RedOx reaction, meaning that the exchange of electrons is what drives the reaction. Fortunately for us, this exchange of electrons happens in different domains of the battery cell, namely, the anode and the cathode. Hence, we can decompose a battery cell reaction into two processes called *half cells*. One half cell describes the process of oxidation which occurs at the anode. The other half cell describes in the cathode the process of reduction. We describe them below

Half reactions:

Oxidation process

A oxidation process in a RedOx reaction, is when electrons are being detached from a molecule. At the anode, this reaction is the following

$$LiC_6 \rightarrow Li^+ + e^- + C_6 \tag{5.2}$$

This means that a molecule of LiC_6 is decomposed into a cation of Li^+, an electron e^- and an atom of C_6. The electrons are detached when the electric circuit of the battery is closed due to the difference of electric potential between anode and cathode. The electron travels to the external circuit while the atom of C_6 remains in the anode and the cation of Li^+ is expelled towards the electrolyte due to differences of electrochemical potential. We must highlight that ideally the electrolyte acts as an electric insulator Xu [2004], imposing a high resistance for the electrons, that is why we assume electrons and cations have to traverse different paths to reach the cathode.

Reduction process

The reduction process in a RedOx reaction, is when electrons are gained by a molecule. This is what happens at the cathode. As explained above, electrons are sent to the cathode by an external circuit, once they reached the cathode, the chemical reaction produced at the cathode is the following

$$Li_{(1-x)}CoO_2 + xLi^+ + xe^- \rightarrow LiCoO_2 \tag{5.3}$$

In the cathode, there are molecules of $Li_{(1-x)}CoO_2$ which react with an x amount of cations Li^+ arriving from the electrolyte and the same amount of electrons e^- arriving from the external circuit. Both incoming molecules are the result of the oxidation process described above. The reaction creates a molecule of $LiCoO_2$ at the electrode.

Therefore, we can see that the reactions (5.2) and (5.3) from the half cells combined, described the whole RedOx process in (5.1). Notice that the reactants and end products on the reaction equation (5.1) are in each case distributed between anode and cathode. The process above describes the chemical reaction when the battery is being discharged. In contrast while charging, an external source promotes the movement of electrons and Li^+ back to the electrode where the C_6 molecules where left, producing the inverse process. Therefore, depending on whether the battery is being charged or discharged, the definition of the electrodes as anode and cathode becomes ambiguous. Hence, by definition, oxidation takes place at the anode, and reduction at the cathode as proposed by Ehrl [2017]. In general we will be talking of the discharged process of the battery.

5.1.1.1 Battery cell anatomy

We have mentioned that the most simple spatial description of a battery cell composition is through the electrodes and the electrolyte. We focus now on the types of electrochemical coupling which might take place in each of part of the battery cell. We add the interface region electrolyte/electrode since it is a spatial region where interface coupling is expected to occur. The different spatial zones of coupling we mention are shown in figure 5.2.

Electrolyte: In the electrolyte the transport of ions between electrodes takes place. When we focus on the electrolyte as shown in figure 5.2a the type of coupling we are dealing is bulk coupling. A minimal model of the electrolyte, requires a strong coupling between chemistry and electricity. The later is roughly justified since the ions move through the electrolyte driven by the gradient of chemical potential *(diffusion)*. However, as ions, they also move electric charge which starts to build up an opposing gradient of electric potential. The movement of ions due to an electrical field is called *migration*. This migration and diffusion phenomena has been studied in electrochemistry for more than a 100 years. Some of the first succesful models which focus on the migration-diffusion process can be seen in the works of Nernst [1889] and Planck [1890]. The bulk coupling of the electrolyte is displayed in figure 5.2a

Electrodes: In contrast with the electrolyte where we assume the only particles are ions, in the electrodes we consider also the electrons. The electrons are expected to move through conductors embedded in the electrode and are the main cause for the generation of electric current inside the electrode. Therefore inside the electrodes the electrochemical bulk coupling can be considered to be weak or even uncoupled [Fang et al., 2017]. The rationale to avoid a strong coupling is that electrons are scattered over the domain, therefore, local electric potential due to electrons is weak with comparison the strength of the mechanical structure of the electrode, which is normally considered to be rigid or elastic. However, if we would describe accurately the electrode, the following couplings should be considered. Thermal and mechanical effects should be strongly coupled with the chemistry, since the adsorption and ejection of ions should influence the mechanical structure of the electrode. Depending on the material, the electrodes are expected to undergo large elastic and plastic deformations Salvadori et al. [2015], leading also to thermal fluctuations. Furthermore, the electric forces despite being weakly coupled with the chemistry, are in contrast, strongly coupled with the mechanics and heat conduction, since the displacement of the electrons, specially at high electrical currents can lead to electron migration and heat dissipation. Nevertheless, for the sake of presenting different ways to construct the VF we are proposing, we use the uncoupled model used in [Fang et al., 2017].

Electrode / Electrolyte interface: The region between the electrolyte and the electrodes is where interface coupling takes place. The coupling from an electrochemical point of view, is generated by the reaction of Li ions which are absorbed *(lithiated)* or expelled *(delithiated)* from the electrodes. *Lithiation* is the process of absorption of Li ions from the electrolyte into the electrode, while *delithiation* is when Li ions are expelled from the electrode into the electrolyte. However, more complete models used further interface regions, as it is the surface electrolyte interface (SEI), as mentioned in Newman and Thomas-Alyea [2004], Xu [2004], Bucci et al. [2014]. As before, we omit further refinement of the model to keep the focus on the modelling via the VF proposed. The simple interface region is enough to provide us with the opportunity to show how to implement interface coupling with the VF. The region of interface coupling of the electrolyte with the anode and cathode is displayed in figure 5.2b

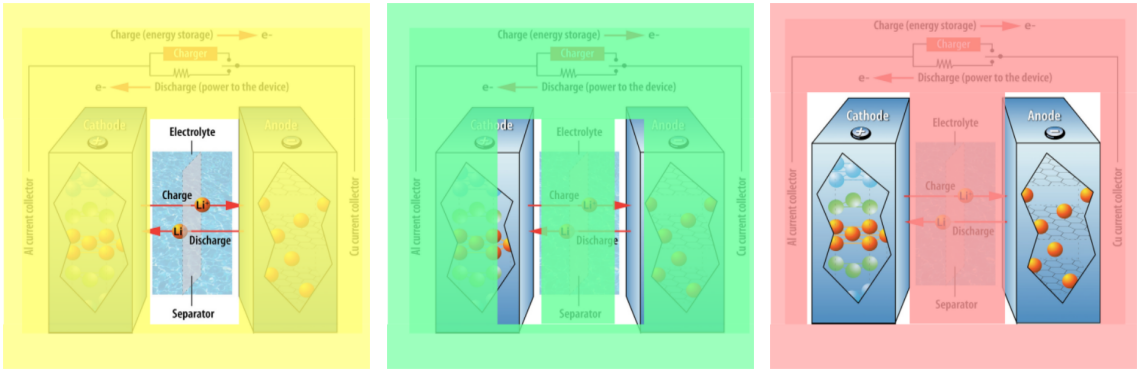

(a) Electrolyte (bulk) (b) Electrolyte/Electrode (interface) (c) Electrodes (bulk)

Figure 5.2: Battery cell coupling

5.1.2 Framework: Local irreversible thermodynamics

Different approaches are used when we model the electrochemistry behaviour in a battery, mainly due to spatial and time scales. To understand the main difference, a dimensional analysis of the problem is taken, resulting on the parameter *Debye length* r_D. The *Debye length* represents the distance surrounding an ion at which its electric potential is screened in its surroundings. A popular postulate which simplifies set of equations to solve is the so-called ElectroNeutrality condition (ENC). ENC is not a fundamental law, but rather an approximation of Gauss' law, one of Maxwell's equations. The ENC holds for spatial scales bigger than the Debye length [Jackson, 1974, Newman and Thomas-Alyea, 2004, Dickinson et al., 2011, Salvadori et al., 2015]. Based on a *local equilibrium hypothesis* we will consider volume elements bigger than the Debye length, such that the ENC holds. Moreover, the implications of the Debye length r_D also extend to the temporal domain by means of the *Debye time* $t_D := r_D^2/D$ where D is the diffusion coefficient of the medium. Hence, we further consider a temporal domain bigger than the *Debye time* t_D. For temporal domains smaller than the *Debye time* t_D, the volume elements are not longer a valid representation of the system, and thus the local equilibrium approach does not hold. In this case, a plausible solution is the use of *extended irreversible thermodynamics*, which we will not pursue in this work.

Thus, the following VF is developed under the framework of *local equilibrium thermodynamics* assuming the postulate of the ENC. The Debye parameters are given by

$$r_D := \sqrt{\frac{RT\epsilon_s\epsilon_0}{2FC*}} \qquad \text{(Debye length)} \tag{5.4a}$$

$$t_D := \frac{r_D^2}{D} \qquad \text{(Debye time)} \tag{5.4b}$$

where RT/F is the *thermal volt* coefficient, ϵ_s is the *relative permittivity of the medium*, ϵ_0 is the *permittivity of free space*, $C*$ is the *bulk concentration* of the electrolyte, N_A the *Avogadro constant* and $F := q_e N_A$ is the *Faraday constant*, with q_e as the electron charge. The derivation of the equations above can be found in Dickinson et al. [2011].

5.1.3 Further details

Before presenting the specifics of the model for each region of the battery, we make a supplementary distinction, in line with the review by Ramadesigan et al. [2012]. As mentioned above, different approaches are used to model lithium-ion batteries. Ramadesigan et al. [2012] proposes to group the models into four categories, namely, *empirical models*, *electrochemical engineering models*, *multiphysics models*, and *molecular/atomistic models*, this work can be classified in the set of electrochemical and/or multiphysic models.

5.2 Electrolyte

For the electrolyte we explore three different approaches from the literature to obtain the flux-type equations describing the electrolyte behaviour: the *Stefan-Maxwell*, *Nernst-Planck* and *Ion-transport* model. These models will be used to define the functions needed by the VF. To model the electrolyte, any of these three approaches are used together with balance laws for mass and electric charge [Kontturi et al., 2008, Ehrl, 2017, Latz and Zausch, 2011]. We will derive a general condition to check if each approach is prone to fit our VF. This condition is equivalent to Onsager's reciprocal theorem, as we will also show. In addition, we refer to the spatial area occupied for the electrolyte as Ω_{el}

The electrolyte section is presented as follows. We start by introducing in §5.2.1 the conservation laws and in §5.2.2 the constitutive laws describing the electrolyte. Afterwards, we continue with the contribution of this work. We begin in §5.2.3 by defining a set of conditions required in the flux-type equations such that the VF can be constructed. Furthermore, we will demonstrate the equivalence between the condition we derived and the Onsager relations. In §5.2.4 we develop specific definitions of the functions for the VF based on the different approaches.

5.2.1 Conservation laws

The conservation laws shown in the general electrochemical framework in §4.3.1 are simplified for the electrolyte model we present. We consider the system to be closed, where any type of sources or reactions within the domain are not allowed. In addition, we assume the ElectroNeutrality condition (ENC) holds within the spatial and time interval scales we consider. The later reduces the balance laws into conservation laws, plus the use of the ENC turns the conservation of electric charge into a zero divergence statement. We start showing the conservation law for mass, afterwards, we derive and justify the use of the ElectroNeutrality condition. Finally, we present and reduce the conservation of electric charge by means of the ENC. We conclude by summarizing the set of conservation laws for the electrolyte and present the corresponding VF functional we propose for it.

5.2.1.1 Conservation of mass

The particles constituting the electrolyte come from the solute and the ionic particles. Assuming the absence of chemical reactions inside the electrolyte and exchange of ions only through the boundaries, the conservation of mass for the electrolyte becomes

$$\dot{c}_{el} + \nabla \cdot \vec{j}_{el} = 0\,; \qquad \forall \vec{x} \in \Omega_{el} \qquad \textit{(mass conservation)} \tag{5.5}$$

where c_{el} is the concentration of Li^+, and $\vec{j}_{el}$ is the flux associated to the Lithium cations (Li^+) in the electrolyte. For a general electrolyte of n species we have $\cdot_{el}$ to be exchanged by $\cdot_k$ where $k \in$

$\{0, 1, \ldots, , n+1\}$, where it is common to use $k = 0$ to denote the solute. For a detailed derivation confer to Kontturi et al. [2008].

5.2.1.2 ElectroNeutrality condition (ENC)

A popular postulate in electrochemical systems is based on the fact that aqueous electrolyte solutions are neutral [Wright, 2007], which is true under certain conditions we detail below. To describe electric charge transport, we make use of *Gauss law* from electromagnetism, one of Maxwell's equations.

$$\frac{\rho}{\epsilon_s \epsilon_0} - \nabla \cdot \vec{E} = 0 \qquad \textit{(Gauss law)} \tag{5.6}$$

where we recall ρ as the *electric charge density*, $\vec{E}$ is the electric field, ϵ_s is the *relative permittivity of the medium* and ϵ_0 is the *permittivity of free space*. Assuming the only charge carriers in the electrolyte are the disassociated ions, the total charge Q of the system is given by

$$Q := \sum_k q_e z_k N_k \tag{5.7}$$

where for the species k , N_k is the *number of particles per volume* V, z_k is the corresponding *charge number* and q_e is the *electron charge constant*. Since we assume dissociate ions are the only charge carriers, we can state the charge density ρ and electric current density $\vec{i}$ as

$$\rho = \frac{Q}{V} = \frac{1}{V} \sum_k q_e z_k N_k = F \sum_k z_k C_k \,; \qquad \vec{i} = F \sum_k z_k \vec{j}_k \tag{5.8}$$

recalling that the *total concentration* expressed in moles/volume of a substance is defined as $C := \frac{N}{N_A V}$ where N_A is the *Avogadro constant* and $F := q_e N_A$ is the *Faraday constant*. Substituting the definition of charge density in (5.8) into the Gauss law (5.6) we get

$$\frac{1}{\epsilon_s \epsilon_0} F \sum_k z_k C_k - \nabla \cdot \vec{E} = 0 \qquad \underset{\text{dimensional analysis}}{\longrightarrow} \qquad \sum_k z_k c_k = 2 r_D^2 \frac{F}{RT} \nabla \cdot \vec{E} \tag{5.9}$$

where $c_k = C_k / C*$ is the *relative concentration* of the species k in the electrolyte and r_D is the *Debye length* as defined in (5.4a). For a detailed derivation of the dimensional analysis shown above, refer to Dickinson et al. [2011]. Finally, using the dimensional analysis we can postulate the use of the so-called ElectroNeutrality condition (ENC)

$$\sum_k z_k c_k \approx 0; \qquad \textit{(electroneutrality condition)} \tag{5.10}$$

this approximation is considered valid for large scale such that the Debye length tends to zero. The Debye length represents the extend over which the electric field can vary having possible large values before being screened in the electrolyte. Thus, the ENC is valid at such scales since the divergence of the electric field becomes insignificant compared with the charge of the ions.

For more detailed information please refer to Jackson [1974], Newman and Thomas-Alyea [2004], Salvadori et al. [2015]. An interesting discussion on regard the validity of the ENC is given in Dickinson et al. [2011], and insightful results on the implications of it can be seen in the work of Danilov and Notten [2008].

5.2.1.3 Conservation of electric charge

The conservation of electric charge is derived from Maxwell's equations by applying the divergence to Ampere's law and substituting Gauss law into it [Kontturi et al., 2008].

$$\dot{\rho}_{el} + \nabla \cdot \vec{i}_{el} = 0\,; \qquad \forall \vec{x} \in \Omega_{el} \qquad \textit{(electric charge conservation)} \tag{5.11}$$

where we recall $\vec{i_{el}}$ is the *electric current density* within the electrolyte. Under the postulate of ENC (5.10) we have that ρ_{el} is constant in time. Hence, the conservation law for electric charge becomes

$$\nabla \cdot \vec{i}_{el} = 0\,; \qquad \forall \vec{x} \in \Omega_{el} \qquad \textit{(electric charge conservation assuming ENC)} \tag{5.12}$$

Therefore, the use of the ENC imposes a zero divergence on the electric flux density.

5.2.1.4 Electrochemical conservation laws and VF functional

Summarizing the results above, the two conservation equations to which an electrolyte is subjected are

Chemical	**Electrical**	
$\dot{c}_{el} + \nabla \cdot \vec{j}_{el} = 0$	$\nabla \cdot \vec{i}_{el} = 0$	(*Conservation laws*)

(5.13)

Conservation laws and its associated natural (Neumann) boundary conditions are enough to define the functional which needs to be optimized in our VF, as described in §4. Starting from the general electrochemical functional we derived in (4.37), using the conservation laws (5.13) we obtain the following VF

$$\{\dot{c}_{el}, \mu_{el}, \phi_{el}\} = \arg \inf_{\mu_{el}, \phi_{el}} \sup_{\dot{c}_{el}} \Pi_{el}[\dot{c}_{el}, \mu_{el}, \phi_{el}] \tag{5.14a}$$

$$\Pi_{el}[\dot{c}_{el}, \mu_{el}, \phi_{el}] = \int_{\tau} \left[\int_{\Omega_{el}} \left(\dot{U}(c_{el}) - \sum_{el} \mu_{el} \dot{c}_{el} - \chi^*(\vec{g}_{el}, \vec{E}_{el}) \right) dV - \int_{\partial_{j_{el}} \Omega_{el}} \overline{j_{el}}(\mu_{el}) dS - \int_{\partial_i \Omega_{el}} \overline{i}_{el}(\phi_{el}) dS \right] dt \tag{5.14b}$$

Notice that the only difference between (4.37) and (5.14) is that we have removed the dependence of the rate of internal energy $\dot{U}$ on the electric charge density ρ as a result of using the ENC. Now, we present the constitutive equations which will define the different material models for the VF.

5.2.2 Constitutive laws

We present two types of constitutive laws used for an electrolyte. One concerning the relation between chemical potential μ_{el} and concentration c_{el}, plus, the flux-type equations or transport equations as suggested in this context in Kontturi et al. [2008]. The *flux-type equations* describe the associated flux-type quantity and may embed implicitly the constitutive law for the chemical potential. However, we need to introduce some concepts before. We start with the definition of preliminary concepts such as that of a *binary electrolyte solution*. This allows to present the constitutive equation for the chemical potential within the electrolyte. Afterwards, we introduce the concept of *electrochemical potential* and present three different approaches to obtain the flux-type equations for the electrolyte, namely, the *Stefan-Maxwell*, *Nernst-Planck* and *Ion-transport* model. The different approaches will help us define in different ways the functions in the VF, as long as they satisfy the conditions we have imposed in §4. Each definition will correspond to a specific material model inside the VF .

5.2.2.1 Binary electrolyte solution

To simplify the model we consider a *binary electrolyte*, which is defined as an electrolyte which contains a single salt in a single solvent [Newman and Thomas-Alyea, 2004]. For an overview on the lithium salts used in advanced Lithium-ion batteries confer to Younesi et al. [2015]. We consider a neutral *salt* to be a substance that dissociates when dissolved, such as salt in water [Job et al., 2015], in essence,

$$\mathrm{A}_{\nu_+}\mathrm{B}_{\nu_-} \leftrightarrows \nu_+\mathrm{A}^{z_+} + \nu_-\mathrm{B}^{z_-} \tag{5.15}$$

where AB is the *component* in its solid state, A and B are the *dissociated elements*, the subindex + and − relate to the dissociated cathodic and anodic species respectively, being ν the *stoichiometric coefficient*, and z the *charge number*. In a salt the relation between concentrations is equal to the ratio between their stoichiometric coefficients

$$\frac{c_+}{c_-} = \frac{\nu_+}{\nu_-} \qquad \rightarrow \qquad c := \frac{c_+}{\nu_+} = \frac{c_-}{\nu_-} \quad \text{or} \quad m := \frac{m_+}{\nu_+} = \frac{m_-}{\nu_-} \tag{5.16}$$

The implications of the process above, allow us to define the equations in term of the dissociated species or the salt. Where we have defined the concentration of the salt c in terms of any of its components. Furthermore, using the ElectroNeutrality condition in (5.10), and substituting the component concentrations for the salt concentration, we can arrive to the condition for a neutral salt

$$\sum z_k\nu_k c = (z_+\nu_+ + z_-\nu_-)c = 0 \qquad \rightarrow \qquad z_+\nu_+ + z_-\nu_- = 0 \tag{5.17}$$

The derivation above, shows the validity of the neutral salt condition. In essence, the neutral salt condition directly depends on the validity of the ENC.

5.2.2.2 Chemical Potential

In §3 we established a connection between chemical potential and concentration of a species k, known as the *logarithmic mass action law* (3.2), which we rewrite below

$$\mu_k = \mu_{k_0} + RT\ln\left(\frac{c_k}{c_{k_0}}\right) \qquad (\textit{logarithmic mass action law}) \tag{5.18}$$

Nevertheless, in the literature, a more specific relation is sometimes used. In Newman and Thomas-Alyea [2004] the chemical potential of a substance is expressed as

$$\mu = RT\ln\lambda = \underbrace{RT\ln c}_{:=\mu^c} + \underbrace{RT\ln fa^\theta}_{=:\mu^{ex}} \tag{5.19}$$

where λ is the *absolute activity*, and is represented through μ^c, an ideal term dependent on the concentration used to approximate the chemical potential μ which is coined as the *second reference state* and μ^{ex} the *correction term* of the chemical potential which usually is independent of concentration. The *absolute activity* for a species k in a mixture is expressed in electrochemistry, through its molality or molarity.[1]. Defining the *absolute activity* for a species k through is molality is done as follows

$$\lambda_k = m_k\gamma_k\lambda_k^\theta \tag{5.20}$$

where m_k is the molality, γ_k the molal activity coefficient and λ_k^θ is a proportionality constant. Nevertheless, sometimes a similar expression for the absolute activity is defined in molar terms is used

$$\lambda_k = c_k f_k a_k^\theta \tag{5.21}$$

[1] the *molality* is defined as the number of moles of solute per kilogram of solvent, while *molarity* defines the number of moles of solute per liter of solution.

where c_k is the molarity of the species, f_k is the molar activity coefficient and a_k^θ the corresponding proportionality constant. Both definitions, can be linked through the relations

$$m_k = \frac{c_k}{c_0 M_0}; \qquad \lambda_k^\theta = \rho_0 a_k^\theta \tag{5.22}$$

where the subindex 0 denotes the solvent, being c_0 its molarity, M_0 its molar mass and ρ_0 is its density. A relation between equations (5.20) and (5.22) is given through

$$\lambda_k = \frac{c_k}{c_0 M_0}\gamma_k \lambda_k^\theta \tag{5.23}$$

The equations above can help us to construct more complex expressions for chemical potentials, such as the chemical potential of a neutral salt, which we derive below.

Chemical potential of a binary salt

The molar chemical potential of a binary salt [2], is expressed as the linear combination of its dissociated components weighted through their corresponding stoichometric coefficient. Using (5.21) for the dissociated components we have

$$\begin{aligned}
\mu_A &= RT \ln (c f_A a_A^\theta) && \text{(5.24a)}\\
&= \nu_+ \mu_+ + \nu_- \mu_- \\
&= RT \ln [(c_+ f_+ a_+^\theta)^{\nu_+} (c_- f_- a_-^\theta)^{\nu_-}] \\
&= RT \ln (\nu_+^{\nu_+} \nu_-^{\nu_-}) + \nu RT \ln (c f_\pm a_\pm^\theta) && \text{(5.24b)}
\end{aligned}$$

where the subindex + and − denote the corresponding positive and negative species on which the salt dissociates. We have used the definitions $\nu := \nu_+ + \nu_-$, $f_\pm := f_+^{\nu_+} f_-^{\nu_-}$ and $(a_\pm^\theta)^\nu := a_+^{\nu_+} a_-^{\nu_-}$, [3]. The terms in (5.24a) and (5.24b) are related by $f_A = f_\pm^\nu \nu_+^{\nu_+} \nu_-^{\nu_-} c^{\nu-1}$. We will use the equation above (5.24) to define the internal energy U for some models. However, for other models we can apply the same process for a salt as above but instead we use (5.20).

$$\begin{aligned}
\mu_A &= RT \ln \left(m \gamma_A \lambda_A^\theta\right) && \text{(5.25a)}\\
&= RT \ln (\nu_+^{\nu_+} \nu_-^{\nu_-}) + \nu RT \ln (m \gamma_\pm \lambda_\pm^\theta) && \text{(5.25b)}
\end{aligned}$$

A further expression for the chemical potential of a salt can be produced by means of (5.16) and (5.22) such that

$$m = \frac{m_k}{\nu_k} = \frac{1}{\nu_k}\left(\frac{c_k}{c_0 M_0}\right) = \frac{\nu_k}{\nu_k}\left(\frac{c}{c_0 M_0}\right) = \frac{c}{c_0 M_0} \tag{5.26}$$

which substituting in (5.23) leads to

$$\begin{aligned}
\mu_A &= RT \ln \left(\frac{c}{c_0 M_0}\gamma_A \lambda_A^\theta\right) && \text{(5.27a)}\\
&= RT \ln (\nu_+^{\nu_+} \nu_-^{\nu_-}) + \nu RT \ln \left(\frac{c}{c_0 M_0}\gamma \pm\right) + RT \ln (\lambda_\pm^\theta) && \text{(5.27b)}
\end{aligned}$$

The equations (5.24), (5.25) and (5.27) give us three options to represent the chemical potential of a salt.

[2] see §5.2.2.1

[3] we omit the θ upper index in the dissociated components, to overload the notation in the expression

Diffusion coefficients Above we have defined different constitutive expressions for the chemical potential. The chemical potential, is not just a constitutive property of a substance, its gradient is also considered as the driving force for chemical reactions and diffusion Newman and Thomas-Alyea [2004], Job et al. [2015]. This means that the flux of species $\vec{j}$ is defined proportionality to the gradient of the chemical potential $\nabla\mu$. However, for historical and some experimental reasons it is a common practice to relate the flux of species $\vec{j}$ as dependent on the concentration as it is done when using Fick's first law (3.1a). Both expressions can be matched through the definition of a diffusion coefficient D^{ch} as follows

$$\vec{j}_k = -c_k \mathfrak{m}_k \nabla\mu_k \equiv D_k^{ch} \nabla c_k \tag{5.28}$$

where we recall that for a species k, $\mathfrak{m}_k$ is the mobility coefficient and D_k^{ch} is the chemical diffusivity. It is a common procedure in the literature to relate both expression through the chemical diffusivity. We present below different expressions for the chemical potential and relate some of them to the chemical diffusivity D_k^{ch}. The process developed on these steps will turn useful when defining the different models of the VF. This process, can be related to the process we define in §4.2.5.1.

Molar relation

If we let the chemical potential be defined through (5.24) the expression in (5.28) becomes

$$\vec{j}_k = -c_k \mathfrak{m}_k \nabla\mu_k \tag{5.29}$$

$$= \nu D_k \left(\nabla c_k + c_k \nabla \ln f_\pm + c_k \nabla \ln a_k^\theta \right) \equiv D_k^{ch} \nabla c_k \tag{5.30}$$

where D_k is the tracer diffusivity, defined as $D_k := \mathfrak{m}_k RT$. Therefore the chemical diffusivity can be expressed as

$$D_k^{ch} = \nu D_k \left(1 + \frac{\partial \ln f_\pm}{\partial \ln c_k} + \cancelto{0}{\frac{\partial \ln a_k^\theta}{\partial \ln c_k}} \right) \tag{5.31}$$

the last term cancels out, since the proportionality constant a_k^θ is defined by most authors to be independent of c_k.

Molal/molar relation

Another option is to let the chemical potential be defined through (5.27). In that scenario the expression in (5.28) becomes

$$\vec{j}_k = -c_k \mathfrak{m}_k \nabla\mu_k \tag{5.32}$$

$$= \nu D_k \left(\nabla c_k - c_k \nabla \ln c_0 + c_k \nabla \ln \lambda_\pm + c_k \nabla \ln \gamma_k^\theta \right) \equiv D_k^{ch} \nabla c_k \tag{5.33}$$

where D_k is the tracer diffusivity, defined as $D_k := \mathfrak{m}_k RT$. Therefore the chemical diffusivity can be expressed as

$$D_k^{ch} = \nu D_k \left(1 - \frac{\partial \ln c_0}{\partial \ln c_k} + \frac{\partial \ln \lambda_\pm}{\partial \ln c_k} + \cancelto{0}{\frac{\partial \ln \gamma_k^\theta}{\partial \ln c_k}} \right) \tag{5.34}$$

as the other example above, the last term cancels out, since the proportionality constant γ_k^θ is defined to be independent of c_k.

5.2.2.3 Electrochemical potential

In electrochemistry for experimental reasons, it is preferred to work with the electrochemical potential ψ instead of the pure electric potential ϕ. Both variables are related to each other via the chemical potential. The electrochemical potential is presented having different units for different authors, we select the definition of the electrochemical potential presented by Latz and Zausch [2011]

$$\psi_k = \phi_k + \frac{1}{z_k^+ F}\mu_k \tag{5.35}$$

where z_k^+ is the *charge number of a positive ion* from the species k, and F the *Faraday constant*. As shown in (5.35), the units of the electrochemical potential are the same units of the electric potential. A useful relation we can derive from (5.35) is to solve for ϕ_k and take the gradient, in essence

$$-\nabla\phi_k = -\nabla\psi_k - \frac{1}{z_k^+ F}(-\nabla\mu_k) \qquad \text{or} \qquad \vec{E}_k = \vec{\Psi}_k - \frac{1}{z_k^+ F}\vec{g}_k \tag{5.36}$$

where we recall the definitions of the fields $\vec{E}_k := -\nabla\phi_k$, $\vec{\Psi}_k := -\nabla\psi_k$ and $\vec{g}_k := -\nabla\mu_k$.

5.2.2.4 Flux-type equations

Nernst-Planck approach The classical Nernst-Planck equation defines the constitutive law for the species flux[4] as a contribution of the ionic diffusion and migration as

$$\vec{j}_k = -D_k\left(\nabla c_k + \frac{F}{RT}z_k c_k \nabla\phi\right) \qquad \forall k \neq 0 \qquad \textit{(classical Nernst-Planck equation)} \tag{5.37}$$

as pointed out in Kontturi et al. [2008] this equation takes as frame of reference the solvent −Hittorf's reference frame−. An alternative formulation for the Nernst-Planck approach is presented in Ehrl [2017], where the flux-type equations are defined for a binary electrolyte solution as

$$\vec{j} := -\mathbb{D}_\pm \nabla c + \frac{t_+}{\nu_+ z_+ F}\vec{i} \qquad \textit{(ionic flux)} \tag{5.38}$$

$$\vec{i} := -\kappa\nabla\phi + \frac{\nu}{\nu_+ z_+}\frac{RT}{F}\kappa\left(\frac{\nu_-}{\nu} - t_+\right)\nabla \ln c \qquad \textit{(electric current)} \tag{5.39}$$

where for a species k we have, ν_k is the *dissociation number*, t_k is the *transference number*, for the binary salt we have $\mathbb{D}_\pm$ is the *dilute binary diffusion coefficient*, $\nu := \nu_+ + \nu_-$ is the *dissociation number*, κ is the *conductivity* of the electrolyte solution and ϕ is the *electrostatic potential* within the electrolyte solution. Notice that one should be careful when working with component concentrations (e.g. c_+ or c_-), or the salt concentration c, since the the conductivity κ depends on the concentrations also as shown below.

The definition of the transport parameters given above is

$$\mathbb{D}_\pm := \frac{(z_+ - z_-)D_+ D_-}{z_+ D_+ - z_- D_-}; \qquad \kappa := \frac{F^2}{RT}\Big(z_+ D_+ - z_- D_-\Big)z_+ c_+ \tag{5.40a}$$

$$t_+ := \frac{z_+ D_+}{z_+ D_+ - z_- D_-}; \qquad t_- := \frac{-z_- D_-}{z_+ D_+ - z_- D_-} \tag{5.40b}$$

[4] except the solvent species

Stefan-Maxwell approach The Stefan-Maxwell models concentrated solutions Newman and Thomas-Alyea [2004]. It defines the flux-type equations through of equilibrium of forces, namely, the driving force and frictional force [Kontturi et al., 2008]. According to Ehrl [2017] the flux-type equations described by this approach are

$$\vec{j} := -D_{\pm}\nabla c + \frac{t_+}{\nu_+ z_+ F}\vec{i} \qquad \textit{(ionic flux)} \tag{5.41a}$$

$$\vec{i} := -\kappa\nabla\psi - \frac{\kappa}{\nu_+ F}\left(\frac{s_+}{n} - \frac{t_+}{z_+} - \frac{s_0\nu_+}{nc_0}\right)\nabla\mu_{\pm} \qquad \textit{(electric current)} \tag{5.41b}$$

where $D_{\pm}$ is the *binary diffusion coefficient*, s the *stoichiometric coefficient* for reactions at the electrode interface, n is the *number of available electrons* at the electrode with $s_+z_+ + s_-z_- = -n$, the subindex $_+$, $_-$ and $_0$ correspond to the cations, anions and solvent. It is important to highlight the correction done in (5.41b), where Newman and Thomas-Alyea [2004] uses a dependence on the electric pontential ϕ instead of the electrochemical potential ψ. This change, is proposed in Latz and Zausch [2011] since the dependence on ϕ violates the Onsager relations. The parameters in (5.41) are described by

$$\Xi := \left(1 - \frac{\partial \ln c_0}{\partial \ln c}\right); \qquad D_{\pm} := D\Xi \tag{5.42a}$$

$$\frac{1}{\kappa} := -\frac{1}{z_+z_-C^*}\frac{RT}{F^2}\left(\frac{c_0t_-}{c_+D_{0-}} + \frac{1}{D_{+-}}\right) \qquad D := \frac{(z_+ - z_-)D_{0+}D_{0-}}{z_+D_{0+} - z_-D_{0-}} \tag{5.42b}$$

where D is the molecular diffusion coefficient related to the coefficient appearing in Fick's law of diffusion and Ξ the *thermodynamic factor*. For the derivation process for the Stefan-Maxwell approach please refer to Kontturi et al. [2008], Ehrl [2017]

Ion-transport approach The ion-transport approach proposed in Latz and Zausch [2011] not only encompass the flux-type equations for ion flux and electric current, it also defines heat conduction. However, we will focus only on the electrochemical part of this model. This approach is based on rigorous derivation of the equations based exclusively on the general principles of nonequilibrium thermodynamics under the postulate of the ENC, a binary salt such that $\nu_+ = \nu- = 1$ and no convection forces. The flux-type equations proposed in this approach are given by

Chemical	**Electrical**	
$\vec{j} := -D_{el}\nabla c + \frac{t_+}{z_+F}\vec{i}$	$\vec{i} := -\kappa\nabla\Phi - \kappa\frac{t_+}{z_+F}\nabla\mu_{el}$	*(Flux-type equations)* (5.43)

where D_{el} is the diffusion coefficient of the electrolyte, and μ_{el} the electrolyte's chemical potential, ions and solvent included. The rest of the coefficients are defined such that they satisfy the Onsager relations. Notice that the chemical potential is that of the electrolyte, where we consider as electrolyte the ions and the solvent.

As it will be shown *Ion-transport approach* from Latz and Zausch [2011], shows a direct correspondence with the method General VF method we have proposed.

5.2.3 VF Conditions

The constitutive laws presented above by the equations, (5.38, 5.41, 5.43) are plausible models for the VF in (5.14). Hence, we abstract the similarities in the equations to define a general rule to construct the internal energy and dissipation potential required for the VF.

$\forall \vec{x} \in \Omega_{el}$	**Chemical**	**Electrical**	
Evolution eq.	$\dot{c}_{el} + \nabla \cdot \vec{j}_{el} = 0$	$\nabla \cdot \vec{i} = 0$	(5.44a)
Flux-type eq.	$\vec{j}_{el} = \partial_{g_{el}} \chi(\vec{g}_{el}, \vec{E}_{el})$	$\vec{i}_{el} = \partial_{E_{el}} \chi(\vec{g}_{el}, \vec{E}_{el})$	(5.44b)

where we consider only the transport of lithium cations within the electrolyte, as it is done for a lithium-ion battery cell. The equations above highlight that all approaches use the same evolution equations. As it is for the flux-type equations they may differ, which is indicated for the now generic partial derivatives of the dissipation potential $\chi(\vec{g}_{el}, \vec{E}_{el})$. Notice that we have changed the dependencies of the thermodynamics fluxes $(\vec{j}_{el}, \vec{i}_{el})$ to be now given by their conjugates, in essence, the thermodynamic forces $(\vec{g}_{el}, \vec{E}_{el})$. The relation between fluxes and forces must satisfy

$$\vec{j} := \frac{\partial \chi}{\partial \vec{g}} = L_{j,g}\vec{g} + L_{j,E}\vec{E} \tag{5.45a}$$

$$\vec{i} := \frac{\partial \chi}{\partial \vec{E}} = L_{i,g}\vec{g} + L_{i,E}\vec{E} \tag{5.45b}$$

$$\begin{bmatrix} \vec{j} \\ \vec{i} \end{bmatrix} = \begin{bmatrix} L_{j,g} & L_{j,E} \\ L_{i,g} & L_{i,E} \end{bmatrix} \begin{bmatrix} \vec{g} \\ \vec{E} \end{bmatrix} \tag{5.45c}$$

where we have omitted the subindex $\cdot_{el}$ and use $L_{x,y}(z)$ to denote the coefficients from the partial derivatives. The notation express that the partial derivative with respect to y helps to represent the variable x. The use of this notation allows to highlight the interplay between variables. Furthermore, the linear dependence shown rises due to the thermodynamic conditions. We proposed χ to be quadratic in order to satisfy the convexity condition the model requires according to the linear theory of irreversible processes.

5.2.3.1 Holonomic condition

We derive now a condition on the flux-type constitutive equations to see if they are viable for the construction of the dissipation potential χ, in the sense that it satisfies thermodynamic conditions. We will refer to such condition as the **holonomic condition**[5]. We construct the constraint based on the method of exact differentials for PDEs. From equations (5.38, 5.41, 5.43) it can be seen that all flux-type equations satisfy a similar relation. Specially, the species flux $\vec{j}$ is defined through the electric current $\vec{i}$. This relation is shown at the left in the equations below, and at the right next to it we show how this relates with the general coefficients proposed in (5.45)

$$\vec{j} = \tilde{L}_{j,g}\vec{g} + \alpha\vec{i} = (\tilde{L}_{j,g} + \alpha L_{i,g})\vec{g} + \alpha L_{i,E}\vec{E} \quad \Longleftrightarrow \quad L_{j,g} = \tilde{L}_{j,g} + \alpha L_{i,g} \tag{5.46a}$$

$$\vec{i} = L_{i,g}\vec{g} + L_{i,E}\vec{E} \quad \Longleftrightarrow \quad L_{j,E} = \alpha L_{i,E} \tag{5.46b}$$

We can benefit from these similarities to find the conditions and to construct the *dissipation potential* $\chi(\vec{g}, \vec{E})$. Therefore, we use the flux-type equation for $\vec{i}$ in (5.46b) and integrate it with respect to $\vec{E}$ as expected from the conjugate relation (5.45) to get

$$\chi\Big|_{\vec{g}-fix} = \int \left(L_{i,g}\vec{g} + L_{i,E}\vec{E}\right) d\vec{E} = L_{i,g}\vec{g} \cdot \vec{E} + \frac{1}{2}L_{i,E}\vec{E} \cdot \vec{E} + H(\vec{g}) \tag{5.47}$$

where $H(\vec{g})$ is a dummy function arising from the integration. In addition, we recall the coefficients $L_{i,g}$ and $L_{i,E}$ are independent of $\vec{E}$ and $\vec{g}$. We derive the function above respect to $\vec{g}$ and match the result with $\vec{j}$ in (5.46a).

$$\frac{\partial \chi}{\partial \vec{g}} = L_{i,g}\vec{E} + \frac{dH}{d\vec{g}} = \vec{j} = (\tilde{L}_{j,g} + \alpha L_{i,g})\vec{g} + \alpha L_{i,E}\vec{E} \tag{5.48}$$

[5]The etymology for holonomic comes from the Greek words, (*"hol" : whole*) and (*"onomy": set of rules*), plus the Latin (*"icus":pertaining to*), therefore, *holonomic* can be interpreted as pertaining to a set of rules for a whole

For the equation above to have an exact differential, it needs to satisfy the following relation

$$L_{i,g} = \alpha L_{i,E} \qquad \textbf{(Holonomic condition)} \tag{5.49}$$

we refer to this relation as the *holonomic condition*.

5.2.3.2 Dissipation potential

In the case the flux-type equations satisfy the *holonomic condition* above. We define the dummy function $H(\vec{g})$ as

$$\frac{dH}{d\vec{g}} = (\tilde{L}_{j,g} + \alpha L_{i,g})\vec{g} \qquad \rightarrow \qquad H(\vec{g}) := \frac{1}{2}(\tilde{L}_{j,g} + \alpha L_{i,g})\vec{g}\cdot\vec{g} \tag{5.50}$$

Finally, substituting the above in (5.47) and integration the index of species k for generality, the dissipation potential has the following form

$$\textbf{(Dissipation potential)} \quad \chi(\vec{g}_K, \vec{E}) := \frac{1}{2}L_{i,E}\vec{E}\cdot\vec{E} + \frac{1}{2}(\tilde{L}_{j_k,g_k} + \alpha^2 L_{i,E})\vec{g}_k\cdot\vec{g}_k + \alpha L_{i,E}\vec{g}_k\cdot\vec{E} \tag{5.51}$$

Hence, now the dissipation potential can be defined without using the exact differential method, thanks to the holonomic condition. First we need to transform the flux-type equations at hand in the form dictated by (5.45). If this expression satisfies the holonomic condition (5.49), then we just need to write the dissipation potential as expressed in (5.51). A similar statement to the *holonomic condition* can be traced to Biot [1956] where he requires the differential of entropy in a thermoelastic system to be an exact differential.

5.2.3.3 Connection with the Onsager relations

The physical validity of the *holonomic condition* (5.49) is reinforced with its equivalence to the Onsager relations [Onsager, 1931]. We recall that the holonomic condition has being obtained by the method of exact differentials on the dissipation potential, while Onsager relations is derived from a matrix, the Onsager matrix. The Onsager relations are considered as mentioned in de Groot and Mazur [1984] as a law of nature which is supported by microscopic considerations, or as an example of Newton's third law [Newman and Thomas-Alyea, 2004]. We show that both conditions are equivalent, sketching our holonomic requirement as a physical principle. We start by rewriting (5.45) through the *Onsager matrix*. The Onsager relations imposes that the matrix below needs to be symmetric

$$\begin{bmatrix}\vec{j}\\ \vec{i}\end{bmatrix} = \begin{bmatrix}L_{j,g} & L_{j,E}\\ L_{i,g} & L_{i,E}\end{bmatrix}\begin{bmatrix}\vec{g}\\ \vec{E}\end{bmatrix} \tag{5.52}$$

if we plug the specifics of the electrolyte's flux-type equations highlighted in (5.46) into the Onsager Matrix above, we have

$$\begin{bmatrix}\vec{j}\\ \vec{i}\end{bmatrix} = \begin{bmatrix}\tilde{L}_{i,g} + \alpha L_{i,g} & \alpha L_{i,E}\\ L_{i,g} & L_{i,E}\end{bmatrix}\begin{bmatrix}\vec{g}\\ \vec{E}\end{bmatrix} = \begin{bmatrix}\tilde{L}_{i,g} + \alpha^2 L_{i,E} & \alpha L_{i,E}\\ \alpha L_{i,E} & L_{i,E}\end{bmatrix}\begin{bmatrix}\vec{g}\\ \vec{E}\end{bmatrix} \tag{5.53}$$

where the second equality is obtained by substituting the *holonomic condition* (5.49). This last equality shows the symmetry of the Onsager matrix. Thus, this shows that the *holonomic condition* implies the *Onsager relations* in our scenario.

5.2.3.4 The Pre-Onsager matrix

A mathematical curiosity arises from the Onsager matrix in (5.53), but it has important implications. In essence, we can see that the Onsager matrix is the result of a row operation as follows

$$\begin{bmatrix} \tilde{L}_{i,g} & 0 \\ \alpha L_{i,E} & L_{i,E} \end{bmatrix} \qquad \mathbf{R}_j \to \mathbf{R}_j + \alpha \mathbf{R}_i \qquad \begin{bmatrix} \tilde{L}_{i,g} + \alpha^2 L_{i,E} & \alpha L_{i,E} \\ \alpha L_{i,E} & L_{i,E} \end{bmatrix} \tag{5.54}$$

where $\mathbf{R}_j$ and $\mathbf{R}_i$ correspond to the row for the species flux and electric current respectively. The matrix on the left is what we call here as the *Pre-Onsager* matrix. A row operation on it given by $\mathbf{R}_j \to \mathbf{R}_j + \alpha \mathbf{R}_i$ can define the Onsager matrix. As shown in (5.46a) the massic flux $\vec{j}$ depends directly on the other flux-type variable, i.e. the electric current i. The *Pre-Onsager matrix* along with the row operation shows this type of dependence. The later also explains the need in the *Osanger matrix* of only two parameters and a constant, namely, $L_{i,E}$, $\tilde{L}_{i,g}$ and α, instead of the three parameters we would normally expect. Hence, the existence of the *Pre-Onsager matrix* denotes a coupling between flux-type variables instead of a coupling through forces as more generally suggested by the Onsager Matrix (5.52).

5.2.4 VF material models

Once presented the evolution equations, constitutive equations and the holonomic condition, we are ready to derive the models which will be used for the VF (5.14). The main difference in the material models presented is tied to the flux-type equations presented in §5.2.2. For each case we adapt the flux-type equations to the thermodynamic forces desired to describe the problem. We check if the adapted equations satisfy the holonomic condition and if so, construct the dissipation potential. Finally, since the internal energy is not coupled with the charge density due to the ENC. We select the corresponding expression for the chemical potential to define the internal energy.

5.2.4.1 Nernst-Plank model

For the Nernst-Planck equations in (5.38) we rewrite as

$$\vec{j}_{el} := -\mathbb{D}_{\pm} \left(\frac{\partial^2 U}{\partial c_{el}^2} \right)^{-1} \vec{g}_{el} + \frac{t_+}{\nu_+ z_+ F} \vec{i}_{el} \qquad \textit{(ionic flux)} \tag{5.55}$$

$$\vec{i}_{el} := \kappa \vec{E}_{el} + \frac{1}{\nu_+ z_+} \frac{\kappa}{F} \left(t_+ - \frac{\nu_-}{\nu} \right) \vec{g}_{el} \qquad \textit{(electric current)} \tag{5.56}$$

This model can not be set into a VF as we propose since it does not satisfy the holonomic condition (5.49).

5.2.4.2 Stefan-Maxwell model

The Stefan-Maxwell model summarized in (5.41) requires a further substitution. We also need to change from electrochemical potential to electric potential by means of (5.36).

$$\vec{j}_{el} = D_{\pm} \left(\frac{\partial^2 U}{\partial c_{el}^2} \right)^{-1} \vec{g}_{el} + \frac{t_+}{\nu_+ z_+ F} \vec{i}_{el} \tag{5.57a}$$

$$\vec{i}_{el} = \kappa \vec{E}_{el} + \frac{\kappa}{\nu_+ z_+ F} \left(1 + \frac{s_+ z_+}{n} + t_+ - \frac{s_0 z_+ \nu_+}{n c_0} \right) \vec{g}_{el} \tag{5.57b}$$

As pointed out by Ehrl [2017], "in battery science the most common reference electrode is the lithium reference electrode with normal surface reaction $\mathrm{Li} \leftrightarrows \mathrm{Li}^+ + e^-$". Hence the coefficients from the reference

electrode become, $s_+ = -1$, $s_- = 0$, $s_0 = 0$, $n = -z_+$ and the equation above is reduced to

$$\vec{j}_{el} = D_{\pm}\left(\frac{\partial^2 U}{\partial c^2}\right)^{-1}\vec{g}_{el} + \frac{t_+}{\nu_+ z_+ F}\vec{i}_{el} \tag{5.58a}$$

$$\vec{i}_{el} = \kappa\vec{E}_{el} + \kappa\frac{t_+}{\nu_+ z_+ F}\vec{g}_{el} \tag{5.58b}$$

Thus, from (5.46) the parameters in (5.58) are

$$\tilde{L}_{j,g} = D\left(\frac{\partial^2 U}{\partial c^2}\right)^{-1}; \qquad \alpha = \frac{t_+}{\nu_+ z_+ F}; \qquad L_{i,g} = \kappa\frac{t_+}{\nu_+ z_+ F}; \qquad L_{i,E} = \kappa; \tag{5.59}$$

which, satisfies the holonomic condition (5.49). This result supports the change from electric field $\vec{E}$ to electrochemical field $\vec{\Psi}$ in the original equations from Newman and Thomas-Alyea [2004] as proposed by Latz and Zausch [2011]. We can now substitute the values from (5.59) into (5.51) to construct the dissipation potential of the model

$$\chi_{el}(\vec{g}_{el}, c_{el}) := \frac{\kappa}{2}\vec{E}_{el}\cdot\vec{E}_{el} + \frac{1}{2}\left[\underbrace{D\left(\frac{\partial^2 U}{\partial c^2}\right)^{-1}}_{\mathfrak{m}\text{: mobility}} + \left(\frac{t_+}{\nu_+ z_+ F}\right)^2\kappa\right]\vec{g}_{el}\cdot\vec{g}_{el} + \kappa\frac{t_+}{\nu_+ z_+ F}\vec{g}_{el}\cdot\vec{E}_{el} \tag{5.60}$$

The diffusion parameter used for the Stefan-Maxwell model in (5.42a) is similar to the one shown by the molar relation in (5.34). Therefore, we select the chemical potential defined in (5.27) for a salt, combining molar and molal parameters in its absolute activity.

$$\begin{aligned}\mu_A = \frac{\partial U}{\partial c} &= \nu_+\mu_+ + \nu_-\mu_- \\ &= \nu RT\ln\lambda_A^{\theta} + \nu RT\ln\left(c\frac{\gamma_{\pm}}{c_0 M_0}\right) + RT\ln(\nu_+^{\nu_+}\nu_-^{\nu_-})\end{aligned} \tag{5.61}$$

Finally, integration over c for the equation above defines the internal energy of the model as

$$U_{el}(c_{el}) := \left[\nu RT\ln\left(c_{el}\frac{\gamma_{\pm}}{c_0 M_0}\lambda_A^{\theta}\right) + RT\ln(\nu_+^{\nu_+}\nu_-^{\nu_-}) - \nu RT\right]c_{el} + c_{el}(t_0) \tag{5.62}$$

where $c_{el}(t_0)$ is an initial concentration of the salt. This final step defines the needed functions for the VF version of the concentrated solution approach taken in Newman and Thomas-Alyea [2004]. We summarize the material model as follows

Stefan-Maxwell Model

Internal energy

$$U_{el}(c_{el}) := \left[\nu RT \ln\left(c_{el}\frac{\gamma_\pm}{c_0 M_0}\lambda_A^\theta\right) + RT\ln(\nu_+^{\nu_+}\nu_-^{\nu_-}) - \nu RT\right] c_{el} + c_{el}(t_0) \tag{5.63}$$

Dissipation Potential

$$\chi_{el}(\vec{g}_{el}, c_{el}) := \frac{\kappa}{2}\vec{E}_{el}\cdot\vec{E}_{el} + \frac{1}{2}\left[\underbrace{D\left(\frac{\partial^2 U}{\partial c_{el}^2}\right)^{-1}}_{\mathfrak{m}\text{: mobility}} + \left(\frac{t_+}{\nu_+ z_+ F}\right)^2 \kappa\right]\vec{g}_{el}\cdot\vec{g}_{el} + \kappa\frac{t_+}{\nu_+ z_+ F}\vec{g}_{el}\cdot\vec{E}_{el} \tag{5.64}$$

Stefan-Maxwell electrochemistry The model above, can be changed to use the electrochemical potential instead of the electric field. This change of dependence can be derived directly by substituting into (5.64) the electrochemical field instead of the electric field as defined in (5.36).

$$\chi_{el}(\vec{g}_{el}, \vec{\Psi}_{el}) := \frac{\kappa}{2}\vec{\Psi}_{el}\cdot\vec{\Psi}_{el} + \frac{1}{2}\left[\underbrace{D\left(\frac{\partial^2 U}{\partial c_{el}^2}\right)^{-1}}_{\mathfrak{m}\text{: mobility}} + \left(\frac{t_+ - 1}{\nu_+ z_+ F}\right)^2 \kappa\right]\vec{g}_{el}\cdot\vec{g}_{el} + \kappa\frac{t_+ - 1}{\nu_+ z_+ F}\vec{g}_{el}\cdot\vec{\Psi}_{el} \tag{5.65}$$

The definition above of the dissipation potential, leads to the following results

$$\vec{i}_{el} = \frac{\partial\chi}{\partial\vec{\Psi}_{el}} = \kappa\vec{\Psi}_{el} + \kappa\frac{t_+ - 1}{\nu_+ z_+ F}\vec{g}_{el} \tag{5.66a}$$

$$\begin{aligned}\vec{j}_{el} = \frac{\partial\chi}{\partial\vec{g}_{el}} &= \left[\underbrace{D\left(\frac{\partial^2 U}{\partial c_{el}^2}\right)^{-1}}_{\mathfrak{m}\text{: mobility}} + \left(\frac{t_+ - 1}{\nu_+ z_+ F}\right)^2 \kappa\right]\vec{g}_{el} + \kappa\frac{t_+ - 1}{\nu_+ z_+ F}\cdot\vec{\Psi}_{el} \\ &= D\left(\frac{\partial^2 U}{\partial c_{el}^2}\right)^{-1}\vec{g}_{el} + \frac{(t_+ - 1)}{\nu_+ z_+ F}\vec{i}_{el}\end{aligned} \tag{5.66b}$$

Thus, the model for the concentrated solution theory using the electrochemical potential is described by

Stefan-Maxwell Model (ψ)

Internal energy

$$U_{el}(c_{el}) := \left[\nu RT \ln\left(c_{el}\frac{\gamma_{\pm}}{c_0 M_0}\lambda_A^{\theta}\right) + RT\ln(\nu_+^{\nu_+}\nu_-^{\nu_-}) - \nu RT\right] c_{el} + c_{el}(t_0) \tag{5.67}$$

Dissipation Potential

$$\chi_{el}(\vec{g}_{el}, \vec{\Psi}_{el}) := \frac{\kappa}{2}\vec{\Psi}_{el}\cdot\vec{\Psi}_{el} + \frac{1}{2}\left[\underbrace{D\left(\frac{\partial^2 U}{\partial c_{el}^2}\right)^{-1}}_{\mathfrak{m}\text{: mobility}} + \left(\frac{t_+ - 1}{\nu_+ z_+ F}\right)^2 \kappa\right]\vec{g}_{el}\cdot\vec{g}_{el} + \kappa\frac{(t_+ - 1)}{\nu_+ z_+ F}\vec{g}_{el}\cdot\vec{\Psi}_{el} \tag{5.68}$$

5.2.4.3 Ion-transport model

The flux-type equations (5.43) proposed by the ion-transport approach posed in terms of the electric and chemical potential are

$$\vec{j}_{el} = D\left(\frac{\partial^2 U}{\partial c_{el}^2}\right)^{-1}\vec{g}_{el} + \frac{t_+}{z_+ F}\vec{i}_{el} \tag{5.69a}$$

$$\vec{i}_{el} = \kappa\vec{E}_{el} + \kappa\frac{t_+}{z_+ F}\vec{g}_{el} \tag{5.69b}$$

From the equations above we derive the relations in (5.46)

$$\tilde{L}_{j,g} = D\left(\frac{\partial^2 U}{\partial c_{el}^2}\right)^{-1}; \qquad \alpha = \frac{t_+}{z_+ F}; \qquad L_{i,g} = \kappa\frac{t_+}{z_+ F}; \qquad L_{i,E} = \kappa; \tag{5.70}$$

it can be seen that the terms above satisfy the holonomic condition (5.49). Hence, we use (5.51) to define the dissipation potential. The parameters in this approach are not predefined, thus we use the mass action law for the chemical potential (5.18) to define the internal energy. The corresponding material model then becomes

Ion-transport Model

Internal energy

$$U_{el}(c_{el}) = \mu_0 c_{el} + RT\left[c_{el}\ln\left(\frac{c\gamma}{c_0}\right) - c_{el} + c_0\right] \tag{5.71}$$

Dissipation Potential

$$\chi_{el}(\vec{g}_{el}, c_{el}) := \frac{\kappa}{2}\vec{E}_{el}\cdot\vec{E}_{el} + \frac{1}{2}\left[\underbrace{D\left(\frac{\partial^2 U}{\partial c_{el}^2}\right)^{-1}}_{\mathfrak{m}\text{: mobility}} + \left(\frac{t_+}{z_+ F}\right)^2 \kappa\right]\vec{g}_{el}\cdot\vec{g}_{el} + \kappa\frac{t_+}{z_+ F}\vec{g}_{el}\cdot\vec{E}_{el} \tag{5.72}$$

5.3 Electrodes

For the electrodes, we select an uncoupled model for the chemical and electrical fields as in Fang et al. [2017]. The conservation and flux-type equations in this model are given by

Chemical	**Electrical**	$\forall x \in \Omega_{ed} \times (0, t_f)$	
$\dot{c}_{ed} + \nabla \cdot \vec{j}_{ed} = 0$	$\nabla \cdot \vec{i}_{ed} = 0$	*(Conservation laws)*	(5.73a)
$\vec{j}_{ed} := -D\nabla c_{ed} = -\mathfrak{m}\vec{g}_{ed}$	$\vec{i}_{ed} := -\kappa\nabla\phi_{ed}$	*(Flux-type equations)*	(5.73b)

where Ω_{ed} is the spatial region covered by the electrode, c_{ed} and $\vec{j_{ed}}$ are the lithium concentration and flux density, D the solid-state diffusion coefficient of lithium, $\vec{i}_{ed}$ the electric current density, κ the electric conductivity and $-\nabla\phi_{ed}$ the electric potential. All the variables are only defined inside the electrode phase and boundaries.

The conservation laws in (5.73a) are similar to those of the electrolyte. However, a close look to the flux-type equations shows that the system is uncoupled. Therefore, we need to solve two independent problems, one per each type of Physic. Nevertheless, the functional for both cases is the same

Chemical: $$\{\dot{c}_{ed}, \mu_{ed}\} = \arg\inf_{\mu_{ed}}\sup_{\dot{c}_{ed}} \Pi_{ed}[\dot{c}_{ed}, \mu, \phi_{ed}] \tag{5.74a}$$

Electrical: $$\{\phi_{ed}\} = \arg\inf_{\phi_{ed}} \Pi_{ed}[\dot{c}_{ed}, \mu_{ed}, \phi_{ed}] \tag{5.74b}$$

$$\Pi_{ed}[\dot{c}_{ed}, \mu_{ed}, \phi_{ed}] = \int_\tau \left[\int_{\Omega_{ed}} \left(\dot{U}_{ed}(c_{ed}) - \mu_{ed}\dot{c}_{ed} - \chi^*_{ed}(\vec{g}_{ed}, \vec{E}_{ed}) \right) dV - \int_{\partial_j\Omega_{ed}} \bar{j}(\mu_{ed}) dS - \int_{\partial_i\Omega_{ed}} \bar{i}(\phi_{ed}) dS \right] dt \tag{5.74c}$$

$$= \int_\tau \left[\int_{\Omega_{ed}} \left(\dot{U}_{ed}(c_{ed}) - \mu_{ed}\dot{c}_{ed} - \chi^*_{ed}(-\nabla\mu, -\nabla\phi) \right) dV - \int_{\partial_j\Omega_{ed}} \bar{j}(\mu_{ed}) dS - \int_{\partial_i\Omega_{ed}} \bar{i}(\phi_{ed}) dS \right] dt \tag{5.74d}$$

Despite the VF uses the same functional as it is for the electrolyte, the potentials' definitions provide the VF model with the specifics of the problem. The set of flux-type equations (5.73b), defines the internal energy and dissipation potential for the electrode as shown in (5.75) and (5.76) correspondingly. Since the equation for the lithium flux density is similar to Fick's first law, we use the mass action law (5.18) for the chemical field to define the internal energy $U_{ed}(c)$. As it is for the construction of the dissipation potential, we set the equations in (5.73b) to depend on their correspondent driving force and integrate them afterwards.

Electrode uncoupled model

Internal energy

$$U_{ed}(c_{ed}) = \mu_{ed_0} c_{ed} + RT \left[c_{ed} \ln\left(\frac{c_{ed}\gamma}{c_{ed_0}} \right) - c_{ed} + c_{ed_0} \right] \tag{5.75}$$

Dissipation Potential

$$\chi_{ed}(\vec{g}_{ed}, c_{ed}) = \frac{\kappa}{2}\vec{E}_{ed} \cdot \vec{E}_{ed} + \frac{1}{2}\left(\frac{\partial^2 U}{\partial c_{ed}^2} \right)^{-1} \vec{g}_{ed} \cdot \vec{g}_{ed} \tag{5.76}$$

Notice that the dissipation potential satisfies the entropy-like condition (4.21). This is to be expected, since the relations in (5.73b) are linear.

5.4 Interface

The boundary interface between the two bulk domains of the electrolyte and electrode $\Gamma_{BV} := \Omega/(\Omega_{ed} + \Omega_{el})$, is an important area when modeling the battery cell. In this area, the interface coupling of the problem takes place. The Butler-Volmer current density i_{BV} is a common approach to model this interface [Fang et al., 2017, Newman and Thomas-Alyea, 2004]

$$\textbf{Butler-Volmer current:} \qquad i_{BV} := i_0 \left(\exp\left(\frac{\alpha_a F \eta}{RT} \right) - \exp\left(\frac{-\alpha_c F \eta}{RT} \right) \right) \qquad \forall \vec{x} \in \Gamma_{BV} \tag{5.77}$$

where i_0 is the exchange current density, α_a and α_c the anodic and cathodic transfer coefficients, η the interface overpotential, R the gas constant and T a fixed temperature. The exchange current density i_0 is given by

$$i_0 := k F c_{ed}^{\alpha_c} \left(c_{ed,max} - c_{ed} \right)^{\alpha_a} c_{el}^{\alpha_a} \tag{5.78}$$

where k is the rate constant of the charge transfer reaction, c_{ed} and c_{el} are the concentration of lithium at the electrode and anode correspondingly and $c_{ed,max}$ is the maximum saturation concentration of intercalated lithium. As it is for the interface overpotential η, it is defined by the electric potentials as follows

$$\eta := \phi_{ed} - \phi_{el} - \phi_0 \tag{5.79}$$

where ϕ_{ed} and ϕ_{el} are the electric potentials at the electrode and electrolyte phase correspondingly, ϕ_0 is the equilibrium potential which is modeled by

$$\phi_0 = \frac{\Delta G}{F} + \frac{RT}{F} \ln\left(\frac{1 - X_{ed}}{X_{ed}} \right) + \sum_m \frac{A_m}{F} \left((2X_{ed} - 1)^{m+1} - \frac{2mXed(1 - X_{ed})}{(2X_{ed} - 1)^{1-m}} \right) \tag{5.80}$$

where ΔG is the change of Gibbs free energy during lithium intercalation, A_m are the polynomial Redlich-Kister coefficients for a given values of m and X_{ed} is the mole fraction of intercalated lithium at the electrode surface

$$X_{ed} = \frac{c_{ed}}{c_{ed,max}} \tag{5.81}$$

To conclude, the conservation of mass and electric charge in the interface is proportional to the Faraday constant F, in essence

$$\vec{j}_{ed} \cdot \vec{n}_\Gamma = \vec{j}_{el} \cdot \vec{n}_\Gamma = \frac{1}{F} \vec{i}_{ed} \cdot \vec{n}_\Gamma = \frac{1}{F} \vec{i}_{el} \cdot \vec{n}_\Gamma = \frac{1}{F} \vec{i}_{BV} \cdot \vec{n}_\Gamma \qquad \forall \vec{x} \in \Gamma_{BV} \tag{5.82}$$

a deeper discussion of te Butler-Volmer equation in relation with batteries can be found in Newman and Thomas-Alyea [2004]. The model for the interface corresponds to that one shown by Fang et al. [2017].

5.4.1 Butler-Volmer VF

The Butler-Volmer conditions can be embedded within our VF through the definition of an interface functional $\Pi_{\Gamma_{BV}}$. This interface functional can be derived by direct integration of equation (5.77) with respect to ϕ and μ, where the relation between both is given by (5.82) . We define the energy rate $\dot{Q}$

$$\Pi_{\Gamma_{BV}} := \int_\tau \left[\int_{\Gamma_{BV}} \dot{Q}(\mu_{ed}, \mu_{el}, \phi_{ed}, \phi_{el}) dS \right] dt \tag{5.83a}$$

$$\begin{aligned} \dot{Q}(\mu_{ed}, \mu_{el}, \phi_{ed}, \phi_{el}) := i_0 \frac{RT}{F} \Bigg[& \frac{1}{\alpha_a} \left(\exp\left(\alpha_a \frac{F}{RT} \eta \right) + \exp\left(\alpha_a \frac{1}{RT} [\mu_{el} + \mu_{ed}] \right) \right) \\ & + \frac{1}{\alpha_c} \left(\exp\left(-\alpha_c \frac{F}{RT} \eta \right) + \exp\left(-\alpha_c \frac{1}{RT} [\mu_{el} + \mu_{ed}] \right) \right) \Bigg] \end{aligned} \tag{5.83b}$$

We do not specify an optimal statement in this case since it is defined outside the interface, meaning, on the electrodes and electrolyte. Notice, that the partial derivatives indeed correspond to the equations (5.77) and (5.82).

5.5 The VF of a Lithium-ion battery cell

The functional for the lithium-ion battery cell has been derived in sections corresponding to specific regions of the cell, namely, in the electrolyte by (5.14), in the electrode by (5.74c) and in the interface electrode/electrolyte by (5.83). All the former together, create the following VF for the battery cell as

$$\{\dot{c}_{el}, \mu_{el}, \phi_{el}, \dot{c}_{ed}, \mu_{ed}, \phi_{ed}\} = \arg \inf_{\mu_{el},\phi_{el},\mu_{ed},\phi_{ed}} \sup_{\dot{c}_{el},\dot{c}_{ed}} \Pi[\dot{c}_k, \mu_k, \phi] \tag{5.84a}$$

$$\Pi[\dot{c}_k, \mu_k, \phi] := \Pi_{el}[\dot{c}_{el}, \mu_{el}, \phi_{el}] + \Pi_{ed}[\dot{c}_{ed}, \mu_{ed}, \phi_{ed}] + \Pi_{\Gamma_{BV}}[\dot{c}_{el}, \mu_{el}, \phi_{el}, \dot{c}_{ed}, \mu_{ed}, \phi_{ed}] \tag{5.84b}$$

Notice that despite the electrode being uncoupled, and therefore defined by two parallel conditions, namely (5.74a) and (5.74b), it can be integrated in the whole VF. This is possible since the material models define the coupling.

5.6 Numerical examples: Electrolyte

To illustrate briefly what is detailed above, we present a numerical example of the electrolyte VF in 1D. The model we use is that of the *ion-transport model* showed in §5.2.4.3, where the internal energy is given by (5.71) and the dissipation potential by (5.72). We consider the functional proposed in (5.14) for the electrolyte. We assume only one specie in the electrolyte, thus, we can remove the subindex $_{el}$. Therefore, the functional we need to discretize becomes

$$\{\dot{c}, \mu, \phi\} = \arg \inf_{\mu,\phi} \sup_{\dot{c}} \Pi[\dot{c}, \mu, \phi] \tag{5.85a}$$

$$\Pi[\dot{c}, \mu, \phi] = \int_\tau \left[\int_\Omega \left(\dot{U}(c) - \sum \mu \dot{c} - \chi^*(\vec{g}, \vec{E}) \right) dV - \int_{\partial_j \Omega} \overline{j}(\mu) dS - \int_{\partial_i \Omega} \overline{i}(\phi) dS \right] dt \tag{5.85b}$$

For the discretization of the system above we consider the same procedure as in §3.3, in essence, a classical FEM approach for the space and a finite difference approximation for time. We used second order elements, thus the corresponding admissible spaces belong to a subset of H^2.

5.6.1 Newton Method Form

Applying the Newton method to the discrete problem leads to the following system per each finite element. The residuals blocks become

$$\mathbb{R}_\mu^{(a)} = \frac{\partial \Pi}{\partial \mu}^{(a)} = \int_\Omega \left(-\Delta c S^{(a)} + \Delta t \frac{\partial \chi}{\partial \vec{g}} \nabla S^{(a)} \right) dV - \int_{\partial_j \Omega} \left(\Delta t \, \overline{j} \, S^{(a)} \right) dS \tag{5.86a}$$

$$\mathbb{R}_c^{(a)} = \frac{\partial \Pi}{\partial c}^{(a)} = \int_\Omega \left(\frac{\partial U}{\partial c} - \mu \right) \nabla S^{(a)} dV \tag{5.86b}$$

$$\mathbb{R}_\phi^{(a)} = \frac{\partial \Pi}{\partial \phi}^{(a)} = \int_\Omega \left(\Delta t \frac{\partial \chi}{\partial \vec{E}} \nabla S^{(a)} \right) dV - \int_{\partial_i \Omega} \left(\Delta t \, \overline{i} \, S^{(a)} \right) dS \tag{5.86c}$$

while the tangent of the problem is given by the blocks

$$\mathbb{T}_{\mu\mu}^{(a,b)} = \frac{\partial \mathbb{R}_{\mu}^{(a)}{}^{(b)}}{\partial \mu} = \int_{\Omega} \left(-\Delta t \frac{\partial^2 \chi}{\partial \vec{g}^2} \nabla S^{(a)} \nabla S^{(b)} \right) dV \tag{5.87a}$$

$$\mathbb{T}_{\mu c}^{(a,b)} = \frac{\partial \mathbb{R}_{\mu}^{(a)}{}^{(b)}}{\partial c} = -\int_{\Omega} \left(S^{(a)} S^{(b)} \right) dV \tag{5.87b}$$

$$= \left[\mathbb{T}_{c\mu}^{(a,b)} \right]^T \tag{5.87c}$$

$$\mathbb{T}_{\mu\phi}^{(a,b)} = \frac{\partial \mathbb{R}_{\mu}^{(a)}{}^{(b)}}{\partial \phi} = \int_{\Omega} \left(-\Delta t \frac{\partial^2 \chi}{\partial \vec{E} \partial \vec{g}} \nabla S^{(a)} \nabla S^{(b)} \right) dV \tag{5.87d}$$

$$= \left[\mathbb{T}_{\phi\mu}^{(a,b)} \right]^T \tag{5.87e}$$

$$\mathbb{T}_{cc}^{(a,b)} = \frac{\partial \mathbb{R}_{c}^{(a)}{}^{(b)}}{\partial c} = \int_{\Omega} \left(\frac{\partial^2 U}{\partial \bar{c}^2} S^{(a)} S^{(b)} \right) dV \tag{5.87f}$$

$$\mathbb{T}_{c\phi}^{(a,b)} = \frac{\partial \mathbb{R}_{c}^{(a)}{}^{(b)}}{\partial \phi} = \mathbb{O} \tag{5.87g}$$

$$= \left[\mathbb{T}_{\phi c}^{(a,b)} \right]^T \tag{5.87h}$$

$$\mathbb{T}_{\phi\phi}^{(a,b)} = \frac{\partial \mathbb{R}_{\phi}^{(a)}{}^{(b)}}{\partial \phi} = \int_{\Omega} \left(-\Delta t \frac{\partial^2 \chi}{\partial \vec{E}^2} \nabla S^{(a)} \nabla S^{(b)} \right) dV \tag{5.87i}$$

The former can also be written in a more compact fashion using the notation introduced in (2.24) and (2.25) as

$$\mathbf{R}_e = \begin{bmatrix} \mathbb{R}_{\mu}^{(a)} \\ \mathbb{R}_{c}^{(a)} \\ \mathbb{R}_{\phi}^{(a)} \end{bmatrix} = \begin{bmatrix} \mathbb{S}_{\mu}^{(a)} \Big(-\Delta c \Big) + \nabla \mathbb{S}_{\mu}^{(a)} \Big(\Delta t \frac{\partial \chi}{\partial \vec{g}} \Big) \\ \mathbb{S}_{c}^{(a)} \Big(\frac{\partial U}{\partial c} - \mu \Big) \\ \nabla \mathbb{S}_{\phi}^{(a)} \Big(\Delta t \frac{\partial \chi}{\partial \vec{E}} \Big) \end{bmatrix} \tag{5.88a}$$

$$\mathbf{T}_e = \begin{bmatrix} \mathbb{T}_{\mu\mu}^{(a,b)} & \mathbb{T}_{\mu c}^{(a,b)} & \mathbb{T}_{\mu\phi}^{(a,b)} \\ \mathbb{T}_{c\mu}^{(a,b)} & \mathbb{T}_{cc}^{(a,b)} & \mathbb{T}_{c\phi}^{(a,b)} \\ \mathbb{T}_{\phi\mu}^{(a,b)} & \mathbb{T}_{\phi c}^{(a,b)} & \mathbb{T}_{\phi\phi}^{(a,b)} \end{bmatrix} = \begin{bmatrix} -\mathbb{K}_{\mu\mu}^{(a,b)} \Big(\Delta t \frac{\partial^2 \chi}{\partial \vec{g}^2} \Big) & \mathbb{M}_{\mu c}^{(a,p)} \Big(-1 \Big) & \mathbb{K}_{\mu\phi}^{(a,b)} \Big(\Delta t \frac{\partial^2 \chi}{\partial \vec{E} \partial \vec{g}} \Big) \\ \mathbb{M}_{c\mu}^{(p,a)} \Big(-1 \Big) & \mathbb{M}_{cc}^{(a,b)} \Big(\frac{\partial^2 U}{\partial c^2} \Big) & \mathbb{O} \\ \mathbb{K}_{\phi\mu}^{(a,b)} \Big(\Delta t \frac{\partial^2 \chi}{\partial \vec{g} \partial \vec{E}} \Big) & \mathbb{O} & -\mathbb{K}_{\phi\phi}^{(a,b)} \Big(\Delta t \frac{\partial^2 \chi}{\partial \vec{E}^2} \Big) \end{bmatrix} \tag{5.88b}$$

5.6.1.1 Boundary conditions

We deal with the BC as follows

Neumann BC :

The Neumann BC have their contributions in the residual of the elements with nodes at the corresponding boundaries $\partial\Omega_j$ or $\partial\Omega_i$ as

$$\mathbf{R}_e = \begin{bmatrix} \mathbb{S}_{\mu}^{(a)} \Big(-\Delta t \, \bar{j} \vec{n}_{D_i}^{(a)} \Big) \\ \mathbb{O} \\ \mathbb{S}_{\phi}^{(a)} \Big(-\Delta t \, \bar{i} \vec{n}_{D_j}^{(a)} \Big) \end{bmatrix} \tag{5.89}$$

where $\vec{n}_{D_y}$ is the normal vector of the boundary D_y where a Neumann boundary condition has been imposed.

Butler-Volmer BC

The functional and potential proposed for the *Butler-Volmer* condition in (5.83) have the following contributions in the residual for nodes located in the Butler-Volmer boundary Γ_{BV}. In contrast with the Neuman BC, notice that the *Butler-Volmer* boundary is imposed for chemical and electrical fields simultaneously since it is a coupling interface. Thus, the residual can have the following contribution at the interface nodes

$$\mathbf{R}_e = \begin{bmatrix} \mathbb{S}_{\mu}^{(a)} \left(i_0 \frac{1}{F} \left[\exp^{\alpha_a \frac{1}{RT}\mu} - \exp^{-\alpha_c \frac{1}{RT}\mu} \right] \vec{n}_{\Gamma_{BV}} \right) \\ \mathbb{O} \\ \mathbb{S}_{\phi}^{(a)} \left(i_0 \left[\exp^{\alpha_a \frac{1}{RT}\eta} - \exp^{-\alpha_c \frac{1}{RT}\eta} \right] \vec{n}_{\Gamma_{BV}} \right) \end{bmatrix} \tag{5.90}$$

while the Tangent matrix also must include the following contributions

$$\mathbb{T}_{\mu\mu}^{(a,b)} = \mathbb{M}_{\mu\mu}^{(a,b)} \left(i_0 \frac{1}{RT} \left[\alpha_a \exp^{\alpha_a \frac{1}{RT}\mu} + \alpha_c \exp^{-\alpha_c \frac{1}{RT}\mu} \right] \vec{n}_{\Gamma_{BV}} \right) \tag{5.91}$$

$$\mathbb{T}_{\phi\phi}^{(a,b)} = \mathbb{M}_{\phi\phi}^{(a,b)} \left(i_0 \frac{F}{RT} \left[\alpha_a \exp^{\alpha_a \frac{1}{RT}\eta} + \alpha_c \exp^{-\alpha_c \frac{1}{RT}\eta} \right] \vec{n}_{\Gamma_{BV}} \right) \tag{5.92}$$

5.6.2 Examples

In this subsection we present the results of three 1D problems solved using the VF above via a MATLAB code.

5.6.2.1 Dirichlet and Boundary BC

The first problem considers a strong electrochemical coupling, using the equations shown above. The domain is defined as $x \in \Omega =: [0, 1]$ with a Dirichlet BC at $x = 0$ and a Neumann BC at $x = 1$ for the chemical potential and concentration, and a Dirichlet BC for both boundaries of the electric potential. Thus, we have values of $\mu(0, t) = 0$, $\phi(0, t) = 0$ and $\phi(1, t) = 1$ for the Dirichlet BC[6]. For the Neumann BC we have $\vec{j}(1, t) = -1e^{-3}$ mol m^{-2} s^{-1}. The initial conditions are given by $\mu(t_0) = 0$, and $\phi(t_0) = 0$. We take a total of $N_x := 50$ spatial elements and let evolve the problem with a time step of $\Delta t := 100$ during 300 steps. The parameters used are shown in the Table 5.1.

Figure 5.3 depicts the evolution of the fields of interest for the problem. Lighter gray color make reference to earlier time steps, while darker colors refer to later time steps. The phase space plots are displayed to show the relations between the chemical potential μ with concentration c and electric potential ϕ. The phase space plot for μ vs c shows the problem is working under the chemical non-linear range.

[6]We recall that the value for $c(0, t)$ is obtained using the first derivative of the internal energy

Parameter	Value	Units
$\overline{\mu}$	$-175.0 \cdot 10^{-3}$	$J\,mol^{-1}$ (Gibbs *"G"*)
μ_0	Eq (3.25) or Eq (3.31)	$J\,mol^{-1}$ (Gibbs *"G"*)
c_0	1	mol m^{-3}
R	8.3144598	kg m^2 sec^{-2} K^{-1} mol^{-1}
T	298.0	K
D	$1 \cdot 10^{-5}$	m^2 sec^{-1}
γ	1	-
κ	1	$C^2m^{-3}kg^{-1}s$
q_e	$1.60217662 \cdot 10^{-19}$	C
N_A	$6.02214086 \cdot 10^{23}$	mol^{-1}
F	$q_e N_a$	-
z_+	1	-
t_+	1	-

Table 5.1: Table of parameters

5.6.2.2 Dirichlet BC with initial discontinuity

The next problem displays the time step solutions of the electrochemical problem having Dirichlet boundary conditions at both ends. The domain is defined as $x \in \Omega =: [0, 1]$ with a Dirichlet BC at $x = 0$ and a Neumann BC at $x = 1$ for the chemical potential an concentration, and a Dirchlet BC for both boundaries of the electric potential. Thus, we have values of $c(0, t) = 1$, $\phi(0, t) = 0$ and $c(1, t) = 5$, $\phi(1, t) = 1$ for the Dirichlet BC where the initial values of the chemical potential are now derived in correspondence with the initial values of the concentration. We take a total of $N_x := 50$ spatial elements and let evolve the problem with a time step of $\Delta t := 100$ during 300 steps. The parameters used are the same of the Table 5.1. The initial conditions are given by $\mu(t_0) = 0$, and $\phi(t_0) = 0$. This example resembles to the one analyzed in §3.4, where a discontinuity between initial conditions and boundary conditions is present but now on a strongly coupled problem. This sort of problems where discontinuities between initial and boundary conditions are important since they put into test the numerical stability of the approach used.

Figure 5.4 depicts the evolution of the fields of interest for the problem. As in the previous problem, lighter gray color make reference to earlier time steps, while darker colors refer to later time steps. The phase space plots are displayed to show the relations between the chemical potential μ with concentration c and electric potential ϕ.

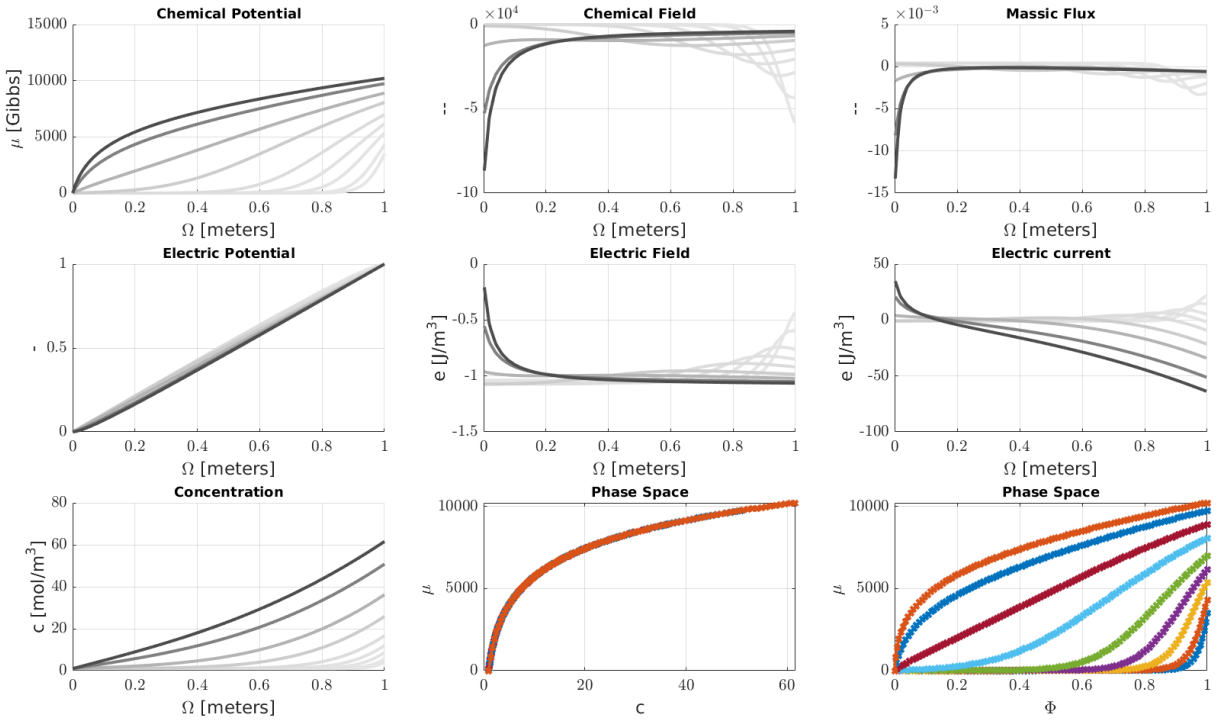

Figure 5.3: Strong bulk coupling, with Dirichlet and Neumann BC.

5.6.2.3 Butler-Volmer BC

Finally, the following problem shows the time step solutions of the electrochemical problem where the Butler-Volmer condition is considered at both ends. In this problem, the domain is defined as $x \in \Omega =: [0, L = 1e-3]$. We take a total of $N_x := 50$ spatial elements and let evolve the problem with a time step of $\Delta t := L^2/(2000D)$ during 20 steps. The parameters used for the chemical part are the same used in §3 which we append to Table 5.2 with the remaining parameters. The initial conditions are given by $c(t_0) = 1$, and $\phi(t_0) = 0.1$.

As in previous figures, Figure 5.5 depicts the evolution of the fields of interest for the problem. Lighter gray color make reference to earlier time steps, while darker colors refer to later time steps. The phase space plots are displayed to show the relations between the chemical potential μ with concentration c and electric potential ϕ.

5.7 Summary

We concluded this chapter by recalling we presented the derivation of the electrochemical VF used as the base for the model of a lithium-ion battery. We mentioned the properties of the generalized VF model we proposed as the definition of internal energy and dissipation potential to encapsulate constitutive laws, the imposition of a thermodynamic consistency in the model, and the flexibility to model strong or weak

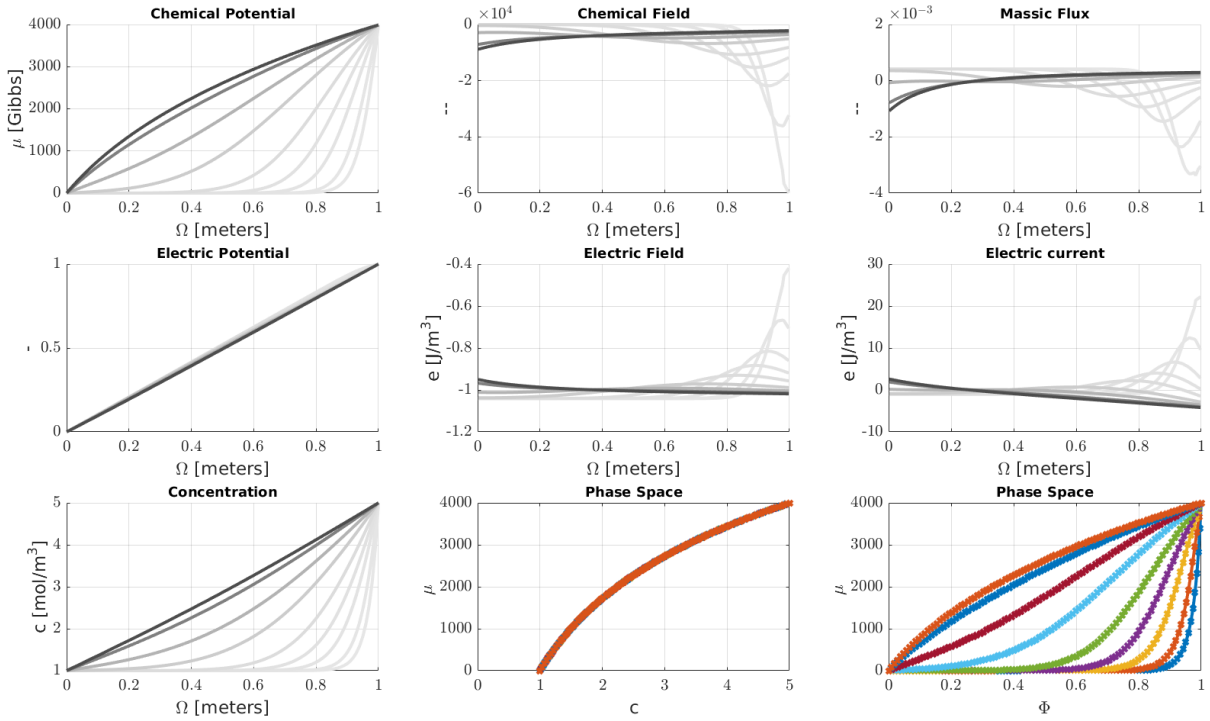

Figure 5.4: Strong bulk coupling, with discontinuity between inital and boundary conditions.

couplings whether at the bulk or the interface. In this chapter based on the formulation we proposed, we derived the Onsager relations in an alternative way. This basic principle of Physics is represented in our framework as the condition required for the dissipation potential to have an exact differential. We explored a strong and weak type of coupling through the electrolyte and electrodes respectively which was located at the bulk. We achieved the interface coupling between electrodes and electrolyte with the definition of the interface potential which encapsulates the Butler-Volmer equation. Nevertheless, these are not all the perks of our formulation, as it will be shown in the next chapter. A further property is the ability to derive different solution strategies to find a numerical solution to the model.

Parameter	**Value**	**Units**
$\overline{\mu}$	$-175.0 \cdot 10^{-3}$	$J\,mol^{-1}$ (Gibbs *"G"*)
μ_0	$-190.0 \cdot 10^{-3}$	$J\,mol^{-1}$ (Gibbs *"G"*)
c_0	Eq (3.25) or Eq (3.31)	mol m^{-3}
R	8.3144598	kg m^2 sec^{-2} K^{-1} mol^{-1}
T	298.0	K
D	$8.4 \cdot 10^{-10}$	m^2 sec^{-1}
γ	1	-
κ	1	$C^2m^{-3}kg^{-1}sec$
q_e	$1.60217662 \cdot 10^{-19}$	C
N_A	$6.02214086 \cdot 10^{23}$	mol^{-1}
F	$q_e N_a$	-
z_+	1	-
t_+	0.5	-
$\phi_{ed}(0)$	0	-
$\phi_0(0)$	0	-
$\phi_{ed}(L)$	0	-
$\phi_0(L)$	0.2	-
η	$\phi_0 - \phi_{el} - \phi_{ed}$	-
η	$\phi_0 - \phi_{el} - \phi_{ed}$	-
i_0	0.1	-
α_a	0.5	-
α_c	0.5	-
L	$1.0 \cdot 10^{-3}$	m
t_f	1190.47619048	sec

Table 5.2: Table of parameters

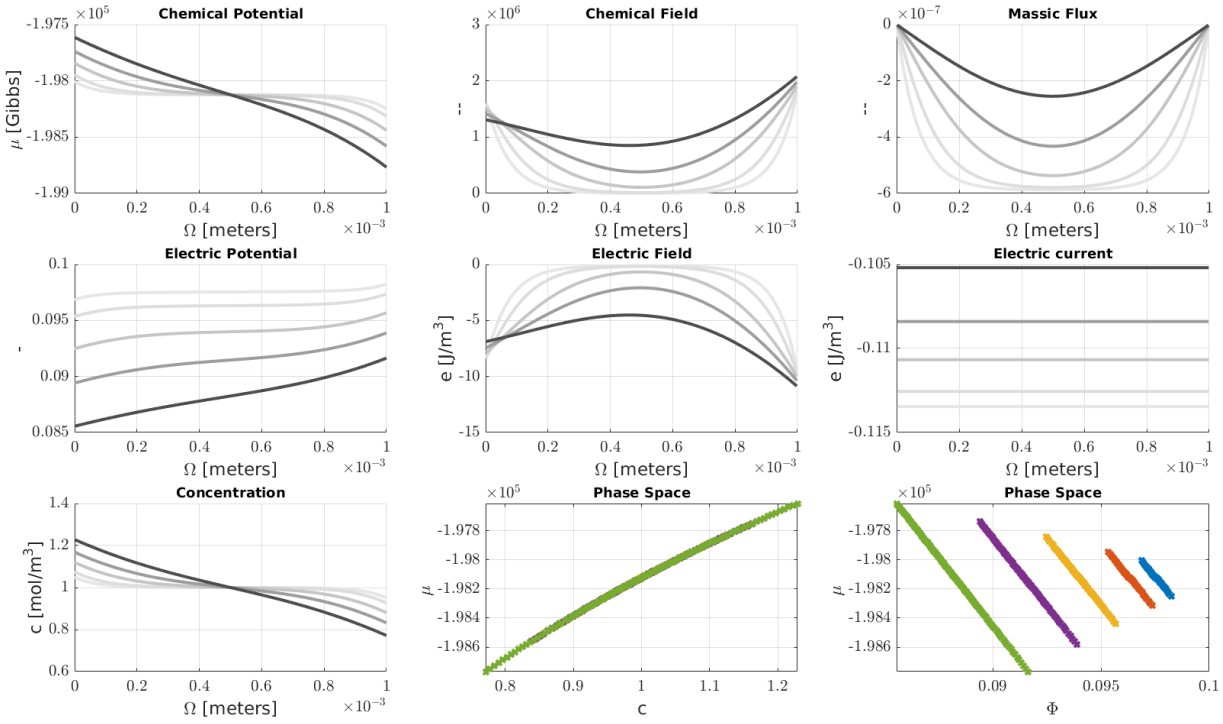

Figure 5.5: Strong bulk coupling using Butler-Volmer BC.

Part III

Solution Strategies

Chapter 6

Solution strategies

Sommaire

Ce chapitre est consacré à la solution numérique des modèles variationnels. Ici, nous présentons et analysons deux familles de stratégies numériques qui peuvent être dérivées du modèle variationnel. Ces stratégies sont généralement présentées comme des algorithmes dépourvus de structure mathématique. Nous montrons la structure mathématique derrière ces algorithmes et allons encore plus loin en soulignant en quoi ces stratégies sont des variantes spécifiques de la méthode de Newton.

> The purpose of computing is insight, not numbers.
>
> R. W. Hamming
> *Numerical Methods for Scientists and Engineers*

The goal of this chapter is to construct a transition from a continuous VF to a discrete version, where a family of solution strategies can be applied to solve the problem numerically. In fact, the family of solution strategies are not just applied but rather derived from the discrete VF model itself. In specific, we explore the family of *monolithic*, *staggered* and *nested* solution strategies. Each specific strategy can be implemented numerically in different ways. The variety of implementations not only changes the computational cost, but can be related to different approximations of the original physical system. Therefore, in this chapter we summarize a smooth transition from a physical system to its numerical solution, which highly contrasts with most of the current solution techniques where numerical strategies are imposed rather than derived. These results are possible thanks to the VF's structure we have detailed in the former chapters. The key idea which holds everything together is the dependencies between our state variables. Thus, a numerical implementation is not only a matter of compromise between computational cost and accuracy, but it can also become a way to increase our understanding in the model and the physics it describes. This is the reason why the quote above from R. W. Hamming has been chosen as opening one for this chapter.

We recall that in the previous three chapters we developed the modeling via a VF for some physical problems. Each chapter derives a continuous functional which describes the problem, but in order to solve

the system we need to move to a discrete form to solve it. In general, time discretization is taken through a finite difference approach, while spatial discretization is done using the Finite Element Method (FEM). Under this specific discretization, we solve the whole system spatially at every time step via the Newton method. In essence, for each time step t_n we end up with a set of classical problem of linear Algebra

$$\mathbf{A}\vec{x} = \vec{b} \tag{6.1}$$

where we have the correspondence of $\mathbf{A}$ being the Hessian Matrix of the functional, $\vec{x}$ the vector of unknown increments for the fields at time t_n, and $\vec{b}$, the vector of residuals. The final system of equations we need to solve (6.1) can become computationally expensive. The number of spatial dimensions of the problem, refinement of the mesh, or an increase on the number of fields to solve, are common reasons which increase the solution cost. In such cases, to reduce the cost as mentioned in [Strang, 2007, Chp. 7,p.563], the task is also to "Find a fast stable algorithm that uses the special properties of the matrix". Starting from our VF models, the system (6.1) has a well defined physical meaning. Therefore, we take a different approach, instead on focusing on the properties of the matrix, we use the physical properties and intuition from the physics and the VF to find a fast stable algorithm.

The structure of this chapter is as follows, we provide some context to our approach by defining key concepts we are going to use along the whole chapter. Afterwards, we give a detailed explanation of the proposed solution strategies we are going to be working with. We analyze the computational complexity of the strategies and as a side result propose a graphical tool to examine iterative strategies. We land these concepts by applying them to the VF problem of chemical diffusion we define in §3. The core ideas and process we propose to develop the strategy solutions are introduced here. The aim for this is to highlight the physical intuition of our method with a specific problem at hand. Subsequently, we abstract the proposed process and present it through mathematical formalism into the context of our general VF shown in §4. By the end of the chapter, we will have specifically tailored a concise method to develop physical-based solution strategies for coupled problems.

6.1 Context

A *strategy* defines an algorithm to solve a system numerically. It is a unique composition of specific *solver*(s) and *preconditioner*(s). The key idea behind the algorithm is to set a predefined series of steps on how the unknowns must be solved. The main strategies we are concerned with are three, namely, *monolithic*, *staggered* and *nested*. To get a better understanding of them, we need to introduce the ideas of *iterative-block*, *block-hierarchy*, *iterative block index*, *transparency-relation* and *iteration sequence* pertaining to system of equations which are divided into blocks.

6.1.1 Block system

Iterative-block: A block-preconditioner can be used to help us split the original system into subsystems which are solved at different steps of the algorithm. We call each of those subsystems an *iterative-block*. Some properties of the strategy are defined with the number of *iterative-blocks*, namely, *computation path* and *power structure*. The number of *iterative-block* defines the *computation path* of the strategy. If the used block-preconditioner is the identity matrix, there will be only one *iterative-block*, hence, the *computation path* is **single** and the *power structure* is **egalitarian**. In the opposite case the block preconditioner is different than the identity, more than one iterative blocks are created, in this case we have the *computation path* is **partitioned** and *power structure* is **hierarchical**. The role of an *iterative-block* inside the strategy can be described by two properties, one global and one local, namely, its hierarchy and

its current state or number of iterations taken.[1]

Block hierarchy: The *block hierarchy* formalizes the *power structure* property from iterative-blocks. It provides a rank to each one of them, defining the blocks uniquely on a global setting of the strategy. The hierarchy establishes the order on which a solution of the iterative-block takes place. In essence, an iterative-block with lower hierarchy is solvable only when iterative blocks with higher rank are solved. Thus, a *block hierarchy* defines an algorithmic dependency between iterative blocks.

Iterative block-index: An *iterative block-index* represents the number of iterations taken by the iterative-block.

6.1.2 Notation

The concepts above provide a general description of the strategy used. Defining a notation for these concepts allow us to describe mathematically a strategy at any time of the solution process. The partition of a system like (6.1) can be thought as a result of block-preconditioning. Let us assume (6.1) has been already partitioned resulting in the following block system

$$\begin{bmatrix} \mathbb{A} & \mathbb{O} \\ \mathbb{O} & \mathbb{D} \end{bmatrix} \begin{bmatrix} \mathbb{X} \\ \mathbb{Y} \end{bmatrix} = \begin{bmatrix} \mathbb{F} \\ \mathbb{E} \end{bmatrix} \tag{6.2}$$

The block matrices $\mathbb{A}$ & $\mathbb{D}$ are considered to be **iterative-blocks**. To highlight the use of block matrices as iterative-blocks we use a set of upper-index square brackets. Inside the square brackets we write down the corresponding *block hierarchy* and *iterative block-index*. The **block hierarchy** is expressed with a Greek letter, whose rank is in accordance with the ordering of the Greek alphabet. The **iterative block-index** is indicated with a subindex at the right of the iterative block. In a general setting, the dependencies are denoted also as subindex but instead to the left of the block hierarchy. Take the following example where the system above states that the iterative block α has undergone i iterations, while the block β has taken j iterations.

$$\begin{bmatrix} \mathbb{A}^{[\alpha_i]} & \mathbb{O} \\ \mathbb{O} & \mathbb{D}^{[{}_i\beta_j]} \end{bmatrix} \begin{bmatrix} \mathbb{X}^{[\alpha_i]} \\ \mathbb{Y}^{[{}_i\beta_j]} \end{bmatrix} = \begin{bmatrix} \mathbb{F}^{[\alpha_i]} \\ \mathbb{E}^{[{}_i\beta_j]} \end{bmatrix} \tag{6.3}$$

It is worth noticing, that the block-matrix used in (6.3), is not properly a matrix. Instead, it represents a series of evolving systems, each one represented by an iterative-block, which are solved asynchronously. In the example of (6.3) this means

$$\begin{bmatrix} \mathbb{A}^{[\alpha_i]} & \mathbb{O} \\ \mathbb{O} & \mathbb{D}^{[\beta_j]} \end{bmatrix} \begin{bmatrix} \mathbb{X}^{[\alpha_i]} \\ \mathbb{Y}^{[\beta_j]} \end{bmatrix} = \begin{bmatrix} \mathbb{F}^{[\alpha_i]} \\ \mathbb{E}^{[\beta_j]} \end{bmatrix} \quad \rightarrow \quad \begin{cases} \mathbb{A}\mathbb{X} = \mathbb{F} & \forall \quad \mathbb{X} \in \alpha_i \\ \mathbb{D}\mathbb{E} = \mathbb{E} & \forall \quad \mathbb{Y} \in \beta_j \end{cases} \tag{6.4}$$

6.1.3 Transparency relations

To emphasize the difference with a matrix we call these systems a *transparency-film* relation or *transparency relation* for short. As a visual aid to understand a *transparency relation* we can refer to figure 6.1. The two equations in braces on (6.4) solve its corresponding unknowns at different times, in essence, asynchronously. Nevertheless, the hierarchy of the blocks puts an order on how those iterations must take place. We can imagine the equations −one per each iteration− for $\mathbb{X}^{[\alpha_i]}$ and the equation for $\mathbb{Y}^{[\beta_j]}$ to be

[1] Notice that *computational path* and *power structure* are independent, e.g., algorithms on parallel computing may have a partitioned computational path and an egalitarian power structure.

written down in independent transparency films, positioned in the place it corresponds according to the matrix structure in the left of (6.4). Stacking one over the other, in accordance on how the iterations must take place − which is defined by a given strategy−, we can project over the transparency films and see something similar to the matrix structure in (6.4). Notice that a *transparency relation* formed by a single iterative-block correspond to different snapshots of a matrix, each snapshot being the matrix solved at a given iteration.

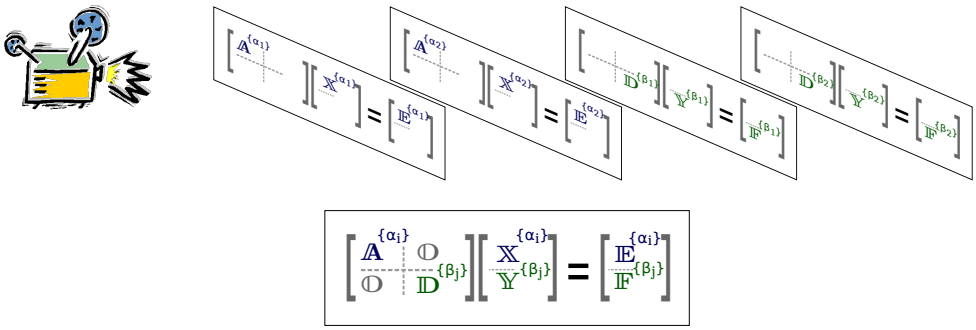

Figure 6.1: Transparency film relation

Thus, a **transparency relation** is a sequence of matrix structures representing a strategy, where its notation prescribes the order of the sequence. In addition, we define the ordered collection of all the *iterative block-indexes* as the **iteration sequence**. The *transparency relation* allows us to analyze in detail the strategies by thinking on each individual iteration as a "film" that constitutes the *transparency relation* itself.

6.2 Proposed strategies

In this work we use and derive three different strategies based on the VF we have discussed on previous chapters. These are the *monolithic*, *staggered* and *nested* solution strategies, we describe them below.

6.2.1 Monolithic

A *monolithic strategy* is the easiest strategy we can define. The block-preconditioner which defines the block system is the identity matrix. Therefore, as mentioned above we only have one iterative block which triggers a strategy having a single computational path, one hierarchy. Therefore, in a *monolithic* strategy, the notions of *iterative-block* and *block hierarchy* are unique. Hence, the corresponding *transparency relation* only describes the iteration state of the strategy.

$$\mathbf{T}^{[\ \alpha_i]}\Delta\mathbf{X}^{[\ \alpha_i]} = \mathbf{R}^{[\ \alpha_i]} \qquad \rightarrow \qquad \begin{bmatrix} \mathbb{A} & \mathbb{B} \\ \mathbb{C} & \mathbb{D} \end{bmatrix}^{[\alpha_i]} \begin{bmatrix} \mathbb{X} \\ \mathbb{Y} \end{bmatrix}^{[\alpha_i]} = \begin{bmatrix} \mathbb{F} \\ \mathbb{E} \end{bmatrix}^{[\alpha_i]} \tag{6.5}$$

as shown above the iterative-block notation is imposed on the transparency relation instead of the individual blocks, to make the notation lighter, since there is no ambiguity. The Newton method is an example of this strategy.

6.2.2 Staggered

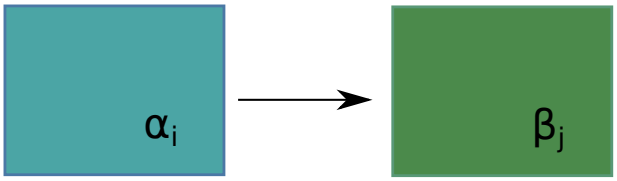

Figure 6.2: Staggered block strategy

A *staggered strategy* is defined by a succession of solutions of iterative-block with no feedback. As an example we can take a matrix similar to that in (6.5), but split into two blocks.

$$\mathbf{T}^{[\ \beta_j]}\Delta\mathbf{X}^{[\ \beta_j]} = \mathbf{R}^{[\ \beta_j]} \quad \rightarrow \quad \begin{bmatrix} \tilde{\mathbb{A}}^{[\alpha_i]} & \mathbb{O} \\ \mathbb{O} & \tilde{\mathbb{D}}^{[\beta_j]} \end{bmatrix} \begin{bmatrix} \mathbb{X}^{[\alpha_i]} \\ \mathbb{Y}^{[\beta_j]} \end{bmatrix} = \begin{bmatrix} \tilde{\mathbb{F}}^{[\alpha_i]} \\ \tilde{\mathbb{E}}^{[\beta_j]} \end{bmatrix} \tag{6.6}$$

this *transparency relation* tells us that we have two *iterative-blocks*, where the block corresponding to the unknown $\mathbb{X}$ is the one with the highest *hierarchy*. For this strategy, we have removed the dependencies index at the left of β due to the open loop property of the strategy. There is no loss of information by this step, since any snapshot at the strategy can be defined uniquely through the iterative-index corresponding to each iterative block. By a succession of solutions with no feedback, we mean that we solve first for the iterative-block α, keeping fixed the unknowns related to β. Once we have achieved a desired approximation for the unknowns in α, we continue to solve for the block β using the last update computed on the previous unknowns from α. Figure 6.2 gives a visual representation of the process.

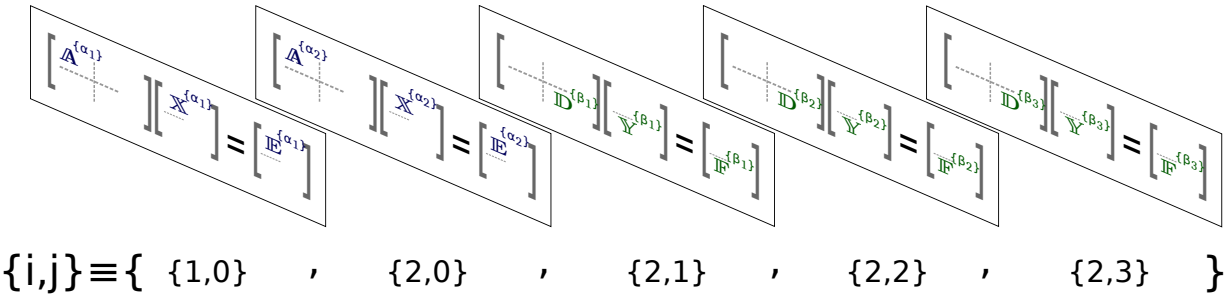

Figure 6.3: Extended transparency-relation for a staggered strategy example, where the system is solved with two iterations for α and three for β

To conclude, we explore the transparency-relation through its *iteration-sequence*. Consider the system (6.6) is solved under two iterations for the block α and three iterations for the block β (See the figure 6.3). Looking at the *iteration-sequence* $\{i, j\}$ we have

$$\{i,j\} \equiv \Big\{ \underbrace{\{1,0\},\{2,0\}}_{\alpha_i}, \underbrace{\{2,1\},\{2,2\},\{2,3\}}_{\beta_j} \Big\}$$

observe the iteration values on the transparency film relation. Each block only sees its iteration-index changing in any of its iteration. This fact, is what justifies the reduction in notation used in (6.6).

In this *staggered* strategy once we solved for the β iterative-block the strategy ends, therefore, there is no feedback on α coming from β. Due to the lack of feedback the strategy can be imagined to resemble an explicit scheme. The *algorithmic coupling* of the staggered strategy is **loose** due to the lack of feedback, therefore it becomes an approximation of our initial system independently of the tolerance error we permit between iterations. This holds true if we consider the physical coupling of the fields in different iterative-blocks as being strongly coupled.

6.2.3 Nested

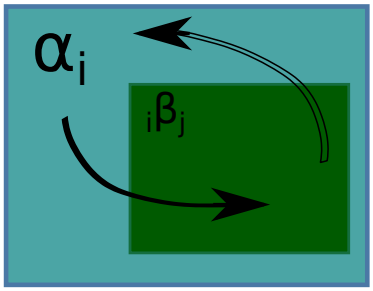

Figure 6.4: Nested block strategy

The last strategy we define is the *nested strategy*. This strategy needs more than one *iterative-block*. Once the blocks have been selected, what we need to do is to iterate in the block with the highest hierarchy once, afterwards we do again one iteration with the next block in the hierarchy and continue this process until the lowest hierarchy block has been reached. When iterating in the lowest hierarchy-block we continue the iterations on it until we have solve for its corresponding variable. After this point a feedback on the strategy starts since we go backwards one level on the hierarchy, repeating again all the process of iterating once and go lower in the hierarchy. This process will be repeated within the lowest two hierarchy blocks until we solve for both of them, once that step is completed we go one hierarchy up and repeat the process. This will continue until we have reached again the highest hierarchy-block and solve also for it. At this moment we consider the completion of the strategy. Figure 6.4 depicts the process for two iterative-blocks

Using the same block preconditioner as used in (6.6), the *nested strategy* can be represented as

$$\mathbf{T}^{[\ {}_i\beta_j]}\Delta\mathbf{X}^{[\ {}_i\beta_j]} = \mathbf{R}^{[\ {}_i\beta_j]} \quad \rightarrow \quad \begin{bmatrix} \hat{\mathbb{A}}^{[\alpha_i]} & \mathbb{O} \\ \mathbb{O} & \hat{\mathbb{D}}^{[{}_i\beta_j]} \end{bmatrix} \begin{bmatrix} \mathbb{X}^{[\alpha_i]} \\ \mathbb{Y}^{[{}_i\beta_j]} \end{bmatrix} = \begin{bmatrix} \hat{\mathbb{F}}^{[\alpha_i]} \\ \hat{\mathbb{E}}^{[{}_i\beta_j]} \end{bmatrix} \tag{6.7}$$

As seen from the equation above, we do not perform any reduction in the notation. To understand the notation we do again an example as depicted in figure 6.5

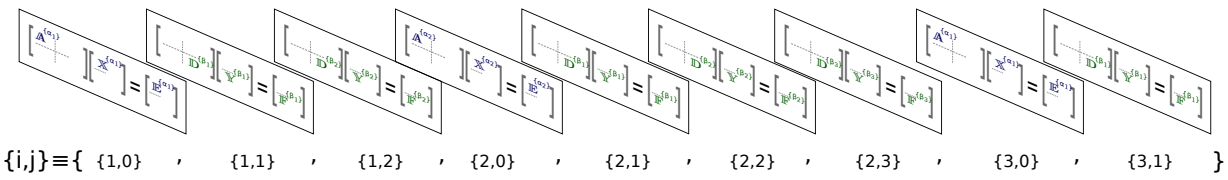

Figure 6.5: Extended transparency-relation for a nested strategy example

Consider that the system in (6.7) is solved under the following *iteration sequence*

$$\{i,j\} \equiv \Big\{ \underbrace{\{1,0\}}_{\alpha_1}, \underbrace{\{1,1\},\{1,2\}}_{\beta_j}, \underbrace{\{2,0\}}_{\alpha_2}, \underbrace{\{2,1\},\{2,2\},\{2,3\}}_{\beta_j}, \underbrace{\{3,0\}}_{\alpha_3} \underbrace{\{3,1\}}_{\beta_j} \Big\}$$

By doing this we can observe that if we want to specify an iteration i on α it does not matter what happens in the lower hierarchy block β. In contrast, for a specific j iteration on β we must say which iteration took place for α. Therefore, for iterations on α it suffices to denote which iteration we want on it as in α_i, but in lower hierarchy blocks we also need to specify the iterations occurring at higher hierarchies as in ${}_i\beta_j$

The *algorithmic coupling* of the nested strategy is **moderate** since it is described by a close loop. Therefore, it approximates the initial system proportionally to the tolerance error we permit between iterations.

6.3 Computational complexity

We presented the strategies above under a simple example of two iterative blocks. Nevertheless, the goal of this work is aimed toward coupled problems. Hence, we need to study the computational complexity and scalability of the strategies, making them independent of the number of partitions and/or iterations. The analysis done gives us important information on the strategies. Emergent properties as the *ordinal limit* arise which can help us define and understand better every strategy.

6.3.1 Ordinal limit analysis

We focus on the strategies as tools which we can use to approximate the exact solution of a discrete system. We expect the approximation to get closer to the solution as we iterate. Hence, we allow the strategy to iterate infinitely so it can arrive to its lowest possible error. Therefore, the *iteration sequence* should transform into a transfinite sequence. By allowing the strategy to iterate an infinite amount of times for an infinity amount of iterative-blocks we can find out an upper bound for the total number of iterations the strategy would need, of course, the result will be a transfinite number which we call the **ordinal limit**. Hence, the *ordinal limit* can be regarded as a open bound of the strategy on regard the iterations it must take.

6.3.1.1 Monolithic strategy

We write down again the system in (6.5) below

$$\mathbf{T}^{[\,\alpha_i]}\Delta\mathbf{X}^{[\,\alpha_i]} = \mathbf{R}^{[\,\alpha_i]} \qquad \rightarrow \qquad \begin{bmatrix} \mathbb{A} & \mathbb{B} \\ \mathbb{C} & \mathbb{D} \end{bmatrix}^{[\alpha_i]} \begin{bmatrix} \mathbb{X} \\ \mathbb{Y} \end{bmatrix}^{[\alpha_i]} = \begin{bmatrix} \mathbb{F} \\ \mathbb{E} \end{bmatrix}^{[\alpha_i]} \tag{6.8}$$

The *ordinal limit* of this strategy is the simplest, since it only contains one iterative-block by definition. To obtain the ordinal limit we only need to iterate the block α an infinite amount of times. Therefore, for the monolithic strategy its **ordinal limit** is ω, which is the first transfinite number.

6.3.1.2 Staggered strategy

Before allowing an undefined number of partitions on the staggered strategy, we check the number of iterations it would take under two iterative-blocks. Therefore, we write down again as an example the

equation (6.6) describing the staggered strategy under two iterative-blocks.

$$\mathbf{T}^{[\ \beta_j]}\Delta\mathbf{X}^{[\ \beta_j]} = \mathbf{R}^{[\ \beta_j]} \quad \rightarrow \quad \begin{bmatrix} \tilde{\mathbb{A}}^{[\alpha_i]} & \mathbb{O} \\ \mathbb{O} & \tilde{\mathbb{D}}^{[\beta_j]} \end{bmatrix} \begin{bmatrix} \mathbb{X}^{[\alpha_i]} \\ \mathbb{Y}^{[\beta_j]} \end{bmatrix} = \begin{bmatrix} \tilde{\mathbb{F}}^{[\alpha_i]} \\ \tilde{\mathbb{E}}^{[\beta_j]} \end{bmatrix} \tag{6.9}$$

The staggered strategy above reach its best approximation when each iterative block is iterated an infinite amount of times. This process is depicted in figure 6.6, it depicts an ordering with open limit 2ω where ω is the first infinite ordinal. We can relate the first infinite process associated with all the natural numbers with the iterations the α block must take. Hence the β block can be related with the ordinals $\omega + j$. The later defines an isomorphism between hierarchy and iterative-block index with the iterations taken in ordinal form. For the staggered strategy (6.9) we have the relation

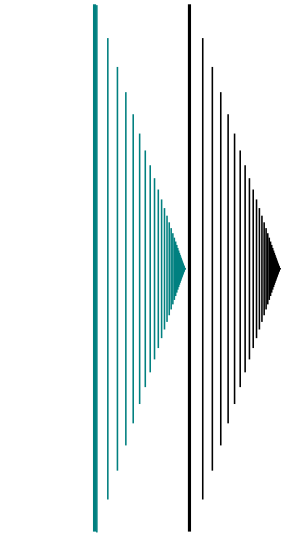

Modified work,
Original By IkamusumeFan - Own work, CC BY-SA 4.0,
https://commons.wikimedia.org/w/index.php?curid=42069842

Figure 6.6: Visualization of staggered strategy iterations for two iterative blocks. The α and β block iterations are depicted with aqua and black color respectively.

$$\begin{aligned} \alpha_i \quad &\rightarrow \quad i \\ \beta_j \quad &\rightarrow \quad \omega + j \end{aligned}$$

The former gives us the clue on how transfinite iterations would take place in a staggered strategy. Now we can generalize the result to an arbitrary number of partitions, i.e., iterative blocks. Let the staggered strategy be defined by k iterative blocks, were we define $h \in [1, 2, ..., k]$, the relation becomes

$$\boxdot^h_{i_h} \rightarrow \quad (h-1)\cdot\omega + i \tag{6.10}$$

where $\boxdot^h$ is a generalization for the Greek letters representing the hierarchy[2]. In relation with the figure 6.6, k colored lined sets should be depicted sequentially, corresponding with the k iterative blocks. Finally, we can obtain the *ordinal limit* for the staggered strategy, by allowing $k \rightarrow \infty$. It can be seen that under this scenario, according to (6.10) if we apply the limit $k \rightarrow \infty$, then, the **ordinal limit** becomes $\omega\,\omega$ which is rewritten as ω^2.

[2] in here we consider for generalization that $\alpha_i \equiv \boxdot^1_{i_1}$, $\beta_j \equiv \boxdot^2_{i_2}$, and so on...

6.3.1.3 Nested strategy

We do the same procedure for the nested strategy as we did above. We write down again as an example the equation (6.7) describing the nested strategy under two iterative-blocks.

$$\mathbf{T}^{[\ {}_i\beta_j]}\Delta\mathbf{X}^{[\ {}_i\beta_j]} = \mathbf{R}^{[\ {}_i\beta_j]} \quad \rightarrow \quad \begin{bmatrix} \hat{\mathbb{A}}^{[\alpha_i]} & \mathbb{O} \\ \mathbb{O} & \hat{\mathbb{D}}^{[{}_i\beta_j]} \end{bmatrix} \begin{bmatrix} \mathbb{X}^{[\alpha_i]} \\ \mathbb{Y}^{[{}_i\beta_j]} \end{bmatrix} = \begin{bmatrix} \hat{\mathbb{F}}^{[\alpha_i]} \\ \hat{\mathbb{E}}^{[{}_i\beta_j]} \end{bmatrix} \tag{6.11}$$

We let the nested strategy iterate each iterative-block infinitely as the strategy says. This process is shown in figure 6.7. The close loops or feedbacks in the strategy make harder to understand the transfinite iterations the strategy takes even with two iterative-blocks. However, the gist of it is to see that each set of decreasing lines corresponds to one cycle of iterations. We already know from the previous strategies that a set of decreasing lines corresponds to ω iterations. Therefore, the number of iteration under two iterative-blocks for the nested strategy corresponds to ω^2 iterations. Each stick corresponds to an ordinal of the form $m \cdot \omega + n$ where m and $n \in \mathbf{N}$. The latter highly contrast with the process taken also for two iterative blocks in the staggered strategy, where the infinite process was represented only with $\omega + j$ ordinals.

The isomorphism between the iterative block notation and the iteration in ordinal form is

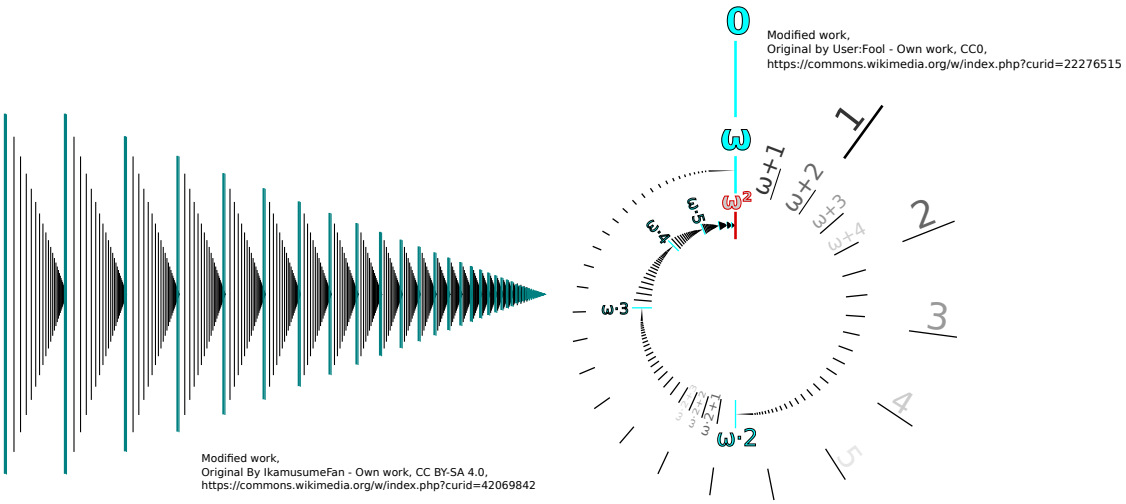

(a) Matchstick (b) Spiral matchstick

Figure 6.7: Visualization of nested strategy iterations for two iterative blocks. The α and β block iterations are depicted with aqua and black color respectively.

$$\begin{aligned} \alpha_i \quad &\rightarrow \quad (i-1)\cdot\omega + 1 \\ {}_i\beta_j \quad &\rightarrow \quad (i-1)\cdot\omega + 2 \end{aligned}$$

Hence, the isomorphism under three partitions becomes

$$\begin{aligned} \alpha_i \quad &\rightarrow \quad (i-1)\cdot\omega^2 + 1 \\ {}_i\beta_j \quad &\rightarrow \quad (i-1)\cdot\omega^2 + (j-1)\cdot\omega + 2 \\ {}_{ij}\gamma_l \quad &\rightarrow \quad (i-1)\cdot\omega^2 + (j-1)\cdot\omega + 3 \end{aligned}$$

Therefore, we generalize for an arbitrary number k of partitions where $h \in [1, k]$

$$\boxdot^k_{i_k} \rightarrow \quad (i_1-1)\cdot\omega^{k-1} + (i_2-1)\cdot\omega^{k-2} + \cdots + (i_h-1)\cdot\omega^{k-h} + \cdots + (i_k-1)\cdot\omega^{k-k} + k \tag{6.12}$$

Finally, to obtain the *ordinal limit* we let $k \to \infty$, i.e., we let the number of partitions of the system be infinite. Thus, in consideration of (6.12), the nested strategy has an **ordinal limit** of given by ω^{ω}.

6.3.2 Path error plot

Figures 6.6 & 6.7 not only provide us a guideline to study the ordinal limit. These same figures can also be used to study the error behavior of the strategy. So far, we have relate the lines in figures 6.6 & 6.7 with each iteration the strategy is taking. If in addition to that, we relate the length of each line to the error between each iterations, we would expect the length of the lines decrease as depicted in the figures. Of course, the iterations would need to be stopped at a certain number of iterations or at a predefined tolerance error.

In the sense of the *path plot error*, figures 6.6 & 6.7 are a pictorial representation of a staggered/nested strategy having a monotonic convergence in each hierarchy level. However, the length of the lines in the figures should be taken qualitatively rather than quantitatively in these images since they have not being deduced from any numerical result.

The use of figures similar to 6.6 & 6.7 as described above would depict the evolution of the error in every step. We refer to this tool as the *path error plot*. The *path error plot* can become a useful tool to measure and make comparison easier between different numerical implementations and strategies. We describe below three properties which it can help us visualize an measure.

Convergence: The slope at which each pattern of lines decreases can help us to have a different representation of convergence.

Speed of convergence: The number of iterations lines contained in a pattern can help to compare the speed of convergence.

Stability: A comparison of a model with small fluctuations in its initial data, should display similar patterns showing the implementation stability.

In addition, the *path error plot* can help us gather information to compare different solvers inside a strategy or even different preconditioners to select the best in a straight manner.

6.3.2.1 Monolithic strategy

To show the use of the *path error plot* described above some first steps have been taken and are shown below. In this case we present the use of the tool for a monolithic strategy. In specific, we show the results from one of the simulations computed for the numerical results in §3.4.1. We take in specific the case using the *Fickean model* using $N_x = 512$ spatial elements and $N_t = 256$ time steps.

Figures 6.8, 6.9 and 6.10 shows a qualitative view of the magnitude of the errors for some time steps of the simulation. As observed figure in 6.8 filters out the first two time steps, figure 6.9 filters out the first eleven time steps. At this point we can perceive a curvature in the decreasing error along all time steps and within each time step. This is expected along time steps due to the parabolic nature of the system we are solving, where as the system evolves differences between neighboring solutions decrease allowing thus to start at each time with a better approximation of the solution since we use the predictor $x^0_{t_{i+1}} = x_{t_i}$[3]. The decrease within each iteration is due to the quadratic convergence of the Newton method. Figure 6.10 shows the results filtering out the first hundred steps.

[3] where $x^0_{t_{i+1}}$ is the initial guess at the time step $i+1$, and x_{t_i} is the solution at time i

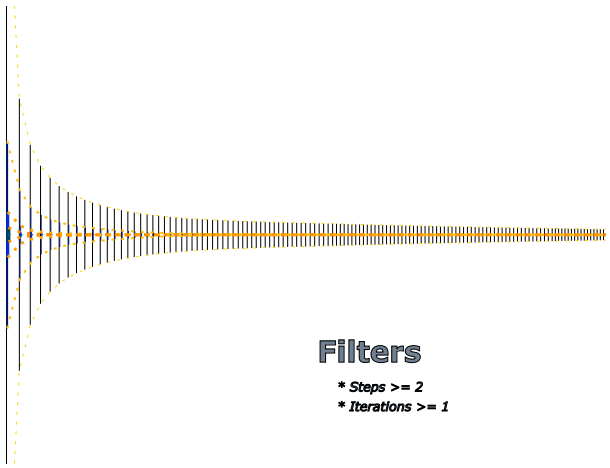

Figure 6.8: Monolithic strategy: Path error plot filtering the first two time steps

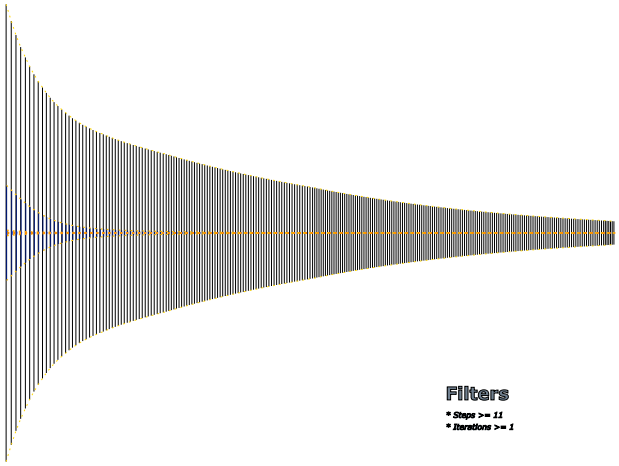

Figure 6.9: Monolithic strategy: Path error plot filtering the first eleven time steps

Vertical lines in figure 6.9 are drawn with different colors. Lines with the same color represent the same number of iteration at each time step, being the black line the first time step. The latter highlights different envelopes in figure 6.9. The outer envelope in black corresponds to the error caused mainly by the first iterations at each time step, an observable inner envelope in dark blue correspond to the second iterations and so on. This can also be filtered out and displayed as shown in figures 6.11 and 6.12. Figure 6.11 shows all the time steps except the first two but displays only the result from the first iteration and figure 6.12 shows the same time steps with all the iterations taken filtering out only the result from the first iteration.

An inspection by time step is also possible as shown in figure 6.13, where we can observe the evolution of the residual per each iteration. Figure 6.13a shows all iterations for the the first time step only, while Figure 6.13b shows it for the second time step.

Finally, notice how the figures showing the evolution of the residual during the simulation of the problem, shown the pattern expected from a monolithic strategy where we mention has an ordinal limit

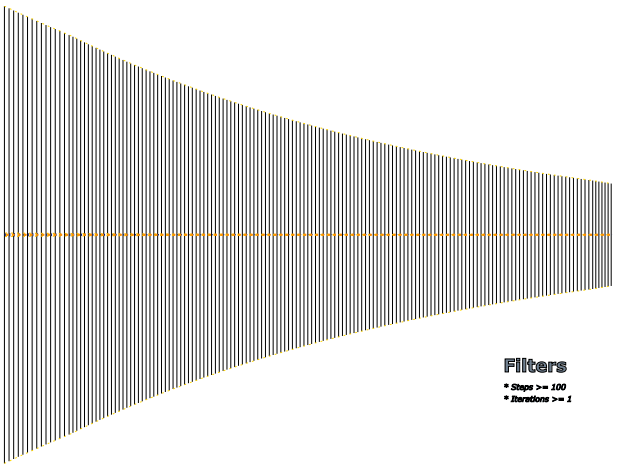

Figure 6.10: Monolithic strategy: Path error plot filtering the first hundred time steps

of ω. This pattern is that one of an arrow, in essence a monotonic decreasing residual.

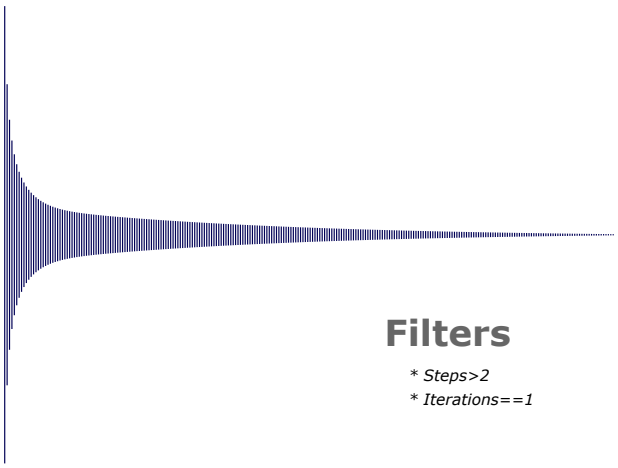

Figure 6.11: Monolithic strategy: Path error plot filtering the first two time steps, showing only the first iteration residual.

6.4 Chemical Diffusion

To implement the different strategies for the multifield VF on chemical diffusion shown in chapter §3 we use the VF shown below

$$\{c, \mu\} = \arg \inf_{c} \sup_{\mu} \Pi[c, \mu] \tag{6.13a}$$

$$\Pi[c, \mu] = \int_{\Omega_h} \pi(c, \mu) dV - \int_{\partial_j \Omega_h} \pi_j(\bar{j}, \mu) dS \tag{6.13b}$$

where we use the definition of the 2-field functional shown in (3.43)

$$\begin{aligned} \Pi[\mu, c] := & \int_{\Omega} \left(\Delta U - \mu \Delta c - \Delta t \chi(\vec{g}, c) + \Delta t \mu f_c(t) \right) dV \\ & - \int_{\partial_j \Omega} \Delta t \mu \bar{j} dS \end{aligned} \tag{6.13c}$$

The system above thanks to the Newton method can be set into a matrix form as shown in (3.49). The system is also presented below

$$\mathbf{T}_{\mathrm{NM}}^{\{\ \alpha_i\}} \Delta \mathbf{X}^{\{\ \alpha_i\}} = -\mathbf{R}_{\mathrm{NM}}^{\{\ \alpha_i\}} \tag{6.14}$$

In general the components of the block are defined by the following relations using the notation described in §2.2.

$$\begin{bmatrix} \mathbb{T}_{\mu\mu}^{(p,q)}\left(\delta_{\mu\mu}\pi\right) & \mathbb{T}_{\mu c}^{(p,q)}\left(\delta_{\mu c}\pi\right) \\ \mathbb{T}_{c\mu}^{(p,q)}\left(\delta_{c\mu}\pi\right) & \mathbb{T}_{cc}^{(p,q)}\left(\delta_{cc}\pi\right) \end{bmatrix}^{\{\ \alpha_i\}} \begin{bmatrix} \hat{\Delta}\mu \\ \hat{\Delta}c \end{bmatrix}^{\{\ \alpha_i\}} = - \begin{bmatrix} \mathbb{R}_{\mu}^{(p)}\left(\delta_{\mu}\pi\right) \\ \mathbb{R}_{c}^{(p)}\left(\delta_{c}\pi\right) \end{bmatrix}^{\{\ \alpha_i\}} \tag{6.15}$$

we use the blocks $\mathbb{R}$ to refer to the residuals and $\mathbb{T}$ to the tangents as needed for the Newton methods when applied to a VF. The specifics forms can be found in (3.50).

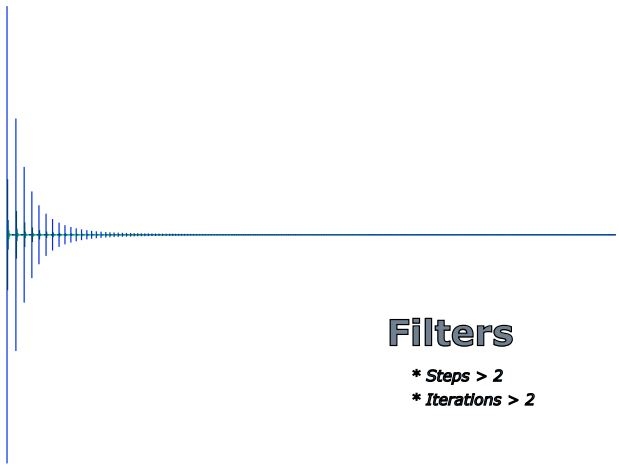

Figure 6.12: Monolithic strategy: Path error plot filtering the first two time steps, showing all the residuals but the first.

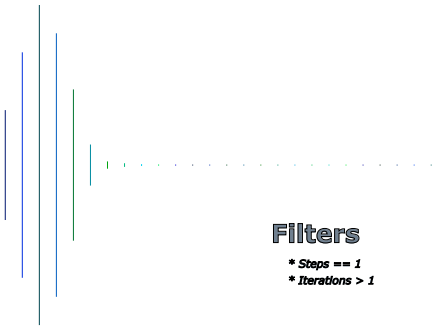

(a) Monolithic strategy: Path error plot first time step, showing all the residuals from the iterations.

(b) Monolithic strategy: Path error plot first time step, showing all the residuals from the iterations.

Figure 6.13: Individual time steps

6.4.1 VF split

The VF split is the partition of the system (4.24) into different blocks field-wise. This split is used to ease the solution of the system by solving smaller systems asynchronously. Hence, this step imposes the *algorithmic coupling* of the strategy. This coupling is independent of the physical coupling of the system. In general, we consider the fields in the original problem to have an implicit dependence between all of them. To partition the VF we modify these implicit dependencies into explicit dependencies. The fields which remain independent belong to the iterative block with the highest hierarchy. The fields belonging to the next iterative block on the hierarchy depend explicitly on the fields in iterative blocks above, and so on. An example amounts to split the VF in (6.13a) into two subproblems by means of the explicit dependency $c(\mu)$. We refer to this specific split $c(\mu)$ as the $c - split$

c-split:

For this split of the functional, the first stage contains an explicit dependency $c(\mu)$ while the second stage contains the independent field μ as a parameter. This is represented through a

semicolon, i.e.

$$\{\hat{\mu}\} = \arg\sup_{\mu} \Pi[\mu, c(\mu)]$$
$$\{\check{c}\} = \arg\inf_{c} \Pi[c; \mu] \tag{6.16}$$

The imposed algorithmic dependency modifies the original system. We observe first the changes occurred on the residuals, which are the first variations of the system acting at each spatial node of the domain Ω_h. For now, we denote the residuals of each iterative block only with its hierarchy.

First stage:
$$\tilde{\mathbb{R}}^{[\alpha]} = \frac{\delta}{\delta\mu^{(p)}}\Pi[c(\mu), \mu] = \mathbb{R}_{\mu}^{(p)}\Big(\delta_{\mu}\pi\Big) + \underbrace{\tilde{\mathbb{R}}_{\mu}^{(p)}\Big(\delta_{c}\pi c_{\mu}\Big)}_{\text{new term}} \tag{6.17a}$$

Second stage:
$$\tilde{\mathbb{R}}^{[\beta]} = \frac{\delta}{\delta c^{(p)}}\Pi[c(\mu); \mu] = \mathbb{R}_{c}^{(p)}\Big(\delta_{c}\pi\Big) \tag{6.17b}$$

6.4.1.1 Analysis of explicit dependency

The residuals of the *c-split* in (6.17a) show an extra term. This is the result of the algorithmic dependency. This new term rises the possibility to select different strategies depending on whether we allow the term to be equal to zero or different. The first stages can be associated with a variant of the *Newton method*. For now, lets see these two possibilities and focus on the direct implications

$$\frac{\delta\pi}{\delta c}\frac{\partial c}{\partial\mu^{(p)}} \equiv 0 \qquad \text{or} \qquad \frac{\delta\pi}{\delta c}\frac{\partial c}{\partial\mu^{(p)}} \neq 0 \tag{6.18}$$

The first thing to notice is that the term on the right leaves us with the same residual as the Newton method, while the term on the left modifies the residual. Therefore we refer to both implications as **Newton-like residual** or **Newton-extended residual** correspondingly. We know from previous chapters that the equivalence between the VF with the SF and WF forms rises from the first variations of the functional Π. On the one hand, a *Newton-extended residual* is actually modifying the physical system we are solving, in essence, we will solve for an approximation of the system. On the other hand, the *Newton-like* leaves the equivalence with other formulations unchanged since the residuals are not modified. In other words, the *Newton-extended* residual approximates the solution in two ways, when we partition the system and when we use an iterative solver. In contrast the *Newton-like* residual only approximates the solution through the use of an iterative solver.

Partial dependencies (explicit dependence): Equation (6.18) shows a partial derivative c_{μ} which emerge as a result of the explicit dependency we imposed. To define these new partial derivatives a general approach is the following.

Optimal conditions

The optimal condition of the problem must satisfy

$$\delta_{\mu}\Big(\delta_{c}\Pi[\mu, c(\mu)]\,(\delta\mu, \delta c)\Big) \equiv 0 \qquad \because \qquad \delta_{c}\Pi[\mu, c(\mu)]\,(\delta\mu, \delta c) \equiv 0$$

The expression above using (6.13) becomes

$$\begin{aligned}\delta_\mu\Big(\delta_c\Pi[\mu, c(\mu)]\,(\delta\mu, \delta c)\Big) &= \delta_\mu\left[\int_{\Omega_h}\left(\frac{\partial U}{\partial c}+\mu\right)\delta c dV\right]\\ &= \int_{\Omega_h}\left(1+\frac{\partial^2 U}{\partial^2 c}\frac{\partial c}{\partial \mu}\right)\delta c\delta\mu dV \equiv 0\\ \iff \quad & 1+\partial_{cc}U c_\mu = 0 \end{aligned} \tag{6.19}$$

from the above we can define the partial relation as

$$\frac{\partial c}{\partial \mu} = -\left(\frac{\partial^2 U}{\partial c^2}\right)^{-1} \tag{6.20}$$

However, for this particular scenario there is a simpler process

Conjugate variables

The same result can be obtained in a straight manner since c and μ are conjugate variables as follows

$$\frac{\partial c}{\partial \mu} = \left(\frac{\partial \mu}{\partial c}\right)^{-1} = \left(\frac{\partial}{\partial c}\frac{\partial U(c)}{\partial c}\right)^{-1} = \left(\frac{\partial^2 U}{\partial c^2}\right)^{-1} \tag{6.21}$$

Notice that this approach is based upon postulated characteristics on the fields c and μ, which we declared in §3.2. In this split, the first stage to solve corresponds to solves for c.

6.4.2 Staggered strategy

We start unveiling the *staggered* strategy behind the *Newton-extended residual*.[4] Thus, we want the extra term in (6.17a) to be different than zero,

$$\frac{\delta\pi}{\delta c}\frac{\partial c}{\partial \mu} \neq 0 \qquad \iff \qquad \frac{\delta\pi}{\delta c} \neq 0 \quad \text{and} \quad \frac{\partial c}{\partial \mu} \neq 0$$

On the one hand, it means that if $c_\mu \neq 0$, it is inevitable for c to change as we apply any variation on μ. This condition is consistent with the formulation of the model, since μ and c are conjugate-related as proposed in §3.2 and therefore, any change on μ must impact c. On the other hand, the first variation being $\delta_c\pi \neq 0$, means that c is not yet an optimal solution while we solve in a first stage for μ. This scheme is in line with the *staggered strategy* as described in §6.2.2. In terms of the algorithm, we put μ and c in the corresponding *iterative-blocks* α and β.

6.4.2.1 Algorithm

The algorithm describing the details on the staggered strategy under a c-split of the VF is given by the following two steps, each one corresponding to the solution of an *iterative-block*.

α Block:

[4] in the literature related to FSI a similar technique is known as a *quasi-direct coupling* [Tezduyar and Sathe, 2007]

The 1st step solves only for the chemical potential which is the only unknown contained within the α block. The problem to solve here becomes

$$\{\hat{\mu}\} = \arg\sup_{\mu} \Pi[\mu, c(\mu)] \qquad \rightarrow \qquad \tilde{\mathbb{T}}^{\ [\alpha_i]} \Delta\mu^{\ [\alpha_i]} = -\tilde{\mathbb{R}}^{\ [\alpha_i]} \tag{6.22}$$

we define the residual $\tilde{\mathbb{R}}^{(p)}_{[\alpha_i]}$ and tangent $\tilde{\mathbb{T}}^{(p,q)}_{[\alpha_i]}$ at the nodes (p,q) as

$$\begin{aligned}
\tilde{\mathbb{R}}^{(p)}_{[\alpha_i]} &= \left[\mathbb{R}^{(p)}_{\mu}\left(\delta_{\mu}\pi\right) + \tilde{\mathbb{R}}^{(p)}_{\mu}\left(\delta_{c}\pi c_{\mu}\right)\right]^{[\alpha_i]} \\
\tilde{\mathbb{T}}^{(p,q)}_{[\alpha_i]} &= \left[\mathbb{T}^{(p,q)}_{\mu\mu}\left(\delta_{\mu\mu}\pi\right) + \tilde{\mathbb{T}}^{(p,q)}_{\mu\mu}\left((\delta_{\mu c}\pi + \delta_{c\mu}\pi)c_{\mu} + \delta_{cc}\pi c^2_{\mu}\right)\right]^{[\alpha_i]}
\end{aligned}$$

where the terms in blue are the new contributions imposed by the explicit dependence. When we substitute the partial relation c_μ from (6.20) into the equation above we get after a cancellation of terms

$$\tilde{\mathbb{R}}^{(p)}_{[\alpha_i]} = \left[\mathbb{R}^{(p)}_{\mu}\left(\delta_{\mu}\pi\right) + \tilde{\mathbb{R}}^{(p)}_{\mu}\left(\delta_{c}\pi c_{\mu}\right)\right]^{[\alpha_i]} \tag{6.24}$$

$$\tilde{\mathbb{T}}^{(p,q)}_{[\alpha_i]} = \left[\mathbb{T}^{(p,q)}_{\mu\mu}\left(\delta_{\mu\mu}\pi\right) - \tilde{\mathbb{T}}^{(p,q)}_{\mu\mu}\left(\delta_{\mu c}\pi(\delta_{cc}\pi)^{-1}\delta_{c\mu}\pi\right)\right]^{[\alpha_i]} \tag{6.25}$$

Which concludes the general form for the α block. We define now the β block

β Block:

In the 2nd step concerning the β Block which contains the concentration, we solve the following problem

$$\{\check{c}\} = \arg\inf_{c} \Pi[c;\mu] \qquad \rightarrow \qquad \tilde{\mathbb{T}}_{\beta_j}\Delta c = -\tilde{\mathbb{R}}_{\beta_j} \tag{6.26}$$

with the local definitions of $\tilde{\mathbb{R}}^{(p)}_{[\beta_j]}$ and $\tilde{\mathbb{T}}^{(p,q)}_{[\beta_j]}$ as

$$\begin{aligned}
\tilde{\mathbb{R}}^{(p)}_{[\beta_j]} &= \left[\mathbb{R}^{(p)}_{c}\left(\delta_{c}\pi\right)\right]^{[\beta_j]} \\
\tilde{\mathbb{T}}^{(p,q)}_{[\beta_j]} &= \left[\mathbb{T}^{(p,q)}_{cc}\left(\delta_{cc}\pi\right)\right]^{[\beta_j]}
\end{aligned}$$

the steps to derive this block are exactly the same as for the corresponding diagonal element of Newton-Method when we solve for c since we do not have to take into account any explicit dependence within this block.

6.4.2.2 Transparency relation

The strategy using *transparency relations* is defined as follows

$$\mathbf{R}_{stag} = \begin{bmatrix} \left[\mathbb{R}^{(p)}_{\mu}\left(\delta_{\mu}\pi\right) + \tilde{\mathbb{R}}^{(p)}_{\mu}\left(\delta_{c}\pi c_{\mu}\right)\right]^{[\alpha_i]} \\ \left[\mathbb{R}^{(p)}_{c}\left(\delta_{c}\pi\right)\right]^{[\beta_j]} \end{bmatrix} \tag{6.27a}$$

$$\mathbf{T}_{stag} = \begin{bmatrix} \left[\mathbb{T}^{(p,q)}_{\mu\mu}\left(\delta_{\mu\mu}\pi\right) - \tilde{\mathbb{T}}^{(p,q)}_{\mu\mu}\left(\delta_{\mu c}\pi(\delta_{cc}\pi)^{-1}\delta_{c\mu}\pi\right)\right]^{[\alpha_i]} & \mathbb{O} \\ \mathbb{O} & \left[\mathbb{T}^{(p,q)}_{cc}\left(\delta_{cc}\pi\right)\right]^{[\beta_j]} \end{bmatrix} \tag{6.27b}$$

As shown in the equations above, the difference between the Newton method in (6.15) and the staggered strategy in (6.27) over the diagonal elements is minimal. The difference is highlighted by the terms in blue. However, we must recalled (6.27) is not a matrix but a transparency relation, defining the sequence for different strategy steps.

6.4.2.3 Algebraic definition

The first step to derive the staggered strategy, was to split the VF which we did by changing some dependencies from implicit to explicit. The later resulted in the partition of the algebraic system of equations. Hence, the block preconditioning we applied was **physically based**. However, some of the perks from the *transparency relation* is that it allow us to define this block-preconditioner also as a matrix, in essence, it can also be understood as being **mathematically based**. To perform this task, we observe that the resulting transparency-relation (6.27) adds some extra terms to the tangent $\mathbf{T}_{stag}$ and residual $\mathbf{R}_{stag}$. A *multiplicative preconditioner*[5] satisfies this behavior. Furthermore, notice that the extra element on the tangent $\mathbf{T}_{stag}$ in the staggered strategy (6.27) is the *Schur complement* from the Newton method strategy (6.15). Moreover, the extra term in $\mathbf{R}_{stag}$ involves the residual for c which element from the row below. The reason of the later observations is that the block-preconditioning we defined algorithmically acts as a step of the Gauss elimination method acting on blocks. The block element we try to reduce to a block of zeros corresponds to the rows defining the chemical potential μ intersecting with the columns multiplied by the the concentrations c. The row instruction we need to perform this operation is

$$\mathbf{r}_\mu \rightharpoonup \mathbf{r}_\mu - \mathbb{T}^{(p,q)}_{\mu c}\Big(\delta_{\mu c}\pi\Big)\Big(\mathbb{T}^{(p,q)}_{cc}\Big(\delta_{cc}\pi\Big)\Big)^{-1}\mathbf{r}_c \tag{6.28}$$

where $\mathbf{r}_\mu$ and $\mathbf{r}_c$ stand for the row-blocks for μ and c respectively. This row operation can be represented by the following block elementary matrix

$$\mathbf{P}_{\text{stagg}} := \begin{bmatrix} \mathbb{I}^{[\alpha_i]} & -\Big[\mathbb{T}^{(p,q)}_{\mu c}\Big(\delta_{\mu c}\pi\Big)\Big(\mathbb{T}^{(p,q)}_{cc}\Big(\delta_{cc}\pi\Big)\Big)^{-1}\Big]^{[\alpha_i]} \\ \mathbb{O}^{[\beta_j]} & \mathbb{I}^{[\beta_j]} \end{bmatrix} \tag{6.29}$$

The term $\mathbb{I}$ stands as an identity block. The equation above is the algebraic definition of the block-preconditioner for the staggered strategy. However, one should be cautious since the block-preconditioner equivalence between algorithmic and algebraic form only holds under special conditions. These special conditions are related to the functional space selected for the field c which needs to be

$$\mathcal{V}_c := \{\, c \mid c \in L^2 \,\} \qquad \rightarrow \qquad c(x,t) \approx \bigcup_{(p)} c^{(p)}(t)\delta(x - x^{(p)})$$

Hence, from the equation above we can see that as long as we satisfy the *null space condition* $(\mathbf{P}-\mathbf{T})\vec{x} = \vec{0}$ we only need to solve the system $\mathbf{P}\vec{x} = \vec{b}$. Basically, the *null space condition* gets rid of the condition which makes the *additive preconditioner* combersome to be used as block-preconditioners.[6]

6.4.2.4 Strategy approximation

The equivalence of the VF with the SF and WF is given through the first variations of the functional. When we solve the system using Newton's method the first variations are the residuals of the method. The change in the residual performed by the strategy implies that we are actually modifying the system

[5] as defined in §2.3.2.1

[6] In the literature the additive preconditioner is used as a point preconditioner for the *Richardson's iterations* methodRichardson [1911].

we are solving. In specific we are not compliant with the mass balance law dictated by the variation of the chemical potential. Therefore, in our modified system the balance law we solve is given by (6.17b) which we rewrite below

$$\tilde{\mathbb{R}}^{[\alpha]} = \frac{\delta}{\delta\mu^{(p)}}\Pi[c(\mu),\mu] = \mathbb{R}_{\mu}^{(p)}\Big(\delta_{\mu}\pi\Big) + \tilde{\mathbb{R}}_{\mu}^{(p)}\Big(\delta_{c}\pi c_{\mu}\Big) \equiv 0 \tag{6.30}$$

recalling that $\vec{j}$ is conjugate to $\vec{g}$, using the partial relation (6.20) and the functional defined in (6.13c) and multiplying by Δt we arrive to

$$\frac{\Delta c}{\Delta t} - f_c + \nabla\cdot\vec{j} = \Big(\frac{\partial U}{\partial c} - \mu\Big)\Big(\frac{\partial^2 U}{\partial c^2}\Big)^{-1}\frac{1}{\Delta t} \tag{6.31}$$

Note that as expected, the term on the RHS of the equation above modifies the original system by modifying the balance law. To understand the implications of the former, we divide the equation above (6.31) by Δt while it tends to zero, thus

$$\lim_{t\to 0}\Big[\Delta c + \Big(\nabla\cdot\vec{j} - f_c\Big)\Delta t\Big] = \lim_{t\to 0}\underbrace{\Big(\frac{\partial U}{\partial c} - \mu\Big)}_{\text{violation}}\underbrace{\Big(\frac{\partial^2 U}{\partial c^2}\Big)^{-1}}_{\text{penalty}} \tag{6.32}$$

In the original system the temporal change of concentration Δc is proportional to the time step Δt. On the contrary, the blue terms impose a correction on Δc which is time independent, providing thus an offset in comparison with the original system. This offset, can be thought as a constraint problem solved by a penalty method. As pointed out in (6.32), the problem to solve is the definition of the conjugate variables where the violation of the constraint is their difference and the penalty term is given by their partial relation.[7] In essence, since U is convex we know $U_{cc} > 0$. Thus, for the extra term to vanish we need

$$\Big(\frac{\partial U}{\partial c} - \mu\Big)\Big(\frac{\partial^2 U}{\partial c^2}\Big)^{-1} \equiv 0 \qquad \Longleftrightarrow \qquad \frac{\partial U}{\partial c} = \mu$$

Furthermore, the units of the extra term $\tilde{\mathbb{R}}_{\mu}^{(p)}\Big(\delta_{c}\pi c_{\mu}\Big)$ have units of concentration. Therefore, it acts as an **artificial added concentration**. The behaviour of this approximated strategy is similar as the artificial added mass effect works in FSI (confeer to Förster et al. [2006] as an example).

6.4.3 Nested strategy

There exist a link between the *nested strategy* and a *Newton-like residual*. For the *Newton-like residual* we want the extra term in (6.17a) to be identical to zero, which means

$$\frac{\delta\pi}{\delta c}\frac{\partial c}{\partial\mu} \equiv 0 \qquad \Longleftrightarrow \qquad \frac{\delta\pi}{\delta c} \equiv 0 \quad \text{or} \quad \frac{\partial c}{\partial\mu} \equiv 0$$

The first option $c_{\mu} \equiv 0$ is not consistent with our formulation since c and μ are conjugate-related. The conjugation implies that if we apply a variation on μ then c must change as well. Therefore, this option is not possible to follow with our original assumptions. The second option involves the first variation to be zero, in essence $\delta_c\pi \equiv 0$. Since we are using a Newton method to solve the system, the first variation is the residual. Therefore, for each variation we apply on μ, we must have a c which is at least an approximated optimal solution. In essence, for each iteration we do for μ, we must solve afterwards for c every time. The later is nothing more than the *nested strategy* as described in 6.2.3. In terms of the algorithm, we put μ and c in the corresponding *iterative-blocks* α and β.

[7] Observe in (6.31) that with a smaller Δt the departure from the original systems increases. Nevertheless, a smaller time step by continuity on U also decreases the value in the violation term. Hence, despite the system not being convergent to the original it can approximate it.

6.4.3.1 Algorithm

The algorithm describing the details on the nested strategy under a c-split of the VF is given by the following two steps, each one corresponding to the solution of an *iterative-block*.

α Block:

The first step solves the iterative-block α which concerns the chemical potential μ. The *Newton-like residual* imposes that per each iteration in the iterative-block α we must solve for the iterative-block β before iterating in the block α once again. Therefore we solve in one iteration

$$\{\hat{\mu}\} = \arg\sup_{\mu} \Pi[\mu, c(\mu)] \qquad \rightarrow \qquad \tilde{\mathbb{T}}_{\ [\alpha_i]} \Delta\mu_{\ [\alpha_i]} = -\tilde{\mathbb{R}}_{\ [\alpha_i]} \tag{6.33}$$

where we define the residual $\tilde{\mathbb{R}}^{(p)}_{[\alpha_i]}$ and tangent $\tilde{\mathbb{T}}^{(p,q)}_{[\alpha_i]}$ at each node as

$$\tilde{\mathbb{R}}^{(p)}_{[\alpha_i]} = \left[\mathbb{R}^{(p)}_{\mu}\left(\delta_{\mu}\pi\right)\right]^{[\alpha_i]} \tag{6.34}$$

$$\tilde{\mathbb{T}}^{(p,q)}_{[\alpha_i]} = \left[\mathbb{T}^{(p,q)}_{\mu\mu}\left(\delta_{\mu\mu}\pi\right) - \tilde{\mathbb{T}}^{(p,q)}_{\mu\mu}\left(\delta_{\mu c}\pi(\delta_{cc}\pi)^{-1}\delta_{c\mu}\pi\right)\right]^{[\alpha_i]} \tag{6.35}$$

where we have already substituted the partial relation (6.20). After one iteration, we solve the β block until we reach or get close to an optimal solution of the β block. This process is repeated until we reach an optimal solution for the α block.

β Block:

The second step solves the β block which concerns the concentration. In this block the system to solve is the following

$$\{\check{c}\} = \arg\inf_{c} \Pi[c; \mu] \qquad \rightarrow \qquad \tilde{\mathbb{T}}_{\beta_j} \Delta c = -\tilde{\mathbb{R}}_{\beta_j} \tag{6.36}$$

with the local definitions of $\tilde{\mathbb{R}}^{(p)}_{[_i\beta_j]}$ and $\tilde{\mathbb{T}}^{(p,q)}_{[_i\beta_j]}$ as

$$\tilde{\mathbb{R}}^{(p)}_{[_i\beta_j]} = \left[\mathbb{R}^{(p)}_{c}\left(\delta_{c}\pi\right)\right]^{[_i\beta_j]}$$

$$\tilde{\mathbb{T}}^{(p,q)}_{[_i\beta_j]} = \left[\mathbb{T}^{(p,q)}_{cc}\left(\delta_{cc}\pi\right)\right]^{[_i\beta_j]}$$

This block is exactly the same as in the staggered strategy since it is the lowest block in the hierarchy.

6.4.3.2 Transparency relation

We summarize the results through its transparency relation.

$$\mathbf{R}_{\text{nest}} := \begin{bmatrix} \left[\mathbb{R}^{(p)}_{\mu}\left(\delta_{\mu}\pi\right)\right]^{[\alpha_i]} \\ \left[\mathbb{R}^{(p)}_{c}\left(\delta_{c}\pi\right)\right]^{[_i\beta_j]} \end{bmatrix} \tag{6.37a}$$

$$\mathbf{T}_{\text{nest}} := \begin{bmatrix} \left[\mathbb{T}^{(p,q)}_{\mu\mu}\left(\delta_{\mu\mu}\pi\right) - \tilde{\mathbb{T}}^{(p,q)}_{\mu\mu}\left(\delta_{\mu c}\pi(\delta_{cc}\pi)^{-1}\delta_{c\mu}\pi\right)\right]^{[\alpha_i]} & \mathbb{O} \\ \mathbb{O} & \left[\mathbb{T}^{(p,q)}_{cc}\left(\delta_{cc}\pi\right)\right]^{[_i\beta_j]} \end{bmatrix} \tag{6.37b}$$

The *transparency relation* shows a great similarity between the Newton method in (6.15) and the staggered strategy in (6.27). Nevertheless, as we expected from the derivation of the strategy, the residual has not changed.

6.4.3.3 Algebraic definition

We have derived the nested strategy starting with a split of the VF by modifying the dependencies of the original system. This step partitioned the original system of equations into two blocks. Once again, through the transparency-relation we can obtain an algebraic definition of the block-preconditioner. In contrast with the staggered strategy, the nested strategy does not modify the residual of the original system, as shown by the *transparency relation* (6.37). Nevertheless, the extra-term in the tangent $\mathbf{T}_{\text{nest}}$ is also the *Schur complement* from the Newton method strategy (6.15). The algebraic definition of the block-preconditioner corresponds to an additive preconditioner (2.31), as shown below

$$\mathbf{P}x = (\mathbf{P} - \mathbf{T})x + b \qquad \textbf{: Additive Identity} \tag{6.38}$$

However, if we use the preconditioner above we will modify the residual. Hence, we need the red term in (6.38) to be equal to zero. Thus, we seek that the matrix $(\mathbf{P} - \mathbf{T})$ is an element of the null space of the solution x

$$(\mathbf{P} - \mathbf{T})x = 0 \qquad \textbf{Null space condition} \tag{6.39}$$

Let $\mathbf{P}$ be the tangent $\mathbf{T}_{\text{nest}}$ from the nested strategy (6.37b) and $\mathbf{T}$ the original tangent from the Newton method (6.15) we arrive to the *null space condition* condition

$$\mathbf{T}_{\text{nest}} - \mathbf{T}_{\text{NM}} = -\begin{bmatrix} \tilde{\mathbb{T}}^{(p,q)}_{\mu\mu}\Big(\delta_{\mu c}\pi(\delta_{cc}\pi)^{-1}\delta_{c\mu}\pi\Big)^{[\alpha_i]} & -\mathbb{T}^{(p,q)}_{\mu c}\Big(\delta_{\mu c}\pi\Big)^{[\alpha_i]} \\ -\mathbb{T}^{(p,q)}_{\mu c}\Big(\delta_{c\mu}\pi\Big)^{[{}_i\beta_j]} & \mathbb{O} \end{bmatrix} \tag{6.40}$$

the first row $\mathbf{r}_\mu$ from (6.40) satisfies the *null space condition*

$$\tilde{\mathbb{T}}^{(p,q)}_{\mu\mu}\Big(\delta_{\mu c}\pi(\delta_{cc}\pi)^{-1}\delta_{c\mu}\pi\Big)\Delta\mu = \mathbb{T}^{(p,q)}_{\mu c}\Big(\delta_{\mu c}\pi\Big)\Delta c$$

Substituting the functional for that in (6.13c) we can write

$$\frac{\Delta c}{\Delta \mu} = \frac{\tilde{\mathbb{M}}^{(p,q)}_{\mu\mu}\Big(\big(\frac{\partial^2 U}{\partial c^2}\big)^{-1}\Big)}{\mathbb{M}^{(a,p)}_{\mu c}\Big(1\Big)}$$

in the last expression, under the assumptions that the solution space for c and μ are both defined under a Sobolev space and making use of Gaussian quadrature we can express the former as

$$\frac{\Delta c}{\Delta \mu} = \Big(\frac{\partial^2 U}{\partial c^2}\Big)^{-1} \tag{6.41}$$

which is exactly the expression we derive as the partial relation c_μ – in 6.20. With this we can conclude that the first row of (6.40) is an element of the null space condition (6.39). Finally, the second row of (6.40) is satisfied automatically due to the iterative process. Namely, the second row is used to solve the second iterative block for which μ is fixed, therefore $\hat{\Delta}\mu \equiv 0$ making thus irrelevant the non-zero block on the second row. Therefore, the *additive preconditioner* is the algebraic definition of the nested strategy, which means the tangent matrix we derived, is itself the preconditioner

$$\mathbf{P}_{\text{nest}} := \mathbf{T}_{\text{nest}} = \begin{bmatrix} \Big[\mathbb{T}^{(p,q)}_{\mu\mu}\Big(\delta_{\mu\mu}\pi\Big) - \tilde{\mathbb{T}}^{(p,q)}_{\mu\mu}\Big(\delta_{\mu c}\pi(\delta_{cc}\pi)^{-1}\delta_{c\mu}\pi\Big)\Big]^{[\alpha_i]} & \mathbb{O} \\ \mathbb{O} & \Big[\mathbb{T}^{(p,q)}_{cc}\Big(\delta_{cc}\pi\Big)\Big]^{[\beta_j]} \end{bmatrix} \tag{6.42}$$

Something interesting from the *nested strategy* is that it can be seen as a generalization of the *global-local* strategy commonly used in the literature, e.g. Miehe et al. [2014]. The *global-local* strategy divides the problem into two different blocks depending on the space they belong to. In essence, in the α block are all the fields which belong to a *Sobolev space* , while in the β block are the fields define in an L^2 *space* . The corresponding names for the blocks are the *global* and *local* to emphasize the nature of their solution spaces. The *global local* strategy create the different block depending if its solution space is *Sobolev* or L^2, this only gives two options. In contrast, the nested strategy defines the block upon explicit dependencies, thus the possibilities for different preconditioners increases.

Finally as a quick summary of the steps taken, one can refer to the image 6.14.

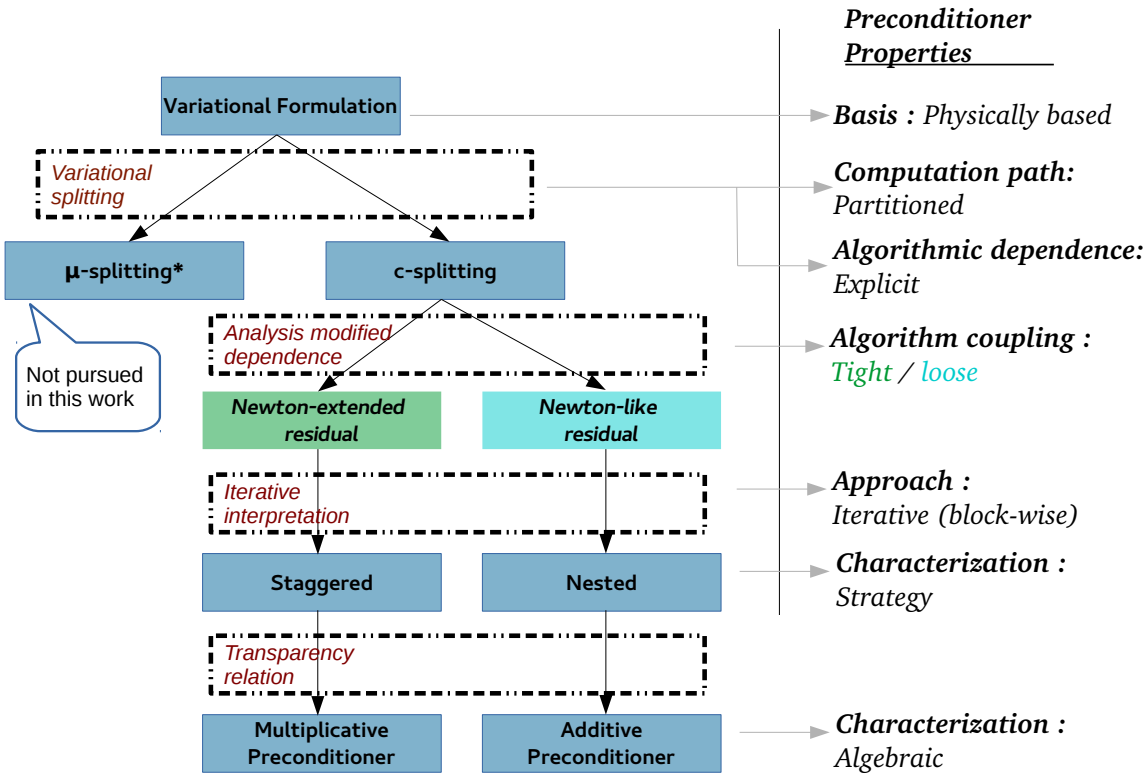

Figure 6.14: Flow process to derive staggered and nested strategies from a VF

6.4.4 Monolithic strategy

The algebraic definitions done for the staggered and nested strategies using additive and multiplicative opened the path for new algebraic preconditioners under a Monolithic strategy. We explore two options below, one using an additive preconditioner and the other a multiplicative preconditioner.

6.4.4.1 Additive preconditioning

In the nested strategy §6.4.3 we used an additive preconditioner as block-preconditioner. For this we need to satisfy the null space condition (6.39). For the nested strategy the expression (6.40) satisfies the *null space condition* for the iterative-block α, in essence on the first row-block $\mathbf{r}_\mu$. The lower row $\mathbf{r}_c$ was satisfied by the fact that chemical potential is fixed while solving the iterative block β. Therefore, we can define the following matrix, which not only satisfy block-row wise the null space condition,

$$\mathbf{P}_{\Delta+} - \mathbf{T} = -\begin{bmatrix} \tilde{\mathbb{T}}^{(p,q)}_{\mu\mu}\left(\delta_{\mu c}\pi(\delta_{cc}\pi)^{-1}\delta_{c\mu}\pi\right) & \mathbb{T}^{(p,q)}_{\mu c}\left(\delta_{\mu c}\pi\right) \\ \mathbb{O} & \mathbb{O} \end{bmatrix} \tag{6.43}$$

This new condition satisfies the null space of our solution even if we do not divide the system into blocks. Therefore, we can solve in a monolithic strategy the following system

$$\mathbf{P}_{\Delta+}\hat{\Delta}\vec{x} = \mathbf{R}_{\Delta+} \tag{6.44}$$

with

$$\mathbf{R}_{\Delta_+} := \begin{bmatrix} \left[\mathbb{R}^{(p)}_{\mu}\left(\delta_\mu\pi\right)\right]^{[\alpha_i]} \\ \left[\mathbb{R}^{(p)}_{c}\left(\delta_c\pi\right)\right]^{[\beta_j]} \end{bmatrix}^{[\alpha_i]} \tag{6.45a}$$

$$\mathbf{P}_{\Delta_+} := \begin{bmatrix} \mathbb{T}^{(p,q)}_{\mu\mu}\left(\delta_{\mu\mu}\pi\right) - \tilde{\mathbb{T}}^{(p,q)}_{\mu\mu}\left(\delta_{\mu c}\pi(\delta_{cc}\pi)^{-1}\delta_{c\mu}\pi\right) & \mathbb{O} \\ \mathbb{T}^{(p,q)}_{\mu c}\left(\delta_{c\mu}\pi\right) & \mathbb{T}^{(p,q)}_{\mu c}\left(\delta_{cc}\pi\right) \end{bmatrix}^{[\alpha_i]} \tag{6.45b}$$

The sub-index in $\mathbf{P}_{\Delta_+}$ is picked to recall the preconditioner is a block-triangular matrix (Δ) arising from an additive preconditioner ($+$).

6.4.4.2 Multiplicative preconditioning

While constructing the algebraic definition of the staggered strategy in §6.4.2 we made use of the multiplicative preconditioner (6.29). We can make use of the same preconditioner but instead of solving the system in different iterative blocks we solve all the system in a single block, thus we have

$$\mathbf{P}_{\Delta_*} := \begin{bmatrix} \mathbb{I} & -\left[\mathbb{T}^{(p,q)}_{\mu c}\left(\delta_{\mu c}\pi\right)\left(\mathbb{T}^{(p,q)}_{cc}\left(\delta_{cc}\pi\right)\right)^{-1}\right] \\ \mathbb{O} & \mathbb{I} \end{bmatrix}^{[\alpha_i]} \tag{6.46}$$

Therefore, in this case we solve the system

$$\mathbf{P}_{\Delta_*}\mathbf{T}\hat{\Delta}\vec{x} = \mathbf{P}_{\Delta_*}\mathbf{R} \tag{6.47}$$

where $\mathbf{T}$ is the tangent and $\mathbf{R}$ residual obtained with the Newton method (6.15). Thus, we get

$$\mathbf{R}_{\Delta_*} = \begin{bmatrix} \left[\mathbb{R}^{(p)}_{\mu}\left(\delta_\mu\pi\right) + \tilde{\mathbb{R}}^{(p)}_{\mu}\left(\delta_c\pi c_\mu\right)\right] \\ \left[\mathbb{R}^{(p)}_{c}\left(\delta_c\pi\right)\right] \end{bmatrix}^{[\alpha_i]} \tag{6.48a}$$

$$\mathbf{T}_{\Delta_*} = \begin{bmatrix} \left[\mathbb{T}^{(p,q)}_{\mu\mu}\left(\delta_{\mu\mu}\pi\right) - \tilde{\mathbb{T}}^{(p,q)}_{\mu\mu}\left(\delta_{\mu c}\pi(\delta_{cc}\pi)^{-1}\delta_{c\mu}\pi\right)\right] & \mathbb{O} \\ \mathbb{T}^{(p,a)}_{c\mu}\left(\delta_{c\mu}\pi\right) & \left[\mathbb{T}^{(p,q)}_{cc}\left(\delta_{cc}\pi\right)\right] \end{bmatrix}^{[\alpha_i]} \tag{6.48b}$$

The sub-index in $\mathbf{P}_{\Delta_*}$ is picked to recall the preconditioner is a block-triangular matrix (Δ) arising from an multiplicative preconditioner ($*$).

6.5 General VF

We formalize the steps for a general VF to develop staggered and nested strategies. In §4 we consider a VF where a first-reduction type has been applied (4.23). Therefore, the functional depends only on the variables $\mathbf{a}_i$ and $\mathbf{a}_i^*$ where $i \in [0, n]$ and n is the number of balance laws we have introduced to develop the VF. Therefore, the problem in VF is

$$\{\dot{\mathbf{a}_i}, \mathbf{a_i}^*\} = \underset{\dot{\mathbf{a}_i}, \mathbf{a_i}^*}{\mathsf{arg\,stat}}\, \Pi \tag{6.49a}$$

$$\Pi[\dot{\mathbf{a}_i}, \mathbf{a_i}^*] := \int_\tau \left[\int_\Omega \left(\dot{U}(\mathbf{a_i}) + \sum_{\forall i} \big(- a_i^* \dot{a_i} + a_i^* b_i \big) + \chi^*(\mathbf{A_i}^*, \mathbf{a_i}) \right) dV - \sum_{\forall i} \int_{\partial_{A_i}\Omega} \Big[a_i^* \overline{A_i} \Big] dS \right] dt \tag{6.49b}$$

After applying finite differences for time discretization and classic FEM for space we arrive to the problem

$$\{\mathbf{a_i}_h^{m+1}, \mathbf{a_i}_h^{*m+1}\} = \underset{\dot{\mathbf{a}_i}_h^{m+1}, \mathbf{a_i}_h^{*m+1}}{\mathsf{arg\,stat}}\, \Pi_h^{m+1} \tag{6.50a}$$

$$\Pi_h^{m+1} = \bigcup_{\forall p \in \overline{\Omega}_h} \Pi_{(p)}^{m+1} \tag{6.50b}$$

$$\Pi_{(p)}^{m+1}[\mathbf{a_i}_h^{m+1}, \mathbf{a_i}_h^{*m+1}] := \left[\int_\Omega \left(\Delta U + \sum_{\forall i} \big(- a_i^* \dot{a_i} + \Delta t a_i^* b_i \big) \Big|^{m+1} + \Delta t \chi^*(\mathbf{A_i}^{*m+1}, \mathbf{a_i}) \right) dV \right. \tag{6.50c}$$

$$\left. - \sum_{\forall i} \int_{\partial_{A_i}\Omega} \Big[\Delta t a_i^* \overline{A_i} \Big] \Big|^{m+1} dS \right] \Big|_{(p)}$$

where the subscript (p) refers to a node p in the discrete mesh $\overline{\Omega}_h := \Omega_h \cup \partial\Omega$, the superscript denotes a time step with reference at the discrete time m. From now on, we only deal with the discrete form. Hence, we consider implicitly the subscripts and superscripts denoting a discretization unless they are necessary. Let $\pi(\mathbf{a}_i, \mathbf{a}_i^*)$ be the integrand of Π. Thus, we have the following partial relations $\forall k \neq i$

$$\frac{\partial^2 \pi}{\partial a_i \partial a_i} = \frac{\partial^2 U}{\partial a_i \partial a_i} \quad ; \qquad \frac{\partial^2 \pi}{\partial a_k \partial a_i} = \frac{\partial^2 U}{\partial a_k \partial a_i} \tag{6.51a}$$

$$\frac{\partial^2 \pi}{\partial a_i^* \partial a_i} = -1 \quad ; \qquad \frac{\partial^2 \pi}{\partial a_k^* \partial a_i} = 0 \tag{6.51b}$$

$$\frac{\partial^2 \pi}{\partial A_i^* \partial a_i} = 0 \quad ; \qquad \frac{\partial^2 \pi}{\partial A_k^* \partial a_i} = 0 \tag{6.51c}$$

$$\frac{\partial^2 \pi}{\partial A_i^* \partial a_i^*} = 0 \quad ; \qquad \frac{\partial^2 \pi}{\partial A_k^* \partial a_i^*} = 0 \tag{6.51d}$$

$$\frac{\partial^2 \pi}{\partial A_i^* \partial A_i^*} = \Delta t \frac{\partial^2 \chi}{\partial A_i^* \partial A_i^*} \quad ; \qquad \frac{\partial^2 \pi}{\partial A_k^* \partial A_i^*} = \Delta t \frac{\partial^2 \chi}{\partial A_k^* \partial A_i^*} \tag{6.51e}$$

The system (6.50) can be solved via the Newton method as

$$\mathbf{T}^{[\,\alpha_i]} \hat{\Delta}\mathbf{x}^{[\,\alpha_i]} = \mathbf{R}^{[\,\alpha_i]} \tag{6.52}$$

where the system is described by one iterative block α, the tangent $\mathbf{T}$ is given by the second variations of the functional, the residual $\mathbf{R}$ by the first variations, the former for an element e is given by

$$\mathbf{T}_e := \begin{bmatrix} \mathbb{T}_{\mathbf{a}_{i_e}\mathbf{a}_{i_e}} & \mathbb{T}_{\mathbf{a}_{i_e}\mathbf{a}^*_{1_e}} \\ \mathbb{T}_{\mathbf{a}^*_{i_e}\mathbf{a}_{i_e}} & \mathbb{T}_{\mathbf{a}^*_{i_e}\mathbf{a}^*_{i_e}} \end{bmatrix} \tag{6.53a}$$

$$= \begin{bmatrix} \delta_{\mathbf{a}_{1_e}\mathbf{a}_{1_e}}\Pi & \delta_{\mathbf{a}_{1_e}\mathbf{a}_{2_e}}\Pi & \cdots & \delta_{\mathbf{a}_{1_e}\mathbf{a}^*_{1_e}}\Pi & \delta_{\mathbf{a}_{1_e}\mathbf{a}^*_{2_e}}\Pi & \cdots & \delta_{\mathbf{a}_{1_e}\mathbf{a}^*_{n_e}}\Pi \\ \delta_{\mathbf{a}_{2_e}\mathbf{a}_{1_e}}\Pi & \delta_{\mathbf{a}_{2_e}\mathbf{a}_{2_e}}\Pi & \cdots & \delta_{\mathbf{a}_{2_e}\mathbf{a}^*_{1_e}}\Pi & \delta_{\mathbf{a}_{2_e}\mathbf{a}^*_{2_e}}\Pi & \cdots & \delta_{\mathbf{a}_{2_e}\mathbf{a}^*_{n_e}}\Pi \\ \vdots & \vdots & \ddots & \vdots & \vdots & & \\ \delta_{\mathbf{a}_{n_e}\mathbf{a}_{1_e}}\Pi & \delta_{\mathbf{a}_{n_e}\mathbf{a}_{2_e}}\Pi & \cdots & \delta_{\mathbf{a}_{n_e}\mathbf{a}^*_{1_e}}\Pi & \delta_{\mathbf{a}_{n_e}\mathbf{a}^*_{2_e}}\Pi & \cdots & \delta_{\mathbf{a}_{n_e}\mathbf{a}^*_{n_e}}\Pi \\ \delta_{\mathbf{a}^*_{1_e}\mathbf{a}_{1_e}}\Pi & \delta_{\mathbf{a}^*_{1_e}\mathbf{a}_{2_e}}\Pi & \cdots & \delta_{\mathbf{a}^*_{1_e}\mathbf{a}^*_{1_e}}\Pi & \delta_{\mathbf{a}^*_{1_e}\mathbf{a}^*_{2_e}}\Pi & \cdots & \delta_{\mathbf{a}^*_{1_e}\mathbf{a}^*_{n_e}}\Pi \\ \delta_{\mathbf{a}^*_{2_e}\mathbf{a}_{1_e}}\Pi & \delta_{\mathbf{a}^*_{2_e}\mathbf{a}_{2_e}}\Pi & \cdots & \delta_{\mathbf{a}^*_{2_e}\mathbf{a}^*_{1_e}}\Pi & \delta_{\mathbf{a}^*_{2_e}\mathbf{a}^*_{2_e}}\Pi & \cdots & \delta_{\mathbf{a}^*_{2_e}\mathbf{a}^*_{n_e}}\Pi \\ \vdots & \vdots & \ddots & \vdots & \vdots & & \\ \delta_{\mathbf{a}^*_{n_e}\mathbf{a}_{1_e}}\Pi & \delta_{\mathbf{a}^*_{n_e}\mathbf{a}_{2_e}}\Pi & \cdots & \delta_{\mathbf{a}^*_{n_e}\mathbf{a}^*_{1_e}}\Pi & \delta_{\mathbf{a}^*_{n_e}\mathbf{a}^*_{2_e}}\Pi & \cdots & \delta_{\mathbf{a}^*_{n_e}\mathbf{a}^*_{n_e}}\Pi \end{bmatrix} \tag{6.53b}$$

$$\mathbf{R}_e := \begin{bmatrix} \mathbb{R}_{\mathbf{a}_{i_e}} \\ \mathbb{R}_{\mathbf{a}^*_{i_e}} \end{bmatrix} \equiv \begin{bmatrix} \delta_{\mathbf{a}_{i_e}}\Pi \\ \delta_{\mathbf{a}^*_{i_e}}\Pi \end{bmatrix} = [\delta_{\mathbf{a}_{1_e}}\Pi, \delta_{\mathbf{a}_{2_e}}\Pi, \cdots, \delta_{\mathbf{a}_{n_e}}\Pi, \delta_{\mathbf{a}^*_{1_e}}\Pi, \delta_{\mathbf{a}^*_{2_e}}\Pi, \cdots, \delta_{\mathbf{a}^*_{n_e}}\Pi]^T \tag{6.53c}$$

the term $\hat{\Delta}\mathbf{x}$ is the corresponding corrections to the set containing $\mathbf{a}_i$ and $\mathbf{a}^*_i$. E.g., for a given triangular element e with vertices $\{p, q, r\}$ we defined them as

$$\begin{aligned} \hat{\mathbf{\Delta}}\mathbf{x}_e &:= \begin{bmatrix} \hat{\Delta}\mathbf{a}_{i_e} & \hat{\Delta}\mathbf{a}^*_{i_e} \end{bmatrix}^T \\ &= \begin{bmatrix} \hat{\Delta}\mathbf{a}_{1_e} & \hat{\Delta}\mathbf{a}_{2_e} & \dots & \hat{\Delta}\mathbf{a}_{n_e} & \hat{\Delta}\mathbf{a}^*_{1_e} & \hat{\Delta}\mathbf{a}^*_{2_e} & \dots & \hat{\Delta}\mathbf{a}^*_{n_e} \end{bmatrix}^T \\ &= [\hat{\Delta}a_{1_{(p)}}, \hat{\Delta}a_{1_{(q)}}, \hat{\Delta}a_{1_{(r)}}, \hat{\Delta}a_{2_{(p)}}, \hat{\Delta}a_{2_{(q)}}, \hat{\Delta}a_{2_{(r)}}, \dots, \hat{\Delta}a_{n_{(p)}}, \hat{\Delta}a_{n_{(q)}}, \hat{\Delta}a_{n_{(r)}} \\ &\quad , \hat{\Delta}a^*_{1_{(p)}}, \hat{\Delta}a^*_{1_{(q)}}, \hat{\Delta}a^*_{1_{(r)}}, \hat{\Delta}a^*_{2_{(p)}}, \hat{\Delta}a^*_{2_{(q)}}, \hat{\Delta}a^*_{2_{(r)}}, \dots, \hat{\Delta}a^*_{n_{(p)}}, \hat{\Delta}a^*_{n_{(q)}}, \hat{\Delta}a^*_{n_{(r)}}]^T \end{aligned} \tag{6.54}$$

where we have expanded the subscripts i according to the number of balance laws and e node-wise. In the following we provide a set of mathematical statements to prove staggered and nested strategies solutions can be deduced from the monolithic VF system described by the Newton method (6.52).

Corollary 6.5.0.1 (VF split through explicit dependencies)**.** *A strongly coupled problem modeled via a generic VF as that in* (6.49) *can be split into two different systems by an explicit change of dependencies leading to the following couple of VF which are solved in a hierarchical sequence.*

$$\{x^{[\ \alpha_i]}\} = \mathit{arg} \quad \underset{x^{[\ \alpha_i]}}{\mathit{stat}}\, \Pi[x^{[\ \alpha_i]}, x^{[\ {}_i\beta_j]}(x^{[\ \alpha_i]})] \tag{6.55a}$$

$$\{x^{[\ {}_i\beta_j]}\} = \mathit{arg} \quad \underset{x^{[\ {}_i\beta_j]}}{\mathit{stat}}\, \Pi[x^{[\ {}_i\beta_j]}; x^{[\ \alpha_i]}] \tag{6.55b}$$

where the upper-indexes $[\alpha_i]$ *and* $[{}_i\beta_j]$ *indicate the corresponding iterative block we are solving. Thus,* $x^{[\ \alpha_i]}$ *is the set of independent fields and* $x^{[\ {}_i\beta_j]}$ *the set of fields where an explicit dependence has been arbitrarily imposed.*

Proof. Since the system (6.49) is a strongly coupled system, all the variables $\mathbf{a}_i$ and $\mathbf{a}^*_i$ depend implicitly on one another. To partition the system we introduce an explicit dependency between the variables. An explicit dependence, e.g. $\mathbf{a}_i(\mathbf{a}^*_i)$ implies that the solution at the field a_i depends on the value of a^*_i while the opposite does not hold, creating thus sequential order to solve the fields and therefore a two block system. ■

Corollary 6.5.0.2. *A split VF* (6.55) *can be solved in each block by the Newton method leading to the following couple of systems to solve.*

$$\mathbb{T}^{[\ \alpha_i]}\hat{\Delta}x^{[\ \alpha_i]} = -\mathbb{R}^{[\ \alpha_i]} \tag{6.56a}$$

$$\mathbb{T}^{[\ {}_i\beta_j]}\hat{\Delta}x^{[\ {}_i\beta_j]} = -\mathbb{R}^{[\ {}_i\beta_j]} \tag{6.56b}$$

where $\mathbb{R}$ is the residual, $\mathbb{T}$ the tangent matrix and $\hat{\Delta}x$ the set of corrections for the fields. The set $\hat{\Delta}x^{[\ \alpha_i]}$ is composed by all corrections to the independent fields whereas $\hat{\Delta}x^{[\ {}_i\beta_j]}$ contains all the corrections to fields where an explicit dependence has been imposed.

6.5.1 Partial relations

Corollary 6.5.0.3. *An explicit dependence between variables in a system like* (6.55) *imposes a set of partial relations in the independent fields. These partial relations are the rate of change of the dependent fields against the independent field.*

Lemma 6.5.1 (Partial relations $a_i(a_k)$)**.** *A split variational form* (6.55) *via the explicit dependence $a_i(a_k)$ has the following partial relation*

$$\frac{\partial a_i}{\partial a_k} = -\left(\frac{\partial^2 U}{\partial a_i^2}\right)^{-1}\frac{\partial^2 U}{\partial a_k \partial a_i} \qquad \forall\, k \neq i \tag{6.57}$$

Proof. Based on corollary 6.5.0.3, consider the VF (6.50) and let the dependent *local* field a_i be a stationary solution, then the first variation with respect to a_i is given by

$$\delta_{a_i}\Pi = \int_{\Omega_h}\frac{\partial \pi}{\partial a_i}\delta a_i dV \equiv 0 \tag{6.58}$$

a further variation with respect the independent also *local* field a_k leads to

$$\delta_{a_k}\big(\delta_{a_i}\big)\Pi = \int_{\Omega_h}\left[\left(\frac{\partial^2 \pi}{\partial a_i^2}\frac{\partial a_i}{\partial a_k} + \frac{\partial^2 \pi}{\partial a_k \partial a_i}\right)\delta a_i \delta a_k\right] dV \equiv 0 \tag{6.59}$$

solving for the partial derivative between the fields a_i and a_k and using the partial derivatives defined in (6.51a) we get

$$\frac{\partial^2 \pi}{\partial a_i^2}\frac{\partial a_i}{\partial a_k} + \frac{\partial^2 \pi}{\partial a_k \partial a_i} = 0 \qquad \Longleftrightarrow \qquad \begin{aligned}\frac{\partial a_i}{\partial a_k} &= -\left(\frac{\partial^2 \pi}{\partial a_i^2}\right)^{-1}\frac{\partial^2 \pi}{\partial a_k^* \partial a_i} \\ &= -\left(\frac{\partial^2 U}{\partial a_i^2}\right)^{-1}\frac{\partial^2 U}{\partial a_k \partial a_i}\end{aligned} \tag{6.60a}$$

since U is smooth enough and piece-wise continuous the partial relation is *well-defined* $\forall\, k \neq i$. ■

Lemma 6.5.2 (Partial relations $a_i(a_k^*)$)**.** *A split variational form* (6.55) *via the explicit dependence $a_i(a_k^*)$ has the following partial relation*

$$\begin{cases} \frac{\partial a_i}{\partial a_i^*} = \left(\frac{\partial^2 U}{\partial a_i^2}\right)^{-1} & \\ \frac{\partial a_i}{\partial a_k^*} = 0 & \forall\, i \neq k \\ \frac{\partial a_i}{\partial A_k^*} = 0 & \forall k \end{cases} \tag{6.61}$$

Proof. Based on corollary 6.5.0.3, consider the VF (6.50) and let the dependent *local* field a_i be a stationary solution, then the first variation with respect to a_i is given by

$$\delta_{a_i}\Pi = \int_{\Omega_h} \frac{\partial \pi}{\partial a_i}\delta a_i dV \equiv 0 \tag{6.62}$$

a further variation with respect the independent *global* field a_k^* leads to

$$\delta_{a_k^*}(\delta_{a_i})\Pi = \int_{\Omega_h} \left[\left(\frac{\partial^2 \pi}{\partial a_i^2}\frac{\partial a_i}{\partial a_k^*} + \frac{\partial^2 \pi}{\partial a_k^* \partial a_i} \right) \delta a_i \delta a_k^* - \left(\frac{\partial^2 \pi}{\partial a_i^2}\frac{\partial a_i}{\partial A_k^*} + \frac{\partial^2 \pi}{\partial A_k^* \partial a_i} \right) \delta a_i \nabla \delta a_k^* \right] dV \equiv 0 \tag{6.63}$$

solving for the partial relation $\partial_{a_k^*} a_i$ and $\partial_{A_k^*} a_i$ and given the variations are arbitrary we must satisfy

$$\frac{\partial^2 \pi}{\partial a_i^2}\frac{\partial a_i}{\partial a_k^*} + \frac{\partial^2 \pi}{\partial a_k^* \partial a_i} = 0 \qquad \rightarrow \qquad \frac{\partial a_i}{\partial a_k^*} = -\left(\frac{\partial^2 \pi}{\partial a_i^2} \right)^{-1} \frac{\partial^2 \pi}{\partial a_k^* \partial a_i} \tag{6.64a}$$

$$\frac{\partial^2 \pi}{\partial a_i^2}\frac{\partial a_i}{\partial A_k^*} + \frac{\partial^2 \pi}{\partial A_k^* \partial a_i} = 0 \qquad \rightarrow \qquad \frac{\partial a_i}{\partial A_k^*} = \left(\frac{\partial^2 \pi}{\partial a_i^2} \right)^{-1} \left(-\frac{\partial^2 \pi}{\partial A_k^* \partial a_i} \right) \tag{6.64b}$$

Substituting the partial relations (6.51) we arrive to the expressions in (6.61) ■

Lemma 6.5.3 (Partial relations $a_i^*(a_k^*)$)**.** *A split variational form* (6.55) *via the explicit dependence* $a_i^*(a_k^*)$ *imposes only* global *restrictions, i.e., over* A_i^**. Therefore, this dependence leads to the following partial relations*

$$\begin{cases} \frac{\partial A_i^*}{\partial A_k^*} = \left(\frac{\partial^2 \chi}{\partial A_i^* \partial A_i^*} \right)^{-1} \left(-\frac{\partial^2 \chi}{\partial A_k^* \partial A_i^*} \right) & \forall\, k \neq i \\ \frac{\partial A_i^*}{\partial a_k^*} = 0 & \forall\, k \neq i \end{cases} \tag{6.65}$$

where no local conditions are imposed, in essence, $\partial_{a_k^*} a_i^*$*,* $\partial_{A_k^*} a_i^*$ *are not determined.*

Proof. Based on corollary 6.5.0.3, consider the VF (6.50) and let the dependent *global* field a_i^* be a stationary solution, then the first variation with respect to a_i^* is given by

$$\delta_{a_i^*}\Pi = \int_{\Omega_h} \left(\frac{\partial \pi}{\partial a_i^*}\delta a_i^* - \frac{\partial \pi}{\partial A_i^*}\delta \nabla a_i^* \right) dV \equiv 0 \tag{6.66}$$

a further variation now with respect to a_k^* leads to

$$\begin{aligned} \delta_{a_k^*}(\delta_{a_i}^*)\Pi = \int_{\Omega_h} \Bigg[& \left(\cancelto{0}{\frac{\partial^2 \pi}{\partial a_k^* \partial a_i^*}} + \cancelto{0}{\frac{\partial^2 \pi}{\partial a_i^* \partial a_i^*}}\frac{\partial a_i^*}{\partial a_k^*} + \cancelto{0}{\frac{\partial^2 \pi}{\partial A_i^* \partial a_i^*}}\frac{\partial A_i^*}{\partial a_k^*} \right) \delta a_i^* \delta a_k^* \\ & - \left(\cancelto{0}{\frac{\partial^2 \pi}{\partial A_k^* \partial a_i^*}} + \cancelto{0}{\frac{\partial^2 \pi}{\partial a_i^* \partial a_i^*}}\frac{\partial a_i^*}{\partial A_k^*} + \cancelto{0}{\frac{\partial^2 \pi}{\partial A_i^* \partial a_i^*}}\frac{\partial A_i^*}{\partial A_k^*} \right) \delta a_i^* \delta \nabla a_k^* \\ & - \left(\cancelto{0}{\frac{\partial^2 \pi}{\partial a_k^* \partial A_i^*}} + \cancelto{0}{\frac{\partial^2 \pi}{\partial a_i^* \partial A_i^*}}\frac{\partial a_i^*}{\partial a_k^*} + \frac{\partial^2 \pi}{\partial A_i^* \partial A_i^*}\frac{\partial A_i^*}{\partial a_k^*} \right) \delta \nabla a_i^* \delta a_k^* \\ & + \left(\frac{\partial^2 \pi}{\partial A_k^* \partial A_i^*} + \cancelto{0}{\frac{\partial^2 \pi}{\partial a_i^* \partial A_i^*}}\frac{\partial a_i^*}{\partial A_k^*} + \frac{\partial^2 \pi}{\partial A_i^* \partial A_i^*}\frac{\partial A_i^*}{\partial A_k^*} \right) \delta \nabla a_i^* \delta \nabla a_k^* \Bigg] dV \equiv 0 \end{aligned} \tag{6.67}$$

canceling out the partial relations equal to zero (6.51) imposes no conditions on $\partial_{a_k^*} a_i^*$ $\partial_{A_k^*} a_i^*$ while the following conditions must be satisfied

$$\frac{\partial^2 \pi}{\partial A_k^* \partial A_i^*} + \frac{\partial^2 \pi}{\partial A_i^* \partial A_i^*} \frac{\partial A_i^*}{\partial A_k^*} = 0 \qquad \Longleftrightarrow \qquad \frac{\partial A_i^*}{\partial A_k^*} = \left(\frac{\partial^2 \pi}{\partial A_i^* \partial A_i^*} \right)^{-1} \left(-\frac{\partial^2 \pi}{\partial A_k^* \partial A_i^*} \right) \tag{6.68}$$

$$\frac{\partial^2 \pi}{\partial A_i^* \partial A_i^*} \frac{\partial A_i^*}{\partial a_k^*} = 0 \qquad \Longleftrightarrow \qquad \frac{\partial A_i^*}{\partial a_k^*} = 0 \tag{6.69}$$

arriving thus to (6.65). ■

Corollary 6.5.3.1. *Let $\{\alpha\}$ and $\{\beta\}$ represent the set of corrections terms from two iterative-blocks and $\hat{\Delta} x$ the set of total correction terms in a VF as in* (6.54)*. As long as $\{\alpha\} \cap \{\beta\} = \emptyset$ and $\{\alpha\} \cup \{\beta\} = \hat{\Delta} x$ a split variational form of two iterative-blocks is well-defined.*

Proof. Using lemmas 6.5.1, 6.5.2 or 6.5.3 the proof follows immediately. ■

6.5.2 Transparency relations

Lemma 6.5.4 (Well-defined first variations)**.** *A variational form* (6.55) *split into two iterative-blocks, where the block with least hierarchy contains only the element a_i and the split is done using the arbitrary explicit dependencies $a_i(\mathbf{a}_k, \mathbf{a}_j^*)$ $\forall k \neq i$ and $\forall j$ has* well-defined *first variations in each iterative block.*

Proof. Consider the functional $\Pi[\mathbf{a}_i, \mathbf{a}_i^*]$ of a VF like (6.55). Under the imposition of arbitrary explicit dependencies $a_i(\mathbf{a}_k, \mathbf{a}_j^*)$ with $k \neq i$ the functional becomes $\Pi[\mathbf{a}_k, \mathbf{a}_k^*, a_i(\mathbf{a}_k, \mathbf{a}_j^*)]$. Thus, the first variations of the functional are given by

$[\alpha]$ **block :**

$$\delta_{a_k} \Pi = \int_{\Omega_h} \left(\frac{\partial \pi}{\partial a_k} + \frac{\partial \pi}{\partial a_i} \frac{\partial a_i}{\partial a_k} \right) \delta a_k dV \qquad \forall \quad k \neq i \tag{6.70a}$$

$$\delta_{a_j^*} \Pi = \int_{\Omega_h} \left[\left(\frac{\partial \pi}{\partial a_j^*} + \frac{\partial \pi}{\partial a_i} \frac{\partial a_i}{\partial a_j^*} \right) \delta a_j^* - \left(\frac{\partial \pi}{\partial A_j^*} + \frac{\partial \pi}{\partial a_i} \frac{\partial a_i}{\partial A_j^*} \right) \delta \nabla a_j^* \right] dV \qquad \forall \quad j \tag{6.70b}$$

$[\beta]$ **block :**

$$\delta_{a_i} \Pi = \int_{\Omega_h} \left(\frac{\partial \pi}{\partial a_i} \delta a_i \right) dV \tag{6.70c}$$

given the functional's integrand π is piece-wise continuous and smooth enough. All the partial derivatives of π from the first variations are well defined. Moreover, as consequence of lemmas 6.5.1 & 6.5.2 the partial relations between fields are well defined. Therefore, the first variations in each iterative block are *well-defined* in each iterative block under the arbitrary imposed explicit dependency $a_i(\mathbf{a}_k, \mathbf{a}_j^*)$. ■

Corollary 6.5.4.1 (Split VF residuals)**.** *The residuals of a split variational form via arbitrary explicit dependencies $a_i^*(\mathbf{a}_j, \mathbf{a}_k^*)$ $\forall k \neq i$ and $\forall j$ are given by*

[α] **block :**

$$\delta_{a_k}\Pi = \int_{\Omega_h} \left(\frac{\partial \pi}{\partial a_k} + \frac{\partial \pi}{\partial a_i}\frac{\partial a_i}{\partial a_k} \right) \delta a_k dV \qquad \forall \quad k \neq i \tag{6.71a}$$

$$\delta_{a_j^*}\Pi = \int_{\Omega_h} \left[\frac{\partial \pi}{\partial a_j^*}\delta a_j^* - \left(\frac{\partial \pi}{\partial A_j^*} + \frac{\partial \pi}{\partial a_i}\frac{\partial a_i}{\partial A_j^*} \right) \delta \nabla a_j^* \right] dV \qquad \forall \quad j \neq i \tag{6.71b}$$

$$\delta_{a_i^*}\Pi = \int_{\Omega_h} \left[\left(\frac{\partial \pi}{\partial a_i^*} + \frac{\partial \pi}{\partial a_i}\frac{\partial a_i}{\partial a_i^*} \right) \delta a_i^* - \left(\frac{\partial \pi}{\partial A_i^*} + \frac{\partial \pi}{\partial a_i}\frac{\partial a_i}{\partial A_i^*} \right) \delta \nabla a_i^* \right] dV \tag{6.71c}$$

[β] **block :**

$$\delta_{a_i}\Pi = \int_{\Omega_h} \left(\frac{\partial \pi}{\partial a_i}\delta a_i \right) dV \tag{6.71d}$$

for variations defined by smooth and piece-wise continuous functions.

Proof. Using lemma 6.5.4, equations (6.70) are reduced to (6.71) by means of lemmas 6.60a & 6.61. Since we imposed variations defined by smooth and piece-wise continuous functions the residuals are well-defined. ■

Lemma 6.5.5 (Well-defined Hessian)**.** *A variational form* (6.55) *split into two iterative-blocks, where the block with least hierarchy contains only the element a_i and the split is done using the arbitrary explicit dependencies $a_i(\mathbf{a}_k, \mathbf{a}_j^*)$ $\forall k \neq i$ and $\forall j$ has* well-defined *second variations in each iterative block.*

Proof. Consider the functional $\Pi[\mathbf{a}_i, \mathbf{a}_i^*]$ of a VF like (6.55). Under the imposition of arbitrary explicit dependencies $a_i(\mathbf{a}_k, \mathbf{a}_j^*)$ with $k \neq i$ the functional becomes $\Pi[\mathbf{a}_k, \mathbf{a}_k^*, a_i(\mathbf{a}_k, \mathbf{a}_j^*)]$. Thus, using the results from (6.70) the second variations of the functional are given by

[α] **block :**

$$\begin{aligned}\delta_{a_k a_l}\Pi = \int_{\Omega_h} \Bigg[\Bigg(& \frac{\partial^2 \pi}{\partial a_l \partial a_k} + \frac{\partial^2 \pi}{\partial a_l \partial a_i}\frac{\partial a_i}{\partial a_k} \\ & + \frac{\partial^2 \pi}{\partial a_i \partial a_k}\frac{\partial a_i}{\partial a_l} + \frac{\partial^2 \pi}{\partial a_i \partial a_i}\frac{\partial a_i}{\partial a_k}\frac{\partial a_i}{\partial a_l} \Bigg) \delta a_k \delta a_l \Bigg] dV \end{aligned} \qquad \forall \quad k,l \neq i \tag{6.72a}$$

$$\begin{aligned}\delta_{a_j^* a_m^*}\Pi = \int_{\Omega_h} \Bigg[& \left(\frac{\partial^2 \pi}{\partial a_m^* \partial a_j^*} + \frac{\partial^2 \pi}{\partial a_m^* \partial a_i}\frac{\partial a_i}{\partial a_j^*} + \frac{\partial^2 \pi}{\partial a_i \partial a_j^*}\frac{\partial a_i}{\partial a_m^*} + \frac{\partial^2 \pi}{\partial a_i \partial a_i}\frac{\partial a_i}{\partial a_j^*}\frac{\partial a_i}{\partial a_m^*} \right) \delta a_j^* \delta a_m^* \\ & - \left(\frac{\partial^2 \pi}{\partial a_m^* \partial A_j^*} + \frac{\partial^2 \pi}{\partial a_m^* \partial a_i}\frac{\partial a_i}{\partial A_j^*} + \frac{\partial^2 \pi}{\partial a_i \partial A_j^*}\frac{\partial a_i}{\partial a_m^*} + \frac{\partial^2 \pi}{\partial a_i \partial a_i}\frac{\partial a_i}{\partial A_j^*}\frac{\partial a_i}{\partial a_m^*} \right) \delta \nabla a_j^* \delta a_m^* \\ & - \left(\frac{\partial^2 \pi}{\partial A_m^* \partial a_j^*} + \frac{\partial^2 \pi}{\partial A_m^* \partial a_i}\frac{\partial a_i}{\partial a_j^*} + \frac{\partial^2 \pi}{\partial a_i \partial a_j^*}\frac{\partial a_i}{\partial A_m^*} + \frac{\partial^2 \pi}{\partial a_i \partial a_i}\frac{\partial a_i}{\partial a_j^*}\frac{\partial a_i}{\partial A_m^*} \right) \delta a_j^* \delta \nabla a_m^* \\ & + \left(\frac{\partial^2 \pi}{\partial A_m^* \partial A_j^*} + \frac{\partial^2 \pi}{\partial A_m^* \partial a_i}\frac{\partial a_i}{\partial A_j^*} + \frac{\partial^2 \pi}{\partial a_i \partial A_j^*}\frac{\partial a_i}{\partial A_m^*} + \frac{\partial^2 \pi}{\partial a_i \partial a_i}\frac{\partial a_i}{\partial A_j^*}\frac{\partial a_i}{\partial A_m^*} \right) \delta \nabla a_j^* \delta \nabla a_m^* \Bigg] dV \end{aligned} \qquad \forall \quad j,m \tag{6.72b}$$

$$\delta_{a_j^* a_l}\Pi = \int_{\Omega_h} \left[\left(\frac{\partial^2 \pi}{\partial a_l \partial a_j^*} + \frac{\partial^2 \pi}{\partial a_l \partial a_i}\frac{\partial a_i}{\partial a_j^*} + \frac{\partial^2 \pi}{\partial a_i \partial a_j^*}\frac{\partial a_i}{\partial a_l} + \frac{\partial^2 \pi}{\partial a_i \partial a_i}\frac{\partial a_i}{\partial a_j^*}\frac{\partial a_i}{\partial a_l} \right) \delta a_j^* \delta a_l \right.$$
$$\left. - \left(\frac{\partial^2 \pi}{\partial a_l \partial A_j^*} + \frac{\partial^2 \pi}{\partial a_l \partial a_i}\frac{\partial a_i}{\partial A_j^*} + \frac{\partial^2 \pi}{\partial a_i \partial A_j^*}\frac{\partial a_i}{\partial a_l} + \frac{\partial^2 \pi}{\partial a_i \partial a_i}\frac{\partial a_i}{\partial A_j^*}\frac{\partial a_i}{\partial a_l} \right) \delta \nabla a_j^* \delta a_l \right] dV \quad \forall\, l \quad \& \quad \forall\, j \neq i \tag{6.72c}$$

$$\delta_{a_k a_m^*}\Pi = \int_{\Omega_h} \left[\left(\frac{\partial^2 \pi}{\partial a_m^* \partial a_k} + \frac{\partial^2 \pi}{\partial a_i \partial a_k}\frac{\partial a_i}{\partial a_m^*} + \frac{\partial^2 \pi}{\partial a_m^* \partial a_i}\frac{\partial a_i}{\partial a_k} + \frac{\partial^2 \pi}{\partial a_i \partial a_i}\frac{\partial a_i}{\partial a_k}\frac{\partial a_i}{\partial a_m^*} \right) \delta a_m^* \delta a_k \right.$$
$$\left. - \left(\frac{\partial^2 \pi}{\partial A_m^* \partial a_k} + \frac{\partial^2 \pi}{\partial a_i \partial a_k}\frac{\partial a_i}{\partial A_m^*} + \frac{\partial^2 \pi}{\partial A_m^* \partial a_i}\frac{\partial a_i}{\partial a_k} + \frac{\partial^2 \pi}{\partial a_i \partial a_i}\frac{\partial a_i}{\partial a_k}\frac{\partial a_i}{\partial A_m^*} \right) \delta a_k \delta \nabla a_m^* \right] dV \quad \forall\, m \;\&\; \forall\, k \neq i \tag{6.72d}$$

$[\beta]$ **block :**

$$\delta_{a_i a_i}\Pi = \int_{\Omega_h} \left(\frac{\partial^2 \pi}{\partial a_i \partial a_i} \right) \delta a_i \delta a_i dV \tag{6.72e}$$

given the functional's integrand π is piece-wise continuous and smooth enough. All the second order partial derivatives of π and partial relations between fields are well-defined due to lemmas 6.5.1 & 6.5.2. Therefore, the second order variations are *well-defined* in each iterative-block under the arbitrary imposed explicit dependency $a_i(\mathbf{a}_k, \mathbf{a}_j^*)$.. ■

Corollary 6.5.5.1 (Split VF tangents)**.** *The tangents of a split variational form via arbitrary explicit dependencies* $a_i^*(\mathbf{a}_j, \mathbf{a}_k^*)$ $\forall k \neq i$ *and* $\forall \quad j \neq i, m \neq i, k \neq i$ *are given by*

$[\alpha]$ **block :**

$$\delta_{a_k a_l}\Pi = \int_{\Omega_h} \left[\left(\frac{\partial^2 \pi}{\partial a_l \partial a_k} + \frac{\partial^2 \pi}{\partial a_i \partial a_l}\frac{\partial a_i}{\partial a_k} \right.\right.$$
$$\left.\left. + \frac{\partial^2 \pi}{\partial a_i \partial a_k}\frac{\partial a_i}{\partial a_l} + \frac{\partial^2 \pi}{\partial a_i \partial a_i}\frac{\partial a_i}{\partial a_k}\frac{\partial a_i}{\partial a_l} \right) \delta a_k \delta a_l \right] dV \tag{6.73a}$$

$$\delta_{a_j^* a_m^*}\Pi = \int_{\Omega_h} \left[\left(\frac{\partial^2 \pi}{\partial a_m^* \partial a_j^*} \right) \delta a_j^* \delta a_m^* - \left(\frac{\partial^2 \pi}{\partial a_m^* \partial A_j^*} \right) \delta \nabla a_j^* \delta a_m^* \right.$$
$$\left. - \left(\frac{\partial^2 \pi}{\partial A_m^* \partial a_j^*} \right) \delta a_j^* \delta \nabla a_m^* + \left(\frac{\partial^2 \pi}{\partial A_m^* \partial A_j^*} \right) \delta \nabla a_j^* \delta \nabla a_m^* \right] dV \tag{6.73b}$$

$$\delta_{a_j^* a_i^*}\Pi = \int_{\Omega_h} \left[\left(\frac{\partial^2 \pi}{\partial a_i^* \partial a_j^*} \right) \delta a_j^* \delta a_i^* - \left(\frac{\partial^2 \pi}{\partial a_i^* \partial A_j^*} + \frac{\partial^2 \pi}{\partial a_i^* \partial a_i}\frac{\partial a_i}{\partial A_j^*} + \frac{\partial^2 \pi}{\partial a_i \partial a_i}\frac{\partial a_i}{\partial A_j^*}\frac{\partial a_i}{\partial a_i^*} \right) \delta \nabla a_j^* \delta a_i^* \right.$$
$$\left. - \left(\frac{\partial^2 \pi}{\partial A_i^* \partial a_j^*} \right) \delta a_j^* \delta \nabla a_i^* + \left(\frac{\partial^2 \pi}{\partial A_i^* \partial A_j^*} + \frac{\partial^2 \pi}{\partial a_i \partial a_i}\frac{\partial a_i}{\partial A_j^*}\frac{\partial a_i}{\partial A_i^*} \right) \delta \nabla a_j^* \delta \nabla a_i^* \right] dV \tag{6.73c}$$

$$\delta_{a_i^* a_m^*}\Pi = \int_{\Omega_h}\left[\left(\frac{\partial^2\pi}{\partial a_m^*\partial a_i^*}\right)\delta a_i^*\delta a_m^* - \left(\frac{\partial^2\pi}{\partial A_m^*\partial a_i^*} + \frac{\partial^2\pi}{\partial a_i\partial a_i^*}\frac{\partial a_i}{\partial A_m^*} + \frac{\partial^2\pi}{\partial a_i\partial a_i}\frac{\partial a_i}{\partial a_i^*}\frac{\partial a_i}{\partial A_m^*}\right)\delta a_i^*\delta\nabla a_m^* - \left(\frac{\partial^2\pi}{\partial a_m^*\partial A_i^*}\right)\delta\nabla a_i^*\delta a_m^* + \left(\frac{\partial^2\pi}{\partial A_m^*\partial A_i^*} + \frac{\partial^2\pi}{\partial a_i\partial a_i}\frac{\partial a_i}{\partial A_i^*}\frac{\partial a_i}{\partial A_m^*}\right)\delta\nabla a_i^*\delta\nabla a_m^*\right]dV \tag{6.73d}$$

$$\begin{aligned}\delta_{a_i^* a_i^*}\Pi = \int_{\Omega_h}\Bigg[&\left(\frac{\partial^2\pi}{\partial a_i^*\partial a_i^*} + \frac{\partial^2\pi}{\partial a_i^*\partial a_i}\frac{\partial a_i}{\partial a_i^*} + \frac{\partial^2\pi}{\partial a_i\partial a_i^*}\frac{\partial a_i}{\partial a_i^*} + \frac{\partial^2\pi}{\partial a_i\partial a_i}\frac{\partial a_i}{\partial a_i^*}\frac{\partial a_i}{\partial a_i^*}\right)\delta a_i^*\delta a_i^* \\ &- \left(\frac{\partial^2\pi}{\partial a_i^*\partial A_i^*} + \frac{\partial^2\pi}{\partial a_i^*\partial a_i}\frac{\partial a_i}{\partial A_i^*} + \frac{\partial^2\pi}{\partial a_i\partial a_i}\frac{\partial a_i}{\partial A_i^*}\frac{\partial a_i}{\partial a_i^*}\right)\delta\nabla a_i^*\delta a_i^* \\ &- \left(\frac{\partial^2\pi}{\partial A_i^*\partial a_i^*} + \frac{\partial^2\pi}{\partial a_i\partial a_i^*}\frac{\partial a_i}{\partial A_i^*} + \frac{\partial^2\pi}{\partial a_i\partial a_i}\frac{\partial a_i}{\partial a_i^*}\frac{\partial a_i}{\partial A_i^*}\right)\delta a_i^*\delta\nabla a_i^* \\ &+ \left(\frac{\partial^2\pi}{\partial A_i^*\partial A_i^*} + \frac{\partial^2\pi}{\partial a_i\partial a_i}\frac{\partial a_i}{\partial A_i^*}\frac{\partial a_i}{\partial A_i^*}\right)\delta\nabla a_i^*\delta\nabla a_i^*\Bigg]dV\end{aligned} \tag{6.73e}$$

$$\delta_{a_j^* a_l}\Pi = \int_{\Omega_h}\left[\left(\frac{\partial^2\pi}{\partial a_l\partial a_j^*} + \frac{\partial^2\pi}{\partial a_i\partial a_j^*}\frac{\partial a_i}{\partial a_l}\right)\delta a_j^*\delta a_k - \left(\frac{\partial^2\pi}{\partial a_l\partial a_i}\frac{\partial a_i}{\partial A_j^*} + \frac{\partial^2\pi}{\partial a_i\partial a_i}\frac{\partial a_i}{\partial A_j^*}\frac{\partial a_i}{\partial a_l}\right)\delta\nabla a_j^*\delta a_l\right]dV \tag{6.73f}$$

$$\delta_{a_i^* a_l}\Pi = \int_{\Omega_h}\left[\left(\frac{\partial^2\pi}{\partial a_l\partial a_i^*} + \frac{\partial^2\pi}{\partial a_l\partial a_i}\frac{\partial a_i}{\partial a_i^*} + \frac{\partial^2\pi}{\partial a_i\partial a_i^*}\frac{\partial a_i}{\partial a_l} + \frac{\partial^2\pi}{\partial a_i\partial a_i}\frac{\partial a_i}{\partial a_i^*}\frac{\partial a_i}{\partial a_l}\right)\delta a_i^*\delta a_l - \left(\frac{\partial^2\pi}{\partial a_l\partial a_i}\frac{\partial a_i}{\partial A_i^*} + \frac{\partial^2\pi}{\partial a_i\partial a_i}\frac{\partial a_i}{\partial A_i^*}\frac{\partial a_i}{\partial a_l}\right)\delta\nabla a_i^*\delta a_l\right]dV \tag{6.73g}$$

$$\delta_{a_k a_m^*}\Pi = \int_{\Omega_h}\left[\left(\frac{\partial^2\pi}{\partial a_m^*\partial a_k} + \frac{\partial^2\pi}{\partial a_m^*\partial a_i}\frac{\partial a_i}{\partial a_k}\right)\delta a_m^*\delta a_k - \left(\frac{\partial^2\pi}{\partial a_i\partial a_k}\frac{\partial a_i}{\partial A_m^*} + \frac{\partial^2\pi}{\partial a_i\partial a_i}\frac{\partial a_i}{\partial a_k}\frac{\partial a_i}{\partial A_m^*}\right)\delta a_k\delta\nabla a_m^*\right]dV \tag{6.73h}$$

$$\delta_{a_k a_i^*}\Pi = \int_{\Omega_h}\left[\left(\frac{\partial^2\pi}{\partial a_i^*\partial a_k} + \frac{\partial^2\pi}{\partial a_i\partial a_k}\frac{\partial a_i}{\partial a_i^*} + \frac{\partial^2\pi}{\partial a_i^*\partial a_i}\frac{\partial a_i}{\partial a_k} + \frac{\partial^2\pi}{\partial a_i\partial a_i}\frac{\partial a_i}{\partial a_k}\frac{\partial a_i}{\partial a_i^*}\right)\delta a_i^*\delta a_k - \left(\frac{\partial^2\pi}{\partial a_i\partial a_k}\frac{\partial a_i}{\partial A_i^*} + \frac{\partial^2\pi}{\partial a_i\partial a_i}\frac{\partial a_i}{\partial a_k}\frac{\partial a_i}{\partial A_i^*}\right)\delta a_k\delta\nabla a_i^*\right]dV \tag{6.73i}$$

[β] **block :**

$$\delta_{a_i a_i}\Pi = \int_{\Omega_h}\left(\frac{\partial^2\pi}{\partial a_i\partial a_i}\right)\delta a_i\delta a_i dV \tag{6.73j}$$

for variations defined by smooth and piece-wise continuous functions.

Proof. Using lemma 6.5.4, equations (6.70) are reduced to (6.71) by means of lemmas 6.60a & 6.61. Since we imposed variations defined by smooth and piece-wise continuous functions the residuals are well-defined. ■

Corollary 6.5.5.2 (Two-block transparency relation $a_i(\mathbf{a}_k, \mathbf{a}_j^*)$)**.** *A split VF* (6.55) *via explicit dependencies of the form* $a_i(\mathbf{a}_k, \mathbf{a}_j^*)$ *with* $k \neq i$ *can be represented by the two block transparency-relation*

$$\begin{bmatrix} \mathbb{T}^{[\ \alpha_i]} & \mathbb{O} \\ \mathbb{O} & \mathbb{T}^{[\ i\beta_j]} \end{bmatrix} \begin{bmatrix} \hat{\Delta}x^{[\ \alpha_i]} \\ \hat{\Delta}x^{[\ i\beta_j]} \end{bmatrix} = - \begin{bmatrix} \mathbb{R}^{[\ \alpha_i]} \\ \mathbb{R}^{[\ i\beta_j]} \end{bmatrix} \tag{6.74}$$

Proof. The former follows immediately from corollaries 6.5.3.1, 6.5.4.1 and 6.5.5.1. ■

Corollary 6.5.5.3 (ϑ-block transparency relation $a_i(\mathbf{a}_k, \mathbf{a}_j^*)$)**.** *A split VF* (6.55) *via explicit dependencies of the form* $a_i(\mathbf{a}_k, \mathbf{a}_j^*)$ *with* $k \neq i$ *can be represented by the* ϑ *blocks through the following transparency relation.*

$$\begin{bmatrix} \mathbb{T}^{[\ \alpha_i]} & \mathbb{O} & \mathbb{O} & \cdots & \mathbb{O} \\ \mathbb{O} & \mathbb{T}^{[\ i\beta_j]} & \mathbb{O} & \vdots & \vdots \\ \mathbb{O} & \mathbb{O} & \mathbb{T}^{[\ i\beta_j]} & \ddots & \vdots \\ \vdots & \vdots & \ddots & \ddots & \mathbb{O} \\ \mathbb{O} & \mathbb{O} & \cdots & \mathbb{O} & \mathbb{T}^{[\ ij\ldots\vartheta_t]} \end{bmatrix} \begin{bmatrix} \hat{\Delta}x^{[\ \alpha_i]} \\ \hat{\Delta}x^{[\ i\beta_j]} \\ \vdots \\ \vdots \\ \hat{\Delta}x^{[\ ij\ldots\vartheta_t]} \end{bmatrix} = - \begin{bmatrix} \mathbb{R}^{[\ \alpha_i]} \\ \mathbb{R}^{[\ i\beta_j]} \\ \vdots \\ \vdots \\ \mathbb{R}^{[\ ij\ldots\vartheta_t]} \end{bmatrix} \tag{6.75}$$

Proof. We can split the VF (6.55) using lemma 6.5.5.2 into the form 6.75. Inside each iterative-block, all the fields are implicit independent from one another. Therefore, we can use in each iterative-block lemma 6.5.5.2 once again. This process can continue until we have defined ϑ iterative-blocks which can be represented through the transparency relation (6.75). ■

Corollary 6.5.5.4. *The dependent iterative-block* $[\beta]$ *from a two block split VF does not change its residual neither its diagonal block element of the tangent from the VF before the split.*

Proof. Equations (6.71d) and (6.73j) complete the proof. ■

6.5.3 Solution strategies

Theorem 6.5.6 (Staggered strategy)**.** *A* staggered strategy *can be deduced from a the Newton Method expression* (6.52) *of a discrete VF.*

Proof. From corollary 6.5.5.2 we obtain a two block transparency-relation of the VF. Let the $[\beta]$ iterative-block consist of only the element $a_i(\mathbf{a}_k, \mathbf{a}_j^*)$. The residual of such two block system for the $[\alpha]$ block has the form (6.71a). The blue terms in (6.71a) represent the extra parameters added by the arbitrary imposed explicit dependency $a_i(\mathbf{a}_k, \mathbf{a}_j^*)$. As consequence, the extra terms can be equal or different than zero. We let them to be different to zero, i.e.

Staggered conditions:

$$\frac{\partial \pi}{\partial a_i}\frac{\partial a_i}{\partial a_k} \neq 0 \qquad \forall\, k \neq i\,,\, \forall j \tag{6.76a}$$

$$\frac{\partial \pi}{\partial a_i}\frac{\partial a_i}{\partial a_k^*} \neq 0 \qquad \forall\, k \neq i\,,\, \forall j \tag{6.76b}$$

$$\frac{\partial \pi}{\partial a_i}\frac{\partial a_i}{\partial A_k^*} \neq 0 \qquad \forall\, k \neq i\,,\, \forall j \tag{6.76c}$$

This implies that independently of the partial relations of a_i the partial derivative $\partial_{a_i}\pi$ should be different to zero. But the residual of the $[\beta]$ block (6.71d) is proportional to the partial derivative $\partial_{a_i}\pi$. Therefore, for the conditions (6.76) to be satisfied, for every iteration of the α block the field a_i does not needs not to be a solution for the $[\beta]$ block. The former suggest a sequence in the iterative-blocks as that dictated by the *staggered strategy.* ■

Theorem 6.5.7 (Nested strategy)**.** *A* nested strategy *can be deduced from a the Newton Method expression* (6.52) *of a discrete VF.*

Proof. From corollary 6.5.5.2 we obtain a two block transparency-relation of the VF. Let the $[\beta]$ iterative-block consist of only the element $a_i(\mathbf{a}_k, \mathbf{a}_j^*)$. The residual of such two block system for the $[\alpha]$ block has the form (6.71a). The blue terms in (6.71a) represent the extra parameters added by the arbitrary imposed explicit dependency $a_i(\mathbf{a}_k, \mathbf{a}_j^*)$. As consequence, the extra terms can be equal or different than zero. We let them to be equal to zero, i.e.

Nested conditions:

$$\frac{\partial \pi}{\partial a_i}\frac{\partial a_i}{\partial a_k} \neq 0 \qquad \forall\, k \equiv i\,,\ \forall j \tag{6.77a}$$

$$\frac{\partial \pi}{\partial a_i}\frac{\partial a_i}{\partial a_k^*} \neq 0 \qquad \forall\, k \equiv i\,,\ \forall j \tag{6.77b}$$

$$\frac{\partial \pi}{\partial a_i}\frac{\partial a_i}{\partial A_k^*} \neq 0 \qquad \forall\, k \equiv i\,,\ \forall j \tag{6.77c}$$

This implies that independently of the partial relations of a_i the partial derivative $\partial_{a_i}\pi$ should be zero. But the residual of the $[\beta]$ block (6.71d) is proportional to the partial derivative $\partial_{a_i}\pi$. Therefore, for the conditions (6.77) to be satisfied, for every iteration of the α block the field a_i needs to be a solution for the $[\beta]$ block. The former suggest a sequence in the iterative-blocks as that dictated by the *nested strategy.* ■

6.5.4 Newton method variations

Nested strategy → Quasi Newton method : In general, we can say the independent iterative-block $[\alpha]$ from a two block split VF solved through a *nested strategy* is a block-diagonal *Quasi-Newton method* of the original VF before the split. A Quasi-Newton method J. E. Dennis and Moré [1977] solves the system

$$\mathbf{B}\hat{\Delta}x = -\mathbf{R} \tag{6.78}$$

where $\mathbf{B}$ is an approximation of the original Hessian matrix. Different techniques to approximate $\mathbf{B}$ are considered to constituted the family of *Quasi-Newton methods.* The system solved by a *nested strategy* by its independent iterative-block $[\alpha]$ solves the original system in the form (6.78). Therefore, the iterative-block $[\alpha]$ belongs to the family of *Quasi-Newton methods* considering the solution of the original block-diagonal form of VF.

Staggered → Inexact Newton method: In a similar fashion, the independent iterative-block $[\alpha]$ from a two block split VF solved through a *staggered strategy* is the block-diagonal *Inexact Newton method* of the VF before the split. An Inexact Newton method Dembo et al. [1982] solves the system

$$\mathbf{T}\hat{\Delta}x = -\mathbf{R} + \mathbf{r} \qquad \text{such that} \qquad \frac{||\mathbf{r}||}{||\mathbf{R}||} \leq \eta \tag{6.79}$$

where η is a *forcing term*, $||\mathbf{r}||/||\mathbf{R}||$ is the *relative residual*, with $\mathbf{r}$ as an extra residual to approximate and solve the original system. The system solved by a *staggered strategy* by its independent iterative-block $[\alpha]$ solves a the system of the form (6.78) by applying a further preconditioning to the the tangent $\mathbf{T}$. Therefore, the iterative-block $[\alpha]$ belongs to the family of *Inexact-Newton methods* if we consider the original problem as the block-diagonal form of the VF corresponding to $[\alpha]$. A mix of such Inexact Newton method and a Quasi-Newton method can be observed in the literature, e.g. M. [2006].

Thus, the proposed VF can be split by explicit dependencies leading to staggered and nested strategies. The preconditioning used to do the split is physical motivated. Nevertheless, by means of the transparency-relation a mathematical formulation can be derived too. This shows a further connection between calculus and linear algebra, mainly, that the explicit added dependencies solved through a staggered strategy is equivalent to solve the system via block Gauss method on the original Newton method. In addition, with the nested strategy we introduced additive preconditioners as block-preconditioners by means of the null-space condition. All the former is possible for coupled problems, since the key ideas depend only on the shape of the functional we optimize, functional which we defined in a general form in §4.

6.6 Numerical example: Electrolyte

Before concluding the chapter we solve the same problem we presented in §5.6.2.2 where a discontinuity between initial and boundary conditions is imposed in chemical and electrical variables. The difference being, we use now a *staggered strategy.*

6.6.1 Staggered Strategy

The staggered strategy we present has been derived by considering the following algorithmic dependence: $\mu, c(\mu), \phi(\mu)$. This means, we split the original monolithic system in two blocks. The α-block with the highest hierarchy will solve for the chemical potential μ while the β-block solves for the concentration c and the electric potential ϕ. Besides the algorithmic difference between strategies, the main in the equations occurs at the α-block due to the algorithmic dependencies. To simplify the equations below, we discard the variations between fields leading to zero.

$$\mathbb{R}_{\mu}^{[\alpha](a)} = \underbrace{\int_{\Omega} \frac{\partial \Pi}{\partial \mu}\frac{\partial \mu}{\partial \mu^{(a)}} + \frac{\partial \Pi}{\partial \vec{g}}\frac{\partial \vec{g}}{\partial \vec{g}^{(a)}} dV}_{\mathbb{R}_{\mu}^{(a)}} + \underbrace{\int_{\Omega} \frac{\partial \Pi}{\partial c}\frac{\partial c}{\partial \mu}\frac{\partial \mu}{\partial \mu^{(a)}} dV}_{\mathbb{S}^{(a)}\left(\frac{\partial \Pi}{\partial c}\frac{\partial c}{\partial \mu}\right)} + \underbrace{\int_{\Omega} \frac{\partial \Pi}{\partial \vec{E}}\frac{\partial \vec{E}}{\partial \vec{g}}\frac{\partial \vec{g}}{\partial \mu^{(a)}} dV}_{\nabla\mathbb{S}^{(a)}\left(\frac{\partial \Pi}{\partial \vec{E}}\frac{\partial \vec{E}}{\partial \vec{g}}\right)} \tag{6.80}$$

where $\mathbb{R}_{\mu}^{(a)}$ is the original residual shown in (5.86) and the other terms under the braces are the expressions using the notation introduced in (2.24) and (2.25). The modified tangent is given by

$$\begin{aligned}\mathbb{T}_{\mu\mu}^{[\alpha](a,b)} = &\underbrace{\int_{\Omega} \frac{\partial^2 \Pi}{\partial \mu^2}\frac{\partial \mu}{\partial \mu^{(a)}}\frac{\partial \mu}{\partial \mu^{(b)}} + \frac{\partial^2 \Pi}{\partial \vec{g}^2}\frac{\partial \vec{g}}{\partial \vec{g}^{(a)}}\frac{\partial \vec{g}}{\partial \vec{g}^{(b)}} dV}_{\mathbb{T}_{\mu\mu}^{(a,b)}} + \underbrace{\int_{\Omega} \frac{\partial^2 \Pi}{\partial c^2}\left(\frac{\partial c}{\partial \mu}\right)^2 \frac{\partial \mu}{\partial \mu^{(a)}}\frac{\partial \mu}{\partial \mu^{(b)}} dV}_{\mathbb{M}^{(a,b)}\left(\frac{\partial^2 \Pi}{\partial c^2}\left(\frac{\partial c}{\partial \mu}\right)^2\right)} \\ &+ \underbrace{\int_{\Omega} \frac{\partial^2 \Pi}{\partial \vec{E}^2}\left(\frac{\partial \vec{E}}{\partial \vec{g}}\right)^2 \frac{\partial \vec{g}}{\partial \mu^{(a)}}\frac{\partial \vec{g}}{\partial \mu^{(b)}} dV}_{\mathbb{K}^{(a,b)}\left(\frac{\partial^2 \Pi}{\partial \vec{E}^2}\left(\frac{\partial \vec{E}}{\partial \vec{g}}\right)^2\right)}\end{aligned} \tag{6.81}$$

Once again the block $\mathbb{T}_{\mu\mu}^{(a,b)}$ is the original tangent shown in (5.86). The next step is to derive the partial dependencies between the fields

$$\begin{aligned}\frac{\partial c}{\partial \mu} &= \frac{d}{d\mu}\left(\frac{\partial \Pi}{\partial c}\right) = \frac{d}{d\mu}\left(\int_\Omega \left(\frac{\partial U}{\partial c} - \mu\right) dV\right) \\ &= \int_\Omega \left(\frac{\partial^2 U}{\partial c^2}\frac{\partial c}{\partial \mu} - 1\right) dV \equiv 0 \qquad \rightarrow \qquad \frac{\partial c}{\partial \mu} = \left(\frac{\partial^2 U}{\partial c^2}\right)^{-1} \end{aligned} \tag{6.82a}$$

$$\begin{aligned}\frac{\partial \vec{E}}{\partial \vec{g}} &= \frac{d}{d\mu}\left(\frac{\partial \Pi}{\partial \vec{E}}\right) = \frac{d}{d\mu}\left(\int_\Omega \left(-\Delta t \frac{\partial \chi}{\partial \vec{E}}\right) dV\right) \\ &= \int_\Omega \left(-\Delta t \frac{\partial^2 \chi}{\partial \vec{E}^2}\frac{\partial \vec{E}}{\partial \vec{g}} - \Delta t \frac{\partial^2 \chi}{\partial \vec{g}\partial \vec{E}}\right) dV \equiv 0 \qquad \rightarrow \qquad \frac{\partial \vec{E}}{\partial \vec{g}} = -\frac{\dfrac{\partial^2 \chi}{\partial \vec{g}\partial \vec{E}}}{\dfrac{\partial^2 \chi}{\partial \vec{E}^2}} \end{aligned} \tag{6.82b}$$

where we have already substituted the functional Π from (5.85). Thus, using the results from (6.80), (6.81) and (6.82) we can write the α-block of the staggered strategy as

α-block

$$\mathbb{R}_\mu^{[\alpha](a)} = \mathbb{R}_\mu^{(a)} + \mathbb{S}^{(a)}\left(\left[\frac{\partial U}{\partial c} - \mu\right]\left(\frac{\partial^2 U}{\partial c^2}\right)^{-1}\right) + \nabla \mathbb{S}^{(a)}\left(\Delta t \frac{\partial \chi}{\partial \vec{E}}\frac{\dfrac{\partial^2 \chi}{\partial \vec{g}\partial \vec{E}}}{\dfrac{\partial^2 \chi}{\partial \vec{E}^2}}\right) \tag{6.83a}$$

$$\begin{aligned}\mathbb{T}_{\mu\mu}^{[\alpha](a,b)} = \mathbb{T}_{\mu\mu}^{(a,b)} &- \mathbb{M}^{(a,b)}\left(\left(\frac{\partial^2 U}{\partial c^2}\right)^{-1}\right) \\ &- \Delta t\, \mathbb{K}^{(a,b)}\left(\frac{\dfrac{\partial^2 \chi}{\partial \vec{g}\partial \vec{E}}\dfrac{\partial^2 \chi}{\partial \vec{E}\partial \vec{g}}}{\dfrac{\partial^2 \chi}{\partial \vec{E}^2}} - 2\frac{\left(\dfrac{\partial^2 \chi}{\partial \vec{E}\partial \vec{g}}\right)^2}{\dfrac{\partial^2 \chi}{\partial \vec{E}^2}}\right)\end{aligned} \tag{6.83b}$$

The β-block then, becomes just a subset of the original block.

β-block

$$\mathbf{R}_e = \begin{bmatrix}\mathbb{R}_c^{(a)} \\ \mathbb{R}_\phi^{(a)}\end{bmatrix} = \begin{bmatrix}\mathbb{S}_c^{(a)}\left(\frac{\partial U}{\partial c} - \mu\right) \\ \nabla \mathbb{S}_\phi^{(a)}\left(\Delta t \frac{\partial \chi}{\partial \vec{E}}\right)\end{bmatrix} \tag{6.84a}$$

$$\mathbf{T}_e = \begin{bmatrix}\mathbb{T}_{cc}^{(a,b)} & \mathbb{T}_{c\phi}^{(a,b)} \\ \mathbb{T}_{\phi c}^{(a,b)} & \mathbb{T}_{\phi\phi}^{(a,b)}\end{bmatrix} = \begin{bmatrix}\mathbb{M}_{cc}^{(a,b)}\left(\frac{\partial^2 U}{\partial c^2}\right) & \mathbb{O} \\ \mathbb{O} & -\mathbb{K}_{\phi\phi}^{(a,b)}\left(\Delta t \frac{\partial^2 \chi}{\partial \vec{E}^2}\right)\end{bmatrix} \tag{6.84b}$$

Using the strategy detailed above, and using the parameters detailed previously in Table 5.1 we arrive to the solutions of the problem depicted in Figure 6.15

If we analyze figures 5.5 and 6.15 which shows the solutions of the same problem using a monolithic and staggered strategy correspondingly, we observe differences at the first time steps as expected from the

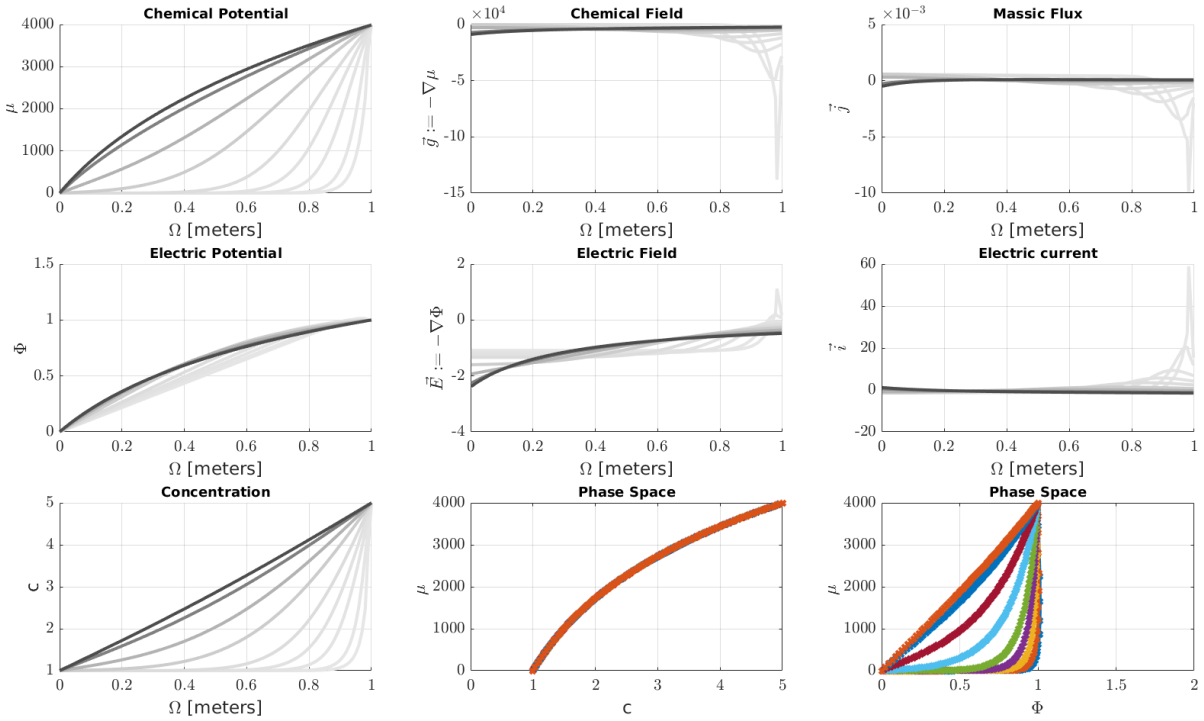

Figure 6.15: Strong bulk coupling with discontinuity between initial and boundary conditions solved using a staggered strategy

already known sensitivity to the discontinuity but also during the evolution of the variables.

In the first time steps, the staggered strategy appears to be more sensitive to the discontinuity for the non-local variables. This is observed in the figures in the first plotted time step by noticing the nodes next to the BC increase its difference with the neighboring nodes to its left or the BC in a more abrupt manner in contrast to what is shown with the solutions from the monolithic strategy. For the electric current $\vec{i}$ and the massic flux $\vec{j}$ the difference with the closest BC is almost tripled, and for the chemical field $-\nabla\mu$ and electric potential $-\nabla\phi$ is doubled. This opposes the results from the monolithic scheme, where it is the BC node the one with the highest magnitude, with the exception of $\vec{j}$, where the difference is less of a ten of a fraction.

During the evolution of the problem, local variables of the chemical field as the chemical potential μ and the concentration c, present similar behavior for both strategies. This comes as no surprise since the chemical field was the variable in the staggered strategy inside the block of highest hierarchy, meaning it was the only algorithmic independent variable. As it is for the electric potential ϕ a clear difference is observed in the solutions of the different strategies. In the monolithic strategy ϕ remains almost constant during the evolution of the problem showing a linear dependence with space, while for the staggered strategy ϕ changes more drastically with time, evolving from a linear dependence with space to whats seems to be an algorithmic relation. This highlights the biggest difference between both strategies, the electric potential $-\nabla\phi$. In the monolithic strategy $-\nabla\phi$ by the end of the simulation has almost reached

a constant value of -1V, not reached by a slight negative slope at the left boundary $x = 0$. In contrast, during the last time steps of the staggered strategy $-\nabla\phi$ shows a concave form highlighted by the positive slope at $x = 0$.

6.7 Summary

Throughout this chapter we presented different options to reduce the computational cost of solving the VF model we have proposed in previous chapters. The first thing to highlight is the derivation from the VF itself the different families of solution strategies, namely, mono, staggered and nested.[8] An algorithmic change of dependencies from implicit to explicit between the variables is the key idea from which all the derivation begins. This produced physically-based block preconditioners leading to the staggered and nested strategies. Furthermore, the common lack of a mathematical definition for physically based block preconditioners Keyes et al. [2013] has been overcome, leading to a dual derivation of the strategies, whether from calculus of variations or a linear algebra process. We explored the generality of the proposed VF when applied to multiphysic problems in two ways. First, starting with the analysis of emergent properties on the obtained strategies. Second, through the derivation of two theorems, namely, the staggered strategy and nested strategy theorems. Thus, as shown the structure of the generalized VF we proposed possess a rich underlying structure which can be exploited to solve the model itself through numerical approximations.

[8] We call them families, since solvers needed at each stage of the solution process also as further point preconditioners are not imposed, but rather the overall sequence on which those are used, leading to a variety of possible strategies having the same underlying structure.

Part IV

Conclusions and perspectives

Chapter 7

Conclusions

Sommaire

C'est le dernier chapitre du manuscrit. Il résume les principaux résultats de ce travail et fournit un aperçu de certaines idées présentées.

> Don't wait to read the most recent research papers. ... Wonder how you could do better. ... Do your own research projects. Take the initiative. ... Ask your own questions — try to answer them. ... At some point you stop being a student and you start being a scientist. ... And it's a completely different skill set ...
>
> Sean M. Carroll
> *(21 April 2018)"Episode 124 - In Search of Reality: A Conversation with Sean Carroll". Waking Up Podcast with Sam Harris.*

The modeling of multiphysic problems is a topic which has gained importance over the last decades. The increasing complexity of current technology and the need to push it forward is one of the main reasons. In addition, as pointed out by Laughlin and Pines [2000] "[for] those of us concerned with the health of physical science [we need] to face the truth that in most respects the reductionist ideal has reached its limits as a guiding principle", suitably, multiphysic leans towards this systematic perspective by incorporating different branches of Physics[1]. Thus, from a practical and theoretical point of view research in multiphysics problems is well justified. There are two main problems encounter by multiphysics. The first one concerns the construction of the multiphysic model. The second is about its solution.

To model a multiphysic problem a *bottom-up* approach is usually performed in the literature. This means that we impose a coupling from the individual branches of Physics to reach the desired model. This has shown some practical drawbacks as most of the knowledge acquired in the area is empirical and the coupling is highly dependent of the specific Physics [Keyes et al., 2013]. From a logical perspective, multiphysics is seen as a consequence of these individual branches rather than the cause of them, which would seem more reasonable. A frequent analogy used by researchers in this area is to think about multiphysics as a puzzle which we can appreciate as we put its parts together. In this work, we explored a *top-down* approach by providing a generic VF model. The abstraction allows to construct a multiphysic

[1] sometimes refer in the literature as *unyphisics*

model regardless of the specifics, by providing a functional based on energies, balance and constitutive laws which are common in all individual branches of Physics. This opens the possibility that the couplings rather than being imposed can be deduced. And still, once we constructed a VF model we know each variation should probe equivalent to the individual branches. Thus, using the puzzle metaphor, instead of putting the puzzle together from its individual pieces we propose a possible picture of the whole puzzle and validate it by dissembling it and observe the individual pieces are the ones we expected.

The solvability of multiphysic models becomes a difficult task since the number of unknowns increases, bringing more dependencies and usually more instabilities to the model itself. As expected, numerical approximations of the solution are the most feasible option despite its computational cost. Therefore, it is a common practice to decrease this cost by different solution strategies. The strategies take advantage of the mathematical structure of the problem or benefit from a physical intuition. Unfortunately, mathematically-based strategies are obtained at the expense of a loss of physical intuition whilst physically-based strategies may lack a mathematical structure which is commonly substitute by an algorithmic description. By taking special care on the distinction of physical and algorithmic dependencies, we have proposed different families of solution strategies which are physically-based but which mathematical structure can also be understood simultaneously. All the former provides a vast option of numerical implementations which can be developed, leading thus to more ways to understand the models being solved.

The purpose of this work is to take advantage of variational principles for the mathematical modeling and development of solutions strategies for multiphysic problems. It has been mostly developed for chemical diffusion, for which mixed formulations can be derived and hence be treated as a multiphysic problem. On regard the mathematical models, we extrapolated the core structure and ideas from chemical diffusion to propose a generic formulation for coupled problems. We validated this generalization by applying it to a specific problem, the model of a lithium-ion battery cell. Thus, the proposed variational model seems suitable for coupled problems in a first instance. Concerning the numerical implementation, we have taken a deviation from common procedures by deriving solution strategies from the model itself rather than imposing them. This has led us to identify three different derivable families of solution strategies, namely, monolithic, staggered and nested. These obtained physically-based solution strategies have the benefit of having also a mathematical representation. The former allows to derive them by means of calculus of variations and/or linear algebra.

7.1 Chapters summary

Each chapter has contributed towards these goals. Furthermore, side conclusions have also been reached. Therefore, we focus on the following to summarize the contribution of each chapter to provide a more detail description of this work.

In the introductory chapter §1, we presented the grounds on which this work has been developed. In chapter §2 we visited basic concepts and stated the definition of properties, drawn distinctions, and relations between strategy, solver, preconditioner. The latter can be considered as the first contribution of this work. This classification is different from different approaches in the literature, which despite presenting a clear understanding of solvers and preconditioners, the role of preconditioners and strategies is fuzzy. The distinction we provided is what allowed us to define algebraically physically-based preconditioners by means of the *transparency-relation*.

The chemical diffusion chapter §3, introduces the ideas needed to develop a generic VF model for coupled problems through the development of the multifield VF for chemical diffusion. To this end, we developed three different variational forms for the problem of coupled chemical diffusion in a continuum

setting. The initial 3-field model was constructed using common concepts among all uniphysics like balance laws, and constitutive laws. The specifics of these concepts become context-free by the use of the internal energy potential U, dissipation potential χ and a constrained functional Π. The further two VF are derived from the 3-field formulation via the Legendre-Fenchel transform. The 2-field VF corresponds to the model proposed in Miehe et al. [2014]. However, the process taken to reach the model is completely different. We reached the model by defining a constrained problem which we later reduced and prove to be equivalent to the SF, while Miehe et al. [2014] derived the model starting from the SF of the problem specified in a given domain. In general we showed, the 3-field and 2-field formulations are equivalent to the SF and WF. As it is for the 1-field formulation, the equivalence is lost. For the specifics of the problem, we present a nonlinear model and its linear counterpart, which we called the *Fickean* and *linear* models correspondingly. We related both models through a specific characterization of the coefficient D. This relation closely relates to the Einstein–Smoluchowski relation [Lindsay, 2009]. Einstein [1905] derived this relation focusing in Brownian motion. Therefore, the benefit of rediscovering this relation through our approach shows that the empirical mass action laws can be regarded as a macroscopic or emergent property between c and μ. We transformed the VF from a continuum to a discrete setting proposing two different schemes −semi-implicit and fully-implicit− for its numerical implementation. Finally, we validated our VF numerically and compare results for the different implementations. The most interesting result comes from the observation that errors in concentration and chemical potential have different order of magnitude and differ also depending on the material model used. This suggests an implicit dependency between these fields, which highly contrasts with the post-process relation −explicit dependence− used in the usual SF or WF.

The use of the core ideas in chemical diffusion to develop a generic VF for coupled problems is laid down in §4. At the end of this chapter, we presented the use of the proposed generic VF model to tackle electrochemical problems. We take this as the starting point to model a lithium-ion battery in §5. For the electrolyte's model, we analyzed three different approaches used in the literature the Nernst-Planck, the Stefan-Maxwell, and the Ion-transport. We introduced the *holonomic condition* which we showed to be equivalent to the Onsager relations. The difference being that the *holonomic condition* establishes the condition on the constitutive laws to be an exact differential of the dissipation potential, while the Onsager relations state the conditions for the Onsager matrix to be symmetric. The Stefan-Maxwell and Ion-transport approach prove to be thermodynamic consistent and we derived the material models for both of them. Furthermore, we presented the *pre-Onsager relation*, which we showed denotes the coupling occurs between the flux-type variables. For the electrolyte's, we use an uncoupled model between the electric and chemical fields, showing the robustness of the VF. Finally, the interface coupling required to satisfy the Butler-Volmer equation, which we achieved by constructing its corresponding function at the electrolyte/electrode interface.

Finally, in §6 we derived different numerical implementations which can be deduced from the VF we proposed. These numerical implementations are achieved by imposing explicit −algorithmic− dependencies. This results in the split of the VF and a field-wise partition of the system which can be solved either through a staggered or nested strategy. Furthermore, we pointed out that the subsystem of the algorithmic independent variables decays into quasi-Newton or inexact Newton method depending if the strategy used is nested or staggered correspondingly. All the former is achieved by means of calculus of variations and the algorithmic explicit dependencies. In addition, we showed the algebraic counterpart of the deduced numerical implementations, which holds under the right solutions' space. The algebraic form of the block-preconditioner for the staggered strategy corresponds to the Gauss elimination method applied block-wise, while for the nested strategy's preconditioner we could obtain it by additive preconditioning using a null space condition. These relations point out interesting relations between calculus and algebra in the context of preconditioning. An important remark is the introduction of concepts like the *transparency-relation*, *iterative-block*, and *block-hierarchy* which give a clear mathematical distinction

between preconditioner and strategy. Moreover, as side results, we explored the complexity of the derived strategies for which we proposed the concept of *ordinal limit*, for which we explored the algorithms under an infinite number of iterations and partitions. Supplementary, we presented a graphical tool for the analysis of strategies. These side results allow studying in a novel way the algorithms, in a context independent of the physics or mathematical structure of the problem.

7.2 Outlook

There is plenty of work which can be continued and further explored from this dissertation. We list below some of this options from the model point of view.

- **Further examples.** A natural next step is to apply these results to thermomechanical and chemomechanical problems. As the model concerns, the main problems would be to expand the generic VF framework to be able to handle nonlinear elasticity and plasticity deformations. However, the works of Yang et al. [2006] and Miehe et al. [2014] can be used as a guide.
- **Noether's theorem.** Theoretically, it would be interesting to draw the connections between Noether's theorem and the generic VF we propose. Noether's theorem qualified as one of the most beautiful theorems in mathematical physics describes the connection between symmetries and conservation laws using the Lagrangian of a system. However, for dissipative systems this might not be the case. The VF we propose can involve dissipative behavior and embeds conservation laws. Hence, it would be interesting to use if possible or adapt Noether's theorem to find the symmetries in our formulation or discard the possibility of the use of this theorem.

As it is from the numerical perspective some options are the following

- **Lithium-ion model.** In order to land the theoretical results, the first natural step is to implement the presented VF for the lithium-ion battery and some of the solution strategies deduced from it. As a personal preference for this task I would use the *FEM library* from `dealii` since it is open source and well documented. The validation of the results besides convergence plots can take place with a comparison of the results using the software ZorgLib or baci which have been developed at the Ècole Central of Nantes and the Technical University of Munich respectively. Equivalent WF of the model have been already implemented and validated on those software.
- **Implementation of solution strategies.** A second step is the implementation of the proposed solution strategies for which `dealii` would also be suitable due to the great amount of resources and flexibility it offers. The difficulty on this regard would be to keep the implementations open for the use of any number of fields, solvers and further preconditioners. However, techniques like sfinae in c++ may provide an answer to overcome this issue.
- **Best null space condition.** Through the algebraic definition of block-preconditioners for the nested strategy we defined the *null space condition*. To achieve the algebraic definition we proposed the partition of the original matrix into the addition of two parts. The null space condition vanishes one of those parts making possible the approximation of the matrix without adding any term to the right hand side of the equation. However, there are an infinite amount of partitions we can do by addition, but one would expect some to be useful while the others not. Hence, this fact raises the following question, For a partition of the matrix in a sum of two parts, is the obtained partition derived by an algorithmic change of dependencies the most optimal approximation of the matrix? Or in short, is that the best null space condition to approximate the system?. A deeper study in this direction could provide many insights not only to understand the effects of the strategy but maybe the model itself, since as we show in our example the null space condition was just a rearrangement of the conjugate definition of the variables which dependence was modified.

- **Path error plot.** Once the model and strategies are implemented, it would be interesting to develop the proposed *path error plot* as a graphical tool to observe convergence results. However, this tool only requires a log file of the solution process and it can be applied to any solution strategy.

- **Ordinal limit analysis.** The ordinal limit provides a tool to explore a emergent property from solution strategies. Therefore, a study which analyses further strategies currently existing in the literature, as it would be AMG as an example, and compare the results obtained may turn helpful in our overall understanding since it may provide or point us to connections or similarities between strategies, or help us categorize them in a different manner from which we may learn new things.

- **Added effect strategies.** In this work, we pointed out an example for which the staggered strategy leads to an algorithm similar to the *added mass-effect* widely used in FSI problems. Therefore, this indicates that it is likely that the staggered strategy could be a generalization of this sort of techniques. A study in this direction could increase our understanding in multiphysics since if true, a wide variety of algorithms from many areas of multiphysic would proof to be similar or would benefit from it.

- **Invariance nested strategy.** As shown the solutions obtained by the nested stategy keep the solution invariant. The invariance of solutions has been already studied for Newton methods in the literature in the book from Deuflhard [2005]. Furthermore, we draw a connection between the nested strategy and a Quasi-Newton method. Hence, it would be interesting to know if this strategy would fit into one of the theories of this book.

Bibliography

McNaught A. D. spinodal decomposition. In *IUPAC Compendium of Chemical Terminology*, volume 1669. Blackwell Science Oxford, 1997. doi: 10.1351/goldbook.s05869. URL https://doi.org/10.1351/goldbook.s05869.

Cynthia A. Lundgren, Kang Xu, Richard Jow, Jan Allen, and Sheng S. Zhang. Lithium-ion batteries and materials. In *Springer Handbook of Electrochemical Energy*, chapter 15, pages 449–494. Springer Berlin Heidelberg, 2017.

Grégoire Allaire and Sidi Mahmoud Kaber. *Numerical Linear Algebra (Texts in Applied Mathematics)*. Springer, 2007. ISBN 0387341595. URL https://www.amazon.com/Numerical-Linear-Algebra-Applied-Mathematics/dp/0387341595?SubscriptionId=0JYN1NVW651KCA56C102&tag=techkie-20&linkCode=xm2&camp=2025&creative=165953&creativeASIN=0387341595.

Juan Alonso and Antony Jameson. Fully-implicit time-marching aeroelastic solutions. In *32nd Aerospace Sciences Meeting and Exhibit*, page 56, 1994.

F. Armero and J. C. Simo. A new unconditionally stable fractional step method for non-linear coupled thermomechanical problems. *International Journal for Numerical Methods in Engineering*, 35(4):737–766, 1992. ISSN 1097-0207. doi: 10.1002/nme.1620350408. URL http://dx.doi.org/10.1002/nme.1620350408.

Owe Axelsson. *Iterative Solution Methods*. Cambridge University Press, 1994. doi: 10.1017/CBO9780511624100.

Santiago Badia, Alberto F. Martín, and Ramon Planas. Block recursive lu preconditioners for the thermally coupled incompressible inductionless mhd problem. *Journal of Computational Physics*, 274:562 – 591, 2014. ISSN 0021-9991. doi: https://doi.org/10.1016/j.jcp.2014.06.028. URL http://www.sciencedirect.com/science/article/pii/S0021999114004355.

N.S. Bakhvalov. On the convergence of a relaxation method with natural constraints on the elliptic operator. *USSR Computational Mathematics and Mathematical Physics*, 6(5):101 – 135, 1966. ISSN 0041-5553. doi: https://doi.org/10.1016/0041-5553(66)90118-2. URL http://www.sciencedirect.com/science/article/pii/0041555366901182.

R. W. Balluffi and B. H. Alexander. Dimensional changes normal to the direction of diffusion. *Journal of Applied Physics*, 23(9):953–956, 1952. doi: http://dx.doi.org/10.1063/1.1702357. URL http://scitation.aip.org/content/aip/journal/jap/23/9/10.1063/1.1702357.

R.W Balluffi and L.L Seigle. Effect of grain boundaries upon pore formation and dimensional changes during diffusion. *Acta Metallurgica*, 3(2):170 – 177, 1955. ISSN 0001-6160. doi: http://dx.doi.org/10.1016/0001-6160(55)90087-0. URL http://www.sciencedirect.com/science/article/pii/0001616055900870.

Margherita Barile. Additive intentity. From MathWorld—A Wolfram Web Resource, a. URL http://mathworld.wolfram.com/AdditiveIdentity.html. Last visited on 18/11/2017.

Margherita Barile. Additive intentity. From MathWorld—A Wolfram Web Resource, b. URL http://mathworld.wolfram.com/MultiplicativeIdentity.html. Last visited on 18/11/2017.

Michele Benzi. Preconditioning techniques for large linear systems: A survey. *Journal of Computational Physics*, 182(2):418 – 477, 2002. ISSN 0021-9991. doi: https://doi.org/10.1006/jcph.2002.7176. URL http://www.sciencedirect.com/science/article/pii/S0021999102971767.

V. Berdichevsky. *Variational Principles of Continuum Mechanics: II. Applications*. Interaction of Mechanics and Mathematics. Springer Berlin Heidelberg, 2009. ISBN 9783540884699. URL https://books.google.de/books?id=m5ZrOK8FLIIC.

J.M. Bergheau and R. Fortunier. *Finite Element Simulation of Heat Transfer*. ISTE. Wiley, 2010. ISBN 9780470394038.

M. A. Biot. Thermoelasticity and irreversible thermodynamics. *Journal of Applied Physics*, 27(3):240–253, 1956. doi: 10.1063/1.1722351. URL https://doi.org/10.1063/1.1722351.

Frederic J. Blom. A monolithical fluid-structure interaction algorithm applied to the piston problem. *Computer Methods in Applied Mechanics and Engineering*, 167(3):369 – 391, 1998. ISSN 0045-7825. doi: https://doi.org/10.1016/S0045-7825(98)00151-0. URL http://www.sciencedirect.com/science/article/pii/S0045782598001510.

Charbel Bouery. *Contribution to algorithmic strategies for solving coupled thermo-mechanical problems by an energy-consistent variational approach*. Theses, Ecole Centrale de Nantes (ECN), December 2012. URL https://tel.archives-ouvertes.fr/tel-00827159.

G. A. Bourdin, B.and Francfort. *Fracture*, pages 107–161. Springer Vienna, Vienna, 2011. ISBN 978-3-7091-0983-0. doi: 10.1007/978-3-7091-0983-0_3. URL https://doi.org/10.1007/978-3-7091-0983-0_3.

S.P. Boyd and L. Vandenberghe. *Convex Optimization*. Berichte über verteilte messysteme. Cambridge University Press, 2004. ISBN 9780521833783. URL https://books.google.de/books?id=mYm0bLd3fcoC.

Achi Brandt. Multi-level adaptive solutions to boundary-value problems. *Mathematics of Computation*, 31 (138):333–333, may 1977. doi: 10.1090/s0025-5718-1977-0431719-x. URL https://doi.org/10.1090%2Fs0025-5718-1977-0431719-x.

Laurence Brassart and Zhigang Suo. Reactive flow in large-deformation electrodes of lithium-ion batteries. *International Journal of Applied Mechanics*, 04(03):1250023, 2012. doi: 10.1142/S1758825112500238. URL http://www.worldscientific.com/doi/abs/10.1142/S1758825112500238.

Laurence Brassart and Zhigang Suo. Reactive flow in solids. *Journal of the Mechanics and Physics of Solids*, 61(1):61–77, 2013.

S. Brenner and L.R. Scott. *The Mathematical Theory of Finite Element Methods*. Texts in Applied Mathematics. Springer New York, 2013. ISBN 9781475736588. URL https://books.google.de/books?id=ServBwAAQBAJ.

William L. Briggs, Van Emden Henson, and Steve F. McCormick. *A Multigrid Tutorial, Second Edition*. Society for Industrial and Applied Mathematics, jan 2000. doi: 10.1137/1.9780898719505. URL https://doi.org/10.1137%2F1.9780898719505.

D L Brown, J Bell, D Estep, W Gropp, B Hendrickson, S Keller-McNulty, D Keyes, J T Oden, L Petzold, and M Wright. Applied mathematics at the u.s. department of energy: Past, present and a view to the future. Technical report, feb 2008. URL `https://doi.org/10.2172/944335`.

Peter N. Brown and Youcef Saad. Convergence theory of nonlinear newton–krylov algorithms. *SIAM Journal on Optimization*, 4(2):297–330, may 1994. doi: 10.1137/0804017. URL `https://doi.org/10.1137%2F0804017`.

Violet Brulliard. *Etude du comportement du Nucleus pulposus à l'aide d'un modèle couplant grandes déformations et diffusion*. PhD thesis, Ecole Centrale de Nantes., 2014.

Giovanna Bucci, Siva P.V. Nadimpalli, Vijay A. Sethuraman, Allan F. Bower, and Pradeep R. Guduru. Measurement and modeling of the mechanical and electrochemical response of amorphous si thin film electrodes during cyclic lithiation. *Journal of the Mechanics and Physics of Solids*, 62:276 – 294, 2014. ISSN 0022-5096. doi: https://doi.org/10.1016/j.jmps.2013.10.005. URL `http://www.sciencedirect.com/science/article/pii/S0022509613002135`. Sixtieth anniversary issue in honor of Professor Rodney Hill.

H.B. Callen. *Thermodynamics and an Introduction to Thermostatistics*. Wiley, 1985. ISBN 9780471862567. URL `https://books.google.de/books?id=XJ0RAQAAIAAJ`.

Patankar S. V. Caretto L. S., Gosman A. D. and Spalding D. B. Two calculation procedures for steady, three-dimensional flows with recirculation. In Temam Roger Cabannes Henri, editor, *Proceedings of the Third International Conference on Numerical Methods in Fluid Mechanics*, pages 60–68, Berlin, Heidelberg, 1973. Springer Berlin Heidelberg. ISBN 978-3-540-38392-5.

E. Chason, B. W. Sheldon, L. B. Freund, J. A. Floro, and S. J. Hearne. Origin of compressive residual stress in polycrystalline thin films. *Phys. Rev. Lett.*, 88:156103, Mar 2002. doi: 10.1103/PhysRevLett.88.156103. URL `http://link.aps.org/doi/10.1103/PhysRevLett.88.156103`.

Ke Chen. *Matrix Preconditioning Techniques and Applications*. Cambridge Monographs on Applied and Computational Mathematics. Cambridge University Press, 2005. doi: 10.1017/CBO9780511543258.

B. M. Clemens. Chapter 4: Diffusion with a chemical concentration gradient. 2005.

Richard Courant and David Hilbert. *001: Methods of Mathematical Physics, Vol. 1*. Wiley-VCH, 1989. ISBN 0471504475.

J. Crank. *The Mathematics of Diffusion*. Oxford science publications. Clarendon Press, 1979. ISBN 9780198534112. URL `https://books.google.co.in/books?id=eHANhZwVouYC`.

Eric C. Cyr, John N. Shadid, and Raymond S. Tuminaro. Teko: a block preconditioning capability with concrete example applications in Navier-Stokes and MHD. *SIAM J. Sci. Comput.*, 38(5):s307–s331, 2016. ISSN 1064-8275; 1095-7197/e. doi: 10.1137/15M1017946.

D. Danilov and P.H.L. Notten. Mathematical modelling of ionic transport in the electrolyte of li-ion batteries. *Electrochimica Acta*, 53(17):5569 – 5578, 2008. ISSN 0013-4686. doi: https://doi.org/10.1016/j.electacta.2008.02.086. URL `http://www.sciencedirect.com/science/article/pii/S0013468608003046`.

Caroline Danowski, Volker Gravemeier, Lena Yoshihara, and Wolfgang A. Wall. A monolithic computational approach to thermo-structure interaction. *International Journal for Numerical Methods in Engineering*, 95(13):1053–1078, 2013. ISSN 1097-0207. doi: 10.1002/nme.4530. URL `http://dx.doi.org/10.1002/nme.4530`.

Timothy A. Davis, Sivasankaran Rajamanickam, and Wissam M. Sid-Lakhdar. A survey of direct methods for sparse linear systems. *Acta Numerica*, 25:383–566, 2016. doi: 10.1017/S0962492916000076.

S.R. de Groot and P. Mazur. *Non-equilibrium Thermodynamics*. Dover Books on Physics. Dover Publications, 1984. ISBN 9780486647418. URL https://books.google.de/books?id=HFAIv43rlGkC.

E.A. de Souza Neto, D. Peric, and D.R.J. Owen. *Computational Methods for Plasticity: Theory and Applications*. Wiley, 2011. ISBN 9781119964544. URL https://books.google.de/books?id=21Q0oLGFZuoC.

Francesco dell'Isola and Luca Placidi. *Variational principles are a powerful tool also for formulating field theories*, pages 1–15. Springer Vienna, Vienna, 2011. ISBN 978-3-7091-0983-0. doi: 10.1007/978-3-7091-0983-0_1. URL https://doi.org/10.1007/978-3-7091-0983-0_1.

Laurent Demanet. Waves and imaging-class notes - 18.325, April 2015. URL http://ocw.mit.edu(Accessed13/02/2018.

Ron S. Dembo, Stanley C. Eisenstat, and Trond Steihaug. Inexact newton methods. *SIAM Journal on Numerical Analysis*, 19(2):400–408, apr 1982. doi: 10.1137/0719025. URL https://doi.org/10.1137%2F0719025.

P. Deuflhard. *Newton Methods for Nonlinear Problems: Affine Invariance and Adaptive Algorithms*. Springer Series in Computational Mathematics. Springer Berlin Heidelberg, 2005. ISBN 9783540210993. URL https://books.google.de/books?id=l20xK__HG_kC.

Edmund J. F. Dickinson, Juan G. Limon-Petersen, and Richard G. Compton. The electroneutrality approximation in electrochemistry. *Journal of Solid State Electrochemistry*, 15(7):1335–1345, Jul 2011. ISSN 1433-0768. doi: 10.1007/s10008-011-1323-x. URL https://doi.org/10.1007/s10008-011-1323-x.

J. Donea and A. Huerta. *Finite Element Methods for Flow Problems*. Finite Element Methods for Flow Problems. John Wiley & Sons, 2003. ISBN 9780471496663. URL https://books.google.de/books?id=S4URqrTtSXoC.

Andreas Ehrl. *Determination of Transport Parameters of Binary Electrolyte Solutions for the Use in Numerical Simulations*. Dissertation, Technische Universität München, München, 2017.

A. Einstein. Über die von der molekularkinetischen theorie der wärme geforderte bewegung von in ruhenden flüssigkeiten suspendierten teilchen. *Annalen der Physik*, 322(8):549–560, 1905. doi: 10.1002/andp.19053220806. URL https://doi.org/10.1002/andp.19053220806.

L.C. Evans. *Partial Differential Equations*. Graduate studies in mathematics. American Mathematical Society, 1998. ISBN 9780821807729. URL https://books.google.com.mx/books?id=5Pv4LVB_m8AC.

Rui Fang, Philipp Farah, Alexander Popp, and Wolfgang A. Wall. A monolithic, mortar-based interface coupling and solution scheme for finite element simulations of lithium-ion cells. *International Journal for Numerical Methods in Engineering*, 2017. doi: 10.1002/nme.5792.

R.P. Fedorenko. The speed of convergence of one iterative process. *USSR Computational Mathematics and Mathematical Physics*, 4(3):227 – 235, 1964. ISSN 0041-5553. doi: https://doi.org/10.1016/0041-5553(64)90253-8. URL http://www.sciencedirect.com/science/article/pii/0041555364902538.

Carlos A. Felippa, K.C. Park, and Charbel Farhat. Partitioned analysis of coupled mechanical systems. *Computer Methods in Applied Mechanics and Engineering*, 190(24):3247 – 3270, 2001. ISSN 0045-7825. doi: https://doi.org/10.1016/S0045-7825(00)00391-1. URL `http://www.sciencedirect.com/science/article/pii/S0045782500003911`. Advances in Computational Methods for Fluid-Structure Interaction.

Richard P. Feynman, Robert B. Leighton, and Matthew Sands. *The Feynman Lectures on Physics*, volume I. 1963. URL `http://www.feynmanlectures.caltech.edu`.

Dr. Adolph Fick. V. on liquid diffusion. *Philosophical Magazine Series 4*, 10(63):30–39, 1855. doi: 10.1080/14786445508641925.

B.A. Finlayson. *The Method of Weighted Residuals and Variational Principles*. Classics in Applied Mathematics. Society for Industrial and Applied Mathematics (SIAM, 3600 Market Street, Floor 6, Philadelphia, PA 19104), 2013. ISBN 9781611973242. URL `https://books.google.de/books?id=_2zPAgAAQBAJ`.

Christiane Förster, Wolfgang Wall, and Ekkehard Ramm. The artificial added mass effect in sequential staggered fluid-structure interaction algorithms. 01 2006.

Christiane Förster, Wolfgang A. Wall, and Ekkehard Ramm. Artificial added mass instabilities in sequential staggered coupling of nonlinear structures and incompressible viscous flows. *Computer Methods in Applied Mechanics and Engineering*, 196(7):1278 – 1293, 2007. ISSN 0045-7825. doi: https://doi.org/10.1016/j.cma.2006.09.002. URL `http://www.sciencedirect.com/science/article/pii/S0045782506002544`.

A. Galántai. The theory of newton's method. *Journal of Computational and Applied Mathematics*, 124 (1):25 – 44, 2000. ISSN 0377-0427. doi: https://doi.org/10.1016/S0377-0427(00)00435-0. URL `http://www.sciencedirect.com/science/article/pii/S0377042700004350`. Numerical Analysis 2000. Vol. IV: Optimization and Nonlinear Equations.

François Gay-Balmaz. A variational derivation of the thermodynamics of a moist atmosphere with rain process and its pseudoincompressible approximation. *Geophysical & Astrophysical Fluid Dynamics*, pages 1–38, 01 2019. doi: 10.1080/03091929.2019.1570505.

M. W. Gee, U. Küttler, and W. A. Wall. Truly monolithic algebraic multigrid for fluid-structure interaction. *International Journal for Numerical Methods in Engineering*, 85(8):987–1016, sep 2010. doi: 10.1002/nme.3001. URL `https://doi.org/10.1002%2Fnme.3001`.

Martin H. Gutknecht. A brief introduction to krylov space methods for solving linear systems. In *Frontiers of Computational Science*, pages 53–62. Springer Berlin Heidelberg, 2007. doi: 10.1007/978-3-540-46375-7_5. URL `https://doi.org/10.1007%2F978-3-540-46375-7_5`.

Klaus Hackl and Franz Dieter Fischer. On the relation between the principle of maximum dissipation and inelastic evolution given by dissipation potentials. *Proc. R. Soc. A*, 464:117–132, 2008.

Bernard Halphen and Quoc Son Nguyen. Sur les matériaux standard généralisés. *Journal de Mécanique*, 14:39–63, 1975. URL `https://hal.archives-ouvertes.fr/hal-00105514`.

Magnus R. Hestenes and Eduard Stiefel. Methods of Conjugate Gradients for Solving Linear Systems. *Journal of Research of the National Bureau of Standards*, 49(6):409–436, December 1952.

Victoria E. Howle, Robert C. Kirby, Kevin Long, Brian Brennan, and Kimberly Kennedy. Playa: High-performance programmable linear algebra. *Sci. Program.*, 20(3):257–273, July 2012. ISSN 1058-9244. doi: 10.1155/2012/606215. URL `http://dx.doi.org/10.1155/2012/606215`.

Ilse C. F. Ipsen and Carl D. Meyer. The idea behind krylov methods. *The American Mathematical Monthly*, 105(10):889–899, 1998. ISSN 00029890, 19300972. URL http://www.jstor.org/stable/2589281.

Jr. J. E. Dennis and Jorge J. Moré. Quasi-newton methods, motivation and theory. *SIAM Review*, 19(1): 46–89, jan 1977. doi: 10.1137/1019005. URL https://doi.org/10.1137%2F1019005.

Julius L. Jackson. Charge neutrality in electrolytic solutions and the liquid junction potential. *The Journal of Physical Chemistry*, 78(20):2060–2064, 1974. doi: 10.1021/j100613a014. URL https://doi.org/10.1021/j100613a014.

G Job and F Herrmann. Chemical potential—a quantity in search of recognition. *European Journal of Physics*, 27(2):353–371, feb 2006. doi: 10.1088/0143-0807/27/2/018. URL https://doi.org/10.1088%2F0143-0807%2F27%2F2%2F018.

G. Job, R. Rüffler, R. Fuchs, and H.U. Fuchs. *Physical Chemistry from a Different Angle: Introducing Chemical Equilibrium, Kinetics and Electrochemistry by Numerous Experiments*. Springer International Publishing, 2015. ISBN 9783319156668.

H. El Kadiri, M.F. Horstemeyer, and D.J. Bammann. A theory for stress-driven interfacial damage upon cationic-selective oxidation of alloys. *Journal of the Mechanics and Physics of Solids*, 56(12): 3392 – 3415, 2008. ISSN 0022-5096. doi: http://dx.doi.org/10.1016/j.jmps.2008.09.001. URL http://www.sciencedirect.com/science/article/pii/S0022509608001506.

David E. Keyes, Lois Curfman McInnes, Carol Woodward, William Gropp, Eric Myra, and et al. Multiphysics simulations: Challenges and opportunities. *International Journal of High Performance Computing Applications*, 27:4–83, 2013.

Roy Kingshuk, Wahid Malik, Puthusseri Dhanya, Patrike Apurva, Muduli Subas, Vaidhyanathan Ramanathan, and Ogale Satishchandra. High capacity, power density and cycling stability of silicon li-ion battery anodes with a few layer black phosphorus additive. *Sustainable Energy & Fuels*, 3(1):245–250, 2019. doi: 10.1039/c8se00476e. URL https://doi.org/10.1039/c8se00476e.

E. Kirkendall, L. Thomassen, and C. Upthegrove. *Rates of Diffusion of Copper and Zinc in Alpha Brass*. University of MICHIGAN, 1938. URL https://books.google.fr/books?id=3GPPAAAAMAAJ.

K. Kontturi, L. Murtomäki, and J.A. Manzanares. *Ionic Transport Processes: in Electrochemistry and Membrane Science*. OUP Oxford, 2008. ISBN 9780191559945. URL https://books.google.de/books?id=IgBv7Gdyvr8C.

Cornelius Lanczos. *The Variational Principles of Mechanics*, volume 4. Toronto, University of Toronto Press, 1949. ISBN 0802017436.

F. Larché and J. W. Cahn. A linear theory of thermochemical equilibrium of solids under stress. *Acta Metall.*, 21(8):1051–1063, 1973.

A. Latz and J. Zausch. Thermodynamic consistent transport theory of li-ion batteries. *Journal of Power Sources*, 196(6):3296 – 3302, 2011. ISSN 0378-7753. doi: https://doi.org/10.1016/j.jpowsour.2010.11.088. URL http://www.sciencedirect.com/science/article/pii/S0378775310020793.

R. B. Laughlin and David Pines. The theory of everything. *Proceedings of the National Academy of Sciences*, 97(1):28–31, 2000. ISSN 0027-8424. doi: 10.1073/pnas.97.1.28. URL https://www.pnas.org/content/97/1/28.

S. Lindsay. *Introduction to Nanoscience*. OUP Oxford, 2009. ISBN 9780191609275. URL https://books.google.de/books?id=KGqSxqyqa10C.

Bergamaschi L. Bru R. Martínez A. Putti M. Quasi-newton preconditioners for the inexact newton method. *ETNA. Electronic Transactions on Numerical Analysis [electronic only]*, 23:76–87, 2006. URL `http://eudml.org/doc/127449`.

Heroux M. A. *AztecOO User Guide*. United States. Department of Energy, 2004. URL `https://books.google.de/books?id=vF1dAQAACAAJ`.

J.M.P. Martins, D.M. Neto, J.L. Alves, M.C. Oliveira, H. Laurent, A. Andrade-Campos, and L.F. Menezes. A new staggered algorithm for thermomechanical coupled problems. *International Journal of Solids and Structures*, 122-123:42 – 58, 2017. ISSN 0020-7683. doi: https://doi.org/10.1016/j.ijsolstr.2017.06.002. URL `http://www.sciencedirect.com/science/article/pii/S0020768317302585`.

Matthias Mayr, Thomas Klöppel, Wolfgang A. Wall, and Michael W. Gee. A temporal consistent monolithic approach to fluid-structure interaction enabling single field predictors. *SIAM Journal on Scientific Computing*, 37(1):B30–B59, 1 2015. doi: 10.1137/140953253. URL `https://doi.org/10.1137%2F140953253`.

C. Miehe. Entropic thermoelasticity at finite strains. aspects of the formulation and numerical implementation. *Computer Methods in Applied Mechanics and Engineering*, 120(3):243 – 269, 1995. ISSN 0045-7825. doi: https://doi.org/10.1016/0045-7825(94)00057-T. URL `http://www.sciencedirect.com/science/article/pii/004578259400057T`.

C. Miehe, S. Mauthe, and H. Ulmer. Formulation and numerical exploitation of mixed variational principles for coupled problems of cahn–hilliard-type and standard diffusion in elastic solids. *International Journal for Numerical Methods in Engineering*, 99(10):737–762, 2014. ISSN 1097-0207. doi: 10.1002/nme.4700. URL `http://dx.doi.org/10.1002/nme.4700`.

Christian Miehe. A multi-field incremental variational framework for gradient-extended standard dissipative solids. *Journal of the Mechanics and Physics of Solids*, 59(4):898 – 923, 2011. ISSN 0022-5096. doi: https://doi.org/10.1016/j.jmps.2010.11.001. URL `http://www.sciencedirect.com/science/article/pii/S0022509610002358`.

Alan Needleman and J. R. Rice. Plastic creep flow effects in the diffusive cavitation of grain boundaries. *Acta Metall.*, 28(10):1315–1332, 1980.

Walther Nernst. Die elektromotorische wirksamkeit der jonen. *Zeitschrift für physikalische Chemie*, 4(1): 129–181, 1889.

J. Newman and K.E. Thomas-Alyea. *Electrochemical Systems*. Electrochemical Society series. John Wiley & Sons, 2004. ISBN 9780471477563. URL `https://books.google.de/books?id=vArZu0HM-xYC`.

Jihun Oh and Carl V. Thompson. The role of electric field in pore formation during aluminum anodization. *Electrochimica Acta*, 56(11):4044 – 4051, 2011. ISSN 0013-4686. doi: http://dx.doi.org/10.1016/j.electacta.2011.02.002. URL `http://www.sciencedirect.com/science/article/pii/S001346861100212X`.

Lars Onsager. Reciprocal relations in irreversible processes. i. *Phys. Rev.*, 37:405–426, Feb 1931. doi: 10.1103/PhysRev.37.405. URL `https://link.aps.org/doi/10.1103/PhysRev.37.405`.

Lars Onsager. Theories and problems of liquid diffusion. *Annals of the New York Academy of Sciences*, 46:241–265, 1945.

M. Ortiz and L. Stainier. The variational formulation of viscoplastic constitutive updates. *Computer Methods in Applied Mechanics and Engineering*, 171(3):419 – 444, 1999. ISSN 0045-7825. doi: https://doi.org/10.1016/S0045-7825(98)00219-9. URL http://www.sciencedirect.com/science/article/pii/S0045782598002199.

C. C. Paige and M. A. Saunders. Solution of sparse indefinite systems of linear equations. *SIAM Journal on Numerical Analysis*, 12(4):617–629, sep 1975. doi: 10.1137/0712047. URL https://doi.org/10.1137%2F0712047.

A. Pandol, Couro Kane, Jerrold E. Marsden, and Michael Ortiz. Time-discretized variational formulation of non-smooth frictional contact. 2001.

F. Parhami, Robert M. McMeeking, A. C. F. Cocks, and Z. Suo. A model for the sintering and coarsening of rows of spherical particles. *Mechanics of Materials*, 31:43–61, 1999.

Matt Pharr, Kejie Zhao, Zhigang Suo, Fan-Yi Ouyang, and Pilin Liu. Concurrent electromigration and creep in lead-free solder. *Journal of Applied Physics*, 110(8):083716, 2011.

Max Planck. Ueber die potentialdifferenz zwischen zwei verdünnten lösungen binärer electrolyte. *Annalen der Physik*, 276(8):561–576, 1890.

V. Ramadesigan, P. W. C. Northrop, S. De, S. Santhanagopalan, R. D. Braatz, and V. R. Subramanian. Modeling and simulation of lithium-ion batteries from a systems engineering perspective. *Journal of the Electrochemical Society*, 159(3):R31–R45, jan 2012. doi: 10.1149/2.018203jes. URL https://doi.org/10.1149/2.018203jes.

M. Reiner. The deborah number. *Physics Today*, 17(1):62–62, jan 1964. doi: 10.1063/1.3051374. URL https://doi.org/10.1063%2F1.3051374.

L. F. Richardson. The approximate arithmetical solution by finite differences of physical problems involving differential equations, with an application to the stresses in a masonry dam. *Philosophical Transactions of the Royal Society A: Mathematical, Physical and Engineering Sciences*, 210(459-470):307–357, jan 1911. doi: 10.1098/rsta.1911.0009. URL https://doi.org/10.1098%2Frsta.1911.0009.

Youcef Saad and Martin H. Schultz. GMRES: A generalized minimal residual algorithm for solving nonsymmetric linear systems. *SIAM Journal on Scientific and Statistical Computing*, 7(3):856–869, jul 1986. doi: 10.1137/0907058. URL https://doi.org/10.1137%2F0907058.

Yousef Saad. *Iterative Methods for Sparse Linear Systems*. Society for Industrial and Applied Mathematics, jan 2003. doi: 10.1137/1.9780898718003. URL https://doi.org/10.1137%2F1.9780898718003.

M. Sala and M. Heroux. Robust algebraic preconditioners with IFPACK 3.0. Technical Report SAND-0662, Sandia National Laboratories, 2005.

M. Sala, K. Stanley, and M. Heroux. On the design of interfaces to sparse direct solvers. *submitted*, 2006a.

M. Sala, K. Stanley, and M. Heroux. Amesos: A set of general interfaces to sparse direct solver libraries. In *Proceedings of PARA'06 Conference, Umea, Sweden*, 2006b.

A. Salvadori, D. Grazioli, and M.G.D. Geers. Governing equations for a two-scale analysis of li-ion battery cells. *International Journal of Solids and Structures*, 59:90 – 109, 2015. ISSN 0020-7683. doi: https://doi.org/10.1016/j.ijsolstr.2015.01.014. URL http://www.sciencedirect.com/science/article/pii/S0020768315000165.

Bruno Scrosati and Jürgen Garche. Lithium batteries: Status, prospects and future. *Journal of Power Sources*, 195(9):2419 – 2430, 2010. ISSN 0378-7753. doi: https://doi.org/10.1016/j.jpowsour.2009.11.048. URL http://www.sciencedirect.com/science/article/pii/S0378775309020564.

F.W. Sears and G.L. Salinger. *Thermodynamics, Kinetic Theory, and Statistical Thermodynamics*. Addison-Wesley principles of physics series. Addison-Wesley Publishing Company, 1975. ISBN 9780201068948. URL https://books.google.de/books?id=3gRRAAAAMAAJ.

Jonathan R Shewchuk. An introduction to the conjugate gradient method without the agonizing pain. Technical report, School of Computer Science Carnegie Mellon University, Pittsburgh, PA, USA, 1994.

J.C. Simo and T.J.R. Hughes. *Computational Inelasticity*. Interdisciplinary Applied Mathematics. Springer New York, 2000. ISBN 9780387975207. URL https://books.google.de/books?id=ftL2AJL8OPYC.

J.C. Simo and C. Miehe. Associative coupled thermoplasticity at finite strains: Formulation, numerical analysis and implementation. *Computer Methods in Applied Mechanics and Engineering*, 98(1):41 – 104, 1992. ISSN 0045-7825. doi: https://doi.org/10.1016/0045-7825(92)90170-O. URL http://www.sciencedirect.com/science/article/pii/004578259290170O.

P. Solin, J. Cerveny, L. Dubcova, and D. Andrs. Monolithic discretization of linear thermoelasticity problems via adaptive multimesh hp-fem. *Journal of Computational and Applied Mathematics*, 234(7):2350 – 2357, 2010. ISSN 0377-0427. doi: https://doi.org/10.1016/j.cam.2009.08.092. URL http://www.sciencedirect.com/science/article/pii/S0377042709005731. Fourth International Conference on Advanced COmputational Methods in Engineering (ACOMEN 2008).

L. Stainier. Consistent incremental approximation of dissipation pseudo-potentials in the variational formulation of thermo-mechanical constitutive updates. *Mechanics Research Communications*, 38(4):315 – 319, 2011. ISSN 0093-6413. doi: https://doi.org/10.1016/j.mechrescom.2011.03.011. URL http://www.sciencedirect.com/science/article/pii/S0093641311000668.

L. Stainier and M. Ortiz. Study and validation of a variational theory of thermo-mechanical coupling in finite visco-plasticity. *International Journal of Solids and Structures*, 47(5):705 – 715, 2010. ISSN 0020-7683. doi: https://doi.org/10.1016/j.ijsolstr.2009.11.012. URL http://www.sciencedirect.com/science/article/pii/S0020768309004478.

J. Stewart. *Calculus*. Cengage Learning, 2015. ISBN 9781305480513. URL https://books.google.ie/books?id=spiaBAAAQBAJ.

G. Strang. *Computational Science and Engineering*. Wellesley-Cambridge Press, 2007. ISBN 9780961408817. URL https://books.google.de/books?id=GQ9pQgAACAAJ.

G. Strang and G. Fix. *An Analysis of the Finite Element Method*. Wellesley-Cambridge Press, 2008. ISBN 9780980232707. URL https://books.google.de/books?id=K5MAOwAACAAJ.

Z. Suo. A continuum theory that couples creep and self-diffusion. *J. Appl. Mech*, pages 646–651, 2004.

Z. Suo, D.V. Kubair, A.G. Evans, D.R Clarke, and V.K. Tolpygo. Stresses induced in alloys by selective oxidation. *Acta Materialia*, 51(4):959 – 974, 2003. ISSN 1359-6454. doi: 10.1016/S1359-6454(02)00499-8. URL http://www.sciencedirect.com/science/article/pii/S1359645402004998.

J. Svoboda and F.D. Fischer. Vacancy-driven stress relaxation in layers. *Acta Materialia*, 57(16):4649 – 4657, 2009. ISSN 1359-6454. doi: http://dx.doi.org/10.1016/j.actamat.2009.06.016. URL http://www.sciencedirect.com/science/article/pii/S1359645409003656.

J. Svoboda and I. Turek. On diffusion-controlled evolution of closed solid-state thermodynamic systems at constant temperature and pressure. *Phil. Mag. B*, 64(6):749–759, 1991.

Tayfun E. Tezduyar and Sunil Sathe. Modelling of fluid–structure interactions with the space–time finite elements: Solution techniques. *International Journal for Numerical Methods in Fluids*, 54(6-8):855–900, 2007. doi: 10.1002/fld.1430. URL https://doi.org/10.1002%2Ffld.1430.

V.K. Tolpygo and D.R. Clarke. On the rumpling mechanism in nickel-aluminide coatings: Part ii: characterization of surface undulations and bond coat swelling. *Acta Materialia*, 52(17):5129 – 5141, 2004. ISSN 1359-6454. doi: http://dx.doi.org/10.1016/j.actamat.2004.07.023. URL http://www.sciencedirect.com/science/article/pii/S135964540400432X.

Ulrich Trottenberg, Cornelius W. Oosterlee, and Anton Schuller. *Multigrid*. Academic Press, 2000. ISBN 012701070X. URL https://www.amazon.com/Multigrid-Ulrich-Trottenberg/dp/012701070X?SubscriptionId=0JYN1NVW651KCA56C102&tag=techkie-20&linkCode=xm2&camp=2025&creative=165953&creativeASIN=012701070X.

F.-J. Ulm, Olivier Coussy, K. Li, and C. Larive. Thermo-chemo-mechanics of ASR expansion in concrete structures. *Journal of Engineering Mechanics*, 126(3):233–242, 2000. URL https://hal-enpc.archives-ouvertes.fr/hal-00586622.

Hirofumi Uzawa and Kenneth J. Arrow. Iterative methods for concave programming. In *Studies in Linear and Non-linear Programming*, Stanford mathematical studies in the social sciences, chapter 9. Stanford University Press, 1958.

H.A. van der Vorst. *Iterative Krylov Methods for Large Linear Systems*. Cambridge Monographs on Applied and Computational Mathematics. Cambridge University Press, 2003. ISBN 9780521818285. URL https://books.google.de/books?id=_WJoLfl19e8C.

Lange M. R. Vaz M. Thermo-mechanical coupling strategies in elastic–plastic problems. *Continuum Mechanics and Thermodynamics*, 29(2):373–383, Mar 2017. ISSN 1432-0959. doi: 10.1007/s00161-016-0537-7. URL https://doi.org/10.1007/s00161-016-0537-7.

Francesc Verdugo and Wolfgang A. Wall. Unified computational framework for the efficient solution of n-field coupled problems with monolithic schemes. *Computer Methods in Applied Mechanics and Engineering*, 310:335 – 366, 2016. ISSN 0045-7825. doi: https://doi.org/10.1016/j.cma.2016.07.016. URL http://www.sciencedirect.com/science/article/pii/S0045782516307575.

A. Wathen. Matrix preconditioning techniques and applications. by k. chen, cambridge university press, 2005. 592 pp. isbn 0521 83828 2. £55 -. *Journal of Fluid Mechanics*, 550:442–443, 2006. doi: 10.1017/S0022112005007986.

A. J. Wathen. Preconditioning. *Acta Numerica*, 24:329–376, 2015. doi: 10.1017/S0962492915000021.

P. Wesseling and C.W. Oosterlee. Geometric multigrid with applications to computational fluid dynamics. *Journal of Computational and Applied Mathematics*, 128(1):311 – 334, 2001. ISSN 0377-0427. doi: https://doi.org/10.1016/S0377-0427(00)00517-3. URL http://www.sciencedirect.com/science/article/pii/S0377042700005173. Numerical Analysis 2000. Vol. VII: Partial Differential Equations.

Margaret Robson Wright. *An Introduction to Aqueous Electrolyte Solutions*. Wiley, 2007. ISBN 0470842938.

Kang Xu. Nonaqueous liquid electrolytes for lithium-based rechargeable batteries. *Chemical Reviews*, 104 (10):4303–4418, oct 2004. doi: 10.1021/cr030203g. URL https://doi.org/10.1021%2Fcr030203g.

Q. Yang, L. Stainier, and M. Ortiz. A variational formulation of the coupled thermo-mechanical boundary-value problem for general dissipative solids. *Journal of the Mechanics and Physics of Solids*, 54(2):401 – 424, 2006. ISSN 0022-5096. doi: https://doi.org/10.1016/j.jmps.2005.08.010. URL `http://www.sciencedirect.com/science/article/pii/S0022509605001511`.

Lily Yau and Adi Ben-Israel. The newton and halley methods for complex roots. *The American Mathematical Monthly*, 105(9):806–818, 1998. ISSN 00029890, 19300972. URL `http://www.jstor.org/stable/2589209`.

Reza Younesi, Gabriel M. Veith, Patrik Johansson, Kristina Edstrom, and Tejs Vegge. Lithium salts for advanced lithium batteries: Li-metal, li-o2, and li-s. *Energy Environ. Sci.*, 8:1905–1922, 2015. doi: 10.1039/C5EE01215E. URL `http://dx.doi.org/10.1039/C5EE01215E`.

Jun Zhang. Preconditioned krylov subspace methods for solving nonsymmetric matrices from cfd applications. *Computer Methods in Applied Mechanics and Engineering*, 189(3):825 – 840, 2000. ISSN 0045-7825. doi: https://doi.org/10.1016/S0045-7825(99)00345-X. URL `http://www.sciencedirect.com/science/article/pii/S004578259900345X`.

Hans Ziegler. Some extremum principles in irreversible thermodynamics with applications to continuum mechanics. In I. E. Sneddon and Rodney Hill, editors, *Progress in Solid Mechanics*, volume 4, pages 92–193. Elsevier North-Holland, 1963.

Index

Acronyms

AAME artificial added mass effect. 127

AMG algebraic multigrid strategy. 24, 27, 28, 30–32, 149

BC boundary conditions. 36, 37

BGS block Gauss-Seidel. 24, 25

CoV Calculus of Variations. 12, 15

ENC ElectroNeutrality condition. 83, 89–93, 97, 99

FEM Finite Element Method. 7, 12, 15, 20, 21, 56, 105, 113, 132, 148

FSI Fluid Structure Interaction. 25, 28, 124, 127, 149

GMG geometric multigrid strategy. 27, 30, 31

GMRES General Minimum Residual. 26

IC initial conditions. 36–38

ILU Incomplete LU. 23, 30

IVD intervertebral disc. 5, 6

KSP Krylov subspace preconditioning. 28

LU lower triangular. 23, 30, 31, 167

MG multigrid strategy. 27, 29, 32

MINRES Minimum Residual. 26

PDE Partial Differential Equation. 8, 26, 38, 54–57, 98

RHS right hand side. 37, 72, 127

SEI surface electrolyte interface. 88

SF strong form. 36–38, 42–44, 54–56, 71, 76–78, 80, 82, 123, 127, 146, 147

SIMPLE Semi-Implicit Method for Pressure-Linked Equations. 24

VF variational form. xv, 4, 7, 12, 13, 21, 23, 35, 36, 38–40, 42–44, 48–52, 54, 57, 59, 69, 71–73, 76–85, 88–90, 92, 94, 97, 99–101, 103–105, 107, 113, 114, 116, 122, 123, 125–129, 131–138, 140–142, 145–148

WF weak form. 36–38, 42–44, 54, 56, 59, 71, 76–78, 80, 82, 123, 127, 147, 148

Glossary

A | M | S

A

additive identity

The identity element of an additive group G, usually denoted 0. In the additive group of vectors, the additive identity is the zero vector 0, in the additive group of polynomials it is the zero polynomial $P(x) = 0$, in the additive group of $m \times n$ matrices it is the $m \times n$ zero matrix. Barile [a]. 25

M

multiplicative identity

In a set X equipped with a binary operation $\cdot$ called a product, the multiplicative identity is an element e such that $e \cdot x = x \cdot e = x \forall x \in X$. Barile [b]. 25

S

sparse matrix

is a matrix with enough zeros that it pays to take advantage of them Davis et al. [2016].. 26

Titre : Développement De Modèles Variationnels Et De Stratégies Algorithmiques Pour Les Problèmes Couplés

Mots clés : méthodes variationnelles, électrochimie; problèmes couplés non linéaires; multiphysique; stratégies numériques, préconditionneurs de blocs.

Résumé : Une approche de modélisation et des techniques de résolution de problèmes couplés sont proposées, basées sur un principe variationnel.

La modélisation repose sur une approche variationnelle utilisée dans des types spécifiques de problèmes couplés. Le modèle proposé est généralisé pour les problèmes couplés indépendamment des types de physique sur lesquels ils s'appuient.

Différentes stratégies de solutions numériques sont dérivées du modèle variationnel proposé. Ces stratégies peuvent être liées à des stratégies empiriques telles que des approches “global/local” et/ou “staggered”.

Les modèles proposés et les techniques de résolution sont présentés pour différents exemples 1D. Le modèle généralisé est utilisé en électrochimie et un modèle variationnel pour une batterie lithium-ion est dérivé. Le cadre variationnel est également utilisé pour comparer différents modèles existants pour l'électrolyte de la batterie.

Title : Development Of Variational Models & Algorithmic Strategies For Coupled Problems

Keywords : variational approach, electrochemistry; nonlinear coupled problems; multiphysics; staggered, strategies, nested strategies, block-preconditioners.

Abstract : A modeling approach and numerical-solution techniques for coupled problems are proposed based on variational principles.

The modeling is based on a variational approach used in specific types of coupled problems. The proposed model is generalized for coupled problems independently of the types of physics on which they are based. Different numerical solution strategies are derived from the proposed variational models. These strategies can be linked to empirical strategies such as « global/local" and/or « staggered" approaches.

The proposed models and the resolution techniques are presented for different 1D examples. The generalized model is used in electrochemistry and a variational model for a lithium-ion battery is derived.

The variational framework is also used to compare different existing models for the battery electrolyte.